2012

Roles of the Methylcitrate and Methylmalonyl-COA Pathways in Mycobacterial Metabolism and Pathogenesis

Manisha Ulhas Lotlikar

ROLES OF THE METHYLCITRATE AND METHYLMALONYL-COA PATHWAYS IN MYCOBACTERIAL METABOLISM AND PATHOGENESIS

A Thesis Presented to the Faculty of

The Rockefeller University

in Partial Fulfillment of the Requirements for

the degree of Doctor of Philosophy

by

Manisha Ulhas Lotlikar

June 2012

ROLES OF THE METHYLCITRATE AND METHYLMALONYL-COA PATHWAYS IN MYCOBACTERIAL METABOLISM AND PATHOGENESIS

Manisha Ulhas Lotlikar, Ph.D.
The Rockefeller University 2012

Mycobacterium tuberculosis has been a human pathogen for the history of mankind, but we are only now beginning to understand how it is able to survive and persist indefinitely in the host. Understanding carbon metabolism of the pathogen during infection is key, not only as a source of potential drug targets, but also for elucidating the environment *in vivo*, so that drugs can be tested under relevant conditions.

Studies have revealed that, during infection, *M. tuberculosis* relies on gluconeogenic carbon sources rather than sugars. Fatty acids, cholesterol, and amino acids have all been demonstrated as usable carbon sources *in vitro* and can all generate propionyl-CoA. The methylcitrate cycle, which, in *M. tuberculosis*, uses a bifunctional isocitrate lyase/methylisocitrate lyase (ICL/MCL), is one of the two routes for metabolism of propionyl-CoA. A mutant strain of *M. tuberculosis* lacking the ICL/MCL was rapidly cleared from the lungs of infected mice. However, the upstream enzymes of this pathway have been demonstrated to be dispensable for infection and survival in the mouse model. The methylmalonyl-CoA route of propionyl-CoA utilization can be activated *in vitro* by addition of the vitamin B12 cofactor of the methylmalonyl-CoA mutase. This route may buffer

the loss of the methylcitrate cycle *in vivo*, depending on B12 availability or production in the host.

The work here examines the relative use of the methylcitrate cycle and methylmalonyl-CoA pathways in *M. tuberculosis* and in the related, non-pathogenic species, *M. smegmatis*, using genetic mutants of either or both of the metabolic routes. It is shown here that, as for *M. tuberculosis*, *M. smegmatis* preferentially uses the methylcitrate cycle for growth on propionate. In the absence of the methylcitrate cycle *M. smegmatis*, in contrast to *M. tuberculosis*, can eventually endogenously activate the methylmalonyl-CoA pathway *in vitro*, presumably through B12 synthesis. In mutants of both species, lacking both pathways, the use of other carbon sources in the media is inhibited in the presence of propionate. This dominant inhibition implies the accumulation of toxic metabolites derived from the inability to metabolize propionate, as has been suggested by previous studies.

To detect propionate-derived intermediates, metabolite analysis by targeted liquid chromatography-tandem mass spectrometry (LC-MS/MS) was used in this study. Accumulation of these metabolites under propionate exposure was identified in a strain of *M. smegmatis* impaired in both metabolic routes, but not in the wild-type. These studies also revealed similar accumulation under glucose growth, where the mutant strain displayed a slight growth defect, and also under no-carbon conditions, where the mutant demonstrated a survival defect compared to wild-type. These findings suggest a role of the propionate

pathways for endogenously derived propionyl-CoA as well as during starvation-induced amino acid and/or fatty acid mobilization.

The *M. tuberculosis* mutant strains generated here were tested in the mouse infection model. The methylmalonyl-CoA mutase was found to be individually dispensable for growth *in vivo*. However, a strain with the additional deletion of the methylcitrate cycle was attenuated during the early stage of infection and caused less tissue pathology, even after the bacterial burden reached wild-type levels. While propionate metabolism may not be required *per se* for *in vivo* growth, the suggested accumulation of toxic intermediates, demonstrated here in *M. smegmatis*, may indicate a required role for ICL/MCL in *M. tuberculosis* for detoxification of propionyl-CoA *in vivo*.

ACKNOWLEDGEMENTS

In a sentence, Prof. John McKinney convinced me that I could benefit humanity through tuberculosis research. In the years since, there have been many subsequent sentences - to the effect of superb scientific advising, absorbing discussions, and consistent mentorship. I am grateful to have had the opportunity to learn from him and work in his lab, which he actively orients towards exciting and quality science. I appreciate his patience in this project, which, like *M. tuberculosis*, grew with a slow but steady doubling time, and for his flexibility with letting me work the 'night shift'.

In addition to John's scientific views, I have greatly admired his integrity and his real pursuit of productive collaborations. This has been to the great benefit of my work. I have had the privilege to work in the lab of Prof. Uwe Sauer at the ETH Zurich, whose expertise led to some of the most exciting findings in my research. I would like to specifically acknowledge Dr. Jörg Büscher and Michael Zimmermann for their invaluable collaboration on this work.

A mutual interest in propionate metabolism also led to our fruitful collaboration with the laboratory of Prof. Valerie Mizrahi at the University of Cape Town, including Dr. Suzana Savvi, Dr. Digby Warner, Dr. Krishnamoorthy Gopinath, and Atica Moosa.

I have been fortunate to work in the presence of those willing to share their scientific talents, insight, and experience. Dr. Anna Upton and Dr. Anna Tischler have been mentors and role models, in everything from BSL3-training to scientific

reasoning. In my every day work, I profit from being just a bay-away from many keen and kind scientific minds, including Cyntia DePiano, Meltem Elitas, and Neeraj Dhar, and those in my Metabolic subgroup: Emre Ozdemir, Tarun Chopra, Paul Murima, and Zeljka Maglica.

I am indebted to Prof. Dianne Newman at Caltech for having introduced me to the fascinating world of environmental microbiology through her dedication to teaching. The opportunity she gave me to work in her lab as an undergrad is certainly what revived my love of science at a critical time, and her mentorship inspired me to continue onwards to grad school. The challenges of working with anaerobic bacteria helped prepare me for the difficulties of *M. tuberculosis*, not just in too-large glovebox-gloves presaging too-large Tyvek suits.

In my extracurricular studies of carbon metabolism, I was joined by Dr. Jeffrey Chen and Jocelyne Lew, head curator of Tuberculist, in extending rigorous scientific curiosity to the nutrient availability in our Lausannois environment. In studies of geography and earth science, I have been accompanied by Dr. Sachin Kotak and Sveta Chakrabarti, scientists and badminton players, both.

Through the quarter of my lifetime spent on this work, I am immensely grateful for the friends who have known me for over half my life, for the constancy of their support and reliability of their hilarity, that make up for the inconstancies and minor tragedies of experimental science; Sasha Sadikot, Nicole Pusateri, Chi Hae Park, Cathy Serpico, and Eda Uca.

Every new year that passed in my PhD has fulfilled the promise of a new experience in a new country with the same collegial crew cultivated from our college days; Matt Johnston, David McKinney, Jared Gabor, Peter Samuelson, and Kevin Duncklee. I am especially grateful for the friendship of Bernadette Heyburn, whom, by cosmic CERN-centric coincidence, was expatriating in Switzerland at the same time as myself.

For the seamless transition to a trans-Atlantic PhD I would like to thank the Rockefeller University Dean's Office (Kristen, Cris, Marta, Emily, Sid, Michelle, and Amber) as well as Suzanne Lamy at EPFL. I would like to thank Prof. George Cross and Prof. Howard Hang for serving on my committee, providing their guidance and insight every year, and to Prof. Sabine Ehrt for the honor of her expertise as my external examiner.

Instrumental in helping me to get to this point:

To my parents, who always have and always would support me in anything, whether I am a country or an ocean apart. To Alpa, to whom I attribute my love of learning, who brought home to share every piece of information she learned at school. To Nimish, Piyusha, Madhavi mami, and Sandeep mama, with whom I have enjoyed the extended support of an extended family.

And to Matt, for the brilliance, the humor, the support, of the every single day type, especially for the many days that turn to many years.

Thank you all.

TABLE OF CONTENTS

LIST OF FIGURES

LIST OF ABBREVIATIONS

13C	carbon-14
14C	carbon-13
2D-PAGE	2-dimensional polyacrylamide gel electrophoresis
ACC	acyl-CoA carboxylase
ACK	acetate kinase
ACN	aconitase
ACS	acetyl-CoA synthetase
ADC	albumin-dextrose-catalase
AdoCbi	adenosylcobinamide
AdoCbl	adenosylcobalamin
ADP	adenosine diphosphate
AHAS	acetohydroxy acid synthase
aph	gene encoding aminoglycoside phosphotransferase
B12	coenzyme B12
BC	biotin carboxylase
BCCP	biotin carboxyl carrier protein
BCG	Bacille Calmette Guérin
BCKDH	branched-chain amino acid dehydrogenase
bp	base pair(s)
cAMP	cyclic adenosine monophosphate
CFU	colony forming unit
CNCbl	cyanocobalamin (vitamin B12)
CO2	carbon dioxide
CoA	coenzyme A
CRP	cAMP receptor protein
CS	citrate synthase
CT	carboxyltransferase
deg	degree
DHFR	dihydofolate reductase
DMB	dimethylbenzimidazole
DNA	deoxyribonucleic acid
dNTP	deoxyribonucleotide triphosphate
E4P	erythrose 4-phosphate
EDP	Entner–Doudoroff pathway
EMPP	Embden-Meyerhof-Parnas pathway
EMSA	electrophoretic mobility shift assay
EPFL	École Polytechnique Fédérale de Lausanne
ETHZ	Eidgenössische Technische Hochschule Zürich
FAD	flavin adenine dinucleotide
FADH2	reduced flavin adenine dinucleotide
FBPase	fructose 1,6 bisphosphatase
FI	flow injection

G + C	guanine-cytosine
GAP	glyceraldehyde 3-phosphate
GC	gas chromatography
GDH	glycine dehydrogenase
GDP	guanosine diphosphate
GTP	guanosine triphosphate
HPLC	high performance liquid chromatography
hr	hour
Hyg	Hygromycin B
hyg	gene conferring resistance to Hygromycin B
ICD	isocitrate dehydrogenase
ICL	isocitrate lyase
Kan	Kanamycin
kb	kilobase
kDa	kilodaltons
KDC	alpha-ketoglutarate decarboxylase
KDH	alpha-ketoglutarate dehydrogenase
lacZ	gene encoding beta-galactosidase
LB	Luria-Bertani or lysogeny broth
LC	liquid chromatography
MCD	methylcitrate dehydratase
MCL	methylisocitrate lyase
MCM	methylmalonyl-CoA mutase
MCS	methylcitrate synthase
MDH	malate dehydrogenase
MDR	multiple-drug resistant
MEZ	malic enzyme
MLS	malate synthase
MMCE	methylmalonyl-CoA epimerase
MMDC	methylmalonyl-CoA decarboxylase
MS	mass spectrometry
MS/MS	tandem mass spectrometry
NAD	nicotinamide adenine dinucleotide
NADH	reduced nicotinamide adenine dinucleotide
NADP	nicotinamide adenine dinucleotide phosphate
NADPH	reduced nicotinamide adenine dinucleotide phosphate
NAMN	nicotinic acid mononucleotide
NMR	nuclear magnetic resonance
OADC	oleic acid-albumin-dextrose-catalase
OD600	optical density at 600 nanometer wavelength
ORF	open reading frame
PBS	phosphate-buffered saline
PCA	pyruvate carboxylase
PCC	propionyl-CoA carboxylase

PCR	polymerase chain reaction
PCS	propionyl-CoA synthetase
PDH	pyruvate dehydrogenase
PDIM	phthiocerol dimycoserosate
PEP	phospho-*enol*-pyruvate
PEPCK	PEP carboxykinase
PI	propidium iodide
PKS	polyketide synthase
PNR/P	peroxynitrite reductase/peroxidase
PPC	PEP carboxylase
PPDK	pyruvate phosphate dikinase
PPP	pentose phosphate pathway
PPS	PEP synthase
PTA	phosphotransacetylase
PYK	pyruvate kinase
R5P	ribulose 5-phosphate
RNA	ribonucleic acid
RNS	reactive nitrogen species
ROS	reactive oxygen species
rTCA	reduced tricarboxylic acid (cycle)
RU	The Rockefeller University
sacB	gene encoding levansucrase
SL	sulfolipid
SNP	single nucleotide polymorphism
SSA	succinic semialdehyde
SSADH	succinic semialdehyde dehydrogenase
TA	toxin-antitoxin
TB	tuberculosis
TCA	tricarboxylic acid (cycle)
TOF	time-of-flight
Tween	polyoxyethylene sorbitan monooleate
WT	wild-type
XDR	extremely drug resistant or extensively drug resistant

1. Background

1.1 Metabolism in mycobacteria

"There have been repeated attempts to fathom the nature of tuberculosis, but thus far without success" - Dr. Robert Koch, 1884, translated

Dr. Koch wrote these words as an introduction to one of his seminal papers, which then went on to elucidate the 'nature' of the disease, yet the unfathomable nature of tuberculosis (TB) persists to the present day, in a different sense. The global burden of the affliction is allocated to those least able to deal with it; of the 3,800 daily worldwide deaths from TB in 2010, 95% were in the developing world (World Health Organization 2011). The bacterium responsible outpaces the efforts to stop it, with a rising incidence of multiple drug resistant (MDR) and extremely drug resistant (XDR) cases.

1.1.1 Mycobacterium tuberculosis

The microorganism that causes tuberculosis in humans was identified in 1882 by Dr. Robert Koch as being 'rod-shaped' and belonging to the 'group of *bacilli*' and came to be known as the 'tubercle bacillus'. *Mycobacterium tuberculosis* is now taxonomically classified as a member of the class Actinobacteria, consisting of gram-positive and G+C-rich bacteria, and the

suborder Corynebacterineae, which lays claim to the important pathogen-containing families of Corynebacterineae (diphtheria-causing *Corynebacterium diphtheria*), Gordoniaceae (pulmonary pathogen *Gordonia bronchialis*), and Nocardianceacea (opportunistic pathogens of *Nocardia* spp., plant pathogen *Rhodococcus fascians*, and livestock and opportunistic human pathogen *Rhodococcus equi*).

Within the genus of *Mycobacterium*, there exist pathogens that are obligate (*M. leprae*), facultative (e.g., *M. bovis*), and opportunistic (e.g., *M. avium*), as well as environmental, non-pathogenic strains (e.g., *M. smegmatis*). The members of the genus display a wide range of growth rates. *M. smegmatis*, considered a 'fast-grower', has an average doubling time in rich media around 3-4 hours, whereas *M. tuberculosis* divides every 20-24 hours, on average.

- Cell wall

The family of Mycobacteriaceae and genus *Mycobacterium* are named for the mycolic acids they produce, a characteristic of the coryneform bacteria, that are a major component of their complex cell walls, which consist of a variety of long chain lipids, glycolipids, and polysaccharides, in addition to the peptidoglycan layer characteristic of Gram-negative bacteria (Brennan 2003). The mycolic acid layer is responsible for recalcitrance of mycobacteria to Gram staining but also the retention of 'acid-fast' Ziehl-Neelsen stain used to identify mycobacteria in clinical samples.

- Tuberculosis disease

Infection characteristically occurs through inhaled bacterium-containing droplets spread by aerosols generated by the coughing or sneezing of individuals with active disease. These aerosolized particles are small enough to pass through the mucociliary action of the bronchi to reach the terminal alveoli, where the bacilli are internalized by the resident immune phagocytic cells (macrophages).

Following phagocytosis, the tubercle bacillus resides in a membrane-bound organelle termed the 'phagosome'. *M. tuberculosis* is able to block the fusion of the phagosome with the acidic lysosome that otherwise occurs as a line of host defense. Thus, the infectious agent is able to survive and replicate within this compartment until the onset of the adaptive T-cell mediated immune response, signaled by activated dendritic cells that traffic to lymph nodes. This trafficking may also spread the infection to other sites within the lung or, in some cases, systemically.

Disease progression involves the recruitment of host immune cells, which form a physical encasement of the infected macrophages, known as a granuloma. The continual balance of replication of mycobacteria and macrophage uptake and killing results in an on-going stimulation of the host immune system.

Individuals that can control the infection are able to contain the bacilli in these granulomas, whereas in some individuals the lesions turn necrotic, with continued replication of the bacteria, phagocytic killing, chronic inflammation, and

concomitant tissue damage. This results in further spread of the bacilli and progressive lung tissue damage from the immune response that, if untreated, results in death of the host.

As the bacteria are not necessarily eliminated from even the 'quiescent' lesions, they are able to persist in a latent form of infection unless and until the immune status of the host is compromised and the granulatomous lesions reactivate, undergo necrosis and caseation, allowing the pathogen to exit the lung in sputum to be spread to new hosts (reviewed in Bloom 1994).

Protective immunity does not appear to be afforded by prior infection, which may explain, in part, the varying efficacy (0% - 80%) reported for the widely-used Bacille-Calmette-Guérin (BCG) vaccine (Behr and Small 1997). This live, attenuated vaccine was developed from a lab-passaged strain of the closely related bovine pathogen *M. bovis.*

- Drug therapy

Although chemotherapeutic agents have existed for over half a century, tuberculosis disease remains a leading cause of morbidity and mortality. This can be attributed to the long duration of treatment times and the spread of drug-resistant bacteria.

The current antibiotics target cell wall mycolic acid biosynthesis (isoniazid (H)), cell wall arabinogalactan synthesis (ethambutol (E)), (putatively) fatty acid synthase I (pyrazinamide (Z)), and RNA polymerase (rifampicin (R)). The long

course of drug therapy, a standard two months of four drugs (HREZ) followed by a continued four months of two drugs (HR), is necessitated by the occurrence of spontaneous single-drug resistant mutants and a persistent fraction of the bacterial load that is not eliminated in the initial phase. Targeting this persistent sub-population is believed to be the key to cutting treatment time and more effectively combating the current epidemiology of the tuberculosis disease.

It is thought that either the physiological environment or the metabolic state of the persistent fraction of bacteria renders this sub-population resistant to killing (Bigger 1944). Examples of phenotypic heterogeneity of clonal populations of bacteria have been known to contribute to differential response to antibiotics (Dhar and McKinney 2007). Until the physiological basis of persistence in tuberculosis is understood, additional antibiotic targets need to be validated for drug discovery efforts to continue and attempt to catch up to the rapidly evolving drug resistance of the pathogen.

1.1.2 Understanding pathogen metabolism

While screening efforts are underway with large chemical compound libraries, natural product libraries, and target-based drug design, it has become evident that to improve the success rate and avoid wasted effort, *in vitro* assay conditions should attempt to approximate the *in vivo* environment experienced by the bacteria. A recent large-scale drug-screening effort, which yielded candidates with potent activity in whole cell assays, failed *in vivo*, as they

inhibited growth in a glycerol-dependent manner. While glycerol was the carbon source used in the synthetic medium for the *in vitro* assays, it was found not to be available to the bacteria *in vivo* (Pethe et al 2010).

Historically, bacteria have been cultivated in laboratory environments on medium components that enabled rapid and abundant growth, usually involving formulations replete in sugars, amino acids, and supplements (Middlebrook and Cohn 1958). However, the pathways employed by bacteria in their natural environment can be vastly different from laboratory conditions in a Petri dish or culture flask.

To understand pathogen metabolism, it is critical to understand what routes of biosynthesis and energy production an organism is capable of, as well as what the nutrient availability and physical constraints of the host environment are like. Historically, the former was interrogated by *in vitro* tests for growth upon various permutations of substrates and trace nutrients. With the advent of genomics and bioinformatics, the metabolic potential of the pathogen, even if it cannot be cultured *in vitro*, can be investigated through the contents of the genome. As newly sequenced genomes are annotated via homology to better studied organisms, a caveat exists that a novel gene function may get overlook or misattributed based on the 'tyranny of the majority' (de Carvalho et al 2010a).

- The genome of M. tuberculosis

The sequencing of the *M. tuberculosis* lab reference strain H37Rv revealed a 4.4 megabase genome of 65.6% G+C content that encoded for around 4,000 genes. The genomic potential indicated prototrophy for essential amino acids, vitamins, and co-factors and the ability to utilize a wide array of carbon substrates, including carbohydrates, alcohols, and carboxylic acids. The pathways of glycolysis and gluconeogenesis, the pentose phosphate pathway, the tricarboxylic acid cycle, and the glyoxylate cycle, as will be described subsequently, were all identified (Cole et al 1998).

The 20 genes encoding P450 cytochrome monoxygenases and associated enzymes, which can act in the oxidation of xenobiotics and organic compounds (e.g., long chain fatty acids, sterols), are thought to be remnants of genes required for a saprophytic, soil-dwelling lifestyle of the evolutionary ancestor (Cole et al 1999).

A large portion of the genome is dedicated to fatty acid metabolism, with over 100 genes sharing homology for fatty acid degradation enzymes. In keeping with the primacy of the complex waxy cell wall that surrounds the bacterium, the genome encodes ‘examples of every known lipid and polyketide biosynthetic system encoded in the genome’ of both mammalian and plant origin (Cole 1999). These include the mycolic acids, the methyl-branched fatty acids, the mycocerosic and mycolipenic acids, and the phthiocerols (Lin et al 2006). (Figure 1.1)

To better understand how the metabolic capabilities of *M. tuberculosis* compare to those of other organisms and to interpret the work described herein, a basic introduction to some central carbon metabolic pathways follows.

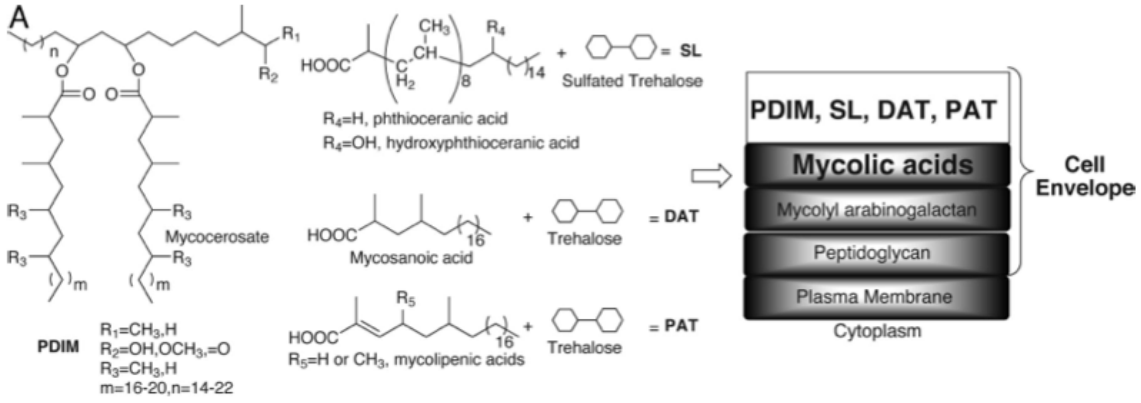

Figure 1.1 Chemical structures of *M. tuberculosis* mycolic acids and multimethyl-branched fatty acids such as A) mycocerosic, B) phthioceranic, hydroxyphthioceranic, C) mycosanoic, and D) mycolipenic acids, which form liposugars phthiocerol dimycocerosate (PDIM), sulfated tetraacyl trehalose (SL), diacyl trehaloses (DAT), and pentaacyl trehalose (PAT), respectively. E) A schematic of a proposed cell envelope architecture (Lin et al 2006).

1.1.3 Overview of central carbon metabolism

- Glycolysis vs. gluconeogenesis

Sugars provide a source of carbon for biosynthesis and energy contained within their bonds. Of the three metabolic routes, the Entner-Duodoroff pathway (EDP), the pentose phosphate pathway (PPP), and the Embden-Meyerhof-Parnas pathway (EMPP), *M. tuberculosis* possesses components of the PPP and EMPP, which will be discussed.

Oxidation of glucose through the PPP results in the formation of a glyceraldehyde-3-phosphate (GAP), the release of 3 molecules of carbon dioxide (CO_2), and the generation of the reduced coenzyme NADPH. The intermediates of this pathway, including ribose-5-phosphate (R5P), one of the pentose phosphates for which it is named, and erythrose-4-phosphate (E4P), act as the precursors for nucleotide biosynthesis and aromatic amino acid synthesis, respectively (Fraenkel 1996).

The EMP can be used in either of two directions, depending on whether the goal is the breakdown or the formation of sugars. In the direction of breakdown, the pathway is known as glycolysis and results in the transformation of the sugar to pyruvate and the release of energy, which is stored in the formation of adenosine triphosphate (ATP) and the reducing equivalents of $FADH_2$ (reduced flavin adenine dinucleotide) and NADH (reduced nicotinamide adenine dinucleotide). The unique steps to this direction, from the irreversible

transformations catalyzed, are the reactions catalyzed by phosphofructokinase (*pfk*) and pyruvate kinase (*pyk*). (Figure 1.2)

The operation of the pathway in the opposite direction, known as gluconeogenesis, is thought to be the original direction in which the pathway was utilized in evolutionary terms (Romano and Conway 1996). In this direction, reducing equivalents and energy are used to generate sugar from non-carbohydrate carbon sources. The unique, 'committed' steps in this direction are the reactions catalyzed by the phospho-enol-pyruvate (PEP) synthase (*pps*) or pyruvate phosphate dikinase (*ppdK*) and fructose-1,6-bisphosphatase (*fbp*). (Figure 1.2)

The end product of glycolysis, pyruvate can then be converted to acetyl-CoA by pyruvate dehydrogenase, for further oxidation and formation of biosynthetic intermediates in the citric acid cycle. In the reverse direction, the entry point metabolite of the gluconeogenic pathway, PEP, can be synthesized by PEP carboxykinase (*pck*) using oxaloacetate generated by the citric acid cycle.

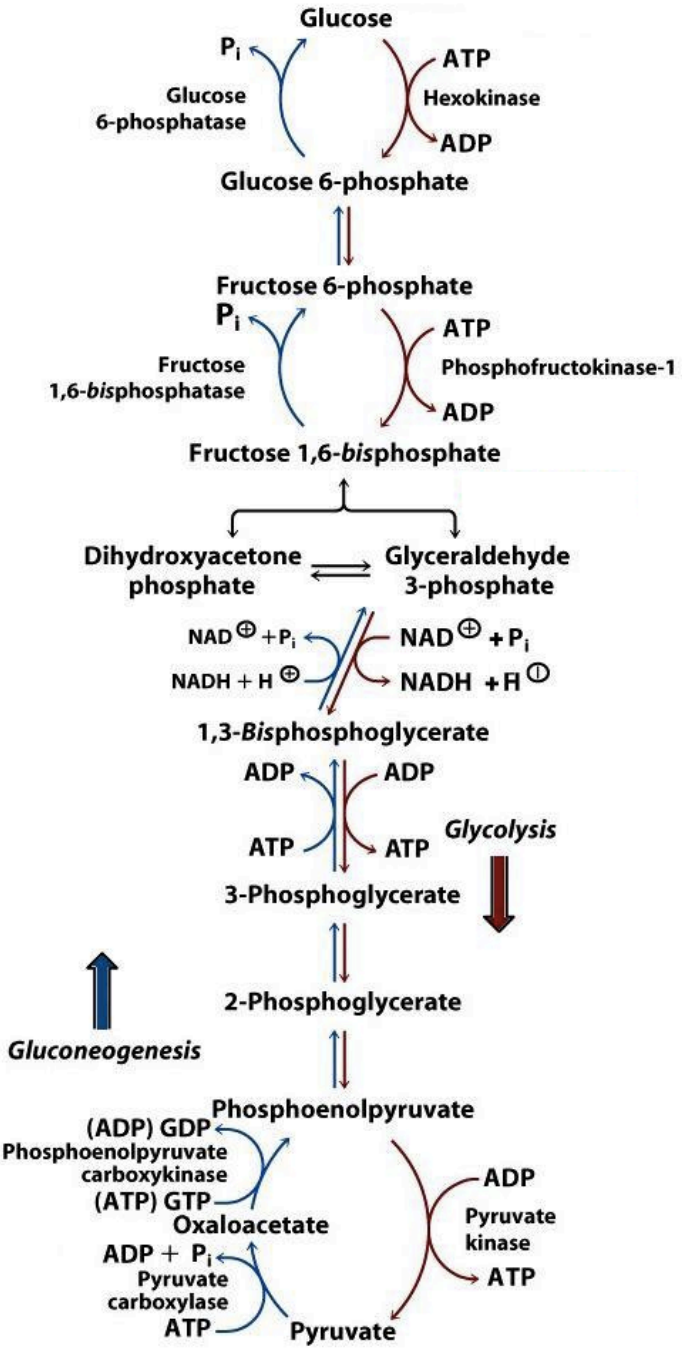

Figure 1.2 Glycolysis and gluconeogenesis proceed in opposite directions using common, reversible reactions and unique, irreversible reactions. Direction-specific reactions are indicated with color-coded one-way arrows (Moran et al 2011).

- Citric acid cycle

The citric acid cycle, also known as the tricarboxylic acid (TCA) cycle or Krebs cycle, serves as a route for energy generation, as well as a pool of biosynthetic precursors that can be siphoned off for formation of amino acids, purines, pyramidines, hemes, and porphyrins. (Figure 1.3A)

However, in the anaerobic conditions that dominated the origins of life, the cycle is believed to have originally run in 'reverse', acting as a reductive TCA (rTCA) cycle, where CO_2 could be fixed into organic compounds by the cell at the energetic cost of the redox transformations involved. (Figure 1.3B) The introduction of oxygen in the atmosphere allowed the cycle to operate in an oxidative direction, which, instead, releases CO_2 and generates reduced energetic equivalents. (Figure 1.3A)

Given the thermodynamic reversibility of most of the reactions of the cycle, the operation of the rTCA cycle requires only two enzymes that do not participate in the oxidative direction: an ATP-(dependent)-citrate lyase and alpha-ketoglutarate synthase. This pathway is still used for CO_2 fixation by some chemoautotrophic bacteria and archaea. A variation thereof is used in heterotrophic anaerobic organisms lacking a complete TCA cycle, or for metabolic flexibility, as in yeast during fermentative metabolism (Srinivasan and Morowitz 2006).

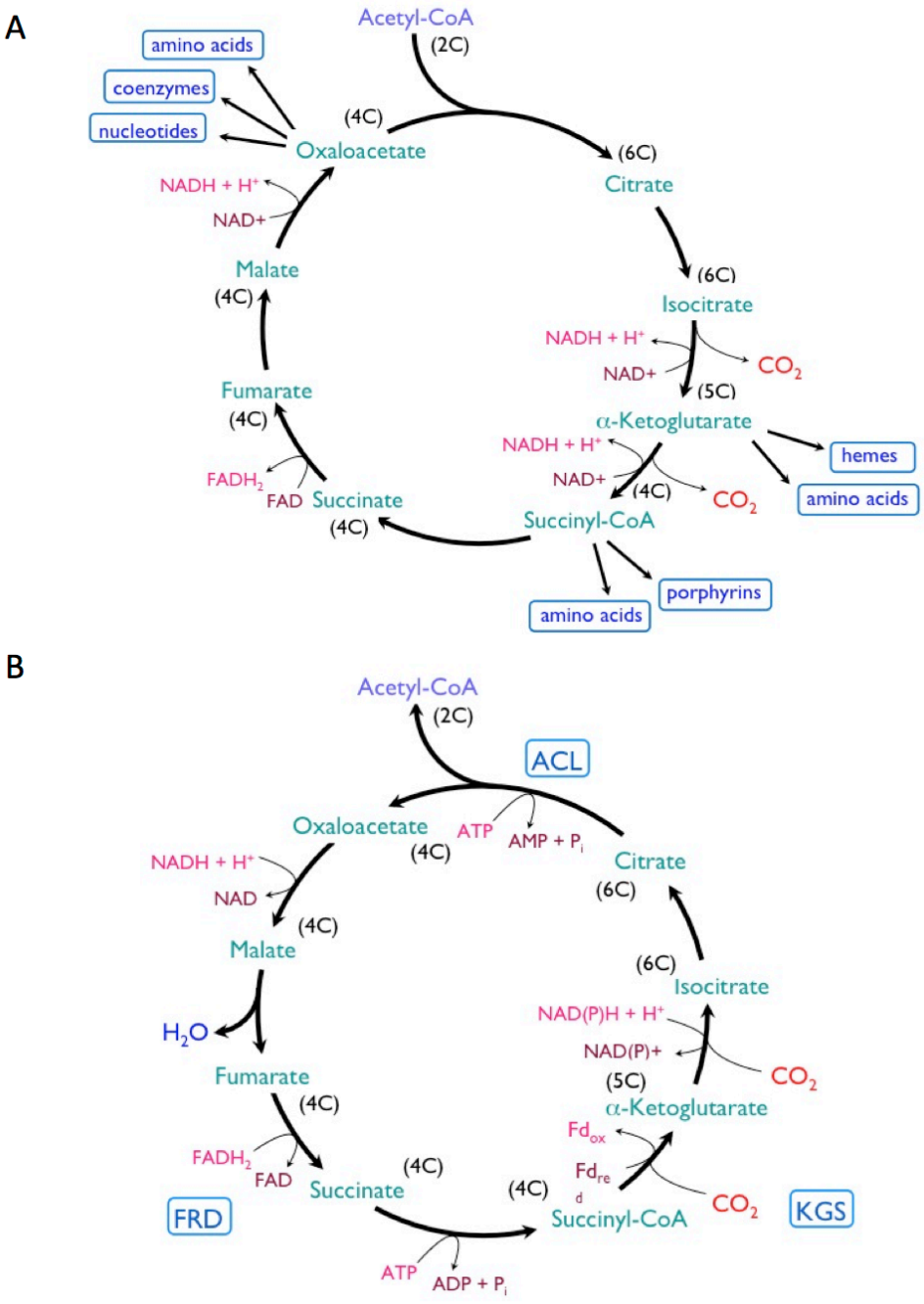

Figure 1.3 A) The TCA cycle is a source of biosynthetic precursors. Run in the oxidative direction, it yields CO_2 and generates reducing equivalents. B) The reductive TCA cycle fixes CO_2 at the expense of reducing equivalents with enzymes: fumarate reductase (FRD), alpha-ketoglutarate synthase (KGS), ATP-citrate lyase (ACL).

As various forms or parts of the TCA cycle are extant in all domains of life, it is believed that the last common ancestor possessed an intact version of the cycle, from which various species, whose TCA cycles posses a different architecture, have retained or lost components. As several components of the TCA cycle (alpha-ketoglutarate, succinyl-CoA, and oxaloacetate) are precursors for essential cellular components (glutamate, heme, and aspartate, respectively), the segments of the cycle involving the formation of these compounds are retained in free-living or facultative organisms (Huynen et al 1999).

Despite the 'central' role of the TCA cycle in aerobic metabolism, the pathogenic lifestyle allows for modifications and 'streamlining' that reduce metabolic flexibility but optimize growth in the adaptive niche. In the extreme case of *Borrelia burgdorferi* (the agent of Lyme disease), the TCA cycle is absent, resulting in obligate pathogenesis (Somerville et al 2003, Cordwell 1999). Incomplete TCA cycles, as for *Yersinia pestis*, result in specific amino acid auxotrophies (Brubaker and Sulen 1971). In other microorganisms, such a *Plasmodium falciparum*, the pathogen may encode for a complete cycle, but still operate it in a branched fashion to meet the constraints of the host environment (Olszewski et al 2010).

- The citric acid cycle of M. tuberculosis

The citric acid cycle of *Mycobacterium* was thought to be complete, but *in vitro* assays failed to detect an alpha-ketoglutarate dehydrogenase (KDH) activity

that converts alpha-ketoglutarate to succinyl-CoA (Tian et al 2005). The activity of an alpha-ketoglutarate decarboxylase (KDC) was proposed to produce a succinic semialdehyde (SSA), which is subsequently converted to succinate via the action of SSA dehydrogenases (SSADH).

However, subsequent assays indicated that the decarboxylase function could be a side reaction of the enzyme, encoded by the apparently essential gene Rv1248c. Assays using the expressed enzyme in a heterologous *M. bovis* BCG extract indicated the formation of hydroxyoxoadipate, formed from alpha-ketoglutarate and glyoxylate, whose significance is still unknown (de Carvalho et al 2010a).

Additionally, an anaerobic-type alpha-ketoglutarate ferredoxin oxidoreductase (KOR) was identified that was able to form succinyl-CoA under ambient atmospheric conditions. This pathway was utilized more during growth on fatty acids and less for use of carbohydrates (Baughn et al 2009).

1.1.4 Alternative carbon sources

In a nutrient-limiting environment, a pathogen may need to rely on alternative, non-sugar carbon sources and utilize the gluconeogenic route described previously for formation of important biosynthetic intermediates. Specific pathways are utilized for metabolizing these substrates in order to derive carbon and energy.

- Beta-oxidation of fatty acids

The bonds forming the hydrocarbon chains of fatty acids are a rich source of energy. The substrate must first be activated via ligation of a CoenzymeA moiety. Acyl-CoA synthetases (*fadD*) perform this step through ATP hydrolysis. The breakdown of these CoA-activated substrates then involves the iterative cycling of reactions that first catalyze oxidation of the acyl chain at the beta-carbon, forming a double bond, with concomitant reduction of FAD^+ via acyl-CoA dehydrogenase (*fadE*). This step is followed by hydration of the double bond by enyl-CoA hydratase (*ech*) and subsequent oxidation of the hydroxyl group to form a keto group, coupled to the reduction of NAD^+ by 3-hydroxyacyl-CoA dehydrogenase (*fadB*). The bond between the keto groups is broken by 3-ketoacyl-CoA thiolase (*fadA*), which adds a CoA group to the end of the truncated chain, releasing a 2-carbon acetyl-CoA unit. (Figure 1.4A)

Repeated cycling of these enzymatic activities results in the fatty acid substrates being sequentially broken down into 2-carbon acetyl-CoA units that can be used for biosynthetic purposes via the citric acid cycle (Clark and Cronan 1996). Odd chain-length fatty acids will produce a terminal 3-carbon propionyl-CoA unit, which must be metabolized via alternative pathways, as described in subsequent chapters, to form intermediates that can be metabolized via the citric acid cycle. (Figure 1.4B)

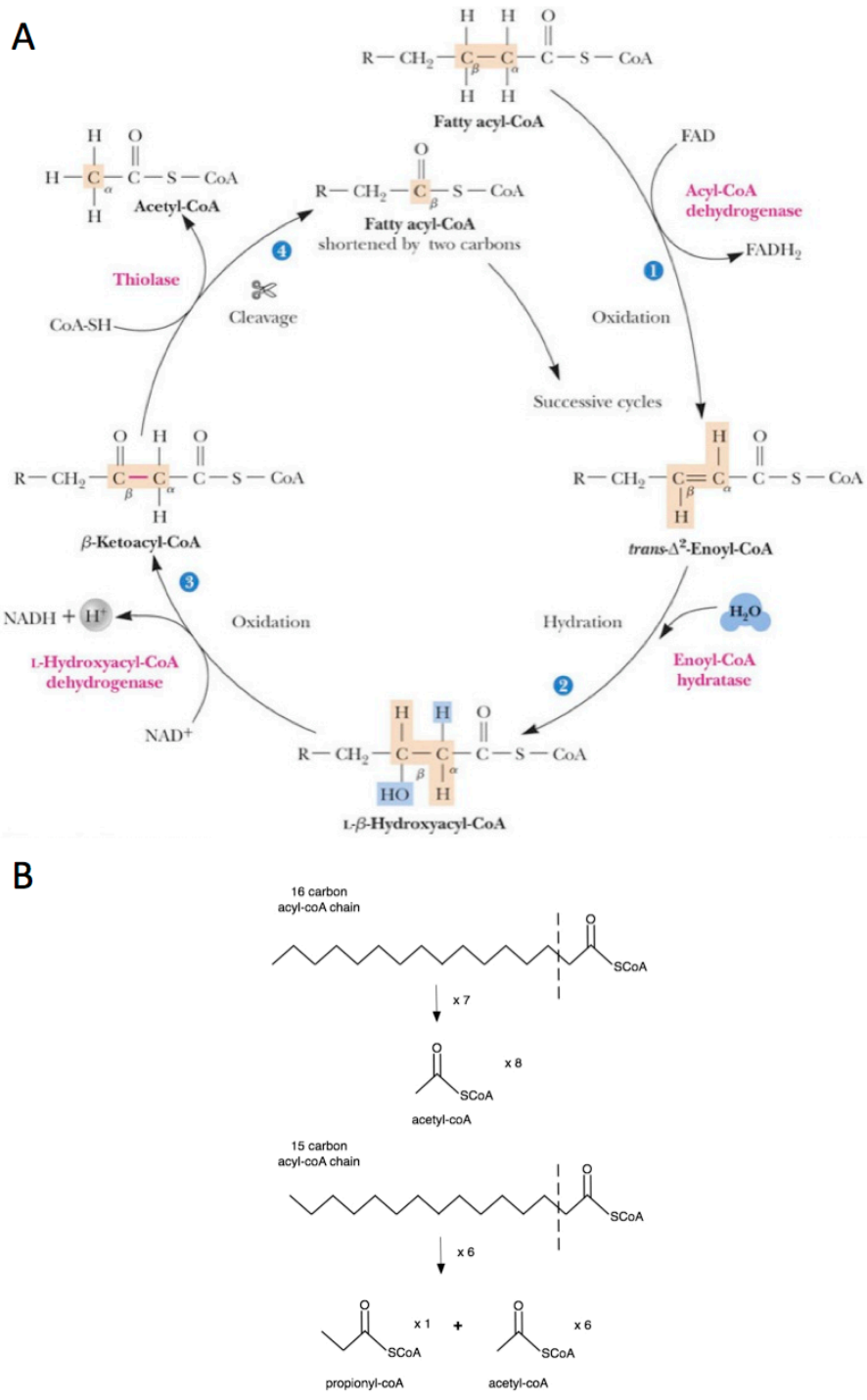

Figure 1.4 A) Beta-oxidation cycle of fatty acids performs iterative breakdown of long acyl-CoA chains into 2-carbon acetyl-CoA units (Campbell and Farrell 2007). B) Even-chain length fatty acids form acetyl-CoA whereas odd-chain length fatty acids produce a terminal propionyl-CoA unit in addition.

- Cholesterol

While the full pathway of cholesterol degradation has not been worked out, it is believed to yield a mixture of acetyl-CoA, propionyl-CoA, and pyruvate. The aliphatic side chain from C17 can be broken down by beta-oxidation to yield an acetyl-CoA and two propionyl-CoA units. The fate of the bicycloalkanone from rings C and D is yet unknown. Enzymatic transformations to cleave the B ring and aromatise and subsequently open the A ring enable the beta-oxidation cleavage to yield pyruvate and a propionyl-CoA unit (van der Geize et al 2007, Griffin et al 2011). (Figure 1.5)

- Amino acids

As well as being formed from TCA cycle intermediates, amino acids can be broken down, using similar pathways, to serve as a carbon source or to replenish the pool of precursors. (Figure 1.6) A few of the routes of amino acid degradation are described here.

Some amino acids are easily deaminated to yield TCA cycle intermediates. In this way, alanine can form pyruvate, and aspartate and asparagine (after hydrolysis to aspartate) can form oxaloacetate, via transamination reactions. Serine forms pyruvate from a dehydratase reaction.

Arginine can be converted to ornithine via arginase, which is, in turn, converted to a glutamate-gamma-semialdehyde that is transaminated to glutamate. Glutamine can also be transformed to glutamate via a glutaminase

reaction. Glutamate can be converted by glutamate dehydrogenase or transaminase to alpha-ketoglutarate.

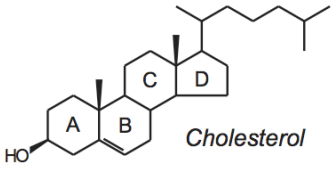

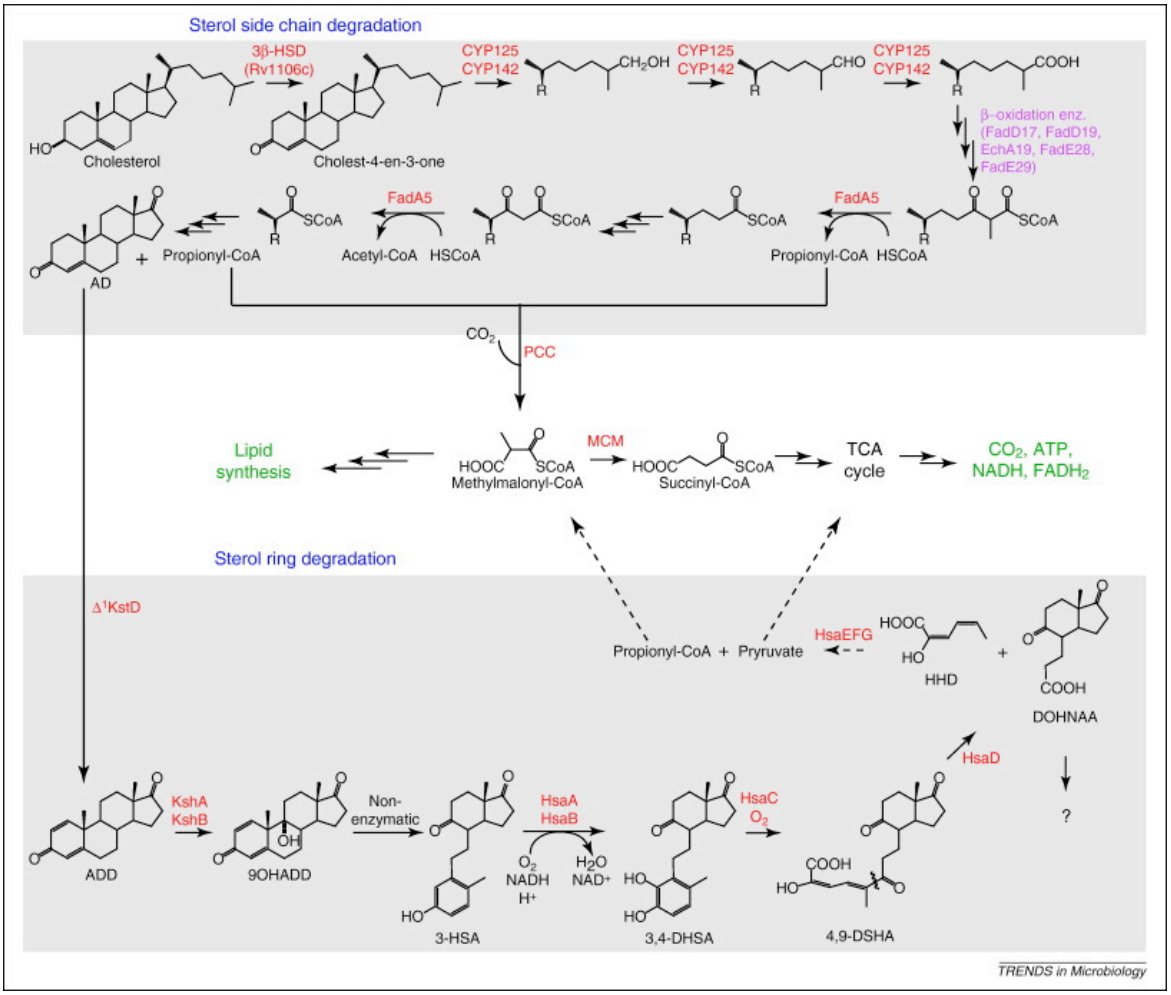

Figure 1.5 Cholesterol degradation pathway, with *M. tuberculosis* proteins in red. Breakdown products include acetyl-CoA, propionyl-CoA, and pyruvate (Ouellet et al 2011).

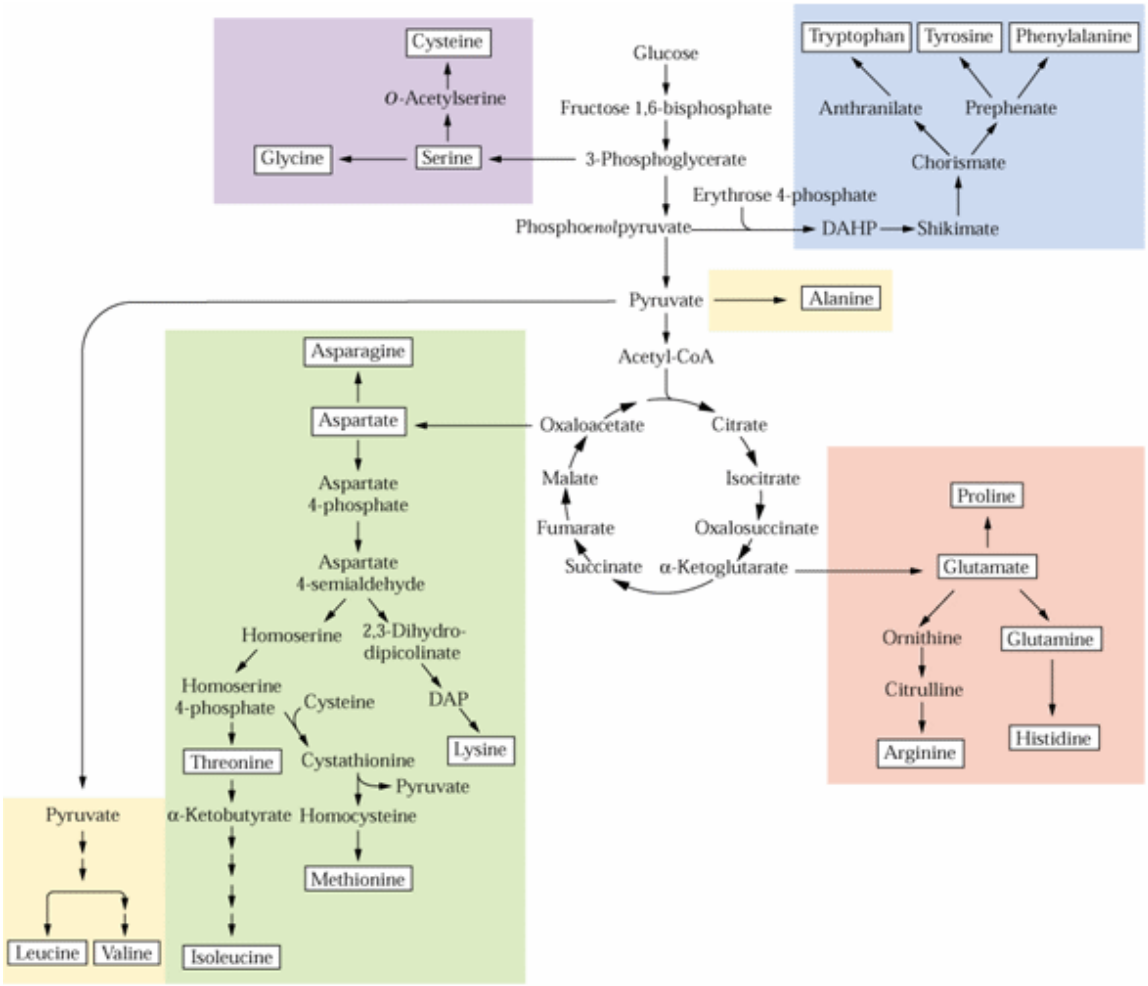

Figure 1.6 Biosynthesis pathways are linked to central carbon metabolism. Amino acids can be formed from sugar and carboxylic acid precursors and serve as precursors themselves for formation of structurally- and chemically- related classes of amino acids (Buchanan et al 2002).

The branched-chain amino acids valine, leucine, and isoleucine undergo the same initial transamination with alpha-ketoglutarate or oxidative deaminative by an amino acid dehydrogenase to yield their respective keto-acids. This is followed by oxidative decarboxylation by the branched-chain alpha-keto acid dehydrogenase (BCKDH) to form their respective acyl-CoA derivatives:

isobutyryl-CoA, isovaleryl-CoA, and 2-methylbutyryl-CoA. An acyl-CoA dehydrogenase forms the methylacrylyl-CoA, tiglyl-CoA, and 3-methylcrotonyl-CoA derivatives. Subsequent independent processing results in the formation of propionyl-CoA from valine, acetyl-CoA from leucine, and both propionyl-CoA and acetyl-CoA from isoleucine (Massey 1976). (Figure 1.7)

Methionine degradation requires a number of steps involving the intermediates S-adenosylmethionine and homocysteine and the subsequent formation of alpha-ketobutyrate and cysteine. An alpha-ketobutyrate dehydrogenase can catalyze the conversion of alpha-ketobutyrate to propionyl-CoA.

A threonine dehydratase forms alpha-ketobutyrate from threonine, which is then oxidatively decarboxylated to form propionyl-CoA (Bell and Turner 1976).

- Anaplerosis

If the citric acid cycle operated solely as a respiratory pathway, the levels of the intermediates would remain balanced. However, whether growth occurs on glycolytic or gluconeogenic carbon sources, citric acid cycle intermediates are withdrawn for biosynthetic purposes (cataplerosis) to form fatty acids, nucleotide bases, porphyrins, hemes, and amino acids. Therefore, for the continued operation of the TCA cycle, these precursors must be replenished by anaplerotic reactions (Kornberg 1965).

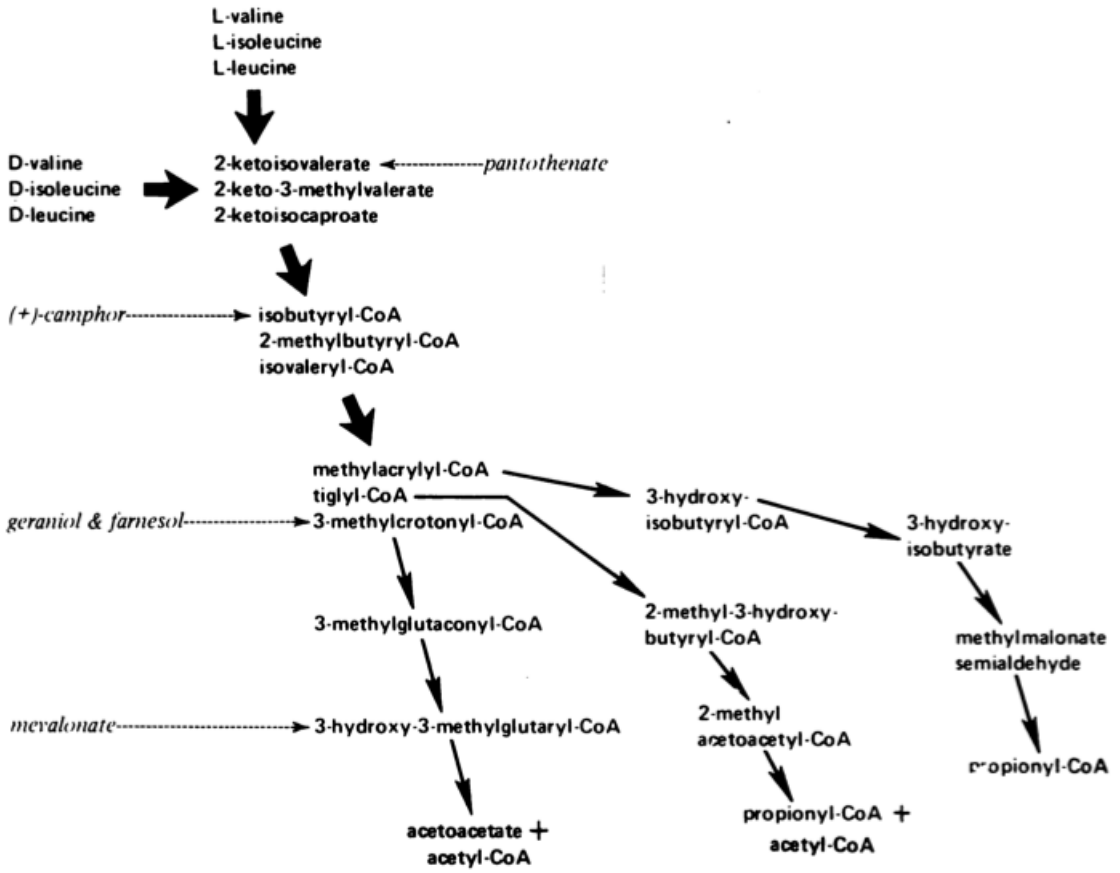

Figure 1.7 Branched-chain amino acid catabolic pathways in bacteria (Massey 1976).

During growth on glucose, carbon anaplerosis can be accomplished by the carbon fixing actions of pyruvate carboxylase (*pyc*) or PEP carboxylase (*pca*) (Kornberg 1965). The PEP carboxykinase (*pck)* reaction can also be run in reverse, albeit inefficiently (Schobert and Bowein 1984).

However, for growth on acetate or fatty acids, the two carbons entering as acetyl-CoA units are lost in the full course of the TCA cycle via the two decarboxylation steps enabling the conversion of isocitrate to alpha-ketoglutarate and subsequent conversion to succinate or succinyl-CoA. Thus, in the absence

of additional sources of carbon, exclusive use of the TCA cycle would result in no net biomass synthesis.

To circumvent this loss of carbon, many organisms that can subsist on fatty acids as the sole carbon source encode a shunt across the TCA cycle to bypass the decarboxylation steps, forming succinate and malate to replenish the key TCA cycle and gluconeogenic intermediates. Carbon anaplerosis via this glyoxylate cycle (GC) is accomplished through the action of two enzymes, isocitrate lyase (ICL) and malate synthase (MLS). (Figure 1.8)

1.1.5 Glyoxylate Cycle

The glyoxylate cycle was originally studied in plants where it plays a role, along with fatty acid beta-oxidation, in the catabolism of stored oils as a carbon source during the germination of seedlings (Kornberg and Beevers 1957). The glyoxylate cycle is also utilized during leaf senescence for the remobilization of carbon sources (Graham et al 1992) and during fruit maturation (Baqui et al 1977). The canonical glyoxylate cycle enzymes from *E. coli* are encoded in the *ace* operon, consisting of malate synthase (MLS - *aceB*), isocitrate lyase (ICL - *aceA*), and the isocitrate dehydrogenase kinase/phosphatase (*aceK*). The AceK kinase/phosphatase controls the flux between the TCA cycle and the glyoxylate cycle by reversibly phosphorylating, and thus inactivating, the gatekeeper enzyme, isocitrate dehydrogenase (ICD). With ICD inactive, ICL is no longer outcompeted for binding to isocitrate and can cleave this substrate to form

glyoxylate and succinate. The glyoxylate can be condensed with another acetyl-CoA unit by MLS to form malate (LaPorte et al 1993, Walsh and Koshland 1985).

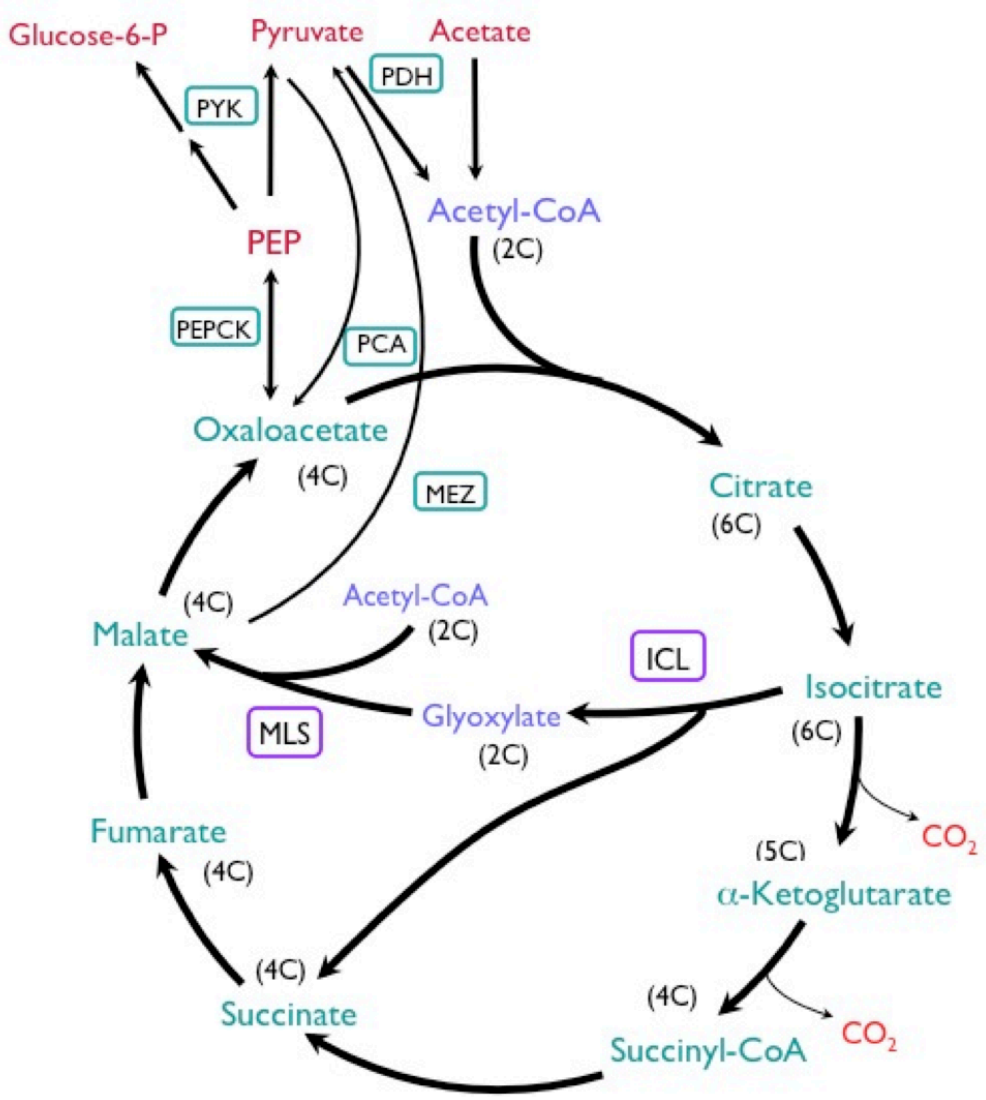

Figure 1.8 Anaplerotic reactions of the TCA cycle. During growth on sugar substrates, carbon can be returned to the TCA cycle through pyruvate carboxylase (PCA) or the PEP carboxykinase (PEPCK) reaction run in reverse. For growth on 2-carbon substrates, the glyoxylate bypass across the TCA cycle avoids loss of carbon from decarboxylation reactions via reactions catalyzed by isocitrate lyase (ICL) and malate synthase (MLS).

- Variations of glyoxylate cycle enzymes

Given the close relationship between the glyoxylate cycle genes, in terms of physical location and coordinate regulation, it is notable that in the nematode *Caenorhabditis elegans* and the unicellular protist *Euglena gracilis*, the ICL and MLS enzyme activities are fused onto a single polypeptide (Liu 1995, Nakazawa et al 2005). In contrast, the genomic loci for ICL and MLS in *Aspergillus nidulans* are unlinked, yet the regulation by carbon source appears coordinate and non-sequential, as an ICL-deficient strain retains MLS activity and *vice versa* (Armitt 1970, Armitt 1971).

Despite defining the 'canonical' glyoxylate cycle, *E. coli* actually encodes two isoforms of malate synthase that are differentially regulated. The type A MLS, encoded by *aceB* and co-located with the ICL-encoding *aceA*, is induced by acetate, whereas the type G MLS, encoded by *glcB*, lies within an operon of genes that are induced by and metabolize glycolate (proceeding via a glyoxylate intermediate) (Molina et al 1994). However, the two MLS enzymes (type A and type G) are able to functionally complement each other in mutants lacking one or the other (Vanderwinkel and de Vlieghere 1968).

The type G MLS has been found in very few organisms, given the wide distribution of the type A MLS across the domains of plants, fungi (and yeasts), and bacteria (Chan and Sim 1998). Besides *E. coli*, *Mycobacterium* spp., *Corynebacterium glutamicum, Pseudomonas aeruginosa*, and *Bacillus halodurans* also encoded the G type MLS by sequence analysis

(Balasubramanian et al 2002). Whereas amino acid similarity between the type A MLS proteins range from ~40% - 98% (with ~40% - 50% across the plant-fungal-bacterial domains), the homology between type A and type G classes shows only 15 - 18% of amino acid sequence similarity. The type G MLSs of *E. coli* and *C. glutamicum* share 59% similarity by amino acid sequence (Chan and Sim 1998).

The budding yeast *Saccharomyces cerevisiae* also encodes two MLS enzymes subject to differential regulation, with MLS1 being carbon responsive and DAL7 being affected by nitrogen metabolism from allantoin degradation (Hartig et al 1992). Both of these enzymes are A type MLS and cluster closely together, phylogenetically, suggesting a chromosomal duplication event (Chan and Sim 1998, Wong and Wolfe 2005).

- The glyoxylate cycle of M. tuberculosis

Mycobacteria encode two isoforms of isocitrate lyase that share only 27% amino acid identity to each other. ICL1 is of bacterial origin whereas the larger ICL2 more closely resembles fungal/eukaryotic ICLs, sharing ~35% amino acid identity, but clustering separately, along with other mycobacterial ICL2s (Munoz-Elias and McKinney 2005). In some strains of *M. tuberculosis*, including the reference strain H37Rv, the *icl2*-coding region has a single nucleotide polymorphism (SNP) that encodes a premature stop codon, thus forming a pseudogene. Assuming there is no read-through based on error-prone

polymerases, these strains would be natural *icl2* mutants. The malate synthase encoded by the *glcB* gene (Rv1837c) is of the more rare G-type. It does not appear to be induced by acetate or any other carbon source that has been tested, aside from a modest (two-fold) induction by glycolate (Smith et al 2003).

In mycobacteria, the genes encoding the enzymes ICL (*icl1*, *icl2*) and MLS (*glcB*) are encoded in separate genomic loci and do not appear to be subject to coordinate regulation. While the RamB regulator of *C. glutamicum* was found to negatively regulate the genes of the *ace* operon and *ack-pta* (Gerstmeier et al 2003), the *M. tuberculosis* homolog (Rv0465c) was found to bind and regulate only the *icl1* gene as well as its own promoter, but was capable of complementing a Δ*ramB* strain of *C. glutamicum* (Micklinghoff et al 2009).

Mutants were generated via marked deletions in the ICL-encoding genes, separately and in combination, in the *M. tuberculosis* Erdman background, denoted as *icl1*::*hyg* and *icl2*::*aph* (Munoz-Elias and McKinney 2005). The *icl1*::*hyg* single mutant and the *icl1::hyg icl2::aph* double mutant were found to have a slight, but reproducible, growth defect in glucose-containing liquid media and a significant 3 week lag to form comparably-sized colonies on plates, relative to wild-type. This suggested some flow of carbon through the glyoxylate bypass during growth on carbohydrate substrates (EJ Munoz-Elias PhD thesis 2005).

The single *icl1*::*hyg* and *icl2::aph* strains were both able to grow on acetate, indicating a degree of functional redundancy for ICL activity, whereas the double mutant was not. The double mutant was also unable to grow on

longer, even-chain fatty acids, consistent with the anaplerotic role of the glyoxylate cycle for this carbon source. The *icl1*::*hyg icl2::aph* strain was additionally unable to grow using propionate, while the single *icl1::hyg* strain showed an attenuated phenotype (Munoz-Elias and McKinney 2005). This result was surprising, as there is not an established role for the glyoxylate cycle for growth on this carbon source. It was subsequently determined that the *icl1* and *icl2* genes of *M. tuberculosis* encoded bifunctional enzymes that also function in the propionate-metabolizing methylcitrate cycle (Munoz-Elias et al 2006), as will be explored later.

The relative importance of the above-described pathways of central carbon metabolism will be looked at in the next section in the context of experimental findings in infection models of *M. tuberculosis*.

1.1.6 Studying the host environment

Acquiring knowledge of the host environment poses a significant challenge given the complex localization of an intracellular pathogen, as *M. tuberculosis* resides within a sub-cellular compartment of human cells, which are further imbedded within the heterogeneous milieu of the granuloma. Some efforts have been made to develop *in vitro* models of granulomas (Peyron et al 2008), to directly assess the metabolic content of lesions (Somashekar et al 2011), to measure the elemental composition of the phagosomes of infected and

uninfected macrophages (Wagner et al 2005), or to detect transcripts *in situ* within lesions (Fenhalls et al 2002).

The pathogen itself can be used as a means of investigating the conditions encountered *in vivo*, by analyzing the transcriptome of bacteria rapidly isolated from macrophage cultures or from infected lungs or by screening for genetic mutants that are attenuated for replication in mice (Schnappinger et al 2003, Camacho et al 1999, Sassetti and Rubin 2003). To confirm and extend these findings, a mutant strain encoding lesions of candidate enzymes or pathways can be tested for the ability to infect, replicate, and persist, with the phenotype taken as the read-out of whether the pathway is required by the pathogen *in vivo*.

1.1.7 Carbon metabolism of Mycobacterium tuberculosis in vivo

- Nutrient limited environment

The aforementioned techniques have been applied to *M. tuberculosis*, whose transcriptome and proteome during *ex vivo* and *in vivo* infection has been used as a 'read-out' to sketch a picture of the intracellular environment. Upregulation of genes involved in fatty acid degradation, gluconeogenesis, iron scavenging, and SOS and DNA damage responses have been found, amongst others (Graham and Clark-Curtiss 1999, Dubnau et al 2002, Schnappinger et al 2003). As *M. tuberculosis* mutants deficient for phosphate transport, pH-dependent magnesium transport, amino acid biosynthesis, or cofactor

biosynthesis are attenuated for growth in macrophages, the scarcity of these nutrients in the phagosome have been inferred (Rengarajan et al 2005, Peirs et al 2005, Buchmeier et al 2000, Appelberg 2006).

- Evidence of fatty acid utilization

In stark contrast to the carbohydrate-rich medium used for *in vitro* culture, the carbon substrates preferentially metabolized by *M. tuberculosis* rapidly extracted from the lungs of infected mice were fatty acids (*n*-heptanoic acid, octanoic acid, and oleic acid) rather than carbohydrates or carboxylic acids (glucose, glycerol, lactate, or pyruvate) (Segal and Bloch 1956). These observations suggested that, *in vivo*, the bacilli are adapted to utilizing fatty acid substrates.

Fatty acids are putatively available to the bacteria within the phagosomal environment of the macrophage, as rat alveolar macrophages were shown to phagocytose and catabolize lung surfactant into free fatty acids and the phagocytic vesicles of rabbit alveolar macrophages showed enrichment of phospholipid (Grabner and Meerbach 1991, Miles et al 1988, Mason et al 1972).

The four phospholipase C genes of *M. tuberculosis*, predicted from whole-genome sequencing and bioinformatics analysis, were found to be jointly required for late-phase growth in the mouse infection model in genetic knockout studies. It was noted that the membrane localization of these apparently non-

secreted enzymes suggests a role for nutrient acquisition rather than host tissue destruction (Wheeler and Ratledge 1992, Raynaud et al 2002).

These findings accord well with the extensive duplication of fatty acid metabolic genes in the genome of *M. tuberculosis* (Cole et al 1998), which may reflect the adaptation of this pathogen for utilizing fatty acid substrates during infection.

- Dispensability of glycolysis

A *de facto* indication of the dispensability of sugar utilization for pathogenesis is found in the genomes of *Mycobacterium bovis* (bovine and human opportunistic pathogen), *Mycobacterium microti* (vole pathogen), and *Mycobacterium africanum* (diverse animal pathogen). All three species 'naturally' contain a SNP in the *pyk* gene encoding pyruvate kinase and are therefore defective in the last step of glycolysis. In the lab, these 'natural' *pyk* mutants require pyruvate supplementation in order to grow on glycerol- or glucose-containing media, yet they remain fully virulent *in vivo* (Keating et al 2005).

- Requirement of gluconeogenesis

As a corollary, a mutant strain generated in *M. bovis* with an insertion in *pckA* encoding PEP carboxykinase, thus interrupting the first committed step of gluconeogenesis, renders the bacillus avirulent in guinea pigs (Collins et al 2002). This finding was extended to *M. tuberculosis* where a deletion of the homologous gene *pckA* (Rv0211) was generated and found to result in a failure of the mutant

strain to survive in murine lungs, with clearance of detectable bacilli before 8 weeks. Moreover, it was shown that 'turning off' this gene, via a doxycycline/tetracycline-inducible copy in the inoculated bacteria, even as late as 6 weeks post-infection, resulted in a sharp decline of the CFU burden, thus validating PEPCK as a potential drug target (Marrero et al 2010). These experiments provided clear evidence that the pathway for generation of sugar intermediates *de novo* was required for survival during infection, suggesting reliance upon alternative, non-glycolytic carbon substrates for this environment.

- Role of cholesterol

Cholesterol appears to be present within the macrophage, specifically accumulating at the site of entry of the pathogen, and may play a role in uptake of mycobacteria (Gatfield and Pieters 2000). Several mutants that were attenuated for intracellular growth (*igr*) mapped to a region (Rv3540c-Rv3545c) previously identified as being upregulated in and required for growth in macrophages and predicted to be required for growth in mice (Chang et al 2007). Although the function of these genes was originally unknown, they were part of a large genomic region (Rv3574-Rv3492c) in *M. tuberculosis* that was largely conserved and homologous to a 58-gene span encoding enzymes involved in cholesterol catabolism in *Rhodococcus* sp. RHA1. This suggested that the locus in *M. tuberculosis* conferred the ability to degrade cholesterol (van der Geize et al 2007).

Mutants defective in the various steps of the cholesterol degradation pathway were generated and tested *in vivo*. Deletion of the *igr* locus attenuates the bacteria for infection in mice by 1-3 $\log_{10}$ CFU until about 10 weeks, by which time the CFU burden of the mutant catches up. (Chang et al 2009) A mutant in the *fadA5*-encoded thiolase (Rv3546), involved in beta-oxidation of the sterol side chain, was found to replicate like wild-type during the initial phases of infection of mice, followed by a decline after the onset of cellular immunity, known as a 'persistence' defect (Nesbitt et al 2010).

A *choD* (Rv3409c) deficient strain, missing the putative cholesterol oxidase responsible for activation of cholesterol, was without an *in vitro* defect, perhaps due to a redundant enzyme activity; however, this strain exhibited a reduced CFU burden in mouse lungs at a single timepoint (Brzostek et al 2007). A mutation of the Rv1106 gene encoding the hypothesized redundant activity did abrogate the ability to use cholesterol *in vitro*, but did not have a phenotype *in vivo* (Yang et al 2011).

The *kshAB*-encoded (Rv3526, Rv3571) two-component oxygenase enzyme is responsible for the hydroxylation reaction leading to the B ring opening and A ring aromatization. In the mouse infection model, the Δ*kshA* and Δ*kshB* strains exhibited a progressive 3-4 $\log_{10}$ loss of CFU over the course of 13 weeks (Hu et al 2010).

A mutation of the *hsaC* (Rv3568c)-encoded dioxygenase responsible for cleavage of the A ring exhibited catechol-intermediate toxicity *in vitro* and

exhibited a modest growth defect in guinea pig lungs and spleen (Yam et al 2009).

Three cytochrome P450 enzymes of *M. tuberculosis* (CYP125, CYP142, and CYP124) were all capable of catalyzing the three sequential oxidation steps *in vitro* that functionalize the sterol side chain before it can be activated to enter the beta-oxidation cycle. Although the different enzymes catalyze different stereospecificities of the products, functional redundancy was seen *in vitro*. Partial complementation resulted in toxicity from cholest-4-en-3-one (Johnston et al 2010).

- Role of amino acids

An *M. tuberculosis* strain lacking a lipoamide dehydrogenase (Δ*lpdC*), a shared component of the pyruvate dehydrogenase (PDH), peroxynitrite reductatse/peroxidase (PNR/P), and the branched-chain keto acid dehydrogenase (BCKADH), was rapidly cleared from the lungs of mice before 1 week post-infection (Venugopal et al 2011). This phenotype was more dramatic than that of a strain lacking dihydrolipoamide acyltransferase (Δ*dlaT*), which is a shared component of the PDH and PNR/P only. Thus, a role for branched chain amino acids as a carbon source in the lung is plausible. This phenotype was somewhat recapitulated by the double deletion of Δ*dlaT* Δ*pdhC*, which additionally eliminates the function of the BCKADH in the PDH- and PNR/P-deficient background. Although the Δ*dlaT* Δ*pdhC* double mutant was not completely cleared from the lungs it was more attenuated than the Δ*dlaT* single

knockout. However, the Δ*pdhC* knockout alone did not cause a phenotype, so branched-chain amino acid metabolism appears to be individually dispensable for growth *in vivo*.

- Role of the glyoxylate cycle

Upregulation of the *icl1* transcript during macrophage infection, in the mouse infection model, and in samples of human tuberculous lesions strongly suggested the importance of this pathway *in vivo* (Graham and Clark-Curtiss 1999, Dubnau et al 2002, Schnappinger et al 2003, Timm et al 2003). An *icl1::hyg icl2*::*aph* strain was attenuated for survival in resting and activated macrophages, and in intravenously infected mice the *icl1::hyg icl2*::*aph* strain was cleared from the lungs in less than four weeks post-infection (Munoz-Elias and McKinney 2005). These experiment were intended to investigate the requirement of the glyoxylate cycle, and thus the need for anaplerosis during growth on C2-forming compounds, during the course of infection. However, this simple interpretation was subsequently cast into doubt by the discovery that the enzymes encoded by *icl1* and *icl2* are bifunctional and participate in both the glyoxylate cycle (as isocitrate lyases) as well as the methylcitrate cycle (as methylisocitrate lyases), a pathway for catabolism of propionate (Munoz-Elias et al 2006).

1.1.8 Role of the glyoxylate cycle in pathogenesis

The role of the glyoxylate cycle was subsequently studied in other pathogens and demonstrated to be required for virulence in several cases, including the opportunistic fungal pathogen *Candida albicans* (Lorenz and Fink 2001), the livestock pathogen *Rhodococcus equi* (Wall et al 2005), and the phytopathogenic fungi *Leptosphaeria maculans* (Idnurm and Howlett 2002) and *Magnaporthe grisea* (Lee et al 2007).

However, there are also examples where ICL was not found to play an essential role in pathogenesis, as in *Salmonella enteria* serovar Typhimurium, where ICL-deficiency only seemed to have a minor role in persistence (Kim et al 2006). Similarly, an ICL-deficient strain of the filamentous fungal pathogen *Aspergillus fumigatus* did not differ in virulence from wild-type (Schobel et al 2007). Although the *Cryptococcus neoformans icl* transcript was upregulated in a rabbit meningitis model, an ICL-deficient strain showed no phenotype in macrophages and perhaps only an early and modest defect in one of two animal infection models (Rude 2002).

There have been fewer studies examining the role of the second enzyme of the glyoxylate pathway, malate synthase. In the phytopathogenic fungus *Stagonospora nodorum*, the apparent role of MLS for pathogenesis was actually due to the requirement of the glyoxylate shunt for germination. When tested in infection assays that did not involve germination, the MLS-deficient strain had comparable virulence to wild-type. The requirement for the glyoxylate cycle for

germination may have contributed to the 'virulence' defect of an ICL-deficient strain of *L. maculans* (Solomon et al 2004). Consistent with the finding of Schobel *et al*., an MLS-deficient strain of *A. fumigatus* also retained full virulence (Olivas et al 2008).

However, in the phytopathogenic *Rhodococcus fascians*, a mutation causing attenuated virulence was mapped to a gene encoding an MLS with high identity to the type G MLS enzymes of *Pseudomonas fluorescens* (72%), *M. tuberculosis* (66%), *M. leprae* (66%), *C. glutamicum* (60%), and *E. coli* (55%). The mutant strain accumulated glyoxylate to levels that appeared to be growth inhibitory. Although behaving like a glyoxylate shunt enzyme on acetate, the MLS was also induced by leafy gall extracts (Vereecke et al 2002a, Vereecke et al 2002b).

Notably, the *R. fascians* gene encoding MLS was unlinked to the genomic location of the gene encoding ICL and, moreover, was located in a region syntenic to that of *M. tuberculosis* and *M. leprae*, including the genes of the glycine cleavage system (gcv), which encode the enzymes responsible for the oxidative decarboxylation of glycine to glyoxylate. Interestingly, a *R. fascians* mutant of the glycine dehydrogenase P (GDH-P) homolog displayed reduced virulence. While the *gcvP* gene was not transcribed when glycine was provided as the sole nitrogen source (as in *E. coli* and *S. cerevisiae*), the expression was induced by plant gall extracts, similar to MLS (Vereecke et al 2002b).

- Non-glyoxylate cycle functions of MLS?

Given the conserved nature of the genomic location of a type G MLS with glycine-metabolizing region of the genome, it is tempting to speculate that the MLS could be acting in a second pathway. Atypical functions of the MLS of *M. tuberculosis* are further suggested by the production of antibodies against the protein in the sera of tuberculosis patients, its presence in culture filtrate (Sonnenberg and Belisle 1997, Laal et al 1997, Samanich et al 2001), and its reported extracellular localization (Kinhikar et al 2006). Some indications of an alternative or additional function for the *M. tuberculosis* MLS stem from a report of an adhesin-like domain at the C-terminus of the enzyme that is not conserved in MLS enzymes in other mycobacteria (Kinhikar et al 2006). This appears to also be the case for the MLS of the pulmonary fungal pathogen *Paracoccidioides brasiliensis (*da Silva Neto et al 2009). While secondary or 'moonlighting' functions for metabolic enzymes have been reported (Huberts and van der Klei 2010), and a laminin-binding function has been suggested for another metabolic enzyme of *M. tuberculosis*, the fructose-1,6-bisphosphatase (de la Paz Santangelo 2011), the evidence from *in vitro* binding assays needs to be supplemented with specific domain deletions that are tested *in vivo* in comparison to catalytic site mutations that impair enzymatic activity while leaving the putative adhesin domain intact.

- Non-glyoxylate cycle functions of ICL?

The bifunctionality of the ICL enzyme in a propionate metabolic pathway has already been alluded to, but another MLS-independent role for ICL has been known to exist in the serine pathway of bacterial species that are capable of growth on one-carbon substrates, such as methanol and methylamine (Anthony 2011).

There is also the possibility that another enzyme, rather than MLS, plays the dominant role in metabolizing ICL-produced glyoxylate. This hypothesis stems from the observation of coordinately high levels of induction of both ICL activity and glycine dehydrogenase (GDH) activity in *M. tuberculosis* during microaerophilic growth (Wayne and Lin 1982). The ICL activity could function to generating glyoxylate for subsequent reduction by GDH, thereby regenerating the oxidized NAD^+ pool during hypoxic conditions. A gene knockout-based study of this activity in *M. tuberculosis* is complicated by the presence of three putative genes encoding this functionality and the predicted essentiality of the most likely candidate, *gcv* (Rv1832) (Cole et al 1998, Wayne and Sohaskey 2001, Sassetti et al 2003).

- Uncoupling the ICL/MCL bifunctionality

The key to understanding the underpinnings of the inability of an ICL/MCL mutant to survive *in vivo* lies in being able to distinguish between the two functional roles of the enzymes in the glyoxylate cycle (ICL) and methylcitrate

cycle (MCL). In effect, the relative contribution of the two pathways that converge at the ICL/MCL enzymes must be tested independently.

To independently interrogate the requirement of the glyoxylate cycle in pathogenesis, the *in vivo* role of the second enzyme of the pathway, MLS, could be tested. However, previous and ongoing efforts have indicated its likely essentiality (E.J. Munoz-Elias PhD thesis, 2005; N. Dhar, personal communication; S. Ehrt, personal communication; Griffin et al 2011). As the glyoxylate cycle is not expected to be essential for growth on glucose, this poses an intriguing but confounding factor. MLS may be required to avoid the accumulation of gloxylate, which may be toxic to the cell; testing this hypothesis will require the use of a mutant strain that is engineered to conditionally express MLS.

To independently interrogate the requirement of the of the methylcitrate cycle in pathogenesis, a separate, independent lesion should be made in this route. This is the approach that was taken previously by the lab, and the results are discussed in the next section.

1.2 Methylcitrate cycle

1.2.1 Propionate

Propionic acid and other short-chain fatty acids are predominant in the soil (Chin & Conrad 1995) as well as in the gut (Cummings et al 1987), where they are formed as by-products of fermentative bacteria, and then oxidized by other commensal bacteria.

Propionate is also of interest in the food production industry for its historically known anti-bacterial and anti-fungal properties, and its consequent use as a preservative (Salmond et al 1984).

For its use as a growth substrate, propionate must first get activated by the addition of a Coenzyme A group via thioesterification, as will be described subsequently. Propionyl-CoA can also be derived from the breakdown of odd-chain length fatty acids (Clark & Cronan 1996), the breakdown of the amino acids valine, isoleucine, methionine, and threonine (Hesslinger et al 1998), the catabolism of the cholesterol side chain (Griffin et al 2012), and the aerobic and anaerobic degradation of 1,2-propanediol (a product of rhamnose and fucose fermentation in the gut) (Obradors et al 1988, Baldoma et al 1988, Bobik et al 1999).

A number of pathways of metabolism have been proposed, based on the possible transformations of the different carbon positions of the common precursor, propionyl-CoA (Wegener et al 1968, Textor et al 1997). (Figure 1.9A) While the dehydrogenation to acryloyl-CoA, subsequent beta-hydration to 3-

hydroxypropionyl-CoA, and reductive carboxylation to 2-oxobutyrate has been reported for certain organisms, these pathways are utilized in the direction of formation of propionate, rather than breakdown (Eisenreich et al 1993, Tholozan et al 1990, Vagelos and Earl 1959).

Despite a number of reports indicating the function of an acrylate pathway in organisms such as *Escherichia coli* (*E. coli*), *Salmonella enterica* serovar Typhimurium (*S.* Typhimurium), and *Pseudomonas aeruginosa* (*P. aeruginosa*), the labeling experiments were found not to distinguish between the operation of the acrylate and methylcitrate pathways (Bramer et al 2002). The oxidation of propionate is now thought to proceed in bacteria and fungi via the methylcitrate cycle and in a wide distribution of organisms via the methylmalonyl-CoA pathway.

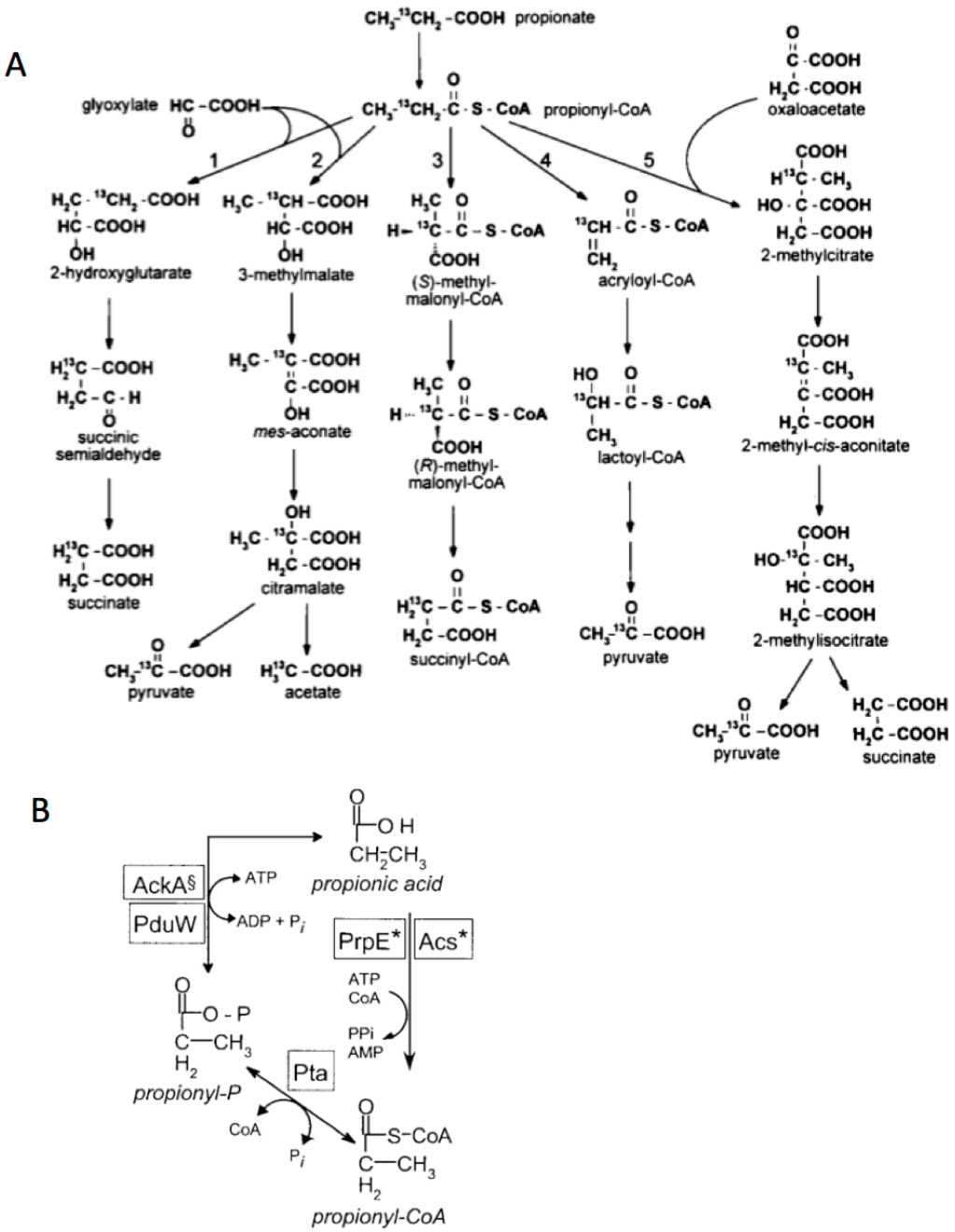

Figure 1.9 A) Proposed routes of propionate breakdown: 1: alpha-hydroxyglutarate, 2: citramalate, 3: methylmalonyl-CoA, 4: acryloyl-CoA, 5: 2-methylcitric acid cycle (Horswill and Escalante-Semerena 1999a). B) Routes for propionate activation in *S.* Typhimurium: acetate kinase (AckA), propionate kinase (PduW), phosphotransacetylase (Pta), propionyl-CoA synthetase (PrpE), acetyl-CoA synthetase (Acs) (Palacios et al 2003).

- Propionate activation to propionyl-CoA

As for acetate conversion to acetyl-CoA, propionate must be activated to propionyl-CoA before it can be utilized in cellular processes. One route, used by acetyl-CoA synthetases (Acs) and propionyl-CoA synthetases (Pcs or PrpE), ligates a Coenzyme A, coupled to ATP cleavage to AMP. A second pathway invokes two proteins, an acetate or propionate kinase (Ack, Pck) and a phosphotransacetylase (Pta), in a sequential reaction of phosphorylation of the fatty acid followed by the transfer of the acetyl- or propionyl- group to Coenzyme A (Chou and Lipmann 1952, Lipmann 1944). Acetyl-CoA and propionyl-CoA may also be formed by a CoA transferase reaction from a Coenzyme A donor to an acetate or propionate acceptor (Heider 2001, Fleck and Brock 2008, Veit et al 2009).

Although dedicated propionate-activating enzymes exist, the substrate specificities of ACS and ACK-PTA enzymes have been known to be 'relaxed' and accept propionate as a substrate. *S.* Typhimurium encodes *ack*, *pta*, *acs* and *prpE* as well as propionate kinases *pduW* and *tdcD*. Unsurprisingly, significant redundancy was seen in knockout mutants (Palacios et al 2003). (Figure 1.9B) Similar overlapping functionality is seen for systems of propionate activation in *E. coli* (Hesslinger et al 1998). *Corynebacterium glutamicum* (*C. glutamicum*) has an ACK-PTA system that utilizes both acetate and propionate as substrates, but is reported not to have an acetyl- or propionyl-CoA synthetase enzyme. However,

this organism possesses a *cat*-encoded CoA transferase that can activate acetate and propionate in the absence of the alternative system (Veit et al 2009).

1.2.2 Methylcitrate cycle

The methylcitrate cycle was first biochemically elucidated in the yeast *Candida* (formerly *Yarrowia*) *lipolytica*, where propionyl-CoA was metabolized to pyruvate and succinate via a set of reactions analogous to those of acetyl-CoA by the glyoxylate cycle. The first step involves the hydrolytic condensation of a propionyl-CoA with oxaloacetate by a methylcitrate synthase (MCS), forming methylcitrate. An isomerization reaction converts methylcitrate to 2-methylisocitrate via a cis-2-methylaconitate intermediate. This step is carried out by the sequential action of a methylcitrate dehydratase (MCD) followed by hydration by an aconitase (ACN). Methylisocitrate is then cleaved by a methylisocitrate lyase (MCL) to produce pyruvate and succinate. The net result is that of the alpha-oxidation of propionate to pyruvate, as succinate re-forms oxaloacetate via the TCA cycle (Tabuchi and Serizawa 1975). (Figure 1.10) As the hydrolysis involved in methylcitrate synthesis is irreversible, this pathway cannot be used for propionate formation (Brock et al 2000).

The genetic basis of this pathway was first identified in *S.* Typhimurium from a mutant strain (*prp*) impaired in propionate metabolism (Hammelman et al 1996). Using genomic mapping, the lesion was localized to two divergent transcriptional units (Horswill and Escalante-Semerena 1997). By homology, a cluster of corresponding genes was identified in *E. coli* (Textor et al 1997).

- prp operon

The genomic region identified in *S.* Typhimurium featured an upstream, divergently-transcribed *prpR* gene, with homology to transcriptional activators of the sigma-45 (RpoN) family. This was designated as the activator of the genes contained within the adjacent *prp* locus. The 264 bp intergenic region separating the transcriptional units was found to contain a consensus binding site for RpoN. Consistent with this, an *rpoN* mutant strain was unable to grow on propionate (Horswill and Escalante-Semerena 1997). (Figure 1.10)

As no internal promoters were identified in the short gaps between the *prpB*, *prpC*, *prpD*, and *prpE* open reading frames, and complementation of single insertion mutants required all the genes (implying polar effects), the *prpBCDE* genes were found to constitute an operon (Horswill and Escalante-Semerena 1997). (Figure 1.10)

Although meaningful homology was difficult to establish at the time for this 'novel' set of genes given the paucity of sequenced organisms, subsequent biochemical studies of the individual mutants with labeled propionate enabled identification of their respective roles. A mutant was not found in *prpE*, as it encodes a propionyl-CoA synthetase (PCS), whose function was found to be redundant with other encoded enzymatic activities, as explained earlier (Horswill and Escalante-Semerena 1999b). *prpC*, homologous to citrate synthases, encoded the methylcitrate synthase (MCS) activity.

prpD, which showed homology only to proteins of unknown function, was found to carry out only the dehydration of 2-methylcitrate to form 2-methyl-cis-aconitate, and thus acted as a methylcitrate dehydratase (MCD). The activity to carry out the hydration of this intermediate to 2-methylisocitrate was determined to be encoded outside of the operon (Horswill and Escalante-Semerena 1997, Horswill and Escalante-Semerena 1999a). It was subsequently found that this aconitase-like reaction was, in fact, carried out by one of the aconitase (ACN) enzymes (encoded by *acnA* or *acnB*) of the TCA cycle (Horswill and Escalante-Semerena 2001). *prpB*, was found to encode the methylisocitrate lyase activity (MCL) (Horswill and Escalante-Semerena 1999a, Grimek et al 2003).

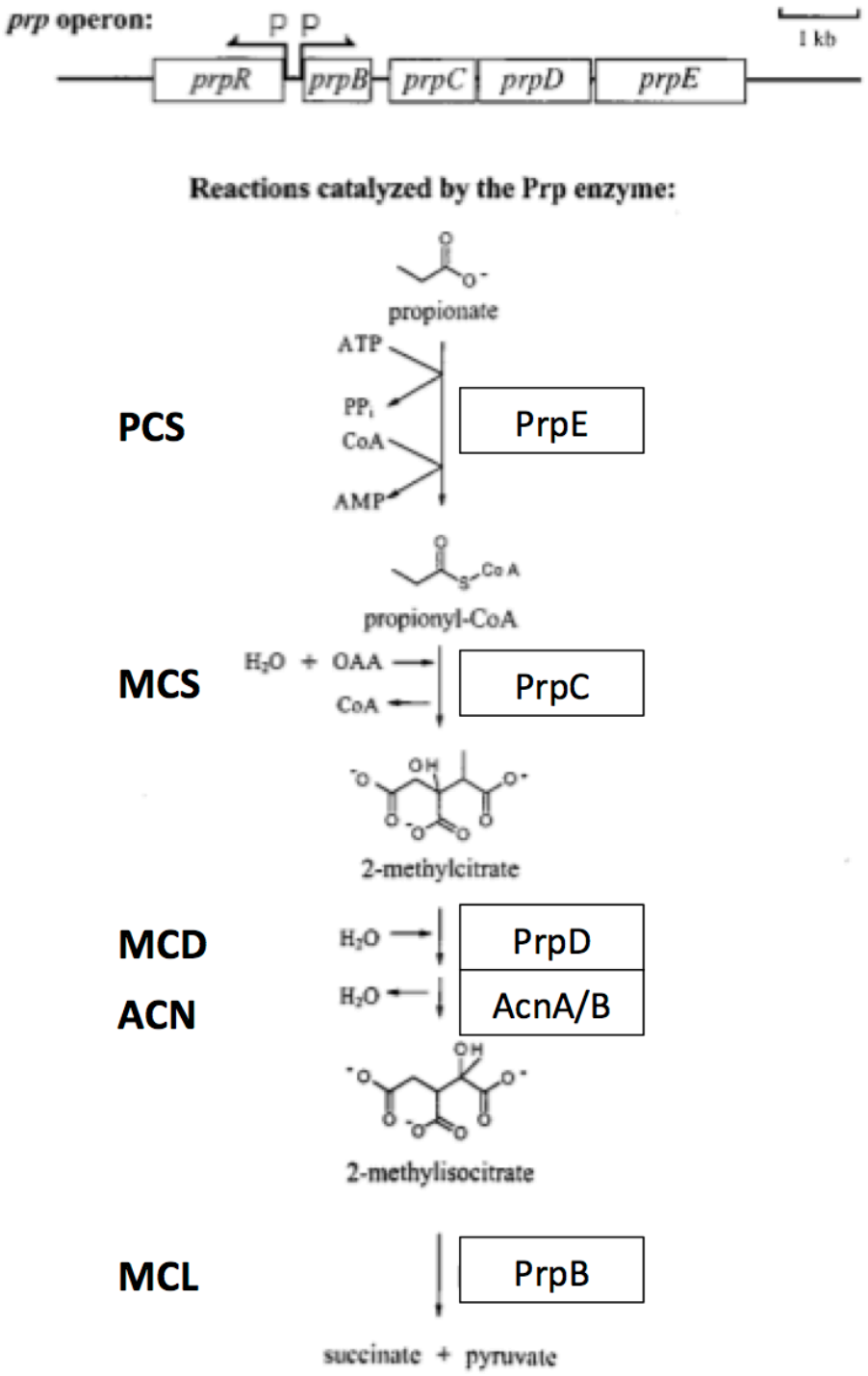

Figure 1.10 Genomic locus of *prp* operon in *S.* Typhimurium and reactions of the methylcitrate cycle. PrpE: propionyl-CoA synthetase (PCS), PrpC: methylcitrate synthase (MCS), PrpD: methylcitrate dehydratase (MCD), AcnA/B: aconitase (ACN), PrpB: methylisocitrate lyase (MCL) (Tsang et al 1998).

The *prp* locus in *E. coli* is syntenic to that in *S.* Typhimurium, with the exception of a region between *prpB* and *prpC* in *E. coli* (Textor et al 1997). Rather than being an ORF, as originally described, Horswill and Escalante-Semerena noted that the increased 'gap' in *E. coli* actually corresponded to four 91-bp repeats, perhaps indicative of genomic rearrangements of the locus. This difference between the operons of the two organisms could affect the relative expression levels of the genes, and thus be responsible for the long lag phase in *E. coli* on propionate (Horswill and Escalante-Semerena 1999a).

- Alternative operon arrangement

Unlike *S.* Typhimurium and *E. coli*, other bacteria seem to encode within their *prp* operons genes homologous to those for aconitate hydratases, but clustering distinctly from the TCA cycle enzymes by phylogeny (Bramer and Steinbuchel 2001). One gene bears homology to the *acnA* of *S.* Typhimurium, and is denoted as *acnD* (elsewhere, *acnM*), whereas the other was denoted *prpF* (previously *ybhH* or ORF5) (Horswill and Escalante-Semerena 2001, Bramer and Steinbuchel 2001, Grimek and Escalante-Semerena 2004). These variations are diagrammed in Figure 1.11.

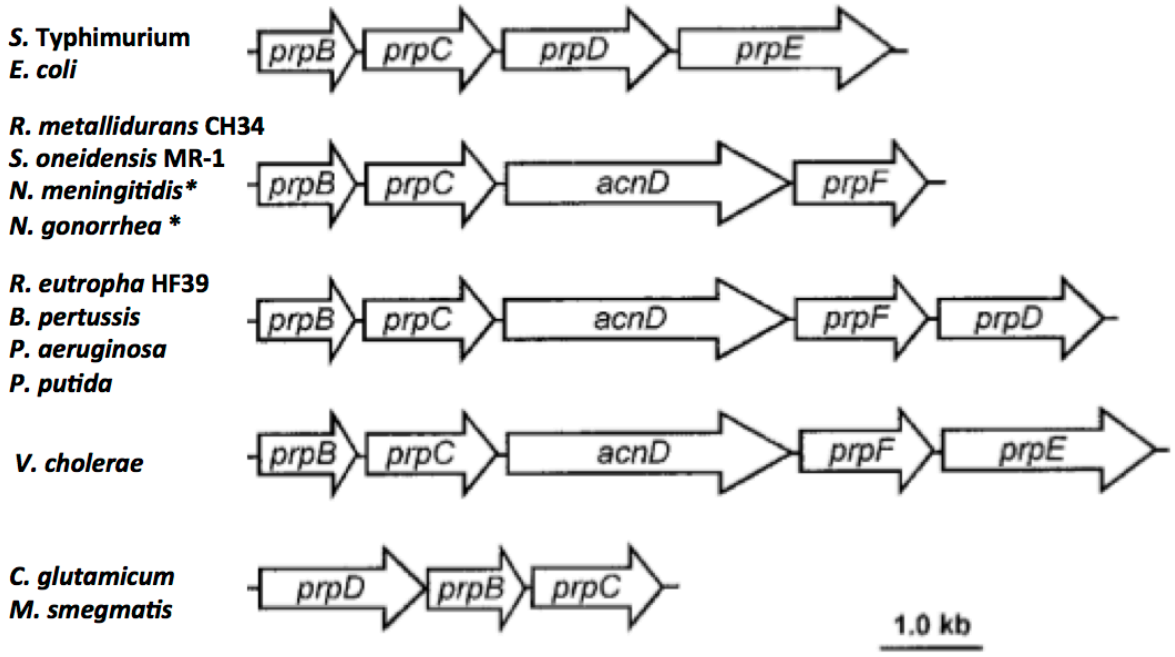

Figure 1.11 Comparison of genomic loci of *prp* operons in different species. prpR: transcriptional regulator, prpB: methylisocitrate lyase, prpC; methylcitrate synthase, prpD: methylcitrate dehydratase, prpE: propionyl-CoA synthetase, acnD: aconitase, prpF: unknown, ackA: acetate kinase – homologous to *E. coli tdcD*, strains marked with an asterisk (*) contain a 789 bp ORF in between *prpC* and *acnD* (Grimek and Escalante-Semerena 2004).

Shewanella oneidensis, *Burkholderia sacchari*, and *Ralstonia metallidurans* (formerly *eutropha*) CH34 encode a *prp* operon with an *acnD* and *prpF* in place of *prpD*, and lack a *prpE* (Bramer and Steinbuchel 2001, Grimek and Escalante-Semerena 2004).

R. eutropha HF39, *Bordetella pertussis*, *Pseudomonas aeruginosa*, and *Pseudomonas putida* have operons resembling the first type, but with the addition of a *prpD* homolog (Grimek and Escalante-Semerena 2004). As a further

variation, a second putative acnD homolog is downstream of, but divergently transcribed from, the *prp* locus of *P. putida* (Bramer and Steinbuchel 2001).

Neisseria spp. have similarly arranged operons to the first type, but with a 789 bp ORF between *prpC* and *prpD* and downstream of *prpF*, a 1200 bp ORF homologous to the *E. coli tdcD*-encoded propionate kinase (Grimek and Escalante-Semerena 2004).

prpR homologs were not identified in *R. metallidurans* CH34 or in *N. meningitidis*, but were found to be transcribed collinearly in the two pseudomonads. The *prp* operon in *Vibrio cholerae* thus appears to be intermediate in these variations, with a collinear *prpR*, an *acnD* and *prpF*, and still retaining a *prpE* (Bramer and Steinbuchel 2001).

A bioinformatics search of the pathogenic *Burkholderia pseudomallei* genome indicated another variation of the *prp* operon structure, with divergently-transcribed *prpR* and *prpB prpC acnD prpF* in one locus and *prpD acnA* genes in a second operon located elsewhere on the same chromosome, both lacking a specific *prpE* (P. Nichayapun M.Sc. thesis, 2005).

Bacillus subtilis has a reduced and rearranged operon structure of *prpCDB*. *Corynebacterium glutamicum*, a close relative to *Mycobacterium tuberculosis* encodes a *prpDBC* arrangement (that has been duplicated) with a regulator that is located downstream of the apparently 'non-functional' duplicated locus (Claes et al 2002, Plassmeier et al 2011). This will be described further in a subsequent section. Pathogens *Corynebacterium diphtheriae* and *Mycobacterium leprae* do

not appear to encode any *prp* homologs (Claes et al 2002). The function of these phylogenetically-distinct aconitase enzymes was investigated further.

- PrpD vs. AcnD/PrpF vs. AcnA/AcnB

The *acnA* and *acnB* genes of *S.* Typhimurium exhibited some overlapping ability to function as methyl-cis-aconitate hydratases, with Δ*acnB* showing a more severe defect, requiring glutamate for growth on propionate. Although the authors concluded that AcnB played a dominant role on propionate (Horswill and Escalante-Semerena 2001), it may be a consequence of the dominant role of AcnB for functioning in the TCA cycle. The double Δ*acnA* Δ*acnB* strain was unable to grow on propionate, with or without glutamate, aerobically or anaerobically, indicating there was no other source of hydratase activity (Horswill and Escalante-Semerena 2001).

The *acnD* and *prpF* genes from both *S. oneidensis* and *V. cholerae* were able to complement a Δ*prpD* strain of *S.* Typhimurium, during aerobic and anaerobic growth on propionate, but only when provided jointly. Both cross-species pairs were functional as well. The *E. coli* YbhJ (with 22% identity and 37% similarity to *S. oneidensis* AcnD) and YbhH (34% identity and 47% similarity with *V. cholerae* PrpF) were unable to complement the *S.* Typhimurium *prpD* mutant, whether provided together (*ybhHIJ*) or in combinations with the *S. oneidensis* and *V. cholerae* enzymes. Neither the *acnD* / *prpF* nor *ybhJ* / *ybhH* gene pairs were able to functionally complement an Δ*acnA* Δ*acnB* stain of *S.*

Typhimurium grown on pyruvate, indicating that the encoded enzymes could not act as aconitases in the TCA cycle (Grimek and Escalante-Semerena 2004).

A Δ*prpD* of *R. eutropha* HF39 did not accumulate 2-methylcitrate or show any phenotype (Bramer and Steinbuchel 2001). Unlike *prpD*, *acnD* of *S. oneidensis* encodes a protein with Fe-S clusters, similar to those in aconitase enzymes, but still was only able to catalyze the first, dehydratase step of the reaction, after anoxic reactivation (Grimek and Escalante-Semerena 2004). PrpF failed to show hydratase or dehydratase activity with any of the tested substrates in oxic or anoxic conditions. Although exhibiting weak homology (~24% amino acid similarity) to the *pduG*-encoded diol dehydratase reactivation factor of *S.* Typhimurium, PrpF did not improve the kinetics when added to reactions with AcnA (Bramer and Steinbuchel, 2001, Grimek and Escalante-Semerena 2004). Thus, while required for 2-methylcitrate dehydratase activity, the precise functional role of PrpF is unknown.

Despite lacking sequence similarities, the MCD enzymes of *S.* Typhimurium and *C. lipolytica* were similar to class II fumarase enzymes in having dehydratase activities in the absence of metal cations, reducing agents, or Fe-S clusters. In contrast, Class I fumarases do contain Fe-S clusters. The existence of multiple aconitase and fumarase systems and the presence of both *acnD* / *prpF* and *prpD* in the *prp* operons of several bacteria (*R. eutropha*, *B. pertussis*, and *Pseudomonas* spp.), could imply that the flexibility of having both

Fe/S-dependent and independent metabolic routes is advantageous (Horswill and Escalante-Semerena 2001, Grimek and Escalante-Semerena 2004).

- prp loci in C. glutamicum

Corynebacterium glutamicum, a soil-dwelling bacterium in the same sub-order of Actinomycetes as *M. tuberculosis*, presents a much reduced *prp* operon structure with a shuffled gene order with respect to *S.* Typhimurium, consisting of *prpDBC*, found in two distinct clusters in the genome. Separated by ~38 kbp, the surrounding regions do not share homology between each other and neither encodes a *prpE* or *acnD* / *prpF*. The paralogs from the two clusters, termed *prpD1B1C1* and *prpD2B2C2* exhibit between 70-75% identity on the nucleotide level and 73%-80% identity of amino acid sequence, indicating a gene duplication event followed by some diversification. Compared to the corresponding genes from *S.* Typhimurium, *C. glutamicum* shares ~26%, ~42%, and ~40% amino acid identity to *prpD*, *prpB*, and *prpC*, respectively. In absence of a PrpE, the activation of propionate is expected to occur via the ACK-PTA system, as ACS was not previously detected nor encoded in the genome (Claes et al 2002, Reinscheid et al 1999).

Growth upon propionate as the sole carbon source caused a 5 to 7 day lag, compared to growth on glucose or acetate. Propionate had a dominant effect even in the presence of glucose, although the lag was reduced to ~36 hr, while growth on acetate was only slightly affected by the presence of propionate.

Growth was monophasic on all mixtures, indicating co-utilization of the substrates (Claes et al 2002).

By a 2D PAGE analysis, all six spots that differed prominently between propionate and acetate grown cultures were assigned by mass spectrometry to the *prpD2B2C2* cluster, with each protein being represented by two spots, suggestive of posttranslational modifications. By mutational analysis, none of the individual or combined deletions in the *prpD1B1C1* operon had an effect for growth on propionate, whereas all individual deletions in the *prpD2B2C2* cluster abrogated growth. This indicated the requirement of the *prp2* gene cluster and the dispensability of the *prp1* locus for propionate growth under the conditions tested (Claes et al 2002). Surprisingly, the *prp1* locus did show upregulation in a microarray of propionate grown cultures compared to acetate cultures (Huser et al 2003).

- Regulation / activation of the prp operon

The activator of the *prpBCDE* operon in *S.* Typhimurium is proposed to be 2-methylcitrate (Tsang et al 1998), as propionate itself did not induce the operon in a lacZ fusion strain (Hammelman et al 1996), and a Δ*prpC* strain had the most severe induction defect. This suggested the product of the PrpC reaction, 2-methylcitrate, was required as the co-activator for PrpR, albeit at low levels (as a leaky plasmid copy could cause induction). Additionally, defects in propionyl-CoA formation, from mutations in the redundant activating systems, also

decreased the levels of induction as they affected an upstream step of 2-methylcitrate formation (Tsang et al 1998).

prpR and consequent *prp* operon induction was shown to be required for propionate utilization, as a Δ*prpR* strain in *S.* Typhimurium was unable to grow on the substrate. The defect could be complemented in *trans*, with the basal, 'leaky' plasmid transcription sufficient for complete rescue. A constitutive expression of the *prp* operon, in a Δ*prpC* strain lacking the putative co-activator, could be obtained by eliminating the activation domain of PrpR, thought to be responsible for signal recognition (Palacios and Escalante-Semerena 2000).

Induction also required the *ntrA* gene (encoding the RpoN (sigma-54) transcription factor), in keeping with the sigma-54 consensus sequence at the promoter of the *prp* operon, as well as the *ihfB* gene, which has been shown to activate sigma-54 promoters (Palacios and Escalante-Semerena 2000). Both *prpR* and the *prp* locus were found to be subject to global cyclic-AMP (cAMP) - cAMP receptor protein (CRP)-mediated catabolite repression under glucose and glycerol in *E. coli* (Lee et al 2005).

No homolog to the *S.* Typhimurium and *E. coli prpR* was found in *C. glutamicum* by sequence similarity. However, a mutant with disregulated MCS activity was isolated and the locus responsible, termed *prpR* (Radmacher and Eggling 2007), contained a lambda repressor-like DNA binding domain. This gene was surprisingly located in anti-parallel orientation to, but downstream of, the genetically dispensable *prpD1B1C1* cluster, rather than the *prpD2B2C2*

cluster that it activates. The protein itself had closest homology (39% identity, 55% positives) within the organism to RamB, the acetate metabolic regulator (Plassmeier et al 2012, in press).

The *prpD2B2C2* transcript appeared to be the only target under propionate addition. Localization or copy number of *prpR* did not affect transcription levels. The *prpR* transcript itself was constitutively expressed, and thus requires a co-activator to induce the operon under propionate conditions (Plassmeier et al 2012, in press).

The PrpR transcriptional start site had a SigA (sig 70, housekeeping) consensus site. The *prpD2B2C2* locus start site had a weaker match to SigA. The *prp* operator was defined to be the 121 bp region between –176 to –56. A clear band shift in an electrophoretic mobility shift assay (EMSA) was only seen with the addition 2-methylcitrate, although structurally similar metabolites citrate and methylisocitrate showed a broadening of the band. This suggested that 2-methylcitrate, as in *S.* Typhimurium, was the co-activator (Plassmeier et al 2012, in press).

The sequence and functional similarity of PrpR and RamB could indicate a shared evolutionary origin. The use of a sigma70 family regulator in *C. glutamicum*, compared to the sigma54 type in *S.* Typhimurium and *E. coli*, suggests a difference in regulation of the *prp* operon by these organisms (Plassmeier et al 2012, in press).

1.2.3 Specificity of citric acid cycle vs. methylcitric acid cycle enzymes

The careful regulation of the *prp* encoding genes could be construed as a safety mechanism to avoid the potential interference of the methylcitric acid enzymes with those catalyzing analogous reactions in the citric acid cycle, as common catalytic mechanisms are assumed (Textor et al 1997). (Figure 1.12)

The ability of these enzymes to 'cross-react' can be assessed by *in vitro* assays, enzymatic activity in extracts grown on different carbon sources, or, most convincingly, by functional complementation in mutant strains. Earlier, the redundant ability of the acetate activation systems to utilize propionate was discussed. Similarly, the evidence for other analogous reactions will be considered.

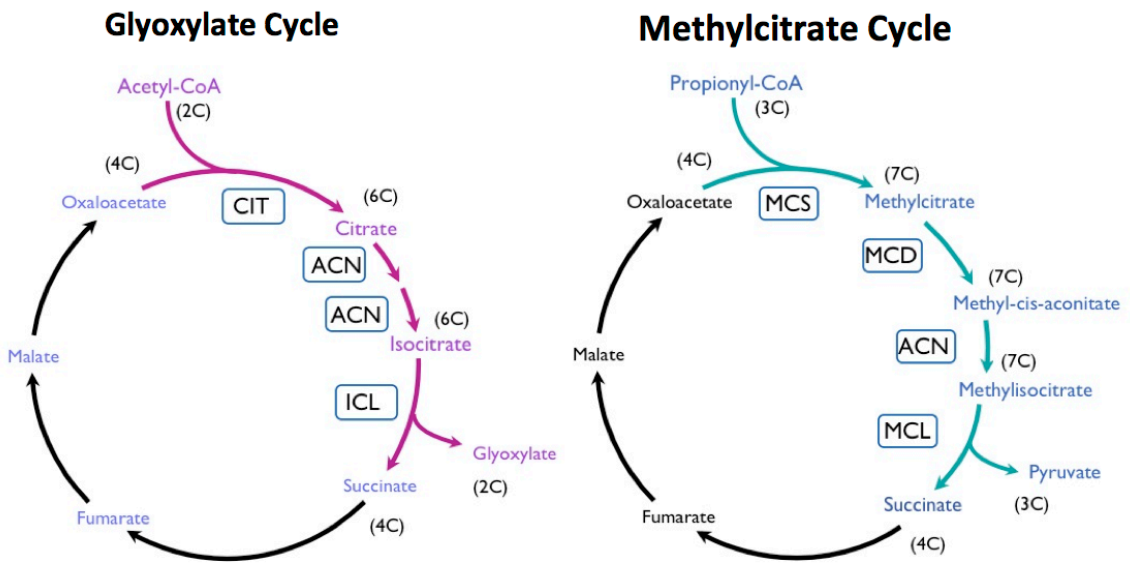

Figure 1.12 Analogous reactions and metabolites of the glyoxylate cycle and the methylcitrate cycle. CS: citrate synthase, ACN: aconitase, ICL: isocitrate lyase. MCS: methylcitrate synthase, MCD: methylcitrate dehydratase, MCL: methylisocitrate lyase. The number of carbons in the intermediates are shown.

- Citrate synthase (CS) vs. Methylcitrate synthase (MCS)

An apparent 'revertant' (but actually a suppressor) of a citrate synthase mutant (Δ*gltA*) of *E. coli* led to the discovery of the 'second citrate synthase' gene (*prpC*) (Patton et al 1993), which indicated the ability of the MCS to functionally complement the CS when overexpressed (Gerike et al 1998, Danson et al 1979). In contrast, the CS of *E. coli* was demonstrated to bind, but not to have activity with propionyl-CoA (Man et al 1995). The relaxed substrate specificity of MCS compared to CS is supported by the crystal structure of *Arthrobacter* MCS having, at the active site, increased substrate accessibility (Gerike et al 2001).

The *gltA*-encoded citrate synthase and *prpC1*/*C2*-encoded methylcitrate synthases of *C. glutamicum* exhibit ~32% amino acid identity (Claes et al 2002). A low level of CS activity of a Δ*gltA* strain was abolished in a Δ*gltA* Δ*prpC1*, indicating that the *prpC* genes could contribute this activity, albeit at levels that could not sustain growth (Radmacher and Eggling 2007). However, the constitutive expression of either *prpC1* or *prpC2* was able to rescue the glutamate auxotrophy of the Δ*gltA* strain (Claes et al 2002).

Similarly, in the filamentous fungus *Aspergillus nidulans*, the MCS could substitute for loss of CS only under de-repressing carbon sources, or with a secondary mutation in the carbon catabolite repressor *creA* site (Murray and Hynes 2010).

In contrast, the CS activity of *prpC* was sufficient to rescue the glutamate auxotrophy of a Δ*gltA* strain of *S.* Typhimurium on propionate. And as will be discussed in a subsequent section, in the absence of *prpC* and consequent excess of propionyl-CoA, the CS of *S.* Typhimurium can form 2-methylcitrate, but does not rescue growth on propionate. (Horswill et al 2001)

Interestingly, the presence of some MCS activity with CS of archaea (Gerike et al 1998) suggests evolution of MCS by duplication of CS. Consistent with this, the closer relatedness of fungal MCS to eukaryotic CS and bacterial MCS to bacterial CS would indicate that the duplication event took place after these branches diverged (Brock et al 2000).

- Aconitase (ACN) vs Methylcitrate dehydratase (MCD)

As the known *prpD*- and *acnD*-encoded enzymes are unable to carry out the hydration of methyl-cis-aconitate to methylisocitrate, the demonstrated use of the citric acid cycle aconitase to perform this reaction already indicates the relaxed substrate specificity of this enzyme (Horswill and Escalante-Semerena 2001).

Purified AcnA (TCA enzyme) of *S.* Typhimurium could utilize citrate, *cis*-aconitate, 2-methyl-*cis*-aconitate, 2-methylisocitrate, and 2-methylcitrate produced by PrpC ('poorly') as substrates (Grimek and Escalante-Semerena 2004, Horswill and Escalante-Semerena 2001). While assays with purified PrpD showed citrate was a poor substrate and isocitrate was not a substrate, *cis*-aconitate could be used, comparably to 2-methylcitrate (Horswill and Escalante-Semerena 2001). Purified AcnD from *S. oneidensis* indicated activity with citrate, *cis*-aconitate, and 2-methylcitrate as substrates (Grimek and Escalante-Semerena 2004), but *acnD*/*prpF* could not complement an Δ*acnA* Δ*acnB* strain of *S.* Typhimurium for growth on pyruvate (Grimek and Escalante-Semerena 2004). In *E. coli*, *prpD* was shown to be responsible for the 5% residual ACN activity in an Δ*acnA* Δ*acnB* strain (Blank et al 2002).

The ability of mammalian Acn and bacterial AcnA and AcnB to catalyze only 2-methylisocitrate dehydration (and not 2-methylcitrate) while being able to perform the full, reversible transformation of citrate to isocitrate, has been attributed to the two ways in which the *cis*-aconitate intermediate can bind to the

enzyme (Lauble and Stout 1995). An analogous rotation of 2-methyl-cis-aconitate, to what would be the 2-methylcitrate position, is predicted to cause a steric clash of the methyl group with the Asp165 residue in the crystal structure of mammalian aconitase, a residue that is conserved in AcnA (Lauble et al 1992). There are reports of an Acn, from a horse heart extract, that can form both 2-methylcitrate and 2-methylisocitrate (Gawron and Mahajan 1966) and of an Fe/S cluster-independent 2-methylisocitrate dehydratase activity in *Y. lipolytica* (Tabuchi et al 1981, Tabuchi et al 1995) that would be exceptions to the trends found in other eukaryotes and methylcitrate cycle enzymes, respectively.

- Isocitrate lyase (ICL) vs. Methylisocitrate lyase (MCL)

Saccharomyces cerevisiae icl2 encodes a dedicated MCL, that even when expressed in multi-copy cannot complement an *icl1* null strain (Heinisch 1996). In contrast, ICL1 can provide some MCL activity in *icl2* null mutants. Both transcripts are expressed under ethanol growth and repressed in glucose, suggesting an evolutionary artifact of cross-regulation. However, *icl2* is specifically expressed with threonine in glucose-limited media (Luttik et al 2000).

An MCL-deficient strain of *A. nidulans* is unable to grow on propionate, but is unaffected on glucose or acetate, thus MCL does not play a role on acetate growth and ICL cannot compensate for loss of MCL activity (Brock 2005). In the plant pathogen *Giberella zaea,* an MCL-deficient strain was unable to utilize propionate, but had no defect on acetate. *icl* transcription was increased on

propionate, although this did not serve a function in the utilization of the substrate in a MCL-mutant and perhaps indicates an evolutionary holdover of transcriptional cross-regulation (Lee et al 2009).

The conserved tryptophan, phenylalanine, and threonine residues of ICL enzymes are thought to define the position of glyoxylate within the active site. The analogous residues in bacterial MCL (phenylalanine, leucine, and proline), are believed to provide a more hydrophobic binding pocket to allow for the methyl group of the pyruvate product (Grimm et al 2003).

The conserved KKCGH sequence, surrounding the catalytic site of all ICLs, is altered to a KRCGH in MCLs (Brock et al 2001). A change in the MCL active site of *S.* Typhimurium from the 'MCL'-type to the 'ICL'-type (R122K), resulted in a 50% loss of activity with 2-methylisocitrate, and no gain of ability to cleave isocitrate. Rather than being important for catalysis, this residue is proposed to serve a similar function to K189 in *M. tuberculosis* ICL (Sharma et al 2000), for closing the active loop site over the substrate (Grimek et al 2003). Further evidence for its non-catalytic role, is the finding that in the *E. coli* structure of PrpB, this residue was found facing away from the active site (Grimm et al 2003). In the complementary experiment, a mutation of the *E. coli* ICL active site to that of MCL results in an 89% loss of ICL activity (Rehman and McFadden 1997).

- Anaplerosis on propionate

The ability of *E. coli* to metabolize propionate was found to be dependent on the glyoxylate cycle (Textor et al 1997). However, in another strain, oxaloacetate regeneration was shown to occur through PEP-synthase and PEPCK (Kay 1972). It appeared that the disparity in dependence on the glyoxylate cycle in the studies was related to the concentration of propionate used in the medium. As the lag on propionate could be decreased by supplementation of the media with 4-carbon substrates, the time for induction of the glyoxylate cycle could account for the delay of growth (Wegener et al 1968).

In *S.* Typhimurium, neither ICL (*aceB*), MLS (*aceA*), nor the ICD kinase/phosphatase (*aceK*) was required for propionate or pyruvate metabolism, whereas PEP-synthase mutants failed to grow on these substrates (Horswill and Escalante-Semerena 1999a). However, the glyoxylate cycle was found to serve an anaplerotic role in *R. eutropha* where ICL1 or MLS-deficient strains exhibited reduced growth on propionate media (Wang et al 2003).

In *C. glutamicum*, the use of anaplerotic pathways was detected by GC-MS analysis of metabolites in wild-type bacteria grown on different carbon substrates. The glyoxylate shunt was less active when propionate was added to acetate in the medium than on acetate alone, with higher levels of alpha-ketoglutarate and lower levels of malate detected. In the presence of propionate, the transcript of *pyc* and the metabolite pool of pyruvate were increased,

suggesting the action of pyruvate carboxylase for anaplerosis (Plassmeier et al 2007).

1.2.4 Role of the methylcitrate cycle in pathogenesis

An MCS-deficient strain of *Aspergillus fumigatus*, the fungal pathogen causing invasive aspergillosis, was shown to be attenuated in the insect infection model, particularly when spores exposed to propionate were used as inoculum (Maerker et al 2005). In a macrophage model of infection, both wild-type and the MCS-deficient *A. fumigatus* strains were taken up and killed at a similar rate. However, the addition of propionate decreased the survival of mutant, but not the wild-type strain, indicating that the inability to catabolize propionyl-CoA, and not propionate itself, was deleterious (Ibrahim-Granet et al 2008).

The spores recovered by bronchial lavage from infected mice at 19 and 48 hours post-infection were also less viable (as assessed by FITC fluorescence) in the case of the mutant, indicating the MCS-deficient strain was killed more *in vivo*. The virulence in mice of the mutant strain was found to be reduced by at least one order of magnitude, as the effect of 10^5 conidia of the mutant represented a more attenuated outcome than infection of 10^4 of the wild-type strain. A histopathology time course demonstrated the delayed onset of inflammation and the reduction of growth and distribution of hyphae in the mutant strain compared to the wild-type (Ibrahim-Granet et al 2008).

Of relevance to the ability of citric cycle enzymes to compensate for loss-of-function of the methylcitrate cycle analogs, an MCL-deficient strain of the cereal pathogen *Gibberella zeae* had a slight defect in one of the infection models. However, the double ICL- and MCL- deficient mutant had reduced disease severity in both plant models tested (Lee et al 2009). In this light, the apparent dispensability of ICL and MCL in *S.* Typhimurium for virulence in the mouse model (Kim et al 2006) may result in their partial redundancy *in vivo*, although this has not been tested.

However, a genome wide transcription study of *S.* Typhimurium isolated from the intestinal lumen of the chicken gut indicated that propionate metabolic genes *prpC, prpD, prpE*, and *pduW* (propionate kinase) were upregulated. The redundancy between the propionyl-CoA synthetase and propionate kinase-*pta* pathways to propionate activation may explain why a *prpE* mutant did not show a reduction in a gut colonization assay. In contrast, expression of the acetate kinase, *ack*, was also upregulated, and mutants in *ack* and *pta* were found to have poor colonization ability (Harvey et al 2011).

Given the similar pulmonary site of infection and intracellular lifestyle of *M. tuberculosis* and the *Legionella pneumophila* pathogen causing Legionnaire's disease, it was interesting that a macrophage- and amoeba-model attenuated strain of *L. pneumophila* was found to have a mutation in *prpD* (Stone et al 1999). It appears from the available genome sequence that in *L. pneumophila*, the *prp*

locus consists of only *prpC* and *prpD* with the annotated putative MCL encoded separately. The glyoxylate cycle does not appear to be present in this organism.

- Methylcitrate cycle in M. tuberculosis

The *prp* locus of *M. tuberculosis* was found to consist of only the MCD-encoding *prpD* (Rv1130) and MCS-encoding *prpC* (Rv1131) genes located downstream of a divergently transcribed regulator (Rv1129c). (Figure 1.13B) The MCL function was found to be provided by bi-functional ICL/MCL enzymes encoded by the *icl1* and *icl2* genes. (Munoz-Elias et al 2006) The crystal structure of the *M. tuberculosis* ICL1 enzyme indicated that the active site could accommodate the methyl group of methylisocitrate, despite the enzyme not having the signature residues of canonical MCLs (Gould et al 2006).

This organization of the *prp* locus is conserved in the closely-related *M. bovis* pathogen. However, the opportunistic pathogens *M. avium* and *M. marinum*, as well as the non-pathogenic *M. smegmatis*, encode a *prpB* between the *prpD* and *prpC* homologs. (Figure 1.13A) In contrast, the pathogen *M. leprae*, known for its reduced genome (Cole et al 2001), lacks the *prp* region altogether. The *prp* locus in *M. tuberculosis* was found to be subject to local regulation by the putative upstream regulator Rv1129c and global regulation by *sigE* (Datta et al 2011).

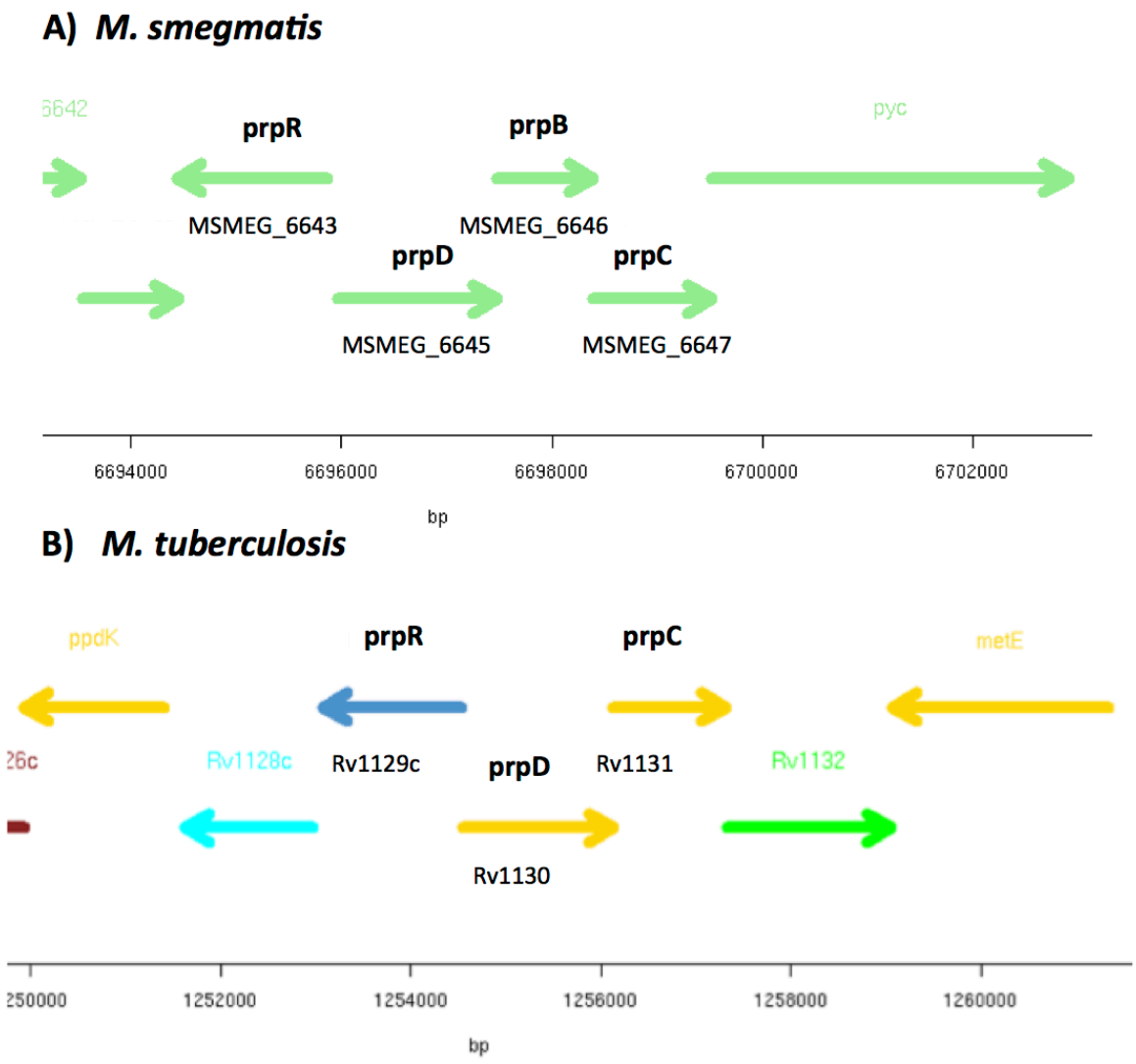

Figure 1.13 Chromosomal locus encoding methylcitrate cycle genes in A) *M. smegmatis* and B) *M. tuberculosis*.

A Δ*prpDC* strain of *M. tuberculosis* was unable to grow on propionate *in vitro*, but was unaffected for growth on acetate. Notably, the strain was dominantly inhibited by propionate, even with the addition of the alternative carbon substrates of glucose or acetate (Munoz-Elias et al 2006). The *icl1*::*hyg icl2*::*aph* mutant of *M. tuberculosis* has been shown to be unable to grow on

either acetate- or propionate-containing media (Munoz-Elias and McKinney 2005), consistent with its identified bifunctional role in the glyoxylate and methylcitrate cycle (Munoz-Elias et al 2006). Cholesterol, from which propionyl-CoA can be derived, was shown to be less-utilized by the Δ*prpDC* and Δ*prpR* (Δ*rv1129c*) strains generated in the H37Rv background of *M. tuberculosis* (Griffin et al 2012).

Pertaining to the possible *in vivo* role of the methylcitrate cycle, transcripts of Rv1129c, *prpC*, and *icl1* were highly upregulated in bacteria in resting and activated macrophages, as well as in bacteria isolated from the mouse lung (Schnappinger et al 2003, Shi et al 2010). PrpD was also detected in 2D gels of proteins from intraphagosomal *M. tuberculosis* (Mattow et al 2006).

Correspondingly, a Δ*prpDC* strain of *M. tuberculosis* was unable to replicate in resting or activated murine bone marrow-derived macrophages (Munoz-Elias et al 2006), although this phenotype was less severe than that of the ICL/MCL-deficient strain (Munoz-Elias and McKinney 2005). However, in an aerosol infection of mice, the Δ*prpDC* strain showed no difference in growth, persistence, or immunopathology compared to the wild-type strain of *M. tuberculosis* (Munoz-Elias et al 2006), and therefore did not recapitulate the phenotype of the ICL/MCL-deficient strain (Munoz-Elias and McKinney 2005).

Thus, while the methylcitrate cycle appeared to be required for growth on propionate and propionyl-CoA-generating carbon substrates *in vitro* and for replication *ex vivo*, it was found to be dispensable for growth *in vivo*. Possible reasons for the disparity included the differences between bone marrow-derived

and alveolar macrophages in terms of nutrient availability or antibacterial ability, the concentration of inhibitory metabolites in macrophages but not in mouse lungs, or the activation of a 'latent' buffering pathway *in vivo* but not during growth *in vitro* or in macrophages (Munoz-Elias et al 2006).

An alternative route for propionate metabolism, the methylmalonyl-CoA pathway, was identified in the genome of *M. tuberculosis*, but its functionality was initially unknown. Moreover, one of the enzymes of the pathway, the methylmalonyl-CoA mutase, utilizes a vitamin B12 coenzyme. Thus, the functioning of this pathway would hinge upon the ability of *M. tuberculosis* to synthesize or acquire this cofactor. These possibilities will be described further.

1.3 Methylmalonyl-CoA pathway

While the methylcitrate cycle has, thus far, only been reported to function in bacteria and fungi, the methylmalonyl-CoA route for propionyl-CoA utilization can be found represented in all domains of organisms, except for plants (Zhang et al 2009). This diversity in distribution is reflected by the array of adaptive uses for this pathway.

The methyl-branched intermediates of the pathway are utilized in the synthesis of complex polyketides by soil bacteria that are of great interest for industrial production of antibiotics and biodegradable polymers. Polyketides are chains resulting from iterative addition of building blocks, such as propionyl-CoA and malonyl-CoA, linked by decarboxylative condensations. Large multienzyme

complexes, called polyketide synthases, are able to perform these reactions in a manner similar to fatty acid synthesis. Complexity is built from altering the starter or chain extension unit, the formation of chiral centers, and cyclizations (Khosla et al 1999).

Addition of methylmalonyl-CoA results in a methyl branch in the chain. Thus, in the production of polyketides, such as antibiotics, there is interest in using succinyl-CoA or sugars as the fermentation carbon source and engineering the methylmalonyl-CoA route into industrial-scale compatible microorganisms, such as *Saccharomyces cerevisiae* and *Escherichia coli* (Mutka et al 2006, Zhang et al 2010).

In the anaerobic and carbohydrate-rich environment of the gut, fermentative bacteria can utilize the pathway in the direction of propionate formation. Humans make use of the pathway in mitochondria, for the degradation of long-chain fatty acids and branched-chain amino acids. The importance of this pathway is evident from the severe metabolic disorders (propionic aciduria and methylmalonic acidemia) that arise from genetic mutations in the enzymes and cofactors involved (Fenton et al 2001).

The pathway has also been of interest to chemists due to the radical chemistry and carbon skeletal rearrangement involved in the methylmalonyl-CoA mutase reaction. This step of the pathway will be discussed in detail later but a basic introduction to the vitamin B12 cofactor and its involvement in these complex rearrangement mechanisms will be given first.

1.3.1 Vitamin B12

Around 20 enzymatic reactions are known that rely on vitamin B12 or one of its variations, falling under the categories of: methylations, isomerizations, ribonucleotide reductases, and the rare halogenations (Martens et al 2002). The process of *de novo* cobalamin synthesis is one of the most complex biological reactions known, requiring at least 25 unique enzymes and up to 20 enzymatic steps, and resulting in a rare carbon-metal bond to a cobalt atom (Raux et al 2000).

- Distribution of B12 utilization vs. B12 synthesis

In addition to *Salmonella enterica* serovar Typhimurium and other well-studied vitamin B12 producers, the full synthetic pathway is known to occur from genome sequences in some other bacteria and archaea. No eukaryotic genome indicates the ability to synthesize B12 (Warren et al 2002). Of the prokaryotes with sequenced genomes that were found to utilize cobalt (evidenced by cobalt-transporters or cobalt-dependent enzymes), 75% of archaea and 50% of bacteria also possessed the B12 biosynthetic pathway. Of the 30.6% of sequenced eukaryotic genomes that appeared to be B12 users, most were of higher order taxonomic groups, with the exception of insects, who appear to have evolved to use nickel-dependent reactions rather than cobalt / B12-type (Zhang et al 2009).

The essentiality of B12 as a nutrient for many eukaryotes is due to the presence of the B12-dependent methionine synthase (MetH) and methylmalonyl-

CoA mutase (Mcm). The half of algal species that require vitamin B12 corresponds to the same subset that have lost the B12-independent methionine synthase (MetE), events that have occurred independently across lineages (Helliwell et al 2011). More perplexing is the subset of bacteria that produce B12 without requiring any of the B12-dependent enzymes for growth (Roth et al 1996).

- Vitamin B12 structure

Briefly, vitamin B12 is composed of four pyrroles in a planar corrin ring, forming a porphyrin-like structure. The rings donate four equatorial nitrogens to coordinate a central cobalt (Co) ion. The cobalt is also ligated by two components in the axial positions, with the upper, beta-ligand lying on one side of the tetracorrinoid core and the lower, alpha-ligand, a nucleotide base, on the other. The substituents at the beta position determine the reactivity of the complex, whereas the variations of alpha-ligands do not (Martens et al 2002, Takahashi-Iniguez et al 2012, in press).

Cyanide as the beta-ligand (an artifact of the industrial purification process), forms the relatively inert cyanocobalamin, which requires activation by the cell via an adenosyltransferase reaction. Methylcobalamin has a methyl group as the upper ligand and is the cofactor for the B12-dependent methionine synthase (encoded by *metH*). Coenzyme B12 or adenosylcobalamin has a 5'-deoxy-5'-adenosine in this beta-position. Cobalamins have 5,6-

dimethylbenzimidazole (Dmb) as the nucleotide base at the alpha-axial position (Takahashi-Iniguez et al 2012, in press).

- Vitamin B12 synthesis

Pseudomonas denitrificans can synthesize B12 under aerobic conditions, whereas *S.* Typhimurium and *Propionibacterium freudenreichii* subspecies *shermanii* (*P. freudenreichii*) only do so anaerobically, with the early steps of the pathway being oxygen sensitive (Jeter et al 1984). The biosynthesis of the central ring is related to that of siroheme, heme, and chlorophyll and is thought to have originated to produce B12 in the context of internal electron sinks for anaerobic small molecule fermentation (Eschenmoser 1988). The components of B12 are synthesized separately and then assembled (Roth et al 1996). (Figure 1.14)

Uroporphyrinogen III (UroIII) is the precursor for the corrinoid ring, which undergoes a number of modifications. Cobalt insertion and adenosylation occurs early or late in the sequence, depending on whether synthesis occurs anaerobically or aerobically, respectively (Mueller et al 1991). An aminopropanol side-chain is formed from threonine and is attached to the ring structure, forming adenosylcobinamide (Ado-Cbi). The dimethylbenzimidazole is synthesized from a flavin precursor, to which ribose, derived from an NAD synthesis intermediate (nicotinic acid mononucleotide), is added, forming the nucleotide DmbMN. This

is then added to the activated form of the aminopropanol side-chain of Cbi (GDP-Cbi), forming the nucleotide loop of the complete Ado-B12 (Roth et al 1996).

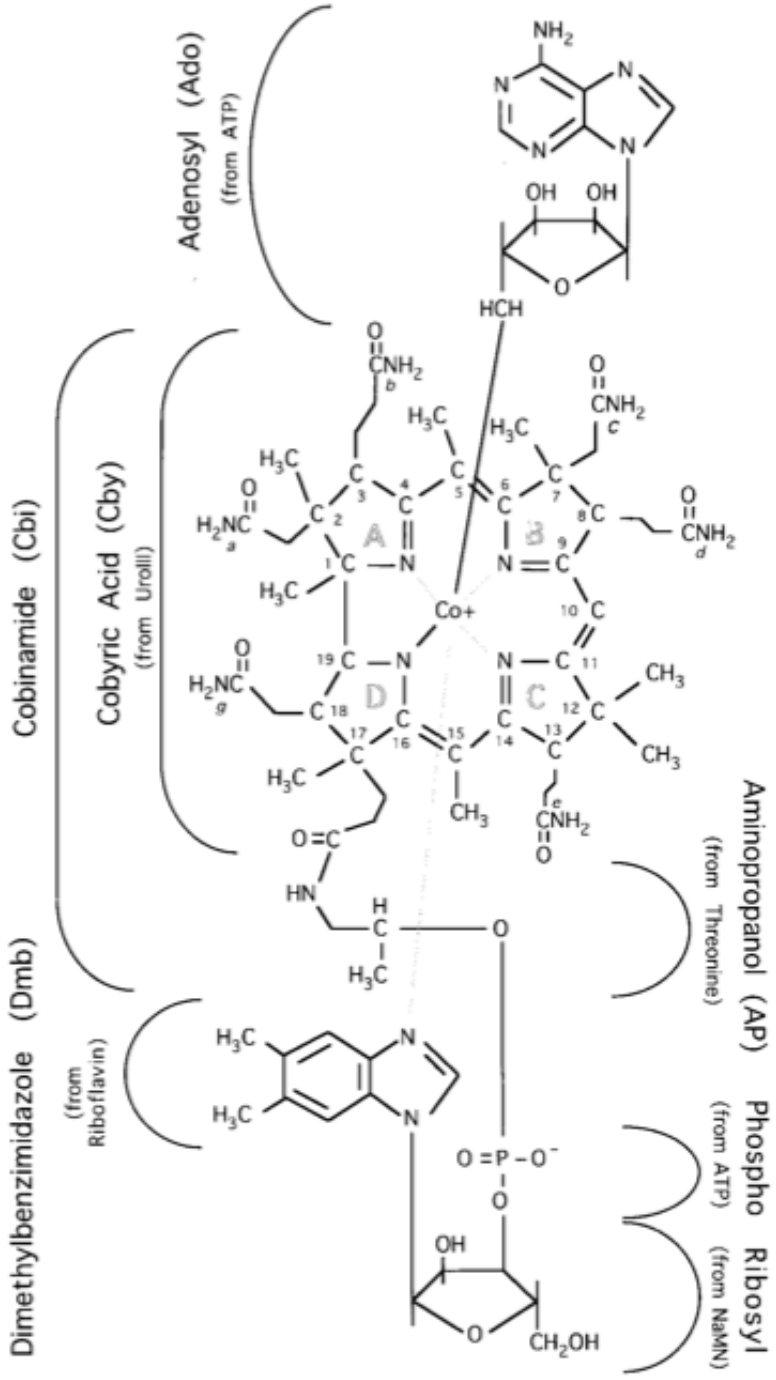

Figure 1.14 Chemical structure of B12 (adenosylcobalamin). Components that are synthesized separately are indicated (Roth et al 1996).

- cob locus of S. Typhimurium

In *S.* Typhimurium, *cbi* mutants in the first 17 genes of a 20 gene locus are rescued by provision of cobinamide (Cbi), which is the corrinoid ring with the aminopropanol side chain. Mutants in the next two genes, *cobU* and *cobS* synthesize Dmb and Cbi, but cannot join them. The last gene, *cobT*, appears to function in both joining the components and in forming Dmb (Roth et al 1996).

A putative cobalt transport system is encoded by the *cbiNQO* gene cluster of the *cob* locus. *cobA*, *cobB*, *cobC*, *cobD*, and *cysG* mutants map outside of this main operon, but rather than functioning in the *de novo* synthesis, they either utilize exogenous precursors for B12 synthesis or play an auxiliary role (Roth et al 1996). (Figure 1.15)

- B12 transporters

E. coli has lost the ability to carry out *de novo* B12 synthesis, but can utilize a cobinamide precursor (Volcani et al 1961). Transport of B12 across the outer membrane of *S.* Typhimurium and *E. coli* has been demonstrated to involve binding of B12 by a high affinity outer membrane transporter BtuB and movement into the periplasm by the energy-coupling protein TonB. Once in the periplasm, B12 associates with a periplasmic binding protein (BtuF in *S*. Typhimurium) before being transported across the inner membrane by BtuC and BtuD, which contains an ATP-binding site (Roth et al 1996).

- The 'paradox' of B12

While *S.* Typhimurium only synthesizes B12 anaerobically, the metabolic pathways that utilize B12 in this organism, those for ethanolamine and propanediol breakdown, require oxygen, when used for growth (Roth et al 1996). Moreover, mutants of *S*. Typhimurium unable to transport or synthesize vitamin B12 have no phenotype *in vitro* (aerobically or anaerobically) or in infection models (Sampson and Gotschlich 1992, Bjorkman et al 1996). The finding of an electron acceptor, tetrathionate, that could be used with propanediol anaerobically (Price-Carter et al 2001), and found to confer a selective advantage in the gut (Winter et al 2010), may provide a resolution of the paradox.

In *S.* typhimurium, the genes encoding the *cob* locus are located downstream and are divergently transcribed from those encoding the *pdu* operon for 1,2-propanediol utilization (Rondon and Escalante-Semerena 1992). In *P. freudenreichii*, the *mutA* and *mutB* genes are similarly placed with respect to the B12 locus. A B12 binding consensus sequence is found in the region between the loci (Roessner et al 2002). The requirement for B12 by these enzymes will be addressed in the following section.

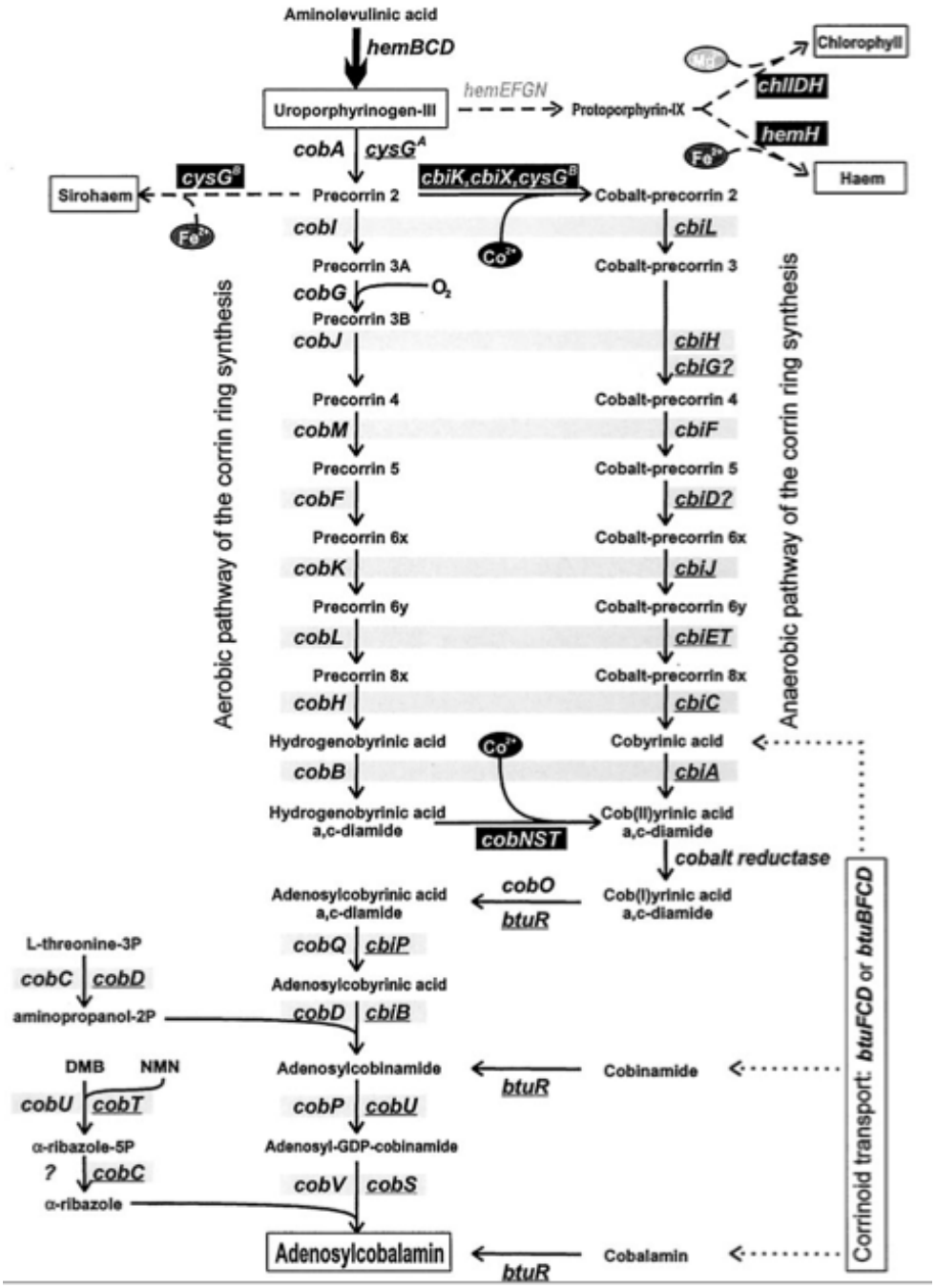

Figure 1.15 Biosynthetic route to B12 (adenosylcobalamin) and other tetrapyrrolic cofactors. Gene names are listed using *S.* Typhimurium nomenclature. Genes similar to *P. denitrificans* are in shared gray blocks, with chelatases in black boxes (Rodionov et al 2003).

- Radical carbon rearrangements

Vitamin B12 serves to generate the radicals that enable the class of 1,2 intramolecular rearrangement reactions, where a carbon-bound hydrogen is exchanged with the group on an adjacent carbon. The family of adenosylcobalamin (AdoCbl)-dependent enzymes catalyzing such carbon skeleton isomerizations consists of methylmalonyl-CoA mutase, ethylmalonyl-CoA mutase, glutamate mutase, methyleneglutarate mutase, and isobutyryl-CoA mutase. Only the methylmalonyl-CoA mutase and B12-methionine synthase are shared between bacteria and humans (Mancia et al 1996, Takahashi-Iniguez et al 2012 in press).

The adenosylcobalamin, or Vitamin B12, co-factor is needed for the mutase reaction to stabilize the radical carbon intermediate during the catalytic transformation. The weakness of the bond between the Co(III) and the 5'-carbon of the 5'-deoxyadenosyl group enables the split that forms two free radicals. This leaves the Co(II) pentacoordinated in the cobalamin and allows the 5'-deoxyadenosyl radical to abstract a hydrogen from the (methylmalonyl-CoA) substrate, generating a substrate radical. After rearrangement (via a migration of the O=C–CoA group), the product radical abstracts a hydrogen from the adenosine, thus re-forming the adenosyl radical and the product (succinyl-CoA), completing the 'radical roulette' (Mancia et al 1996, Takahashi-Iniguez et al 2012 in press). (Figure 1.16) The importance of the vitamin B12 cofactor to the

enzymatic reaction catalyzed by the MCM now established, an explanation of the pathway it takes part in follows.

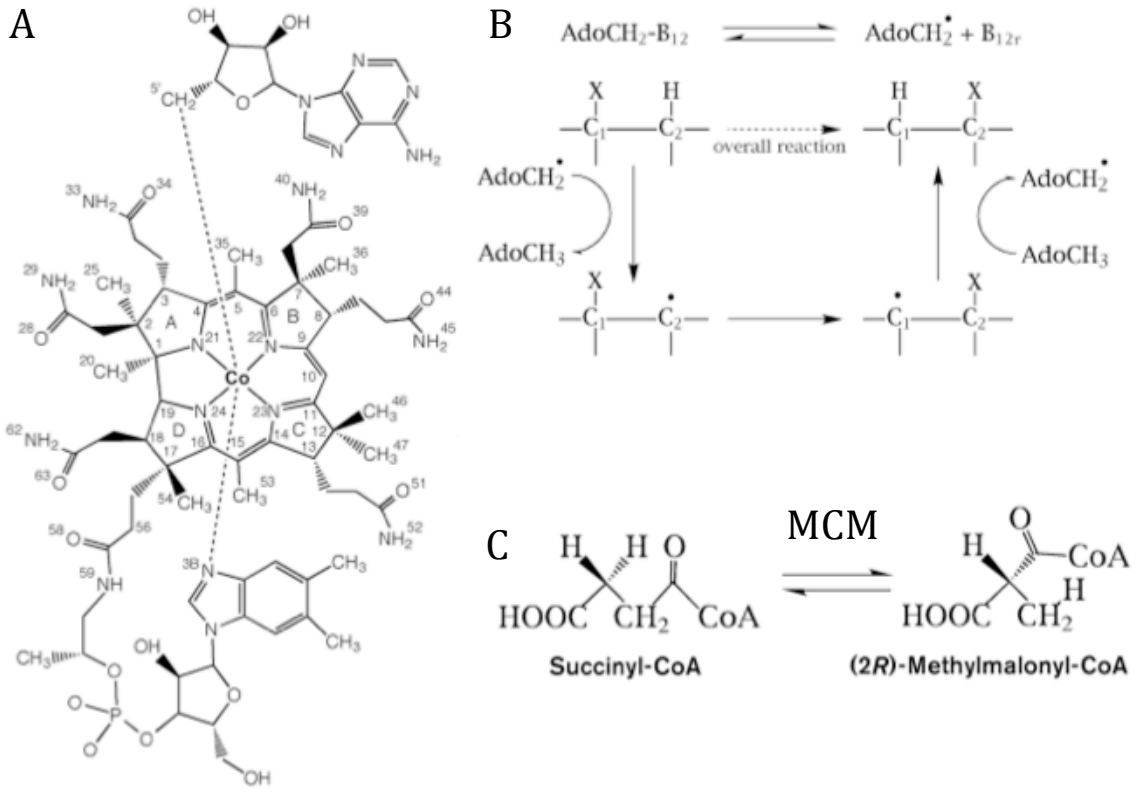

Figure 1.16 Coenzyme B12 and 'radical roulette' catalytic mechanism for carbon skeletal rearrangements. A) 5'-deoxyadenosyl-cobalamin, dashed lines connect to axial coordinating ligands. B) Minimal mechanistic scheme showing radical intermediates and generic (X) migrating group. C) Rearrangement reaction catalyzed by methylmalonyl-CoA mutase (MCM) with migrating O=C-CoA thioester group (Mancia et al 1996)

1.3.2 Methylmalonyl-CoA Pathway

- Pathway description

As mentioned in the previous section, in the direction of propionate utilization, propionate is first activated to propionyl-CoA or propionyl-CoA is derived directly from the catabolism of odd-chain or methyl-branched fatty acids, cholesterol, and the amino acids valine, isoleucine, methionine, or threonine.

Propionyl-CoA undergoes a carboxylation reaction by a propionyl-CoA carboxylase (PCC), a member of the acyl-CoA carboxylase family that uses a biotin prosthetic group, yielding an (S)-methylmalonyl-CoA product. The (S)-form undergoes an isomerization reaction by methylmalonyl-CoA epimerase (MMCE) to generate the (R)-methylmalonyl-CoA form. This intermediate can be used for biosynthetic reactions or as a substrate for the methylmalonyl-CoA mutase (MCM), which uses an adenosylcobalamin (vitamin B12) co-factor to carry out a carbon skeletal rearrangement to generate succinyl-CoA, a TCA cycle metabolite. (Figure 1.17)

- Genes of the MMCoA pathway

The propionyl-CoA carboxylase is encoded by 2 or 3 genes for the different subunits (alpha and beta, or in the case of some actinomycetes: alpha, beta, and epsilon). Most genomic loci consist of a conserved sigma factor regulator, located upstream and transcribed divergently from the structural genes. The epimerase is encoded by an *epi* gene. The methylmalonyl-CoA mutase can

be encoded by 2 genes corresponding to the alpha- and beta- subunits or by a single *mut* gene for homodimeric enzymes. Adjacent to these genes is a conserved associated protection / chaperone factor encoded by *meaB*.

- PCC

Propionyl-CoA carboxylase is a member of the acyl-CoA carboxylase family which further includes methylcrotonyl-CoA carboxylases, geranyl-CoA carboxylases, and acyl-CoA carboxylases of unknown specificity. These enzymes catalyze the formation of precursors for synthesis of long-chain fatty acids and secondary metabolites (Lombard and Moreira 2011).

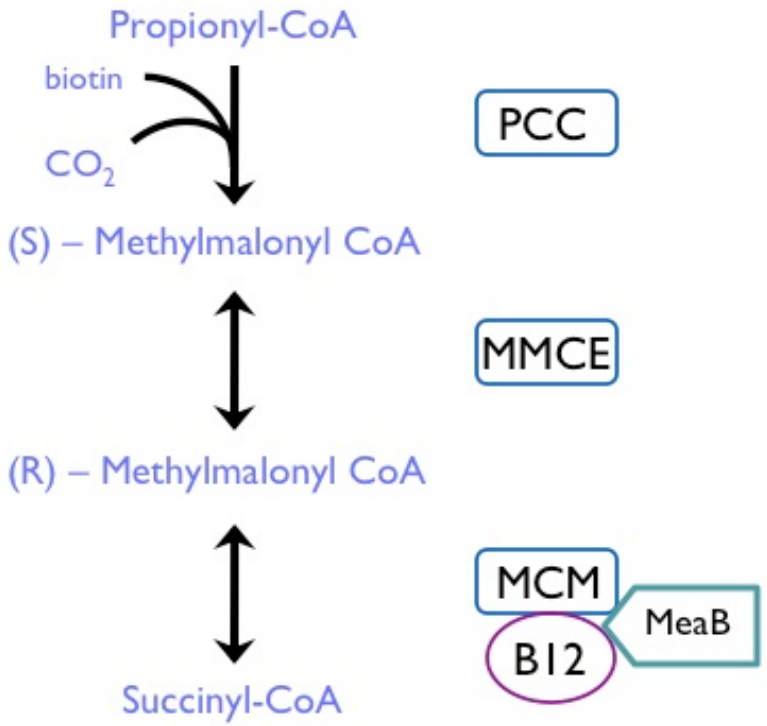

Figure 1.17 Methylmalonyl-CoA pathway. PCC: propionyl-CoA carboxylase, MMCE: methylmalonyl-CoA epimerase, MCM: methylmalonyl-CoA mutase, B12: coenzyme B12 (adenosylcobalamin), MeaB: protection factor.

These enzymes consist of 3 activities: biotin carboxylase (BC), biotin carboxyl carrier protein (BCCP), and carboxyltransferase (CT). In both eukaryotes and bacteria, the highly conserved propionyl-CoA carboxylase enzyme is comprised of two separately encoded chains: an alpha-chain containing the biotin carboxylase (BC) and biotin carboxyl carrier protein (BCCP) domains (Hunaiti and Kolattukudy 1982), and a beta-chain, corresponding to the carboxyltransferase (CT) domain, which confers substrate recognition (Erfle 1973, Henrikson & Allen 1979, Rodriguez et al 2001, Rodriguez & Gramajo 1999). However, for actinomycetal ACCases, a third, epsilon subunit is required for holo complex activity (Diacovich et al 2002, Gago et al 2006). (Figure 1.18)

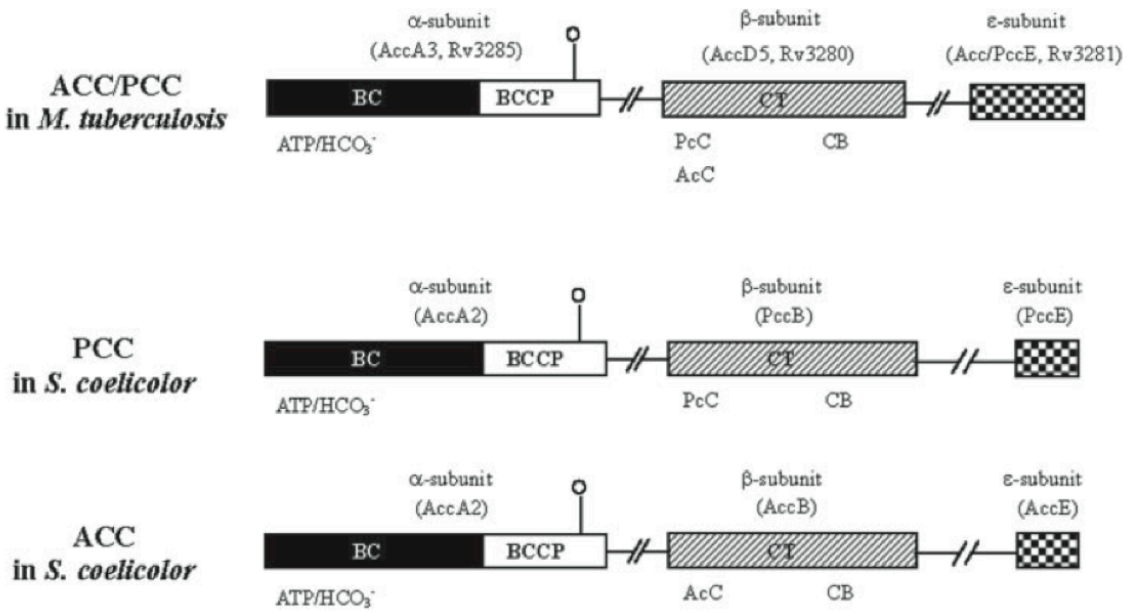

Figure 1.18 Domain organization and similarity between acyl-CoA carboxylase of *M. tuberculosis* and *S. coelicolor*. ACC: Acetyl-CoA carboxylase, PCC: Propionyl-CoA carboxylases BC: biotin carboxylation domain, BCCP: biotin carboxyl carrier protein, CT: carboxyltransferase domain, CB: carboxylbiotin (Oh et al 2006).

A recently recognized domain, denoted as BT, located in between the BC and BCCP regions, was shown to be the site of interaction between the alpha and beta subunits in the crystal structure of the holoenzyme of human PCC (Huang et al 2010). This interaction domain was recognized to be helical in structure. Enzymes that lack this helical region corresponded to those that use the additional AccE subunit for domain interaction. It is suggested that the helical structure of AccEs might be used to compensate for alpha-subunits lacking a BT domain (Lombard and Moreiera 2011).

In the first step of the reaction, the biotin carboxylase domain couples CO_2 to the biotin moiety affixed to BCCP to form carboxybiotin. This is followed by the transfer of the carboxyl group from biotin to the specific acyl-CoA substrate, generating the alpha-carboxylated acyl-CoA product. Carboxylation of acetyl-CoA would yield malonyl-COA, whereas utilization of propionyl-CoA produces methylmalonyl-CoA (Lombard and Moreira 2011).

- MMCE

While the propionyl-CoA carboxylase produces the S-epimer of methylmalonyl-CoA, the conversion to succinyl-CoA by methylmalonyl-CoA mutase requires the R-epimer. The methylmalonyl-CoA epimerase (MMCE), (also called methylmalonyl-CoA racemase) catalyzing this interconversion is metal-ion dependent, forming a dimer with the Co2+ bound at the bottom of the active site (McCarthy et al 2001). The human form was identified by a search by

homology to genes often found adjacent to bacterial and archaeal MCMs. These genes were previously misannotated as lactoylglutathione (LGSH) lyases (Bobik and Rasche 2001).

- MCM

The methylmalonyl-CoA mutase enzyme from *P. freudenreichii* was found to consist of the heterodimeric alpha-subunit (~79 kilodaltons (kDa)) and beta-subunit (~65 kDa). The genes encoding these subunits were found to be located adjacently in the chromosome (Marsh et al 1989).

Subsequent cloning of the human and murine forms of MCM indicated that these enzymes were comprised of homodimeric (two alpha) subunits (Jansen 1989, Wilkemeyer et al 1990). There is not a clear delineation between genomes encoding homodimeric and heterodimeric forms, as both types were found amongst the MCMs encoded by members of the Rhizobiaceae (Miyamoto et al 2003).

Each dimer contains one binding site for the acyl-CoA substrate and for B12. The beta chain does not appear to contribute much to the binding of the substrate or the cofactor, consistent with the sequence having lost many of the key binding and active site residues. (Mancia et al 1996).

In the crystal structure of the *P. freudenreichii* enzyme, the active site was found to be deeply buried in the long tunnel where the substrate is bound, thus protecting the reactive radical intermediates from side reactions. The mutase

enzyme must favor the breaking of the Co-C bond of the coenzyme while disfavoring the formation of the irreversibly inactive hydroxycobalamin (Mancia et al 1996).

The adjacent genes (*mutA*, *mutB*) of *S. cinnamonensis* have overlapping start and stop codons, allowing for translational coupling and production of stoichiometric amounts of each. There is high sequence similarity amongst all the MCM-encoding genes between the large subunits of bacterial enzymes with mammalian enzyme, and between small subunits of bacterial enzymes. The 51% similarity of the small unit to the large subunit is indicative of a gene duplication event (Birch et al 1993).

The high levels of nucleotide sequence conservation between mammalian and bacterial MCM-encoding genes suggest that the constraints placed on the structure by the enzymatic reaction limits genetic drift (Jackson et al 1995).

- MeaB

The susceptibility of radical-driven rearrangement reactions to side reactions and 'suicide' inactivation is evidenced by the class of chaperones that exist to 'reactivate' the enzyme. This class of 'eliminases,' that catalyze the exchange of inactivated co-factor for enzymes such as the glycerol dehydratase, does not function with MCM (Mori et al 1997, Toraya and Mori 1999, Seifert et al 2001).

However, a 'protection' factor, MeaB, was found to be highly conserved in its neighboring location to the MCM-encoding genes. It is commonly misannotated in genomes as a lysine / arginine / ornithine (LAO) transporter, as it was originally identified in a transporter mutant screen of *E. coli*, perhaps due to its GTPase activity (Celis et al 1998). The strong association between the genes encoding MCM and MeaB in the genomes of prokaryotes, led to the identification of the gene in humans. This gene corresponded to the *cblA* complementation group of methylmalonic acidemia-causing defects (Bobik and Rasche 2001, Dobson et al 2002). Other proteins of this P-loop GTPase family are accessory proteins to enzymes with metallic cofactors, and are thought to act in their assembly (Leipe et al 2002).

This factor was first studied in *Methylobacterium extorquens* AM1 where an interrupted *meaB* gene resulted in a loss of MCM activity (Korotkova et al 2002). Complexes of MeaB and MCM were demonstrated in non-denaturing gels and a GTP- and MgCl2-dependent increase in MCM specific activity was seen in the presence of MeaB (Korotkova and Lidstrom 2004). The GTPase activity of MeaB was enhanced, by two orders of magnitude, by MCM. Moreover, the addition of B12 resulted in preferential binding of MCM to the GTP-bound form of MeaB (Padovani et al 2006). However, the catalytic ability to hydrolyze GTP is essential for the binding. Thus, it was determined that MeaB 'gates' B12-binding to the MCM in a GTP-dependent manner. The MeaB protein also seemed to confer oxidative shielding effects to MCM when bound. These effects were GTP-

independent and seemed to be exerted on the level of conformational changes from binding (Padovani and Banerjee 2006). A similar effect of initial protection of MCM and subsequent GTP-dependent reactivation was found using the human homologs, MMAA and MCM (Takahashi-Iñiguez et al 2011).

- Genomic loci

There exist some examples of the close clustering of genes for the enzymes that interact in a pathway. The gene encoding the homodimeric MCM of *Sinorhizobium meiloti* was found to be adjacent to a gene encoding the alpha-subunit of an apparent propionyl-CoA carboxylase. A GntR-type regulator was found further upstream (Charles and Aneja 1999).

In *Streptomyces* sp. DSM4137 the *mutA* and *mutB* genes are found adjacent to those for cobalamin synthesis. These were all found within a cluster for polyketide synthesis of the macrodiolide elaiophylin (Haydock et al 2004).

The coding region for the *epi* gene in the myxobacterium *Sorangium cellulosum* was located just upstream of, and overlapping 9 bp of, the gene encoding a homodimeric MCM. A putative sigma-factor regulator lies upstream of and a *meaB* homolog lies downstream of this *mcm* gene (Gross et al 2006).

- Other functions of MCM or routes to methylmalonyl-CoA

In light of the bifunctional ICL/MCL encoded by *M. tuberculosis*, it seems appropriate to evaluate possible alternative roles of enzymes so observed phenotypes can be interpreted accordingly.

Escherichia coli has been mistakenly thought not to encode a methylmalonyl-CoA mutase although B12 addition had been demonstrated to stimulate growth on propionate (Evans et al 1993). When a gene was identified with homology to known MCMs, it was named *sbm* for 'sleeping beauty mutase' (Roy and Leadlay 1992). The *sbm* was located in a cluster of four genes, adjacent to a *ygfD* gene encoding a protein of undetermined function (Haller et al 2000). This 'undetermined' gene was found to be 75% similar to the *meaB* lying downstream of the *mutAB* genes in *S. cinnamonensis* (Birch et al 1993), 48% similar to *meaB* of *M. extorquens* (Korotkova and Lidstrom 2004), and 46% similar to the human homolog encoding MMAA. The ability of the MeaB protein to bind to the methylmalonyl-CoA mutase *in vitro*, to co-immunoprecipitate from cells, and to possess GTPase function was demonstrated (Froese et al 2009).

Of the remaining two genes in the operon, *yfgG* was found to encode a methylmalonyl-CoA decarboxylase (MMDC) and *yfgH* produced a CoA transferase that showed preference for shuttling CoA between succinate and propionate. However, this decarboxylase did not share sequence similarity to the previously characterized MMDCs that included biotin domains and coupled the energy released from the decarboxylation to sodium transport (Huder and

Dimroth 1993, Bott et al 1997). As *E. coli* was found not to encode a propionyl-CoA carboxylase or an epimerase, the enzymes encoded by the *sbm* locus were predicted to enable a cycle to convert succinate to propionate (Haller et al 2000). The functionality of the *sbm*-encoded enzyme was shown by addition of vitamin B12 (Dayem et al 2002). *E. coli* does not synthesize this co-factor *de novo*, but can synthesize the DMB nucleotide loop and phosphoribosyl-group, and can thus use cobinamide to carry out the final assembly (Lawrence and Roth 1996).

Methylmalonyl-CoA mutase is used in the Wood-Werkman cycle by *P. freudenreichii* to ferment lactate to propionate, releasing CO_2, providing the characteristic flavor and holes of aged Swiss cheese, respectively. This cycle is comprised of the enzymatic activities of MCM, MMCE, and a methylmalonyl-CoA carboxytransferase. A carboxyl group from methylmalonyl-CoA is transferred to pyruvate to produce propionyl-CoA and oxaloacetate (Falentin et al 2010).

Recently, a number of MCM-like enzymes and reactions have been identified, including the isobutyrl-CoA mutase (ICM) that was first thought to be restricted to *Streptomyces* spp., but is now recognized to exist more broadly distributed in archaea and in bacteria. The *icmA* and *icmB* subunits can be encoded together or separately in the genome. The smaller unit possesses the B12-binding function, but the MeaI chaperone factor can associate with either subunit. As a further variation, for some of these species, the ICM activity is provided by an *icmF* 'fused' gene which includes a B12-binding domain, a MeaB-like domain (MeaI), and the ICM large subunit domain (Cracan et al 2010).

Streptomycetes and possibly some strictly anaerobic bacteria seem to be able to form S-methylmalonyl CoA from oxidation of isobutyryl-CoA, formed from the ICM conversion of *n*-butyryl-CoA, which is an intermediate of valine metabolism (Zerbe-Burkhardt et al 1998, Tholozan 1988, Matthies and Schink 1992). This routing appeared active during monensin production of *Streptomyces cinnamonensis* when an oil-based medium was used (Li et al 2004).

As another variation in the canonical roles of enzymes, the epimerase in *Rhodobacter sphaeroides* acts in a promiscuous fashion as the epimerase for the ethylmalonyl-CoA mutase (ECM) in this species (Erb et al 2008).

1.3.3 Acyl-CoA carboxylases (ACCase) in *M. tuberculosis* and related organisms

While most organisms possess 1 or 2 acyl-CoA carboxylases, *Mycobacterium tuberculosis* and *Mycobacterium bovis* encode 3 alpha (BC and BCCP-containing) subunits (*accA1-3*), 6 beta (CT substrate-binding) subunits (*accD1-6*), and 1 epsilon subunit (*accE5* - Rv3281) (Kurth et al 2009). *accA3*, *accD4*, *accD6*, and *accE5* have been predicted to be essential in *M. tuberculosis* by high-density transposon mutagenesis (Sassetti et al 2003).

The massively reduced genome of *M. leprae* contains genes for one alpha-subunit, three beta-subunits, and one epsilon-subunit. The retention of fully functional *accD4* and *accD5* homologs in *M. leprae* and *C. glutamicum* suggests the essential, core-function of these, whereas *accD1*, *accD2*, and

accD6 may account for more mycobacterial-specific functions. *accD4* is found in a genomic locus that is conserved in all *Mycobacterium*, *Corynebacterium*, and *Rhodococcus* genomes analyzed, downstream of *fadD32* and *pks13* (Gande et al 2004).

The closely-related and mycolic acid-producing *C. glutamicum* encodes 1 alpha subunit and 4 beta subunits (Gande et al 2004). The *S. coelicolor* genome encodes for 2 epsilon subunits, for specific interaction with the ACC and PCC complexes (Diacovich 2002).

- Biochemical and genetic studies of the ACCases of mycobacteria

AccD4 appeared to be required for mycolic acid biosynthesis and was correspondingly found to be essential in *M. smegmatis* using a conditional knockout (Portevin et al 2005). This is consistent with its predicted essentiality in *M. tuberculosis* (Sassetti et al 2003).

Reconstituted ACCase 6 (AccA3 + AccD6) showed similar catalytic efficiency with both acetyl-CoA and propionyl-CoA. However, the genomic grouping of *accD6* with genes of the fatty acid synthase II (Fas II) complex, suggested an acetyl-CoA carboxylase function in mycolic acid biosynthesis was the authentic role within the cell (Daniel et al 2007).

While the alpha and beta subunits of AccA3 and AccD5 were able to bind *in vitro*, only a minimal activity was seen. Addition of the epsilon subunit at a 5:1 ratio was required for peak catalytic activity. This ACCase 5 accepts acetyl-CoA

and propionyl-CoA, but with a five-fold preference for propionyl-CoA) (Gago et al 2006).

Despite this activity with acetyl-CoA, the components of ACCase 5 are unable to compensate for the loss of *accD6* in a conditional mutant of *M. smegmatis*, which causes the loss of fatty acid synthesis, growth arrest, and subsequent loss of viability (Kurth et al 2009).

The gene encoding the epsilon subunit (*accE5*) is co-transcribed with *accD5*. During *in vitro* growth, the epsilon subunit is more highly expressed during exponential phase. The organization of this locus is well conserved in *M. tuberculosis*, *M. bovis*, *M. leprae*, and *M. smegmatis* (Oh et al 2006). (Figure 1.19)

- Methylmalonyl-CoA pathway in M. tuberculosis

Methylmalonyl-CoA acts a building block to produce the variety of lipids that contribute to the cell wall architecture and pathogenic lifestyle of *Mycobacterium tuberculosis*, including polyketides, mycolipanoic and mycolipenic acids, and mycocerosic acids (Camacho 2001, Sirakova 2001, Sirakova et al 2003, Dubey et al 2002, Fernandez and Kolattukudy 1997). (Figure 1.1)

Lipid profiles of *in vitro*-grown *M. tuberculosis* exhibited forms of two known virulence lipids, sulfolipid (SL-1) and phthiocerol dimycocerosates (PDIM), of greater mass and abundance when propionate was added in the media. This seemed to imply channeling from propionate to an increased pool of the

methylmalonyl-CoA precursor (Jain et al 2007). A similar shift was seen when cholesterol was provided as the sole carbon source (Yang et al 2009). Interestingly, the lipid profiles of *M. tuberculosis* isolated from the lungs of infected mice were found to share a similar lipid profile of higher mass forms of PDIMs (although SL-1 levels were too low from *in vivo*-isolated extracts to analyze) (Jain et al 2007).

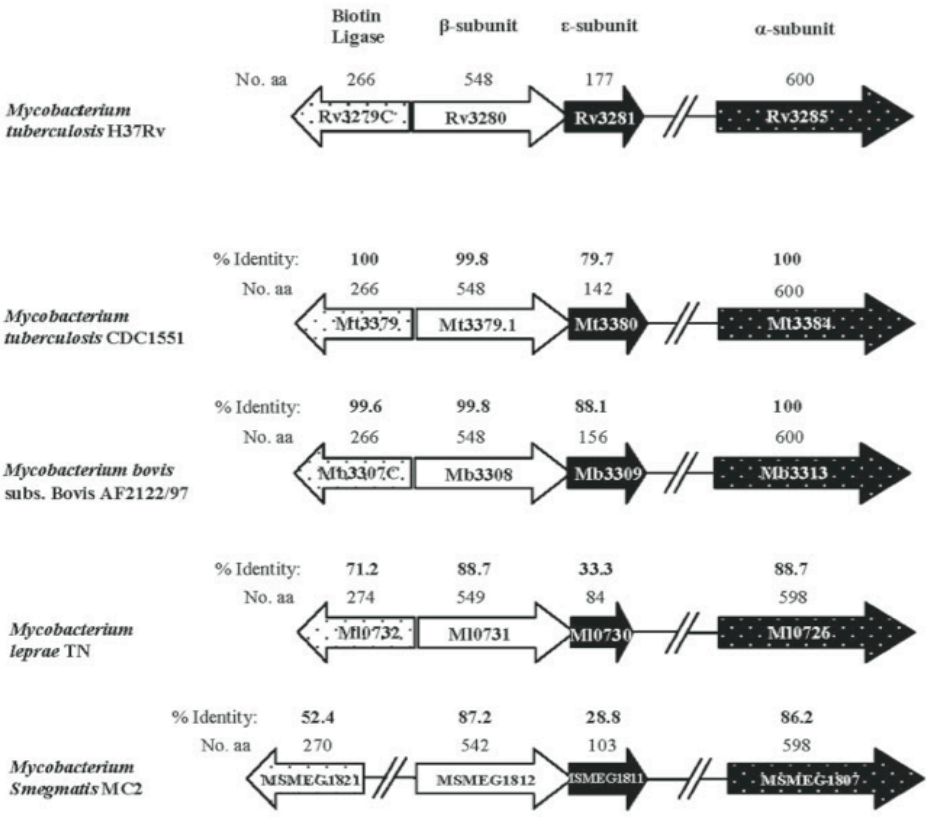

Figure 1.19 Conservation of genes in *Mycobacterium* spp. for biotin ligase, alpha subunit, beta subunit, and epsilon subunit of ACC5 (propionyl-CoA carboxylase) (Oh et al 2006).

Overexpression of the *mutAB*-encoding genes in *M. tuberculosis* caused a shift in the lipid profiles towards increased mass forms of SL-1 and PDIM,

consistent with an increase of the precursor pool. However, this was accompanied by a decreased overall abundance of lipids, thought to be due to draining of TCA intermediates (Jain et al 2007).

While the full functionality of the methylmalonyl-CoA pathway was originally unknown, *M. tuberculosis* is known to encode two other B12-dependent enzymes: the B12-dependent methionine synthase (*metH*) and a class II ribonucleotide reductase (*nrdZ*). In studies on a Δ*metE* strain lacking the B12-independent enzyme, the *metH* was only able to functionally complement the defect when the media was supplemented with cyanocobalamin (vitamin B12). This indicated that *M. tuberculosis* could transport and activate, but not produce, sufficient vitamin B12 for the activity of this enzyme (Warner et al 2007). Surprisingly, *M. tuberculosis* was found to encode the full complement of genes for *de novo* B12 synthesis, via the oxygen dependent route (Raux et al 2000). (Figure 1.20)

Based on the previously described biochemical studies (Gago et al 2006), the genes encoding the alpha, beta, and epsilon subunits of propionyl-CoA carboxylase (PCC) were assigned to *accA3* (Rv3285), *accD5* (Rv3280), and *accE5* (Rv3281). Rv1322A had 40% identity and 60% similarity to the methylmalonyl-CoA epimerases (MMCEs) characterized from *P. freudenreichii* (Leadlay 1981) and *Pyrococcus horikoshii* (Bobik and Rasche 2004). Downstream of a divergently transcribed conserved hypothetical (Rv1491c), the MCM components are encoded by the two adjacent genes *mutA* (Rv1492) and

mutB (Rv1493), for the beta and alpha subunits, respectively. The putative *meaB* (Rv1496)-encoded protection factor was located downstream, separated from the MCM-encoding genes by a MazEF-type toxin-antitoxin module (Savvi et al 2008). (Figure 2.1B)

This pathway appeared unable to compensate for the loss of the methylcitrate cycle in a Δ*prpDC* strain, which could not grow in standard media containing propionate as a carbon source (Munoz-Elias et al 2006). However, addition of cyanocobalamin to the media enabled the growth of this mutant strain (generated in the H37Rv background). When the *mutAB* genes were additionally deleted in the Δ*prpDC* strain, this double knockout (Δ*mutAB* Δ*prpDC*) could no longer be rescued by exogenously supplied B12, demonstrating the MCM-specific effect of the co-factor. In comparison, a Δ*mutAB* strain, also generated in the H37Rv background, was found to be unimpaired in the ability to metabolize propionate compared to the wild-type (Savvi et al 2008). B12 supplementation was also shown to rescue the impaired growth of a Δ*prpDC* strain on the propionyl-CoA generating substrate of cholesterol (Griffin et al 2012).

The role of the methylmalonyl-CoA pathway in the macrophage environment, where the methylcitrate cycle appeared to be essential for *ex vivo* growth of *M. tuberculosis* (Munoz-Elias et al 2006) was recently examined in this context. The addition of B12 to the media of bone marrow-derived macrophages infected with Δ*prpDC M. tuberculosis* resulted in a rescue of the survival defect (Griffin et al 2012).

Whether the full virulence of a Δ*prpDC* strain in the mouse infection model can be attributed to the dispensability for propionate metabolism or to the *in vivo* activation of the methylmalonyl-CoA pathway, had not yet been investigated. Testing the phenotypes of a Δ*mutAB* and Δ*mutAB* Δ*prpDC* strain *in vivo* was one of the goals of this work.

Figure 1.20 Cobalamin biosynthetic gene arrangements. Blue highlighted genes are specific to the oxygen-dependent pathway, yellow highlighted genes are specific to oxygen-independent pathway, and red highlighted genes are found in both pathways. Asterisk * indicates the oxygen-dependent (*cob*) route, other strains considered to contain the oxygen-independent route (*cbi*) (Raux et al 2000).

1.4 Propionate toxicity

Given the long history of fermentation as a method of food preservation and the modern use of propionate as an additive in the food industry, it is perhaps not surprising that this short-chain fatty acid compound is inhibitory to a wide range of fungi and bacteria. The inability to metabolize propionate has been thought to exert adverse effects on the level of acid stress and by the dissipation of the proton-motive force (Baronofsky et al 1984, Salmond et al 1984, Cherrington 1991, Russell 1992). However, the ability to metabolize propionate has been found in microbes residing in soil and gut environments containing high levels of short-chain fatty acids, and may represent a means of detoxification.

Two of these metabolic routes, the methylcitrate cycle and the methylmalonyl-CoA pathway, were described in previous sections. The originally isolated *prp*- mutant strain of *S*. Typhimurium that identified the genomic locus for the methylcitrate cycle was found to grow with a lag on glucose or glycerol in the presence of propionate. Moreover, it was no longer able to use succinate when propionate was added to the media (Hammelman et al 1996). Therefore, propionate appeared to exert a dominant inhibitory effect on the ability of the mutant to catabolize alternative carbon substrates. As the WT strain is not affected in this manner, it would suggest that the lesion in the propionate metabolic pathway is contributing to this negative effect.

In the absence of an alternative pathway for propionate metabolism, it is likely that the breakdown products that form upstream of the defective enzyme

would accumulate. This accumulation could exert a negative effect on other aspects of metabolism. There are many examples of this in the literature and this section will address the cases in methylcitrate cycle mutants.

1.4.1 Dominant inhibition by propionate

While the filamentous fungus *Aspergillus nidulans* is able to utilize propionate as a sole carbon source (albeit with a lag for germination and reduced growth yields), its growth on glucose is dominantly inhibited by the presence of propionate. This inhibition was more pronounced for a MCS-deficient strain. However, in the presence of acetate, propionate was not inhibitory for WT growth and only exerted a mild effect on the MCS-deficient strain. Addition of acetate to mixtures of glucose and propionate improved the growth of both strains on this media, but did not completely alleviate the inhibition (Brock et al 2000).

An MCL-deficient mutant of *A. nidulans*, unaffected for growth on glucose or acetate, was completely inhibited in the ability to use glucose in the presence of propionate, and required acetate at a higher ratio than used for WT, to compete with the effects of propionate (Brock 2005).

In another example, MCS- or MCL- deficient *Corynebacterium glutamicum* strains are able to utilize acetate in the presence of propionate, but an MCD-deficient strain is not (Plassmeier et al 2007). This would suggest the accumulation of different metabolites with different lesions of the pathway, where

some exert inhibition, and others do not. The difference could be addressed by identifying the putative accumulating metabolites in these strains.

1.4.2 Accumulation of propionate-derived metabolites

The accumulation of pathway intermediates has been demonstrated, via 13C-NMR and GC-MS using strains of *S.* Typhimurium and *C. glutamicum*, respectively, with mutations in the MCS, MCD, and MCL activities of the methylcitrate cycle. Propionyl-CoA could not be detected in either method due to technical issues and 2-methyl-cis-aconitate was not detected by GC-MS for lack of an authentic standard. Samples derived from the MCD-deficient strains accumulated 2-methylcitrate. An MCL-deficient strain in *S.* Typhimurium accumulated a mix of 2-methylcitrate, 2-methyl-*cis*-aconitate, and 2-methylisocitrate, by 13C-NMR. Both 2-methylcitrate and 2-methylisocitrate was seen to accumulate in the MCL-deficient strain on *C. glutamicum* by GC-MS. The mix of products detected presumably represented the equilibrium of the reaction forming 2-methylisocitrate, where the activity of MCL is required to drive the reaction to completion (Horswill and Escalante-Semerena 1999a, Plassmeier et al 2007).

In *Ralstonia eutropha*, 2-methylcitrate and 2-methylisocitrate were detected by GC/MS in the supernatants of a *prpB* null-allele mutant incubated in propionate and succinate (Bramer et al 2001). Similarly, in an MCL-deficient strain of the fungus *Aspergillus nidulans*, 2-methylisocitrate, measured

enzymatically, was found to be excreted into the medium, in proportion to the ratio of propionate to the alternative carbon source provided (Brock 2005). Propionyl-CoA accumulation was found, by enzymatic assay, in an MCS-deficient strain of *A. nidulans* incubated in the presence of propionate (Brock and Buckel 2004).

1.4.3 Mechanism of inhibition

While elevated levels of metabolites have been demonstrated, the mechanism by which the metabolite can exert toxic effects is not as clear to establish. From numerous studies on the subject, the suggested target of inhibition varies from enzymes of central carbon metabolism to the more recently identified inhibition of secondary metabolism. Some of these targets will be considered here.

- Inhibition of pantothenic acid synthesis

It was shown that propionate toxicity on *E. coli*, *S. cerevisiae*, and *Acetobacter suboxydans* could be alleviated by addition of beta-alanine, and even more so by pantothenate, but not by pantoic acid (Wright and Skeggs 1946). This suggested that inhibition may be exerted on the level of pantothenate biosynthesis, where propionate, which bears structural similarity to beta-alanine (3-aminopropanoic acid), could compete for binding to the pantoate-beta-alanine ligase enzyme (King and Cheldelin 1948). The requirement for pantothenate in

coenzyme A synthesis and subsequent use of coenzyme A for a number of central metabolic reactions indicates that inhibition at this level could have widespread metabolic effects.

- Inhibition of pyruvate dehydrogenase

The rescue from propionate inhibition by the addition of acetate has been demonstrated for a wide range of organisms, including the gut commensal *Enterococcus* (formerly *Streptococcus*) *faecalis*, the photosynthetic purple bacterium *Rhodobacter* (formerly *Rhodopseudomonas*) *sphaeroides*, the cyanobacteria *Synechococcus elongatus* (formerly *Anacystis nidulans*) and *Gloeocapsa alpicola*, and the filamentous fungus *Aspergillus nidulans* (Hill 1952, Maruyama and Kitamura 1975, Smith and Lucas 1971, Brock et al 2000), suggesting a common mechanism underlying the toxicity.

In cell free extracts of *E. faecalis*, pyruvate oxidation was inhibited by propionate itself as well as by propionyl-P. Addition of lipoic acid and other even chain-length fatty acids improved growth in the presence of propionate, consistent with the enhancement of pyruvate oxidase function. Moreover, the radioactivity from 14C-labeled acetate and 14C-labeled pyruvate added to the mixtures was found to be incorporated into lipid fractions rather than evolved as CO_2, suggesting fatty acid biosynthesis was needed for growth in the presence of propionate (Kamihara 1969).

The excretion of pyruvate by *R. sphaeroides*, *A. nidulans*, and *A. fumigatus* in the presence of propionate also suggested the inhibition of pyruvate dehydrogenase activity (Maruyama and Kitamura 1975, Brock and Buckel 2004, Maerker et al 2005). Propionyl-CoA rather than propionate itself was shown to inhibit the partially purified pyruvate dehydrogenase enzyme, uncompetitive with pyruvate, but competitive with CoA (Maruyama and Kitamura 1985).

Incorporation of propionate was stimulated by the addition of sodium bicarbonate ($NaHCO_3$), but not succinate. This effect was attributed to increased carboxylation of propionyl-CoA and was eliminated in a propionyl-CoA carboxylase (PCC) mutant strain. The growth of this mutant on propionate and glucose could then be restored by addition of acetate. It was concluded that inhibition was exerted at the level of propionyl-CoA and rescue could be enabled by the metabolism of propionyl-CoA by the methylmalonyl-CoA pathway or by the supply of acetyl-CoA from acetate (Maruyama and Kitamura 1985).

It is thought that glucose does not allow for growth in the presence propionate as acetyl-CoA or oxaloacetate may be limiting. However, acetate, which is able to form acetyl-CoA directly from activity of ACS, allows a bypass of this inhibition. Consistent with this, the rescue of an MCS-deficient strain was dependent on acetyl-CoA synthetase function. Moreover, an ACS-deficient strain was inhibited even in propionate and acetate mixtures (Brock et al 2000).

Interestingly, while the addition of acetate to propionate was able to alleviate inhibition of an MCS-deficient strain, propionyl-CoA levels were still high,

indicating that acetate did not rescue the phenotype by competing with propionate for activation (Brock and Buckel 2004).

- Inhibition of TCA cycle enzymes

Given the analogous structures of the methylcitrate cycle intermediates to the authentic TCA cycle metabolites, the accumulation of the former could interfere with the ability of the TCA cycle enzymes to use the latter. Examples of TCA cycle enzymes having affinity and/or catalytic activity with the methylcitrate cycle substrate were discussed in the previous section. A number of examples were cited where a methylcitrate cycle enzyme was able to buffer the loss of the analogous citric acid cycle enzyme, when overexpressed. On the other hand, the TCA cycles do not seem to functionally compensate for methylcitrate cycle mutants, although the *S.* Typhimurium citrate synthase can produce 2-methylcitrate in an MCS-deficient strain (discussed in a subsequent section), it is not sufficient to support growth on propionate (Rocco and Escalante-Semerena 2010).

- Inhibition of aconitase

The mixed data on the ability of 2-methylcitrate to inhibit aconitase is attributed to the differential use of pure enantiomers or synthetic mixtures, as well as variability in aconitase preparations, for the assays (Cheema and Dhadli 1975, Beach et al 1977, Horswill et al 2001). While WT and MCS-deficient *A. nidulans*

were able to utilize glucose in the presence of propionate, an MCL-deficient strain was not. This suggested that a lesion in the pathway at this step resulted in a more severe phenotype. By way of hypothesis, the TCA cycle aconitase, which appears to serve a dual function in the methylcitrate cycle for organisms lacking *acnM,* was suggested as a possible point of inhibition.

Eukaryotic aconitases have been shown to bind and catalyze the reverse reaction of 2-methylisocitrate to methyl-cis-aconitate. Thus, an accumulation of 2-methylisocitrate could inhibit the aconitase function in the TCA cycle, leading to citrate accumulation (Brock 2005). ACN-deficient strains very quickly develop secondary site mutations to compensate for their poor growth phenotypes. This indicates that citrate accumulation could be quite deleterious for the cell (Viollier et al 2001, Koziol et al 2009, Baumgart et al 2011).

- Inhibition of NADP+ isocitrate dehydrogenase

2-methylcitrate, tested against enzymes prepared from rat liver, caused inhibition of a number of enzymes that normally interact with citrate or isocitrate, including citrate synthase, aconitase, NAD+ and NADP+ isocitrate dehydrogenases, and phosphofructokinase. Under the conditions tested, ATP citrate lyase and acetyl-CoA carboxylase were not inhibited. Inhibition of the citric acid cycle enzymes could have the effect of increasing the ratio of acetyl-CoA and acyl-CoA relative to free CoASH as well as blocking gluconeogenesis through a fall in ATP from citric acid cycle inhibition (Cheema and Dhadli 1975).

2-methylisocitrate was found to be a potent inhibitor of the NADP isocitrate dehydrogenase (ICD) enzyme from bovine heart, rat liver, and porcine heart, competitive with isocitrate. The extent of this effect was shown to be dependent on the isomers used, with a mixture or erythro- and threo- decreasing the inhibition seen. D-threo-2-methylisocitrate is the form expected to be produced by the aconitase enzyme (Plaut et al 1975, Beach et al 1977).

The (2R, 3S) 2-methylisocitrate isomer was the only form to competitively inhibit the isocitrate dehydrogenase in crude extracts of *A. nidulans* grown in glucose or acetate. Interestingly, isocitrate dehydrogenase activity measured from extracts on an MCL-deficient *A. nidulans* strain grown on different carbon sources, was higher than WT in every condition, including those with propionate, except on lower concentrations of acetate, where they were similar. This was interpreted as an indication that inhibition by 2-methylisocitrate was sensed and compensated for by upregulation of activity (Brock 2005).

- Sequestration of metabolites

The accumulation of non-metabolizable propionyl-CoA (and methylmalonyl-CoA) could exert inhibition at the level of 'trapping' CoA. This could in turn affect processes that make use of thioesters, including fatty acid, sterol, and polyketide synthesis (Brock et al 2000). In the case of 2-methylcitrate or 2-methylisocitrate accumulation, these metabolites act as a sink of

oxaloacetate, which is competed away from the citrate synthase by MCS, and is not easily regenerated by the alternative carbon source (Brock 2005).

Propionyl-CoA and methylmalonyl-CoA accumulation in rat liver hepatocytes was correlated with a wide range of metabolic sequelae, including decreased pyruvate dehydrogenase activity, fatty acid oxidation, gluconeogenic defects, and ureagenesis defects (Brass 1992, Glasgow and Chase 1976).

- Inhibition of fructose-1,6-bisphosphatase (FBPase)

As FBPase is allosterically bound and stabilized by citrate (Hines et al 2006, Hines et al 2007), it was hypothesized that an excess of 2-methylcitrate could cause binding and inhibition of gluconeogenic activity. Consistent with this, cell extracts from cultures grown with increasing amounts of propionate had decreasing FBPase activity.

Glucose could partially alleviate the growth inhibition of propionate on succinate of the *prpC* mutant of *S*. Typhimurium. In agreement with the hypothesis, overexpression of FBPase could also restore the growth in the absence of glucose on low concentrations of glucose (Rocco and Escalante-Semerena 2010).

- Inhibition of secondary metabolism

High concentrations of propionate resulted in the loss of polyketide-derived spore color in wild-type *A. nidulans*. The same effect was seen for an

MCS-deficient strain but on a mixture of glucose and propionate (Brock et al 2000). Other phenotypes seen in the wild-type on high concentrations of propionate, including the inability to synthesize a polyketide, sterigmatocystin (ST), the loss of a sexual spore pigment, and the inhibition of sexual development, were all phenocopied by an MCS-deficient strain, but in the absence of propionate (Zhang et al 2004).

As an overexpression of MCS-activity helps to alleviate the phenotype and propionyl-CoA was previously found to be accumulating in the MCS-deficient strain (Brock and Buckel 2004), it was proposed that the excess of propionyl-CoA was out-competing the acetyl-CoA substrate used by the polyketide synthase (PKS) enzymes (Zhang and Keller 2004). Accordingly, the addition of acetyl-CoA resulted in the restoration of spore pigmentation (Brock and Buckel 2004), whereas addition of 2-methylcitrate or pyruvate, downstream metabolites of the methylcitrate cycle, did not (Zhang and Keller 2004).

Loss of pigmentation also occurred with the addition of branched-chain amino acids or odd chain-length fatty acids, indicating alternative sources of propionyl-CoA could cause the defects. Overexpression of propionyl-CoA synthetase exacerbated the phenotype whereas an ACS-deficient strain suppressed it (Brock and Buckel 2004). A deletion of the gene encoding the propionyl-CoA synthetase in the MCS-deficient background also reverted these phenotypes, whereas a deletion of the acetyl-CoA synthetase in the MCS-deficient background resulted in partial alleviation. These data therefore implicate

propionyl-CoA as the causative agent of secondary metabolism inhibition (Zhang and Keller 2004).

- Citrate synthase as a suppressor mutant

A mutation of the *gltA*-encoded citrate synthase (CS) was able to rescue the growth of an MCS-deficient strain of *S.* Typhimurium on mixtures of propionate with succinate or malate, but not on mixtures with glucose or glycerol. Toxicity was restored by the introduction of *gltA* on a plasmid. Thus, citrate synthase activity in an MCS-deficient background enabled toxicity on propionate, suggesting the formation of 2-methylcitrate, and not propionyl-CoA, as a toxic metabolite (Horswill et al 2001).

Elimination of the citrate synthase in an MCD-deficient background did not rescue toxicity, supporting the idea of 2-methylcitrate as the toxic metabolite. It was further shown that the CS activity introduced into an MCS-/CS-deficient strain was more toxic that introduction of MCS activity. The authors postulated that the 2-methylcitrate produced by the CS enzyme was more toxic than 2-methylcitrate produced from MCS. The difference between the metabolites produced could arise from the different enantiomers formed by each synthase reaction, and the toxicity from the inability of the stereospecific MCD to utilize them. Thus, the most deleterious effects are not caused just by a general buildup of the metabolite, but rather by the formation of a dominantly toxic form (Rocco and Escalante-Semerena 2010).

Alternatively, citrate synthase can be seen as competing with and reducing the ability of MCS to bind oxaloacetate, causing toxicity at the level of propionyl-CoA. An increased tolerance to propionate was seen in an *A. nidulans* CS-deficient strain, supporting the idea that propionyl-CoA is more efficiently metabolized in the absence of CS, although competition for aconitase could also occur (Murray et al 2010). The hypothesis could be tested further by uncoupling the oxaloacetate binding and catalytic activities, via site-specific mutations, if these functions are contributed by distinct domains.

1.4.4 Toxic metabolite hypothesis

"There are two basic metabolic methods of killing an organism. Either the flux through an essential metabolic pathway can be decreased to the point where life is no longer possible, or a metabolite concentration can be increased to toxic levels."

(Eisenthal and Cornish-Bowden 1998)

It has become evident that it is not just the loss of a pathway and consequent inability to catabolize a substrate that causes a negative growth phenotype, but also lesions within the pathway that can exert toxicity, from intermediate accumulation. The resulting lack of growth can actually be a dominant inhibition of cellular function that is not alleviated in the presence of alternative substrates.

This has been demonstrated for the Δ*prpDC* and Δ*prpR* strains of *Mycobacterium tuberculosis* for growth on propionate (in the presence of acetate or glucose) and cholesterol (in the presence of glycerol), respectively (Munoz-Elias and McKinney 2006, Griffin et al 2012).

A toxic metabolite hypothesis on dominant inhibition (Figure 1.21) postulates that an interruption in a metabolic pathway leads to buildup of intermediates upstream of the lesion. The accumulation may lead to spillover into other, perhaps unrelated, pathways. As a corollary, the growth defects can

be reverted by additionally interrupting a step upstream of the toxic metabolite-generating step, assuming that this lesion does not, itself, generate toxic metabolites. Although the catabolic pathway remains non-functional, an alternative growth substrate can be used.

The demonstration of this reasoning was carried out with mutant strains of the methylcitrate cycle in *Mycobacterium smegmatis*. A strain lesioned in the MCL-catalyzed step of the pathway exhibited dominant inhibition by propionate on the ability to use glucose. This growth inhibition on glucose was relieved by the further elimination of the upstream steps (MCS, MCD) of the pathway. The removal of the pathway served to prevent the formation of the toxic metabolite and, paradoxically, allowed for improved growth on the alternative carbon source (Upton and McKinney 2007).

As there is evidence from a number of organisms on accumulating metabolites and dominant toxicity for mutants of the methylcitrate cycle, the toxic metabolite hypothesis constitutes a third possible explanation for the *in vivo* attenuation of the ICL/MCL-deficient strain of *M. tuberculosis*. Namely that the methylcitrate cycle acts as a detoxification pathway *in vivo* that can be knocked out without consequence (as with Δ*prpDC*), but perhaps cannot be interrupted (as with *icl1::hyg icl2::aph*) due to dominant toxic effects. The work presented here also aims to explore this possibility.

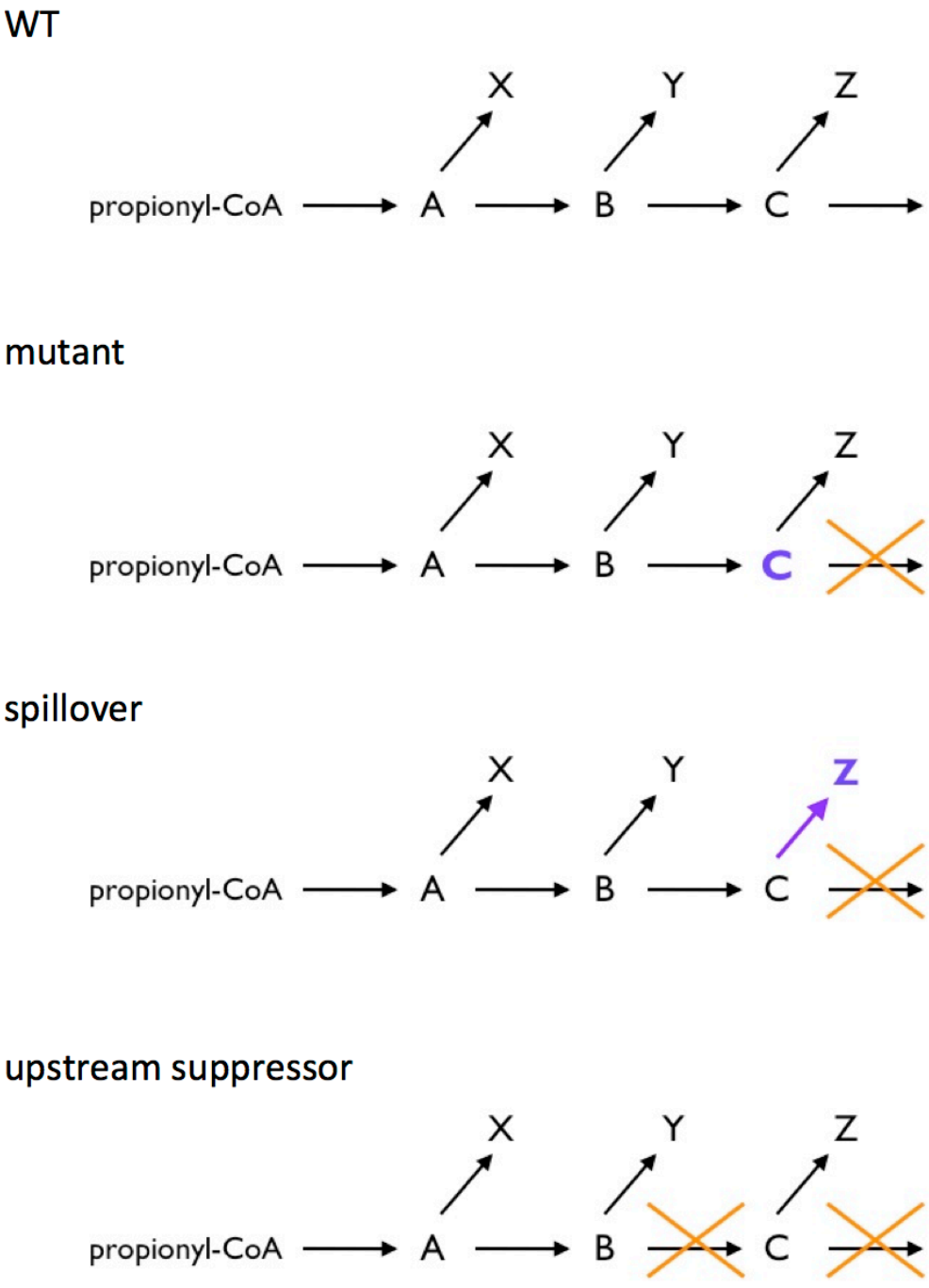

Figure 1.21 Schematic of the toxic metabolite hypothesis. When a pathway is blocked in the mutant strain, accumulation of toxic intermediate C occurs. Excessive amounts of this metabolite may enter alternative or unrelated pathways from spillover. Making an additional mutation upstream of the formation of the toxic metabolite prevents the accumulation and relieves the toxic effects.

2. Experimental Results & Discussion

2.1 Studies of the propionate metabolism pathways of *M. smegmatis*

To investigate carbon metabolism in mycobacteria, the use of *Mycobacterium tuberculosis* as the organism of study presents significant challenges. In addition to the requirement for a BSL3 biohazard facility and a slow doubling-time of ~20-24 hours, there is great difficulty in cultivating the organism on truly minimal media containing only a single potential carbon source. Standard Middlebrook 7H9 growth media contains glutamate, which can serve as both a nitrogen and carbon source for mycobacteria, bovine serum albumin, a potential source of amino acids, and the dispersal agent Tween80, which can be hydrolyzed by mycobacteria to produce oleic acid esters. Dubos medium is based on copious amounts of glycerol and employs asparagine as a nitrogen source, which can also be catabolized as a carbon source. Tyloxapol (WR-1339) can be substituted as the dispersal agent and is widely cited as, and believed to be, 'non-hydrolyzable' (Vandal et al 2008).

In contrast, *Mycobacterium smegmatis*, a close relative of *M. tuberculosis*, is a non-pathogenic mycobacterium with a generation time *in vitro* that is about 4 to 10 times shorter (depending on the medium employed), which has made it a model organism for many aspects of study of the tubercle bacillus. Of relevance

to this study, *M. smegmatis* is capable of growth on minimal salts media without the presence of a dispersal agent, allowing for investigations into single carbon substrate usage with relative ease.

M. smegmatis was initially isolated, and thusly named, from chancre secretions, but is more often found in soil as a saprophytic, free-living organism. The widely used 'wild-type' mc^2155 strain of *M. smegmatis* for genetic studies is actually an 'efficient plasmid transformation' (*ept*) mutant (Snapper et al 1990) isolated from the rough colony variant mc^26 parent (which itself was one of three colony morphotypes found in the reference strain ATCC 607, designated mc^21) (Jacobs 2000).

As the *M. tuberculosis* complex (MTC) comprising several slow-growing pathogenic species is thought to have descended from an ancestral soil bacterium (Cole et al 1998), studying a modern-day soil-dwelling bacterium of the same genus, such as *M. smegmatis*, is of interest from an evolutionary perspective. *M. smegmatis* strains lacking ICLs (Δ*icl1* Δ*icl2*) (L. Merkov PhD thesis, 2006), MCL and ICLs (Δ*prpB* Δ*icl1* Δ*icl2*), and the methylcitrate cycle enzymes MCD, MCL, MCS (Δ*prpDBC*) in combination with ICL (Δ*prpDBC* Δ*icl1* Δ*icl2*) (Upton and McKinney 2007) were previously generated to study the impact of loss or interruption of the methylcitrate cycle in this species.

Here, work is presented that investigates the contribution of an alternative route of propionate metabolism, the methylmalonyl-CoA pathway, to the growth of *M. smegmatis* in various carbon substrates and mutant backgrounds. To

lesion the methylmalonyl-CoA pathway, the last enzyme of the pathway, the vitamin B12-dependent methylmalonyl-CoA mutase, forming the citric acid cycle product succinyl-CoA, was chosen. This strategy avoids disruption of the propionyl-CoA carboxylase (PCC) or methylmalonyl-CoA epimerase (MMCE) reactions, which are required for methyl-branched lipid biogenesis and appear to be essential (Griffin et al 2012).

2.1.1 Methylmalonyl-CoA Mutase (MCM) in *M. smegmatis*

Based on the homology-based annotation of the SmegList database, the corresponding genes encoding the methylmalonyl-CoA mutase enzyme were found in a largely conserved location, 150 base pairs (bp) downstream of a divergently transcribed 'conserved hypothetical' open reading frame (MSMEG_3157) of 245 amino acids (aa). The small subunit *mutA* (MSMEG_3158) of 623 aa, was separated by only a 1 bp gap from the *mutB* large subunit (MSMEG_3159) of 751 aa. Following a 7 bp gap, the *meaB* (MSMEG_3160) homolog was found, of 325 aa in length, misannotated as an 'LAO/AO transport system ATPase'. After a 52 bp intergenic region, a small 166 aa ORF was found (MSMEG_3161) encoding a 'conserved hypothetical protein' with no homolog in *M. tuberculosis*. A BLAST search using the sequence from an analogously located, small gene from the MCM locus in *Saccharopolyspora erythraea* termed *mutR* (Reeves et al 2007) produced a match with the ORF from *M. smegmatis*. (Figure 2.1)

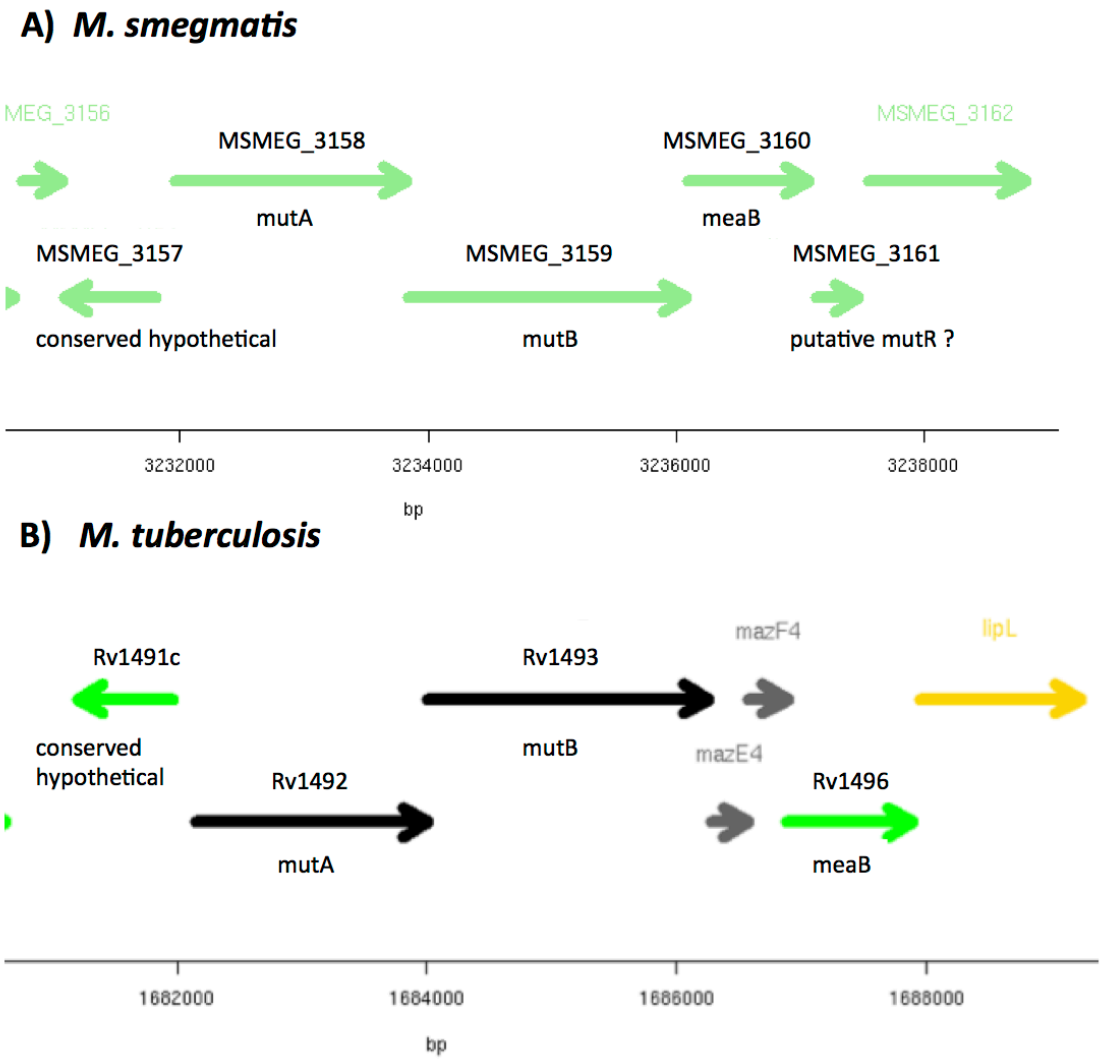

Figure 2.1 Chromosomal locus encoding methylmalonyl-CoA mutase in A) *M. smegmatis* and B) *M. tuberculosis*.

2.1.2 Deletion of *mutAB* in *M. smegmatis*

In-frame and unmarked deletions of the *mutAB* genes were made by allelic exchange, using the two-step counter-selection method (Pelicic et al 1996a, Pelicic et al 1996b). Homologous flanking regions were amplified from genomic DNA that resulted in an in-frame fusion of the first 3 codons of *mutA* to the last 7 codons of *mutB*, with an AvrII site to replace the genomic locus. The Δ*mutAB* deletion was made in the wild-type (WT) mc^2155, Δ*prpDBC*, Δ*icl1* Δ*icl2*, Δ*prpB* Δ*icl1* Δ*icl2*, and Δ*prpDBC* Δ*icl1* Δ*icl2* strain backgrounds (Upton and McKinney 2007, L. Merkov PhD thesis 2006). The Δ*mutAB* deletions were confirmed by PCR amplification using primers binding outside of the cloned region. (Figure 2.2)

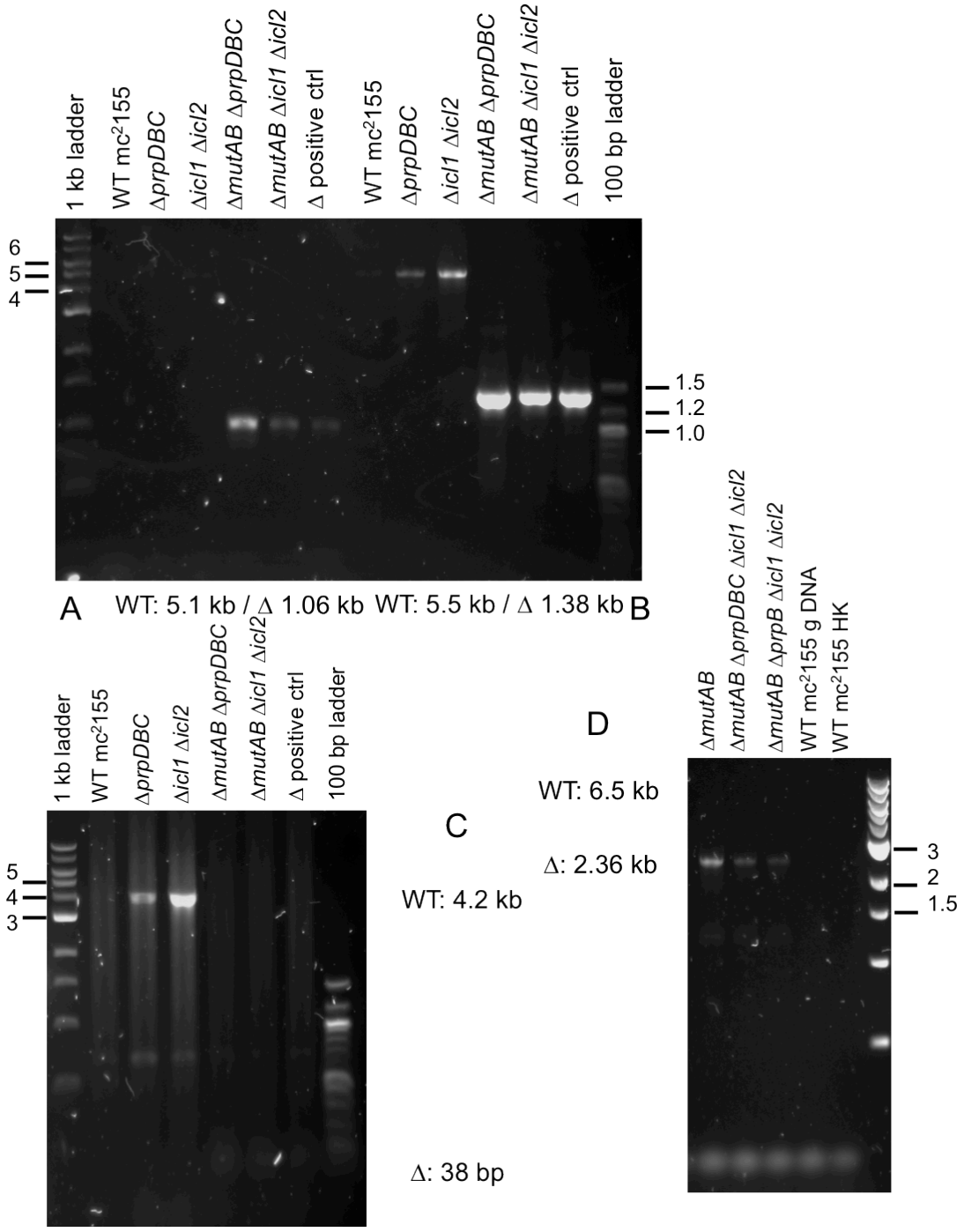

Figure 2.2 PCR confirmation of the chromosomal Δ*mutAB* deletion in *M. smegmatis*. Primers in A & B amplify in 2 parts, Primers in C amplify across gene, Primers in D amplify across homology arms. WT 6.5 kb product is too large to be amplified.

2.1.3 *in vitro* characterization by growth curve analysis

The Δ*mutAB* strains of *M. smegmatis* were initially characterized by growth in liquid culture media, measured by optical density (OD) at 600 nm (OD_{600}), in M9 minimal media base with carbon substrates added at 0.1% or 0.5% weight/volume (w/v) to compare growth to the corresponding parental strains.

- Relative contributions of the methylcitrate and methylmalonyl-CoA pathways

WT *M. smegmatis* could grow quite robustly on 0.5% propionate as a sole carbon source. Higher concentrations were not tested in liquid culture media, but 1% propionate was found to be inhibitory in M9 solid culture medium. The methylmalonyl-CoA mutase mutant (Δ*mutAB*) strain had no detectable phenotype for growth on propionate relative to the WT. In contrast, the methylcitrate cycle mutant (Δ*prpDBC*) strain exhibited a significant lag and slower doubling time for growth. This lag did not disappear upon subsequent re-inoculation from exponential phase cultures. In contrast, the double pathway mutant (Δ*mutAB* Δ*prpDBC*) exhibited no growth on 0.5% propionate. (Figure 2.3) Similar results were obtained when the Δ*mutAB* Δ*prpDBC*) mutant was tested on a lower (0.1%) concentration of propionate (data not shown). Thus, the methylcitrate and methylmalonyl-CoA pathways appeared to be the only routes for propionate metabolism for *M. smegmatis* under the tested conditions.

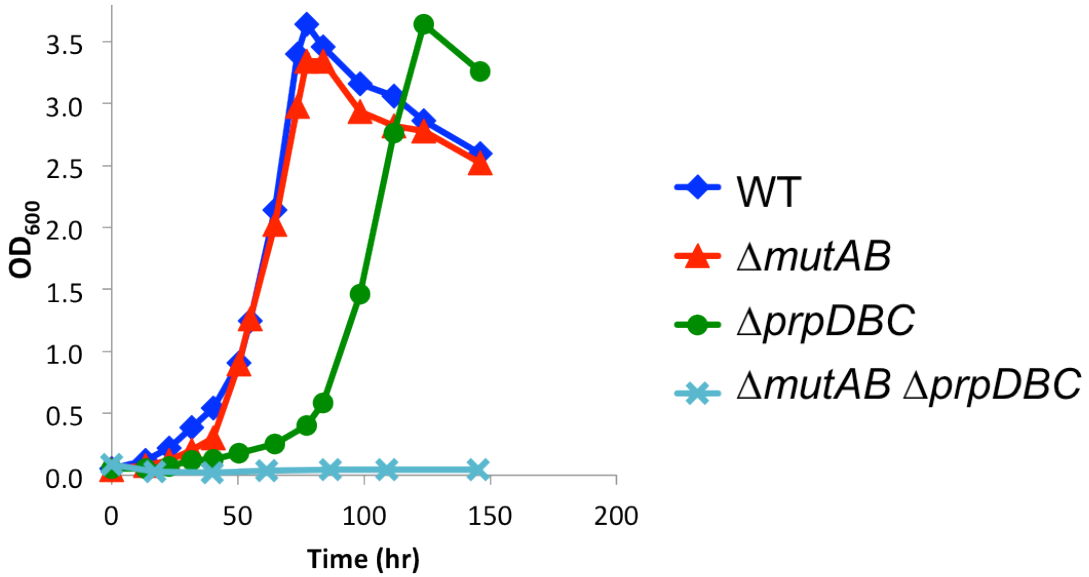

Figure 2.3 Growth of *M. smegmatis* strains in M9 + 0.5% propionate.

- Activation of the methylmalonyl-CoA pathway by B12 supplementation

To determine if the growth 'lag' of the Δ*prpDBC* strain was due to an adaptation period, the propionate-grown cultures were re-inoculated into propionate media from exponential phase in parallel with WT. This procedure did not eliminate the lag or allow for an earlier onset of growth. (Figure 2.4) As this strain would be relying upon the adenosylcobalamin-dependent pathway for growth on propionate, it was hypothesized that perhaps the delay was caused by the time required for B12 synthesis.

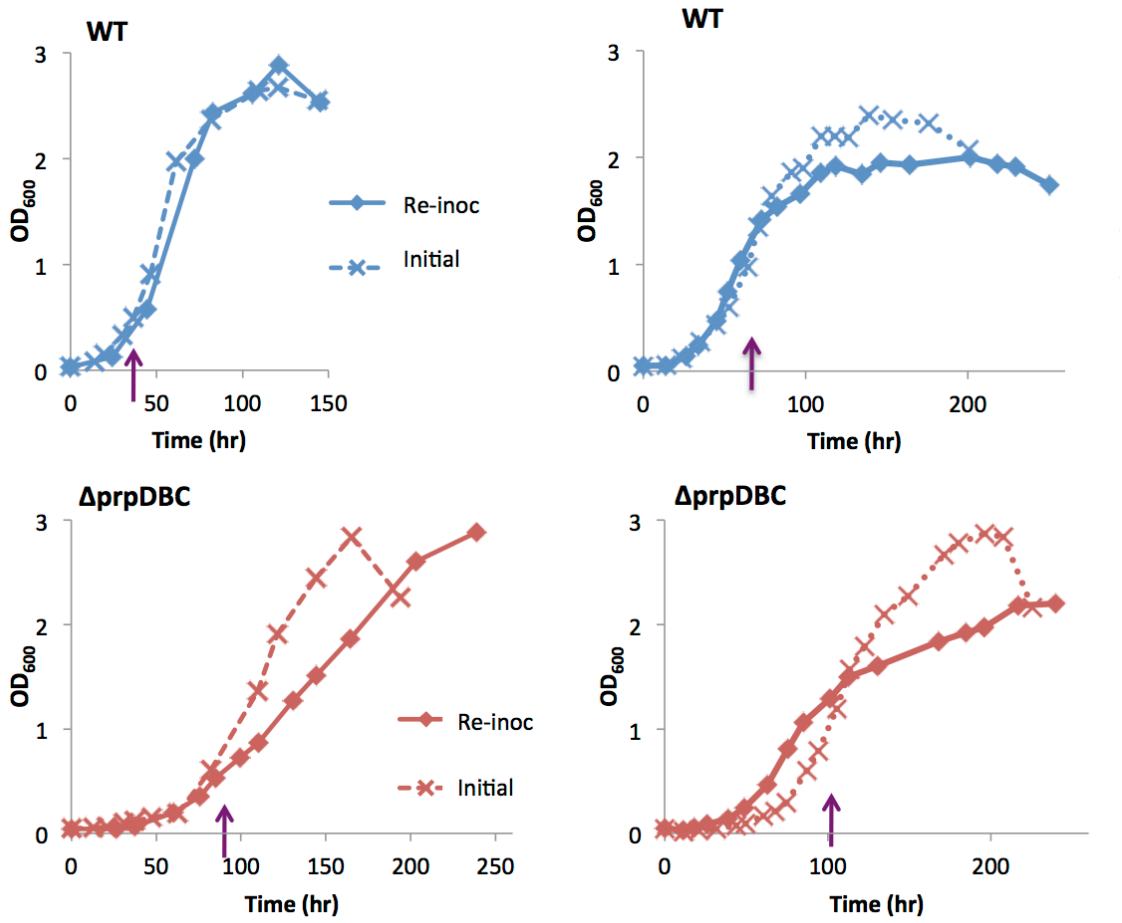

Figure 2.4 Initial vs. re-inoculation (Re-inoc) growth of *M. smegmatis* in M9 liquid medium + 0.5% propionate; arrow indicates time at which initial growth was taken for re-inoculation.

To test whether vitamin B12 was limiting for growth of the Δ*prpDBC* strain on propionate, exogenous B12 was added in the commercially available cyanocobalamin form, at increasing concentrations of 0, 10, 20, 50, and 100 ug/mL. (Figure 2.5A) B12 addition resulted in the dose-dependent improvement of the growth kinetics of the Δ*prpDBC* strain, achieving WT levels at 100 *μ*g/mL. Higher concentrations or pre-incubations of B12 were not tested.

To ensure that the B12 'rescue' was MCM-dependent, 100 μg/mL cyanocobalamin was added to all four strains (the WT parental strain, the Δ*prpDBC* and Δ*mutAB* single-knockout strains, and the Δ*mutAB* Δ*prpDBC* double-knockout strain) when inoculated into propionate media. Despite addition of cyanocobalamin to the medium, the Δ*mutAB* Δ*prpDBC* strain remained unable to grow on propionate as the sole carbon source. The stimulatory effect on growth was seen only for the Δ*prpDBC* strain, suggesting that the methylmalonyl-CoA pathway in the WT strain could not be (further) activated to contribute to growth as measured by OD. (Figure 2.5B) These results suggest that the methylcitrate cycle is the dominant pathway for growth on propionate, under the tested conditions, while the methylmalonyl-CoA pathway plays a secondary role but can fully compensate for loss of the methylcitrate cycle if the growth medium is supplemented with cyanocobalamin.

- Growth phenotypes of the ΔmutAB ΔprpDBC double-knockout strain

All four strains (WT, Δ*prpDBC*, Δ*mutAB*, and Δ*mutAB* Δ*prpDBC*) were capable of growth on M9 minimal medium containing glucose, but the Δ*mutAB* Δ*prpDBC* strain reproducibly exhibited a slower doubling time of ~7-8 hr as compared to ~5-6 hr for WT and single-pathway (Δ*mutAB* or Δ*prpDBC*) mutants (data not shown). The Δ*mutAB* Δ*prpDBC* strain displayed a similar growth defect when cells were grown in 7H9-based media supplemented with ADS (albumin, dextrose, saline). This growth defect in liquid media corresponded to a lag in

appearance of colony-forming units (CFU) on M9, LB, or 7H10+ADS solid culture media as compared to the parental strains. Preliminary results showed that addition of 0.5% glycerol to the 7H10+ADS media eliminated the lag (data not shown). Attempts to test for glycerol 'rescue' in liquid culture were impeded by the excessive aggregation (clumping) of *M. smegmatis* cells on this medium in the absence of detergent, suggesting that glycerol might affect the composition and physical properties of the cell wall.

The Δ*mutAB* Δ*prpDBC* strain also exhibited altered colony morphology on M9 and LB solid culture media, forming smaller, smoother, and rounder colonies, suggestive of differences in cell wall composition (data not shown). Interestingly, it was noticed that both the Δ*mutAB* and Δ*mutAB* Δ*prpDBC* strains had a darker, orange-toned coloration to the pellets formed when cells were collected by centrifugation, presenting a phenotype that is caused by MCM deficiency (data not shown).

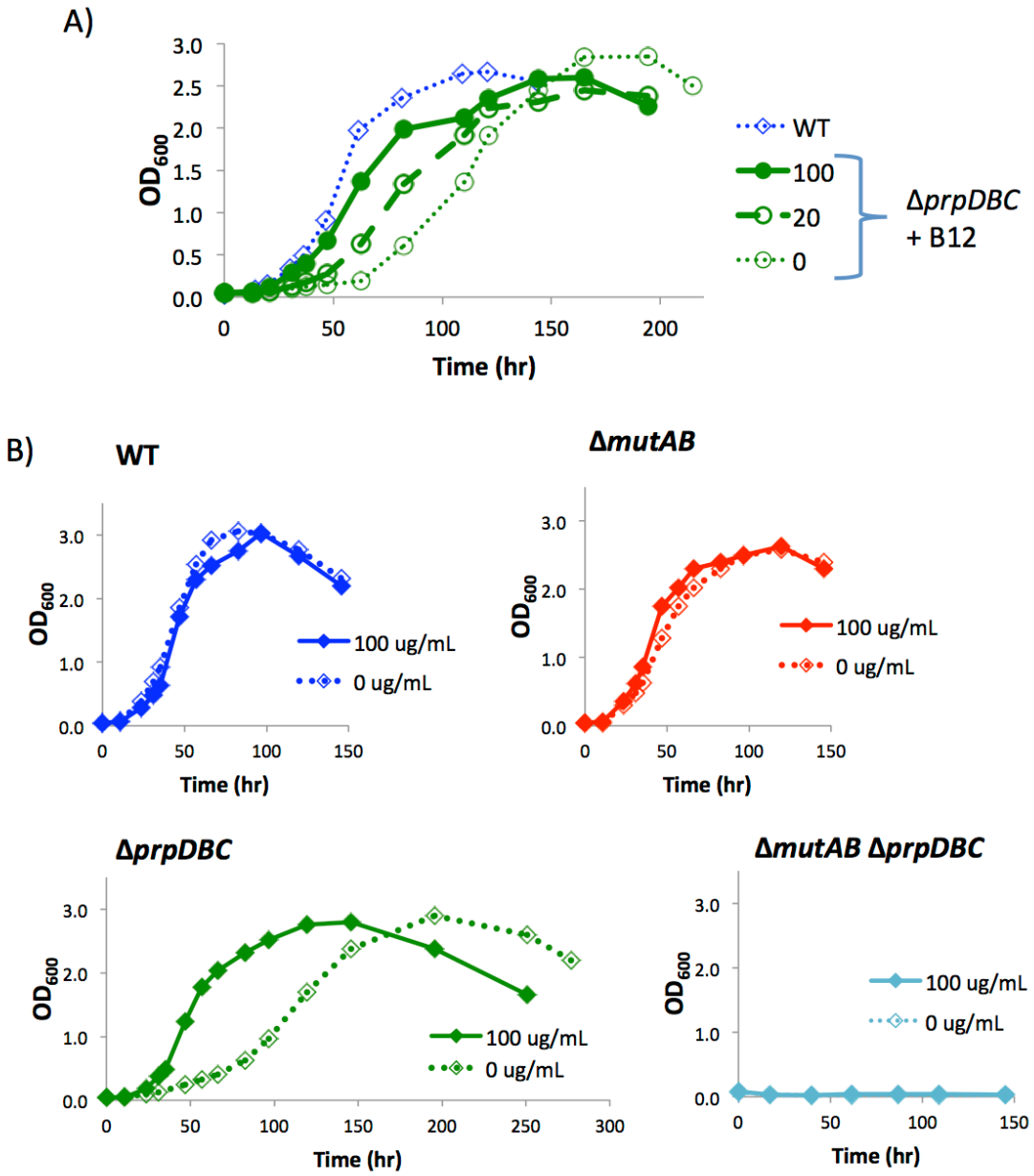

Figure 2.5 A) Addition of cyanocobalamin (Vitamin B12) in μg/mL to *M. smegmatis* grown in M9 + 0.5% propionate. B) Growth of *M. smegmatis* strains in M9 + 0.5% propionate with or without addition of 100 μg/mL cyanocobalamin (vitamin B12).

- Methylcitrate cycle and MCM are dispensable for growth on acetate

Growth of the methylcitrate cycle and methylmalonyl-CoA mutase mutants was examined on acetate-containing media to verify that these propionate-metabolizing pathways did not affect growth upon C2 substrates. The strains were inoculated alongside ICL-deficient (Δ*icl1* Δ*icl2*) and MLS-deficient (Δ*glcB*) strains to confirm their respective phenotypes on acetate. Although dispensable for growth on glucose (data not shown), ICLs were found to be essential for growth upon acetate, while MLS was previously found to be dispensable due to the presence of the alternative glyoxylate-carboligase (*gcl*)-mediated route for glyoxylate metabolism identified in *M. smegmatis* (L. Merkov PhD thesis, 2006).

The WT, Δ*mutAB*, Δ*prpDBC*, and Δ*mutAB* Δ*prpDBC* strains grew with similar kinetics in medium containing 0.5% acetate as the sole carbon source, whereas the Δ*icl1* Δ*icl2* strain was unable to grow and the Δ*glcB* strain grew with a slight lag. (Figure 2.6A) Of potential interest, addition of vitamin B12 to the strains when inoculated into acetate-containing medium appeared to affect the peak OD reached; this effect was MCM-dependent as it was not observed for the Δ*mutAB* or Δ*mutAB* Δ*prpDBC* strains. (Figure 2.6B) Although these findings are preliminary, they might indicate a convergence of acetate metabolism with propionate metabolism at the level of the MCM-catalyzed reaction.

- Role of glyoxylate cycle for anaplerosis on propionate

As the ICL activity of *M. smegmatis* can be eliminated without affecting the methylcitrate cycle (this is not possible for *M. tuberculosis*, which lacks a dedicated MCL enzyme), the requirement for the glyoxylate cycle on both propionate-metabolizing pathways could be addressed directly. To this end, growth of the propionate pathway mutants (Δ*mutAB* and Δ*prpDBC*) was compared in the presence and absence of glyoxylate cycle activity, by introducing the propionate pathway mutations into WT and Δ*icl1* Δ*icl2* genetic backgrounds. The absence or presence of ICL activity had no apparent effect on the growth kinetics of any of the mutant strains tested in 0.5% propionate liquid culture medium. Nor did ICL or MLS deficiency affect growth in liquid medium containing 0.5% propionate, confirming that the glyoxylate cycle is not required for growth on this substrate. (Figure 2.7)

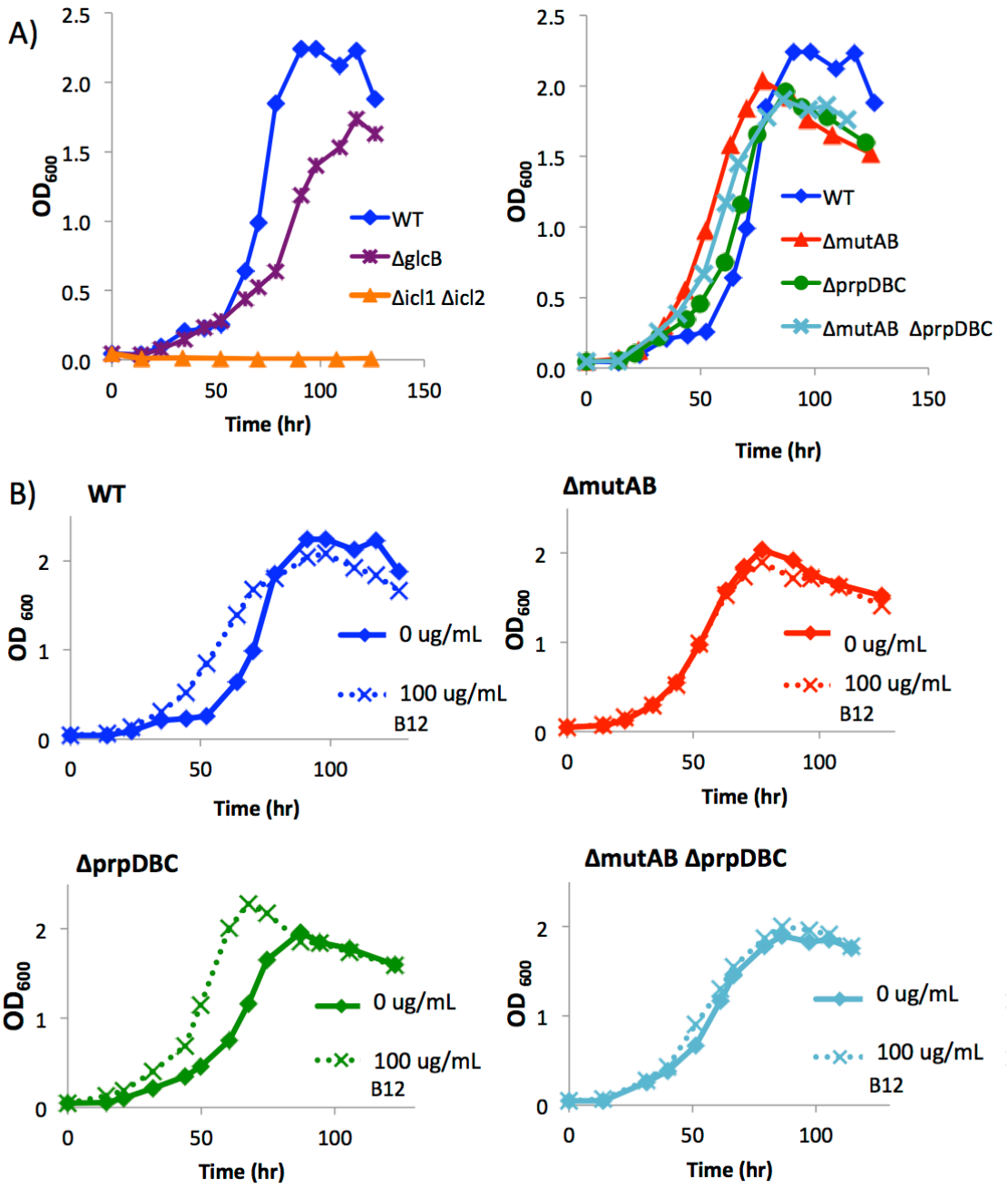

Figure 2.6 A) Growth of *M. smegmatis* strains in M9 + 0.5% acetate. B) Growth of *M. smegmatis* strains in M9 + 0.5% acetate with or without addition of 100 μg/mL cyanocobalamin (vitamin B12).

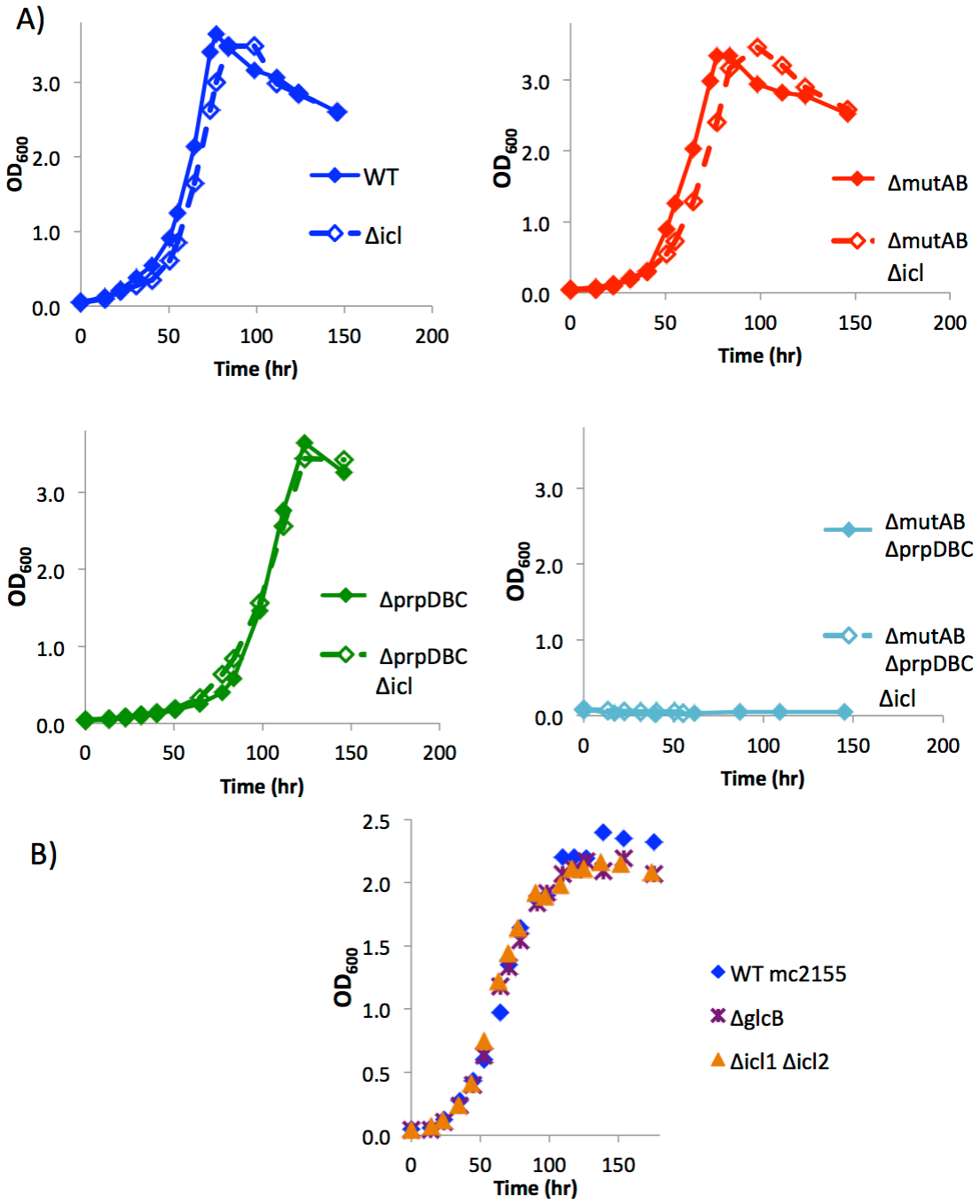

Figure 2.7 A) Growth of *M. smegmatis* strains in M9 + 0.5% propionate. B) Growth of *M. smegmatis* strains in M9 + 0.5% propionate.

2.1.4 Dominant growth inhibition and toxicity of propionate

Although the Δ*mutAB* Δ*prpDBC* strain was capable of growth on medium containing glucose as the sole carbon source, albeit with a slightly slower doubling rate, addition of 0.5% propionate to the medium partially inhibited growth of the mutant on liquid culture medium containing 0.1% glucose; a growth lag and overall lower growth yield were observed as compared to cultures containing glucose alone. (Figure 2.8) In contrast, the WT, Δ*mutAB*, and Δ*prpDBC* strains could utilize both carbon substrates (propionate and glucose). Addition of glucose improved the growth kinetics of the Δ*prpDBC* strain on propionate-containing medium, but did not completely revert the lag. (Figure 2.8) This effect appears to be dependent on the ratio of the two substrates provided and could be overcome by increasing the amount of added glucose. However, growth of the bacteria on equal mixtures of glucose and propionate (0.1% : 0.1%) was found to result in increased clumping, making OD measurements unreliable.

To elucidate the viability of the Δ*mutAB* Δ*prpDBC* strain during non-growth in propionate-containing medium, a time series was done by plating culture aliquots for CFU recovery on agar plates at intervals over the course of incubation. In parallel, aliquots of the culture were imaged by fluorescence microscopy 'snapshots' after staining with propidium iodide (PI). PI is a DNA intercalating dye that is excluded from cells with intact membranes; it can enter and fluorescently stain damaged or dead cells and thus can be used as a surrogate marker of viability.

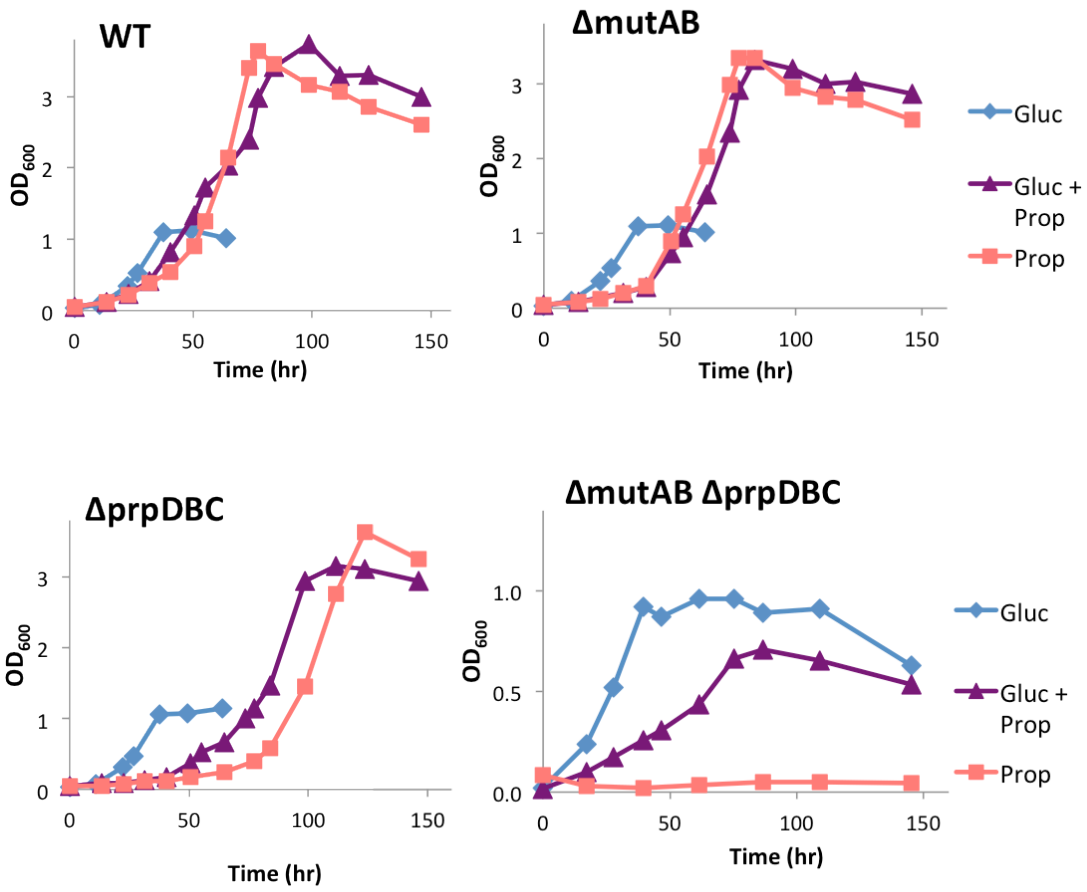

Figure 2.8 Growth of *M. smegmatis* strains in M9 + 0.1% glucose, M9 + 0.5% propionate, or M9 + 0.1% glucose + 0.5% propionate.

Decreasing numbers of CFU were recovered from the culture as a function of time time, resulting in a 'kill curve' kinetic of the Δ*mutAB* Δ*prpDBC* strain from the apparently toxic effects of propionate. (Figure 2.9B) Declining numbers of CFU correlated with an increased proportion of PI-stained cells seen by microscopy, although the latter could not be quantified due to the macroscopically and microscopically visible and progressive aggregation of cells.

(Figure 2.9A) Attempts to use flow cytometry as a means to quantify the PI-positive and PI-negative populations were unsuccessful due to the extent of clumping, which could not be reduced by vortexing with beads, waterbath sonication, or probe sonication.

Surprisingly, incubating the Δ*mutAB* Δ*prpDBC* strain in liquid M9 medium containing no carbon substrate resulted in similar kinetics of cell death as compared to incubation of this strain in medium containing propionate. This effect was not seen when the WT strain was incubated in liquid M9 medium containing no carbon substrate, although the differences in initial inoculation density between experiments gave some variation in the apparent 'stability' of the numbers of CFU over time. (Figure 2.9B) Preliminary data indicates that the Δ*icl1* Δ*icl2* mutant might have a similar, and possibly even more pronounced, phenotype (data not shown).

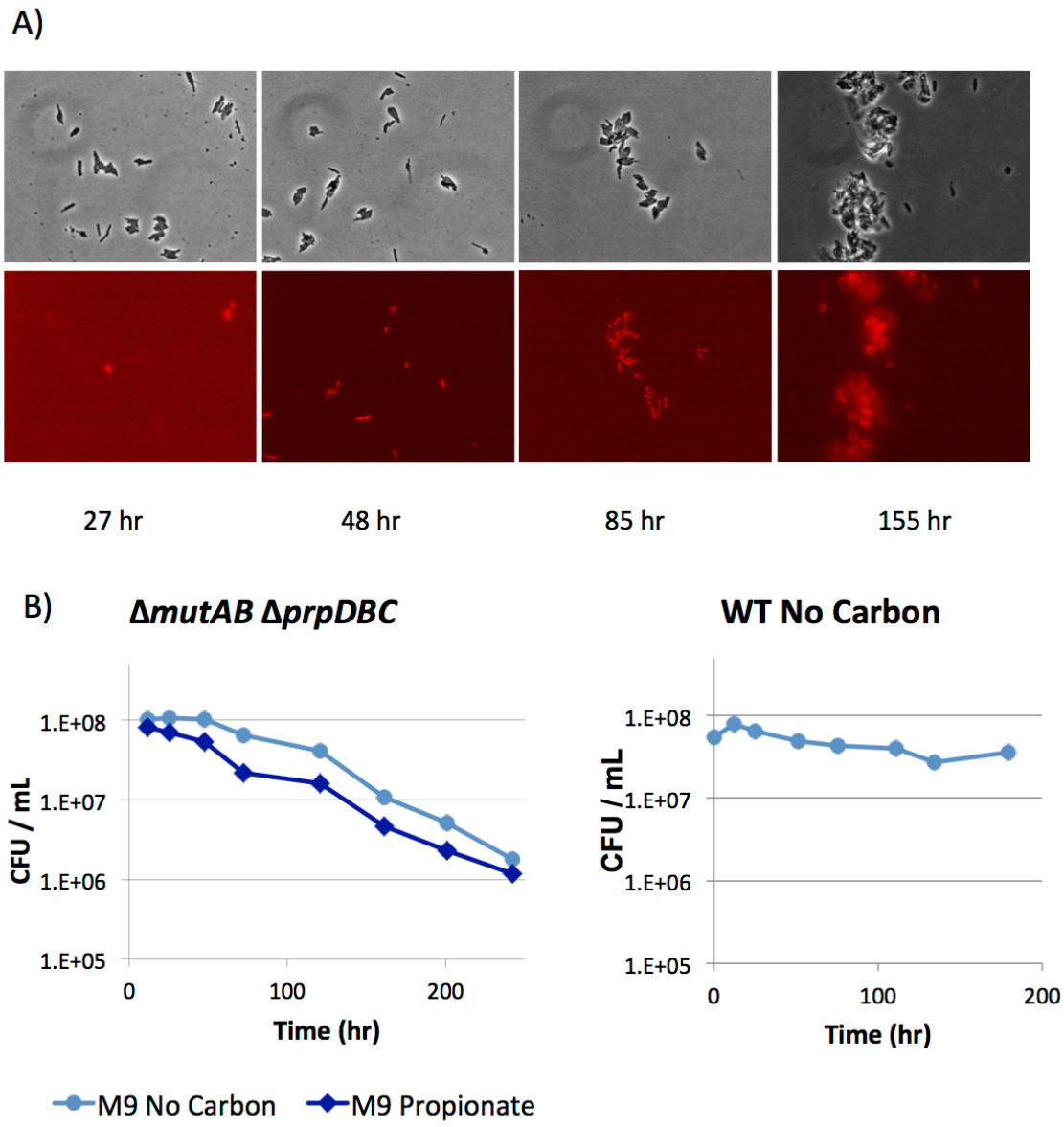

Figure 2.9 A) Propidium iodide (PI) staining, and B) CFU enumeration timecourse of Δ*mutAB* Δ*prpDBC M. smegmatis* incubated in A) M9 + 0.5% propionate, or B) M9 + 0.5% propionate or M9 (no-carbon). Wild-type (WT) control on no-carbon shown.

2.1.5 Complementation with *mutAB* vs. *mutAB meaB* in *M. smegmatis*

Complementation of a Δ*mutAB* Δ*prpDBC* Δ*icl1* Δ*icl2* mutant was attempted using a single-copy *attB*-integrating plasmid that contained the full-length coding sequences of *mutA* and *mutB* along with 174 bp of the upstream intergenic region. This plasmid complemented the growth defect of the Δ*mutAB* Δ*prpDBC* Δ*icl1* Δ*icl2* strain on glucose-containing medium but failed to restore growth on propionate-containing medium.

To account for any promoter elements that might lie further upstream, perhaps within the upstream flanking gene (which is divergently transcribed from *mutAB*), the full-length *mutA* and *mutB* genes were integrated upstream of the Δ*mutAB* deletion, via homologous single-crossover recombination, in a Δ*mutAB* Δ*prpB* Δ*icl1* Δ*icl2* strain. However, this approach still failed to complement the defect for growth on propionate-containing medium.

Taking into consideration the known role of the downstream *meaB*-encoded protection / reactivation factor of the methylmalonyl-CoA mutase enzyme (Korotkova et al 2004), a single-copy *attB*-integrating plasmid was constructed that contained all three genes (*mutA*, *mutB*, and *meaB*) plus 174 bp of the 5'-flanking sequences. Complementation with this plasmid successfully restored growth of the Δ*mutAB* Δ*prpDBC* strain on propionate-containing medium. (Figure 2.10)

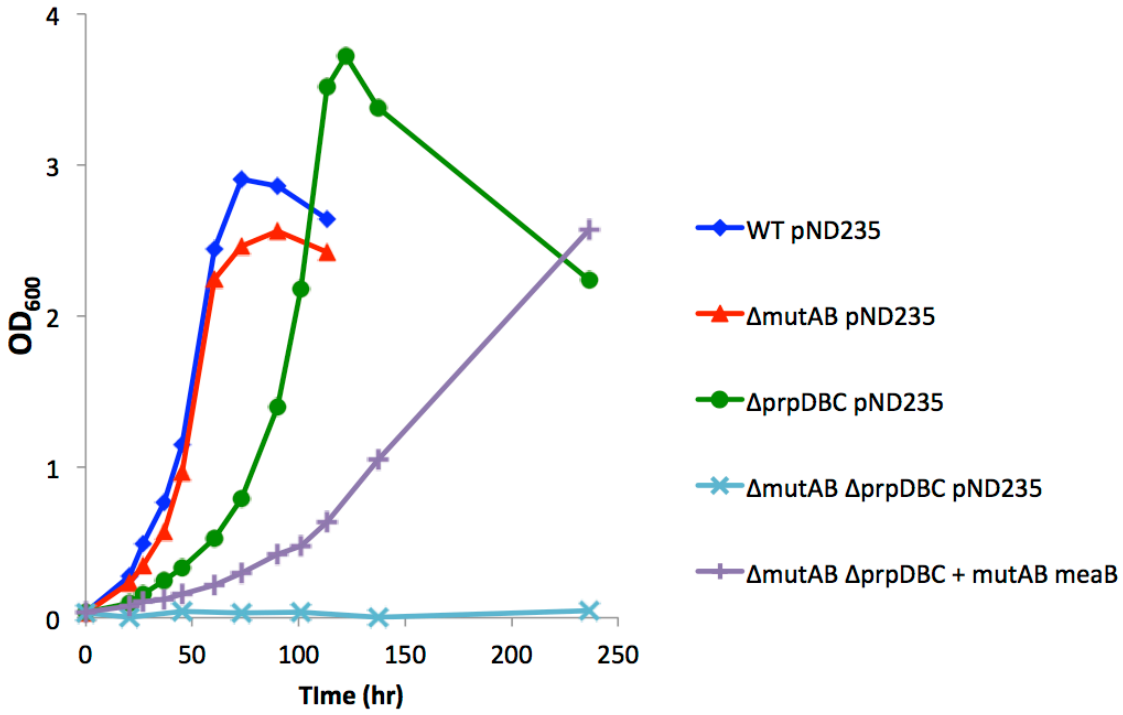

Figure 2.10 Complementation of Δ*mutAB* Δ*prpDBC M. smegmatis* with a single-copy *attB*-integrating plasmid encoding *mutA*, *mutB*, and *meaB*, and strains containing pND235 (empty vector) grown in M9 + 0.5% propionate.

2.1.6 Alternative approaches to studying mutant phenotypes

- Suppressor screen

Initially, a genetic approach was envisaged to elucidate the mechanisms of propionate toxicity by selecting for suppressor mutants that could overcome propionate toxicity and form colonies on agar plates by utilizing an alternative carbon source included in the medium (such as glucose). In practice, however, this approach did not readily work with the Δ*mutAB* Δ*prpDBC* strain, as the 'semi-dominant' nature of 0.5% propionate toxicity in medium that also contained 0.1%

glucose provided only a brief lag period as the window for the selection of 'early' suppressors. Moreover, if the suppressor mutation itself caused a growth defect on the provided alternative carbon source, it would not appear within this window. Thus, despite repeated attempts, no reliably 'early' colonies appeared when the Δ*mutAB* Δ*prpDBC* strain was mutagenized and plated on solid culture medium containing 0.5% propionate and 0.1% glucose.

- Microfluidic-based time-lapse microscopy

The ability to visualize, in real-time, the effect of introducing an inhibitory or toxic compound to a growing population of cells, and the consequence of the compound's withdrawal, would provide a wealth of time-resolved information about the kinetics of growth and the fate of individual cells over time. While the microfluidic-based time-lapse microscopy platform allows for this approach (Balaban et al 2004), a number of confounding factors were found for interpreting the results from this method.

The use of M9 minimal media (vs. the richer 7H9-based medium) resulted in a long adaptation phase to growth in microfluidic devices. The use of fluorescent imaging negatively synergized with 'stress' due to growth on M9 minimal medium and the subsequently added propionate. Thus, cells that were unable to re-grow following a transient exposure to propionate in experiments performed with fluorescence imaging were able to recover when fluorescence was not used.

As an additional complication, there appeared to be a cryptic carbon source in one or more components of the microfluidic device, which was fabricated from a glass cover slip, a micropatterned PDMS chip, and a semi-permeable cellulose membrane. This was evident from the ability of the WT strain to continually grow in liquid medium with no added carbon source in the microfluidic device but not in batch culture flasks with the same medium. Similar results were obtained using an alternative PDMS-based device without the cellulose membrane.

2.1.7 Discussion

Growth assays in which mutants deficient in the known propionate-utilizing pathways of *M. smegmatis* were grown in liquid media containing individual carbon substrates have demonstrated that the methylcitrate cycle and the methylmalonyl-CoA pathway are the only two metabolic routes that appear to operate under these conditions. This conclusion is based on the observation that a Δ*mutAB* Δ*prpDBC* strain with genetic lesions in both pathways was unable to grow with propionate as the sole carbon source. However, the presence of a cryptic pathway for propionate metabolism, which might be operational under different culture conditions, cannot be ruled out.

From the phenotypes of the single-pathway Δ*mutAB* and Δ*prpDBC* mutants, the dominance of the methylcitrate cycle for propionate utilization under standard culture conditions is evident. The lag in the endogenous (but not

exogenous) activation of the methylmalonyl-CoA pathway is presumably due to the time required for induction of *de novo* vitamin B12 synthesis or the time required for a critical level of this cofactor to accumulate (in light of the dose-dependent rescue that was observed). Factors contributing to the regulation of B12 synthesis or of the methylmalonyl-CoA pathway in mycobacteria are yet unknown. The functionality of the putative upstream regulator has not yet been demonstrated. How B12 is able to 'activate' this pathway, whether through transcriptional or post-translational mechanisms, is of interest.

The function of the MeaB protection / activation factor appears to be key, as complementation of the double-mutant Δ*mutAB* Δ*prpDBC* strain was unsuccessful without it. Although the Δ*mutAB* deletion was in-frame, it is possible that a regulatory element for *meaB* expression is located within the coding sequence of *mutB* and is thus missing in the Δ*mutAB* mutant. Alternatively, the proximity of the genes during coupled transcription-translation might have an effect on the subsequent physical association of the translated proteins. The residual difference in growth kinetics of the Δ*prpDBC* strain as compared to the complemented Δ*mutAB* Δ*prpDBC* + *mutAB meaB* strain might indicate that a regulatory factor is absent. This factor could be the identified *mutR* locus that, in *S. erythrea*, led to additional activity of the MCM when included in the plasmid (Reeves et al 2007).

While exogenous addition of the vitamin B12 cofactor for the methylmalonyl-CoA mutase enzyme eliminates the lag of the Δ*prpDBC* strain for

growth on propionate-containing medium, it does not have a further stimulatory effect on the WT strain compared to the Δ*mutAB* strain. This would be consistent with inhibition of the methylmalonyl-CoA pathway by operation of the methylcitrate cycle, or it could imply that the 'maximal' metabolism of propionate is already occurring via the methylcitrate cycle. Either of these hypothetical explanations could be the result of greater affinity of the methylcitrate cycle for the common propionyl-CoA precursor and a rate-limiting activation step. It is also possible that the additional activation of MCM leads to changes in carbon routing that are not measured by the OD readout, such as changes in cell wall composition. However, the latter interpretation is inconsistent with studies in *E. coli* where the addition of vitamin B12 to radiolabeled propionate cultures did not change the routing of the label (Evans et al 1993, Textor et al 1997).

The interesting phenotypes of the Δ*mutAB* and Δ*mutAB* Δ*prpDBC* strains with respect to culture pigmentation (both strains) and colony morphology (Δ*mutAB* Δ*prpDBC* strain) suggest that MCM deficiency might affect the biosynthesis of chromogenic compounds and cell wall components, perhaps due to alterations in the methyl-branched precursor pool upstream of MCM (Zhang et al 2004).

The growth deficiency of the Δ*prpDBC* strain on propionate-containing liquid medium without vitamin B12 supplementation, which persisted when the strain was re-passaged on the same medium, suggests that the routing of propionate through the methylmalonyl-CoA pathway in the absence of

exogenous B12 stimulation is less efficient than the use of the methylcitrate cycle. Alternatively, the persistent growth defect of the Δ*prpDBC* strain could be due to the continual formation and presence of a growth-inhibitory factor that cannot be removed via the methylmalonyl-CoA pathway unless this pathway is further activated by exogenous B12.

The dominant negative effect of propionate on the ability of the Δ*mutAB* Δ*prpDBC* strain to grow on glucose, and the inability of glucose to 'rescue' the lag of the Δ*prpDBC* strain on propionate, both support the idea that defective metabolism of propionate by strains lacking the methylcitrate cycle might result in the accumulation of growth-inhibitory metabolites. Whether or not these metabolites are directly responsible for the 'toxic' effect of propionate on the survival of Δ*mutAB* Δ*prpDBC* cells cannot be determined by these assays, especially in light of the similar kill kinetics of this strain under 'No Carbon' conditions. The unexpected growth phenotype of the Δ*mutAB* Δ*prpDBC* mutant on glucose might indicate some basal carbon flux through the methylcitrate and methylmalonyl-CoA pathways even in the absence of exogenous propionate. One approach to confirm these phenotypes, and to elucidate the underlying mechanisms, is to measure intracellular metabolite levels directly.

2.2 Metabolite analysis of *M. smegmatis*

"Metabolites are the end products of cellular regulatory processes, and their levels can be regarded as the ultimate response of biological systems to genetic or environmental changes." - Oliver Fiehn, 2002

The field of metabolomics, although implying a sense of global coverage, actually involves a number of tradeoffs in the preparation and analysis of samples. Targeted metabolite analysis provides highly quantitative measurements of a limited number of pre-selected metabolites of interest. Alternatively, metabolite profiling provides an unbiased but semi-quantitative approach to identify peaks or patterns of interest among all detectable metabolites (Fiehn et al 2002).

The choice of analytical method determines what information can be retrieved from a sample and how much sample is needed. Approaches based on nuclear magnetic resonance (NMR) spectroscopy provide non-destructive sample analysis but require relatively large amounts of material. Alternatively, approaches based on mass spectrometry (MS) start with the destructive ionization of the sample, often followed by electron bombardment and fragmentation of the sample components, but require only small amounts of material. While MS can accurately measure the analyte 'mass' (actually, the mass-to-ion (m/z) ratio), allowing for identification by formula but unable to

distinguish between mass isomers, NMR provides information about the structure and connectivity of the compound, thus distinguishing between isomers.

Mass spectrometers detect the differences in the m/z ratios of ionized compounds, which are identified either by their accurate mass or by a combination of the 'parent' ion m/z and the subsequently fragmented 'daughter' ion m/z. To increase the analytical power of mass spectrometry, a compound separation step can be performed first, using gas chromatography (GC), liquid chromatography (LC), capillary electrophoresis (CE), or similar techniques, although this adds analysis time and introduces an additional bias of what types of compounds can be detected.

For the measured extract to be a reflection of the state of the metabolites that are present when the sample is taken, the inactivation or 'quenching' of the cell's metabolism, via extreme treatments of cold (liquid nitrogen), heat (boiling), acid, or base, to avoid any subsequent transformations of the contents, should aim to be faster than the cell's turnover of metabolites. Moreover, whether or not the cell mass is 'harvested' and separated from the culture medium before or after the quench step reflects the tradeoff between speediness of quenching and cleanliness of extraction. As there is no 'universal' solvent, the choice of extraction buffer will again introduce biases as to which compounds can be dissolved and detected.

To study the metabolite content of *M. smegmatis*, an effective method of extraction first needed to be identified and validated for the ability to detect

propionate pathway metabolites. This work has been carried out in collaboration with the laboratory of Prof. Uwe Sauer at ETH Zürich. Prof. Sauer is an internationally recognized authority in the field of MS-based microbial metabolomics and all of the MS-based metabolite analysis discussed in this thesis was done in his laboratory. These studies were done with the invaluable assistance, technical expertise, and insight of Michael Zimmermann and Dr. Jörg Büscher.

2.2.1 Extraction methodology

Two extraction methods from the scientific literature – the rapid centrifugation / liquid nitrogen quench / hot buffered ethanol extraction used for *Bacillus subtilis* (Buescher et al 2010) and the fast filter separation / cold methanol : acetonitrile : formic acid quench/extraction solution used for *E. coli* (Rabinowitz et al 2007) – were tested (with some variations) and compared using cultures of wild-type (WT) *M. smegmatis* grown on M9 liquid medium with glucose or propionate as the sole carbon source. Samples were separated by an ion-pairing liquid chromatography (LC) method, optimized for central carbon metabolites, before detection by tandem MS/MS. Metabolites were identified by their retention time (RT) on the LC and optimized parent / daughter mass-ion combination.

The two aforementioned protocols resulted in 'complementary' profiles of detected metabolites. The 'rapid centrifugation' method provided better

extraction of sugar-phosphates, nucleotides, and energy cofactors; the 'fast filter' method provided better extraction of citric acid cycle intermediates, sugars, and propionate-specific metabolites. (Figure 2.11, bracketed) Switching to a hot (78˚C) extraction for the 'fast filter' method enabled improved extraction of CoA-containing molecules (a key aim for this work) and this protocol was preferentially used.

It is not clear whether it is the faster quench times in the 'rapid centrifugation' method or the difference in buffer composition that accounts for the differences in the metabolite profiles. In future, further testing of hybrid techniques or the use of 'serial' extraction to try to capture the residual metabolite content with the alternative buffer could be done to try to optimize the protocol.

2.2.2 Identification of propionate metabolism intermediates

As not all of the propionate pathway metabolites are commercially available, initial detection parameters (tube lens and collision energy) were set by analogy to the structurally related citric acid cycle intermediate, with the requisite change in mass (e.g., methylcitrate parameters based on those for citrate, methylisocitrate adjusted from isocitrate). Notably, when a methylcitric acid standard became available during the course of this work, the authentic parameters matched the predicted set, instilling confidence in their reliability for 2-methyl-cis-aconitate.

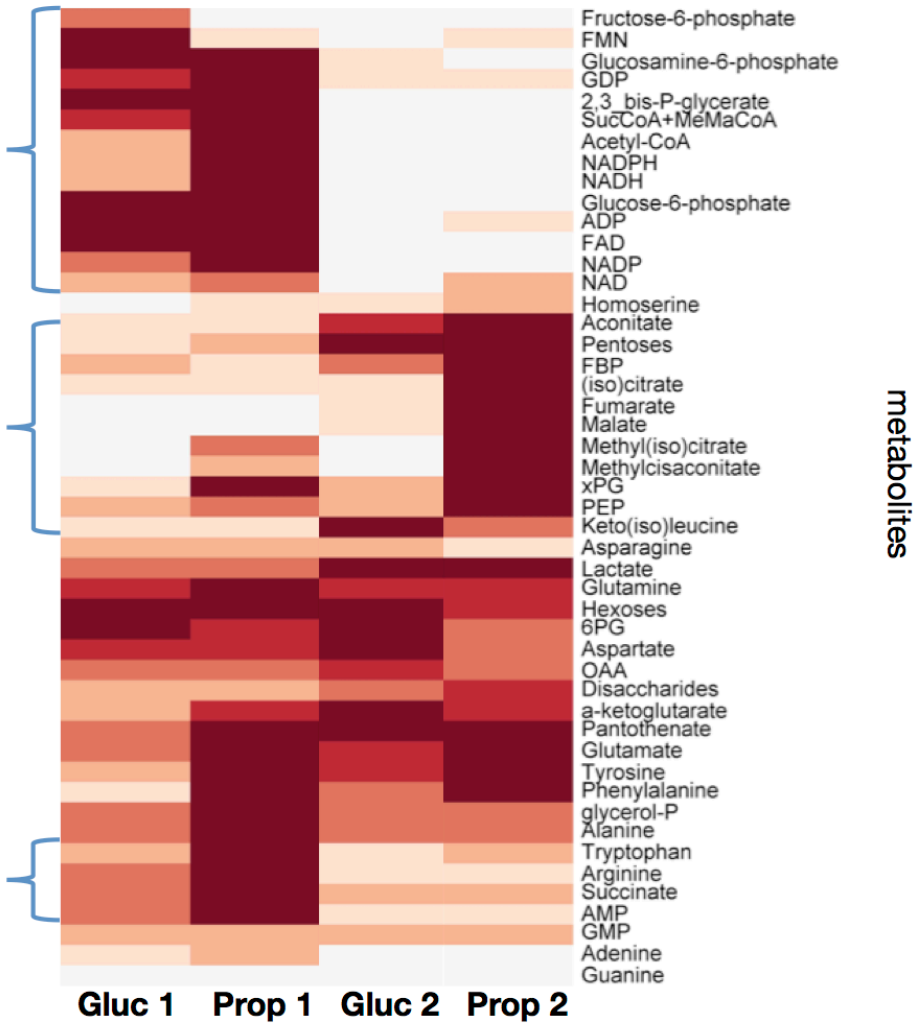

Method	Sampling	Quench	Extract
1	'rapid' spin	liquid N_2	78 deg 60% EtOH + 10 mM NH_4Ac pH 7.2
2	fast filter	-20 deg 40% ACN : 40% MeOH: 100 mM formic acid	

Figure 2.11 Comparison of metabolite profiles of WT *M. smegmatis* grown in M9 + 0.1% glucose or + 0.1% propionate, extracted with Method 1 or Method 2.

In lieu of authentic standards for methylisocitrate and methyl-cis-aconitate, WT and MCL-deficient (Δ*prpB* Δ*icl1* Δ*icl2*) strains of *M. smegmatis* were grown in liquid culture medium with glucose or propionate as the sole carbon source and metabolite extracts were compared as further confirmation of the MS peaks identified as methylisocitrate and methyl-cis-aconitate. Three metabolites that are specific to the methylcitrate cycle (methylcitrate, methylisocitrate, and methyl-cis-aconitate) are expected to accumulate in MCL-deficient bacteria, given the equilibrium of the corresponding reactions in the absence of MCL activity (Horswill and Escalante-Semerena 1999a, Horswill and Escalante-Semerena 2001). (Figure 2.12)

Mass isomers (e.g., methylmalonyl-CoA and succinyl-CoA), which do not separate on a column, might be distinguished by unique fragments generated from the collision reaction or might be calculated from the ratio between the unique peak for the other isomer and the combined peak for common fragments – in effect, subtracting out the contribution of the identifiable isomer. Using this approach, succinyl-CoA was found not to contribute significantly to the measured peak for methylmalonyl-CoA plus succinyl-CoA (data not shown), which will be referred to as 'methylmalonyl-CoA' in the subsequent measurements. The settings for the mass isomers isocitrate and citrate and the isocitrate-unique fragment were previously determined. However, the mass isomers methylcitrate and methylisocitrate could not be distinguished without an authentic standard for methylisocitrate.

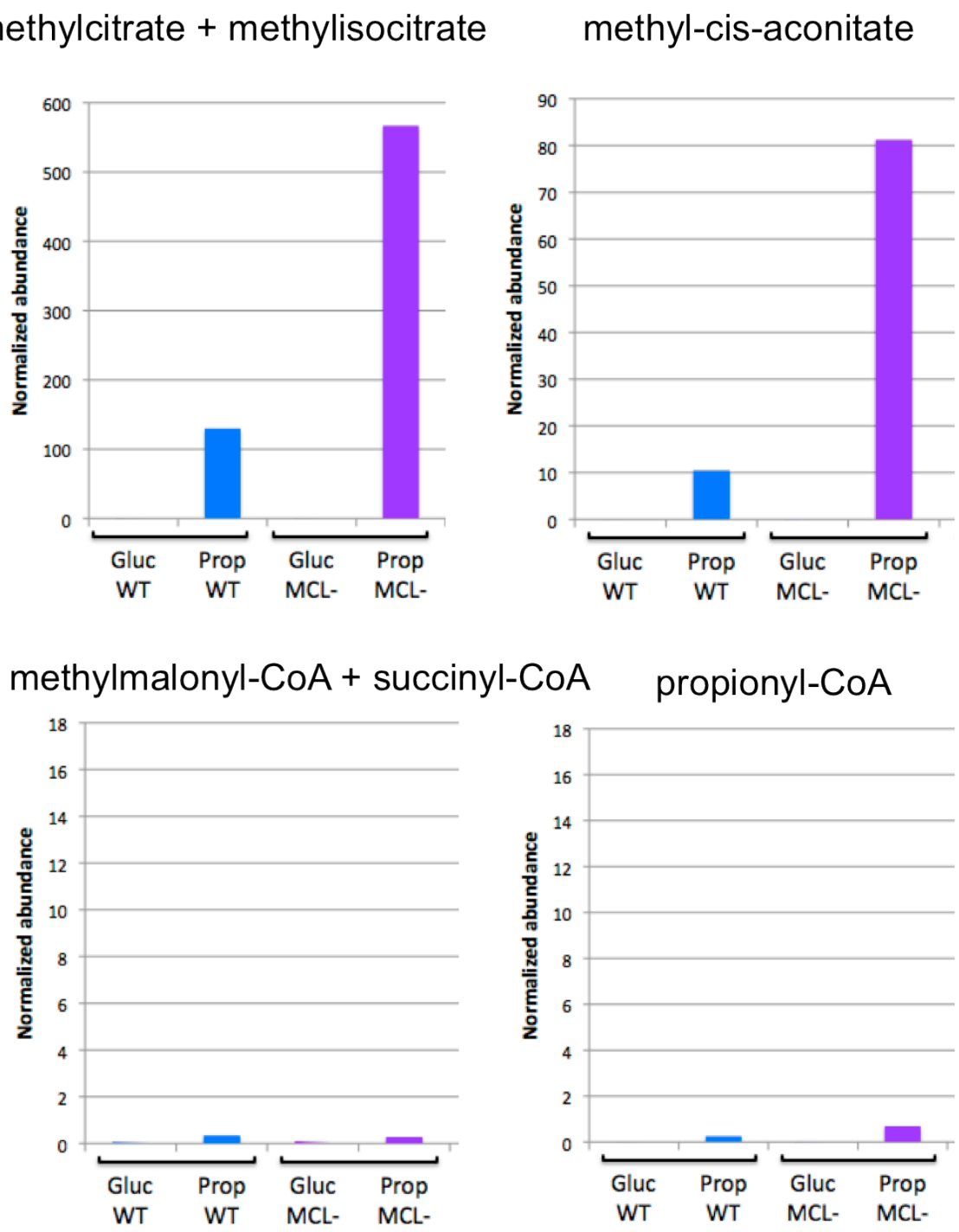

Figure 2.12 Comparison of propionate-specific metabolites from extracts of WT and Δ*prpB* Δ*icl1* Δ*icl2 M. smegmatis* grown in M9 + 0.1% glucose or M9 + 0.1% propionate.

2.2.3 Targeted metabolite analysis

Single time-point extraction experiments were carried out using both methods, with two technical replicates each, but a subsequent 24 hour time course was done with only the fast filtration method and with two independently extracted technical replicates, per culture flask, per time-point. *M. smegmatis* WT, Δ*mutAB*, Δ*prpDBC*, and Δ*mutAB* Δ*prpDBC* strains were grown in M9 liquid culture medium with 0.5% glucose, 0.5% propionate, or 'no-carbon' added. Targeted metabolite data are shown as an average of the replicates at each time-point. Untargeted metabolite data are displayed with dots representing the double measurement of each replicate.

Supernatant samples taken at each time-point were analyzed by HPLC to help establish that the carbon substrates in the media were being 'depleted' as they were (presumably) taken up by the bacteria. The HPLC traces show that propionate was depleted at a lower rate by the Δ*prpDBC* and Δ*mutAB* Δ*prpDBC* strains as compared to the Δ*mutAB* and WT strains. No noticeable differences were detected in the HPLC traces of glucose-grown culture supernatants. (Figure 2.13)

Traces of the methylmalonyl-CoA pathway intermediates depict a time-dependent accumulation of propionyl-CoA and methylmalonyl-CoA in Δ*mutAB* Δ*prpDBC* and, initially, in Δ*prpDBC* cells. Interestingly, the levels of these metabolites in Δ*prpDBC* cells appear to decline at later time-points, which is consistent with the delayed utilization of propionate by this strain. (Figure 2.14)

Evaluation of the methylcitrate cycle metabolites yielded the surprising observation that methylcitrate and methylisocitrate accumulated in Δ*mutAB* Δ*prpDBC* cells. (Figure 2.14) As the methylcitrate cycle enzymes that canonically catalyze these reactions have been knocked out, it seems likely that in the presence of high levels of propionyl-CoA, the corresponding citric acid cycle enzymes are enabling these transformations.

Similarly, the presence of methyl-cis-aconitate in the methylcitrate cycle (Δ*prpDBC*) mutants suggests the spurious action of the citric acid cycle aconitases on the accumulating 2-methylcitrate. (Figure 2.14) The lower levels of methyl-cis-aconitate measured in the Δ*prpDBC* mutants would suggest a decreased efficiency of this 'side'-transformation as compared to the formation of 2-methylcitrate.

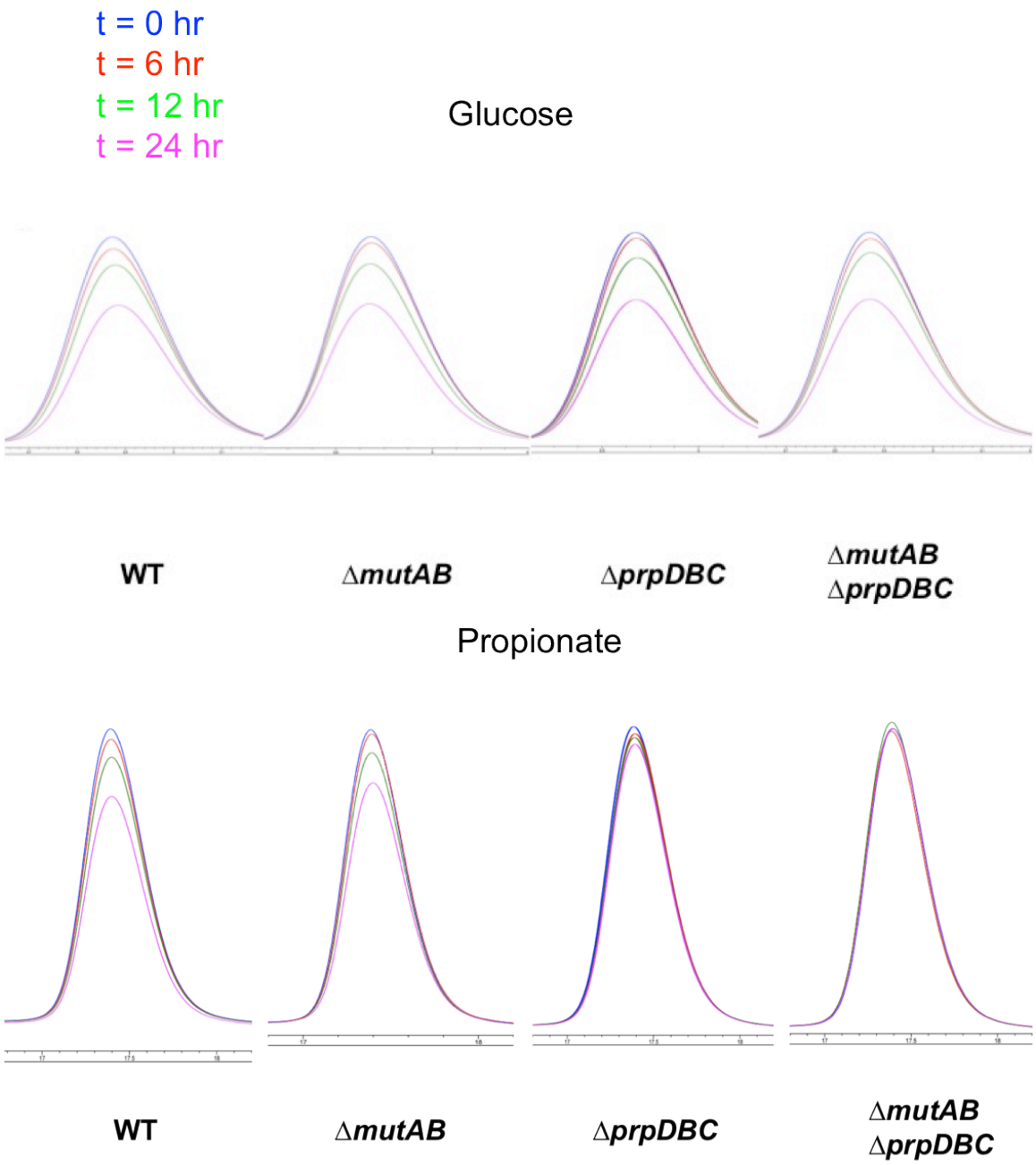

Figure 2.13 HPLC detection of glucose and propionate in culture supernatants from strains of *M. smegmatis* grown in M9 + 0.5% propionate and sampled over a time course (0 hr, 6 hr, 12 hr, 24 hr), scaled for comparison.

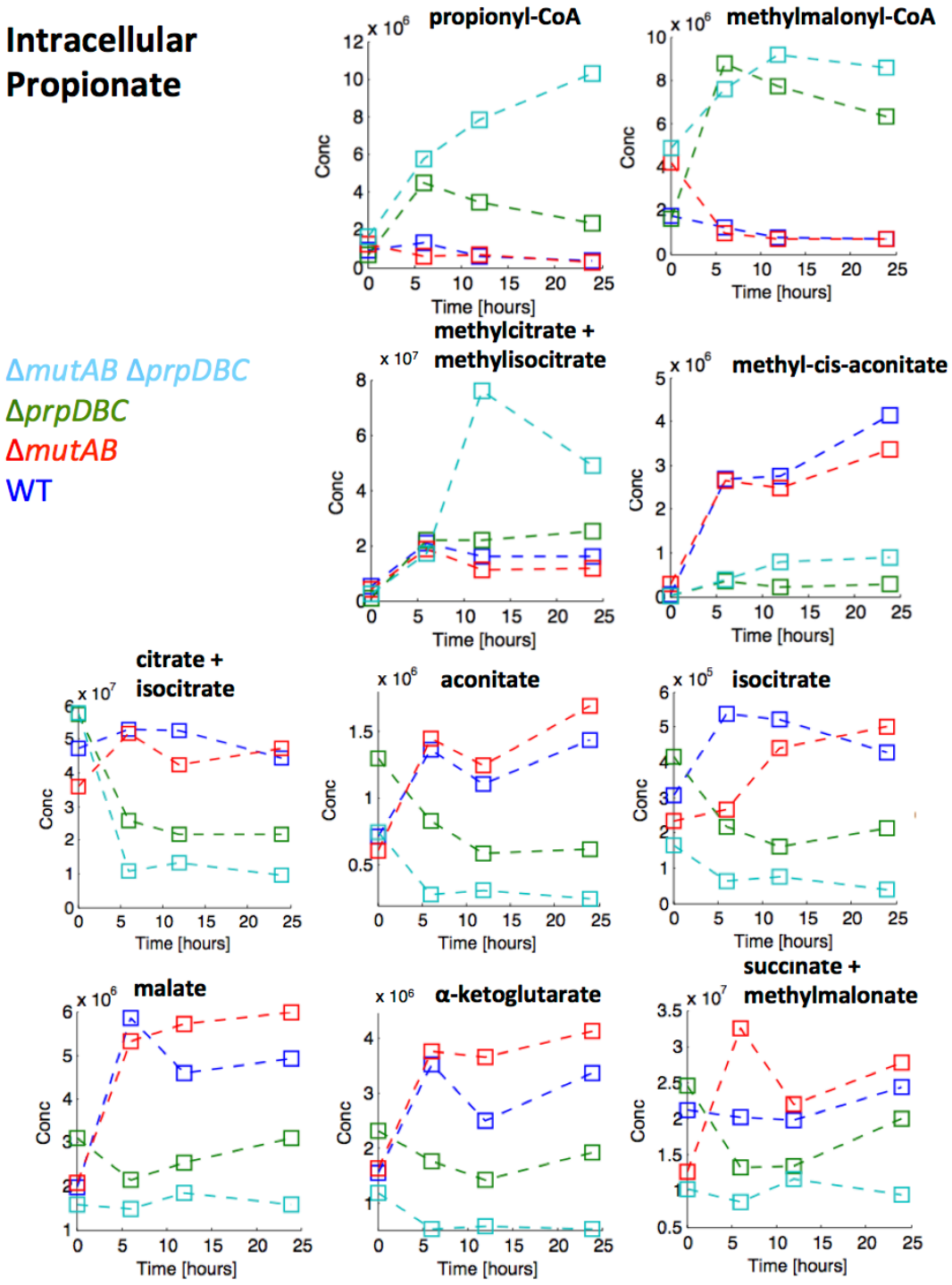

Figure 2.14 LC-MS/MS detection of targeted metabolites from strains of *M. smegmatis* grown in M9 + 0.5% propionate and sampled over a time course (0 hr, 6 hr, 12 hr, 24 hr); each point is an average of two replicates.

Coordinate with the increase in methylcitrate cycle and methylmalonyl-CoA pathway metabolites in the Δ*mutAB* Δ*prpDBC* and Δ*prpDBC* strains are the decreasing levels of the citric acid cycle metabolites (citrate/isocitrate, aconitate, isocitrate, alpha-ketoglutarate, succinate/methylmalonate, and malate) over the time course of incubation in propionate-containing medium. (Figure 2.14)

Another unexpected finding was the accumulation of methylcitrate cycle and methylmalonyl-CoA pathway metabolites in the Δ*mutAB* Δ*prpDBC* strain during growth on glucose. (Figure 2.15) This accumulation could represent a 'basal' activity of the propionate pathways due to endogenously derived propionyl-CoA precursors. Interestingly, the propionate pathway metabolites accumulated in parallel to an apparent depletion of citric acid cycle metabolites in Δ*mutAB* Δ*prpDBC* cells. The presence of methylcitrate cycle metabolites in glucose-grown Δ*mutAB* cells, but not in glucose-grown Δ*prpDBC* cells (Figure 2.15), might suggest that the putative 'basal' flow of propionyl-CoA is normally routed to the methylmalonyl-CoA pathway rather than the methylcitrate cycle.

Under no-carbon culture conditions, the levels of most metabolites decreased over time for all of the strains. However, in the Δ*mutAB* Δ*prpDBC* strain, levels of methylcitrate and methylmalonyl-CoA pathway intermediates increased over time (Figure 2.16), suggesting that an endogenous source of propionyl-CoA might be mobilized during starvation conditions. Endogenous sources of propionyl-CoA could include odd-chain fatty acids and branched-chain amino acids.

The increased intracellular levels of tyrosine and tryptophan detected for all of the strains under no-carbon culture conditions might suggest a mobilization of amino acids during carbon starvation as an adaptive response. The apparent accumulation of the aromatic amino acids may be due to the difficulty in metabolizing them. Notably, the Δ*mutAB* Δ*prpDBC* strain also exhibited high levels of tryptophan and tyrosine when incubated in medium containing propionate as the sole carbon source. Furthermore, the Δ*prpDBC* and Δ*mutAB* Δ*prpDBC* strains also exhibited higher cell-associated levels of disaccharides when incubated in propionate-containing culture medium, and this elevation was matched by all of the strains under no-carbon culture conditions. (Figure 2.17)

A set of metabolites (glutamine, citrulline, diaminopimelate), linked through arginine metabolism pathways (Voellym and Leisinger 1976), showed similar profiles under the different culture conditions. Although glutamate is also part of this pathway, the levels of this metabolite were not coordinated with the other metabolites for a given condition, except that lower levels of all four metabolites were detected in the Δ*mutAB* Δ*prpDBC* strain. (Figure 2.18)

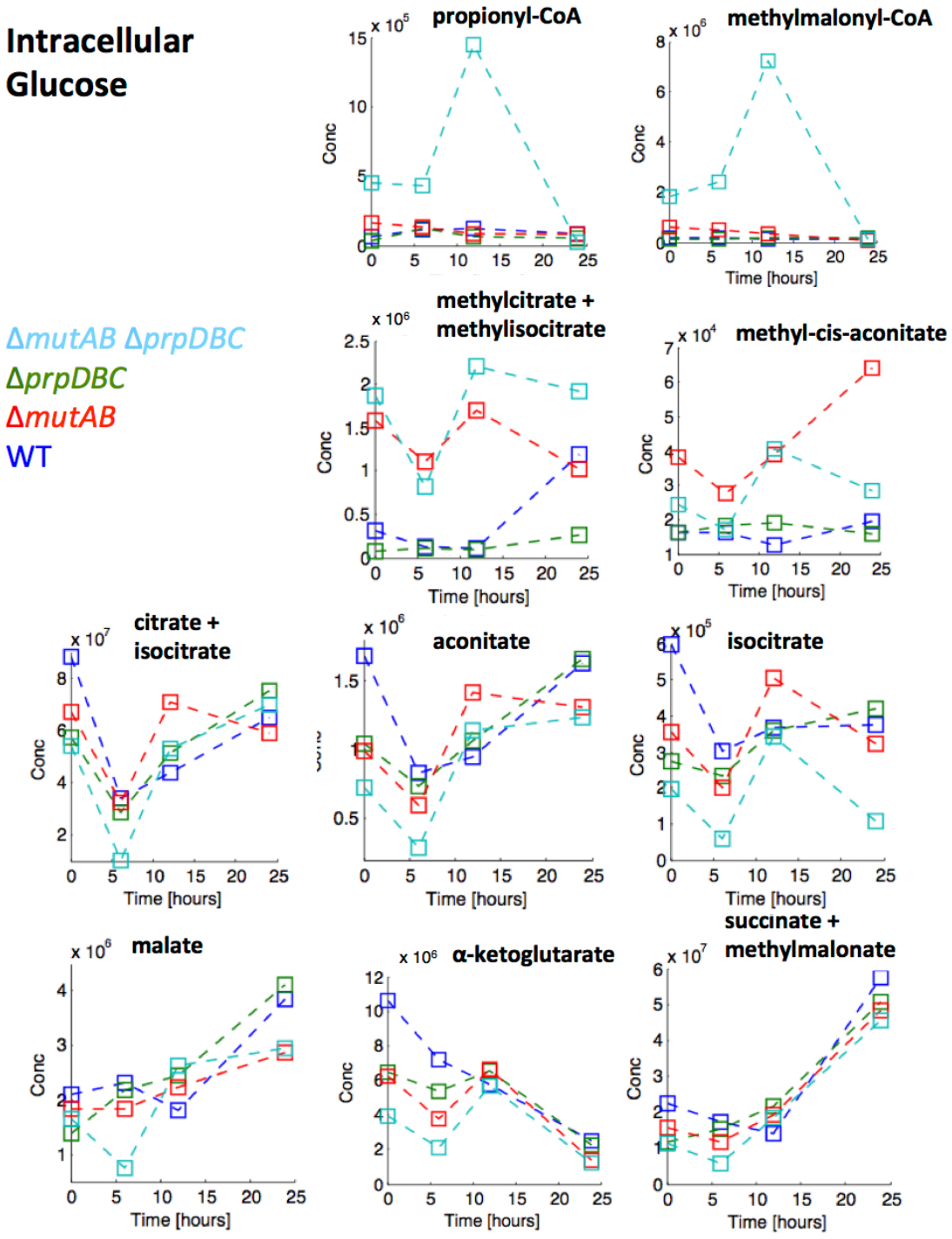

Figure 2.15 LC-MS/MS detection of targeted metabolites from strains of *M. smegmatis* grown in M9 + 0.5% glucose and sampled over a time course (0 hr, 6 hr, 12 hr, 24 hr); each point is an average of two replicates.

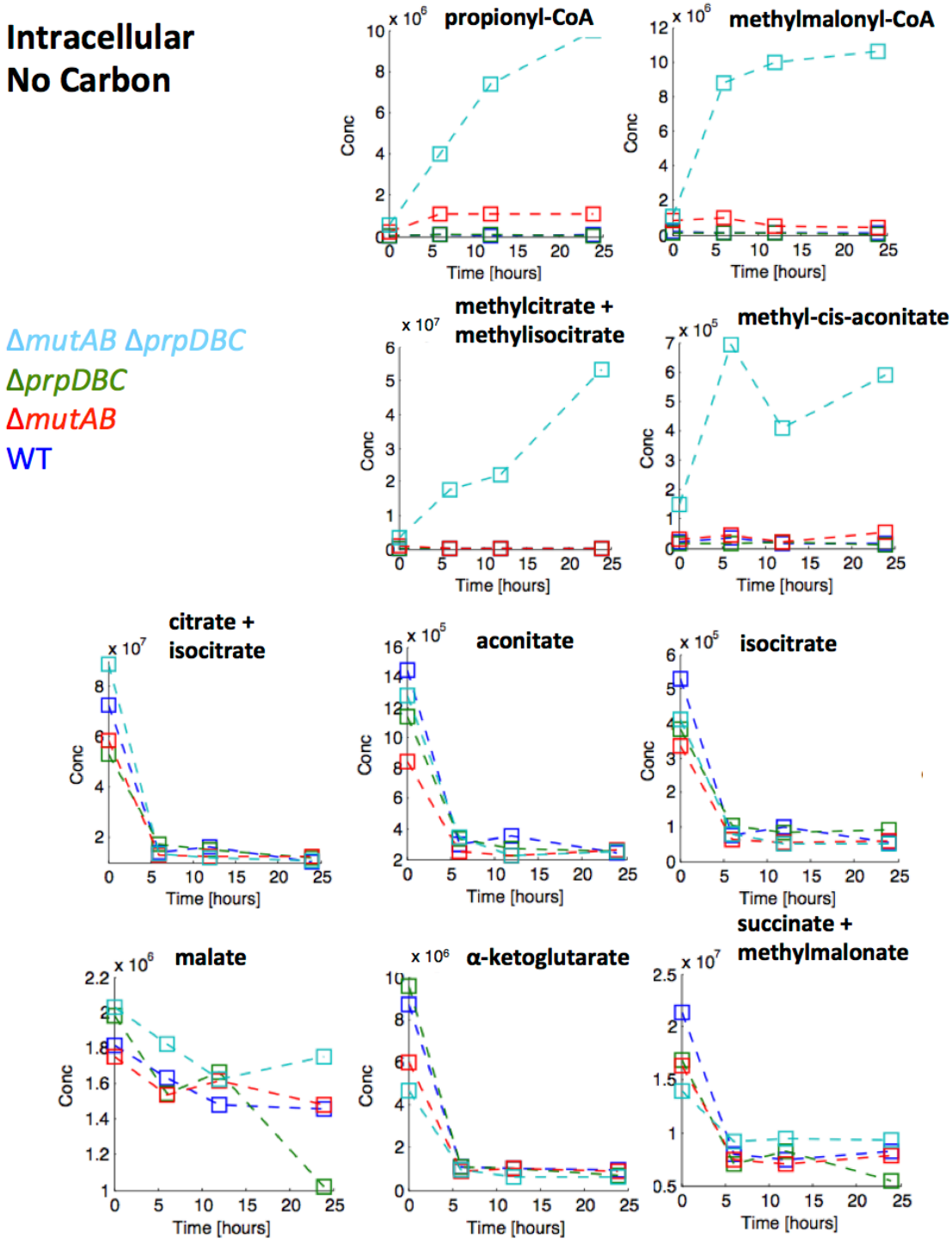

Figure 2.16 LC-MS/MS detection of targeted metabolites from strains of *M. smegmatis*, grown in M9 (no-carbon) and sampled over a time course (0 hr, 6 hr, 12 hr, 24 hr); each point is an average of two replicates.

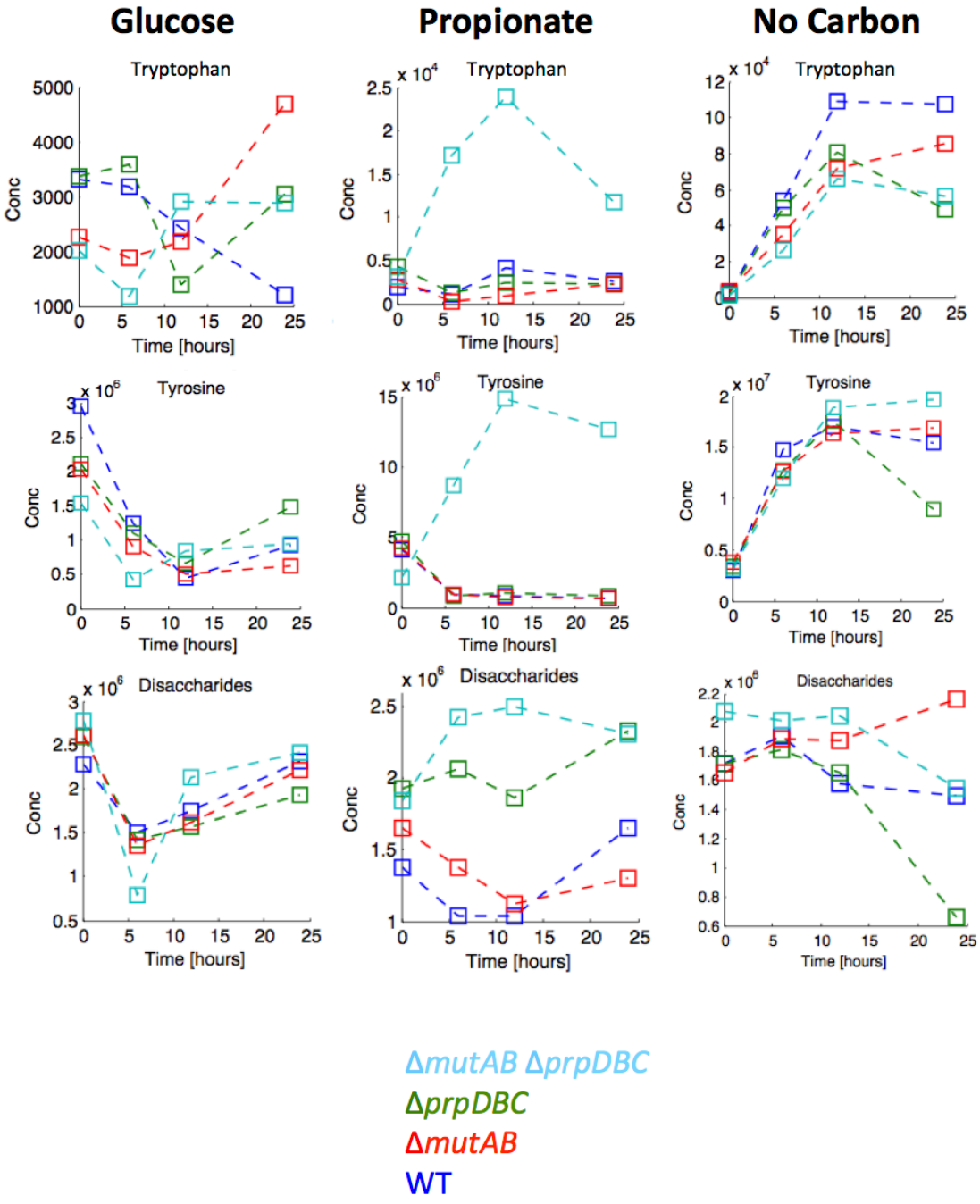

Figure 2.17 LC-MS/MS detection of targeted metabolites from strains of *M. smegmatis* grown in M9 + 0.5% glucose, M9 + 0.5% propionate, or M9 (no-carbon) and sampled over a time course (0 hr, 6 hr, 12 hr, 24 hr); each point is an average of two replicates.

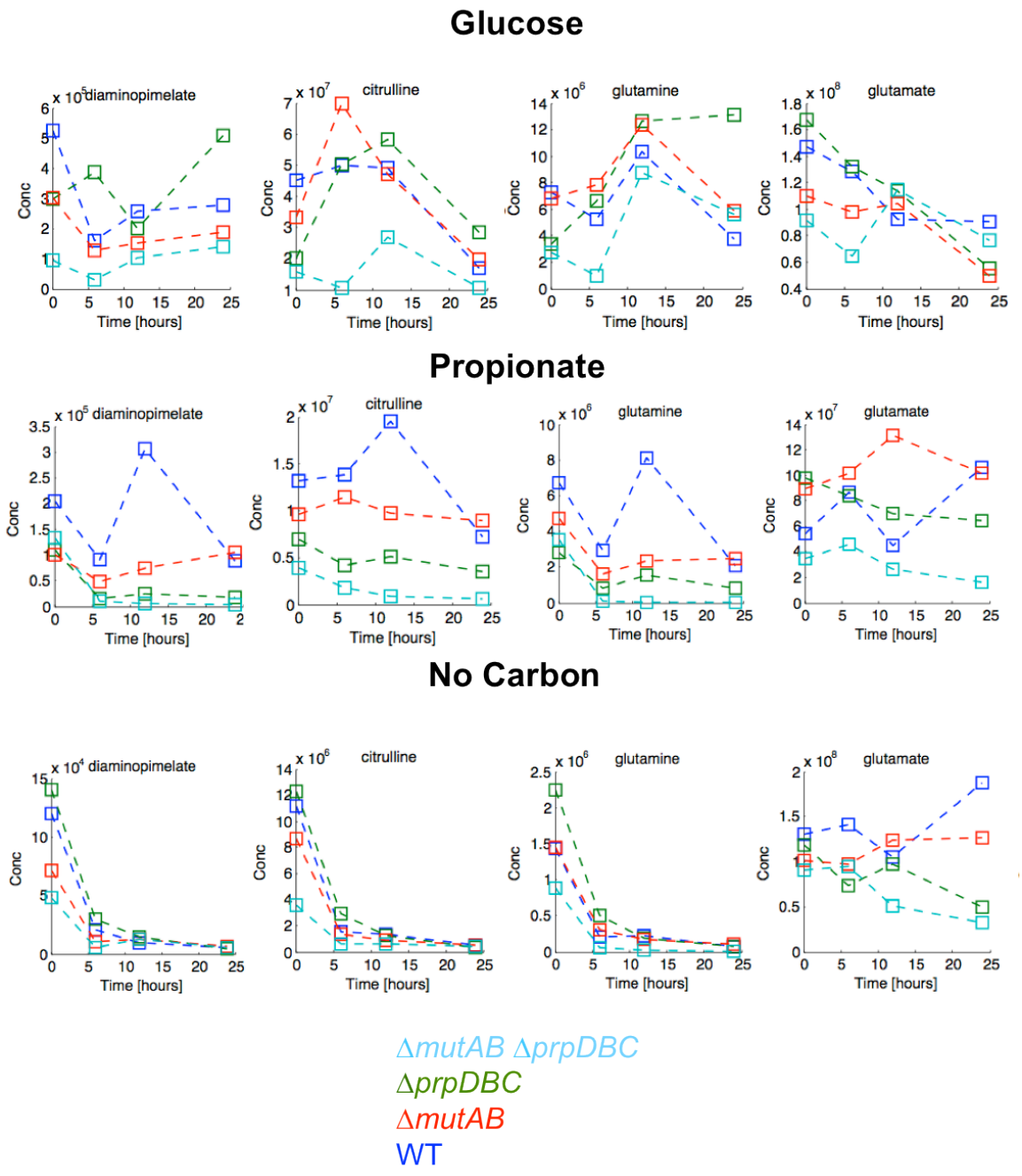

Figure 2.18 LC-MS/MS detection of targeted metabolites from strains of *M. smegmatis* grown in M9 + 0.5% glucose, M9 + 0.5% propionate, or M9 (no-carbon) and sampled over a time course (0 hr, 6 hr, 12 hr, 24 hr); each point is an average of two replicates.

2.2.4 Untargeted metabolomics

As a complementary approach to targeted metabolite analysis with authentic standards, a method based on 'metabolite profiling' was applied to a set of metabolite extracts from the same cultures, using direct flow injection (FI) of samples into a time-of-flight (TOF)-MS for rapid and accurate measurement of hundreds to thousands of metabolite peaks, without prior separation (Fuhrer et al 2011). Putative identification was made by mass alone; therefore, interesting 'hits' should be reconfirmed using the targeted method.

As with the targeted approach, the untargeted approach detected a number of metabolites (4-aminobutanoate, L-ornithine, glutamate, and glutamine) that are associated with arginine metabolism (Voellym and Leisinger 1976). The Δ*mutAB* Δ*prpDBC* strain showed the lowest levels of these metabolites in propionate-grown cultures, followed by the Δ*prpDBC* strain. Under no-carbon conditions, the Δ*prpDBC* strain did not differ from WT or Δ*mutAB* (Figure 2.19), which might indicate that propionyl-CoA generated during carbon starvation can be utilized through the methylmalonyl-CoA pathway. Glutamine and glutamate detected by the FI-TOF-MS method are shown to illustrate the correspondence with the data obtained by the LC-MS/MS method. (Figure 2.18)

Metabolites were identified whose levels were elevated in Δ*mutAB* Δ*prpDBC* cells incubated in propionate-containing medium. For valine and 2-aminoadipate, this elevation also corresponded to the high levels detected in Δ*mutAB* Δ*prpDBC* cells during no-carbon incubation, whereas all of the strains

contained similar levels of 4-methylene-L-glutamate. (Figure 2.20) Such metabolites that show a differential accumulation between these strains as well as between conditions will help distinguish between metabolites that represent normal (wild-type) adaptations to starvation conditions and metabolites that hyper-accumulate only in the mutant strains and that might contribute to toxicity.

This methodology can also make use of supernatant samples to detect metabolites that are excreted into the surrounding medium. Over the time courses, the culture supernatants of all strains under all carbon conditions that were tested accumulated rhamnose, a component of the mycobacterial cell wall (Ma et al 2002). Culture supernatants of the Δ*mutAB* Δ*prpDBC* mutant accumulated the highest levels of rhamnose over time. This elevated excretion (or release) of rhamnose from cells incubated in medium containing propionate, glucose, or no-carbon, is perhaps indicative of cell wall remodeling or cell lysis. (Figure 2.21)

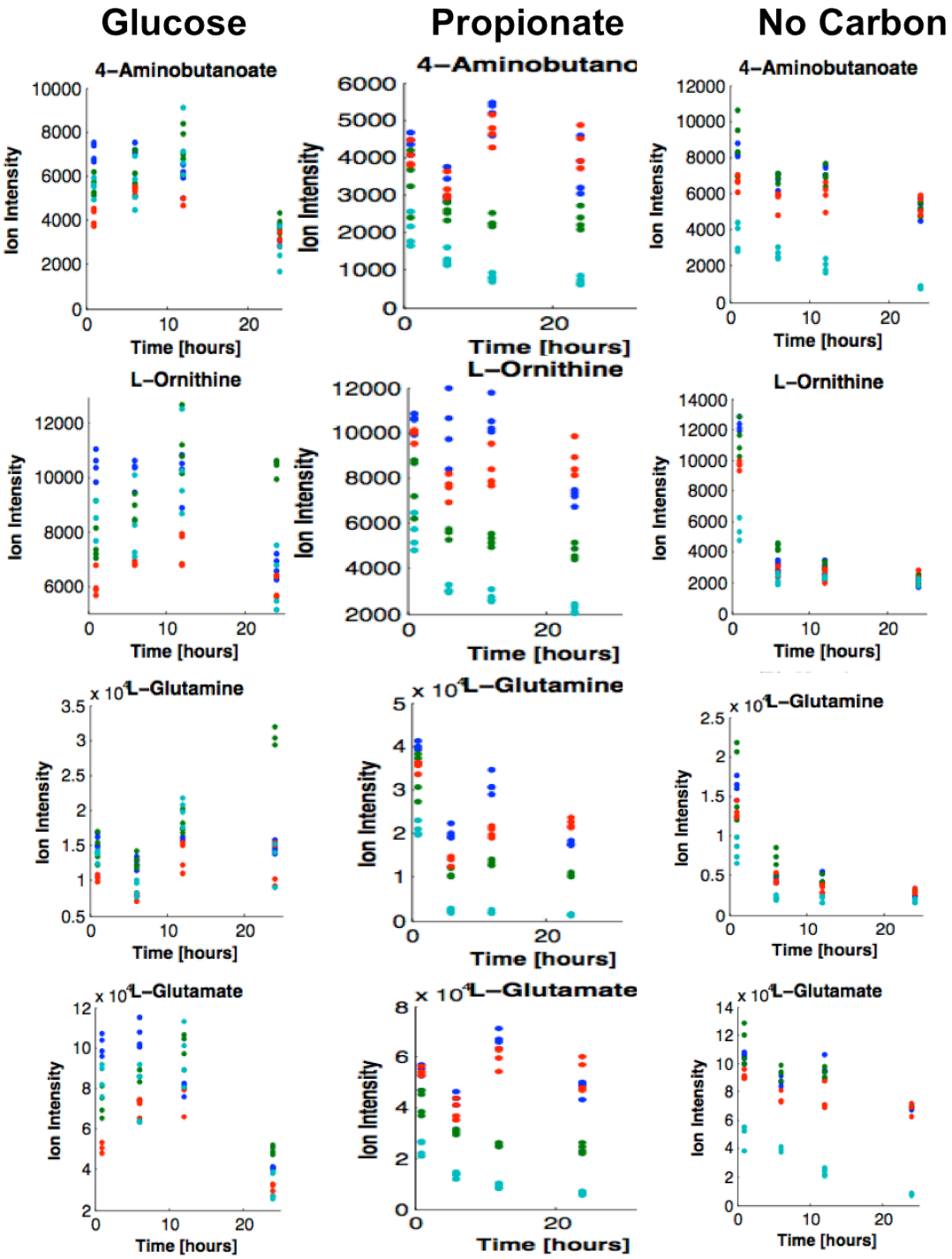

Figure 2.19 FI-TOF-MS detection of untargeted metabolites from strains of *M. smegmatis* grown in grown in M9 + 0.5% glucose, M9 + 0.5% propionate, or M9 (no-carbon) and sampled over a time course (0 hr, 6 hr, 12 hr, 24 hr); 4 points per strain represent 2 replicates with repeat injections. WT (blue), Δ*mutAB* (red), Δ*prpDBC* (green), Δ*mutAB* Δ*prpDBC* (teal).

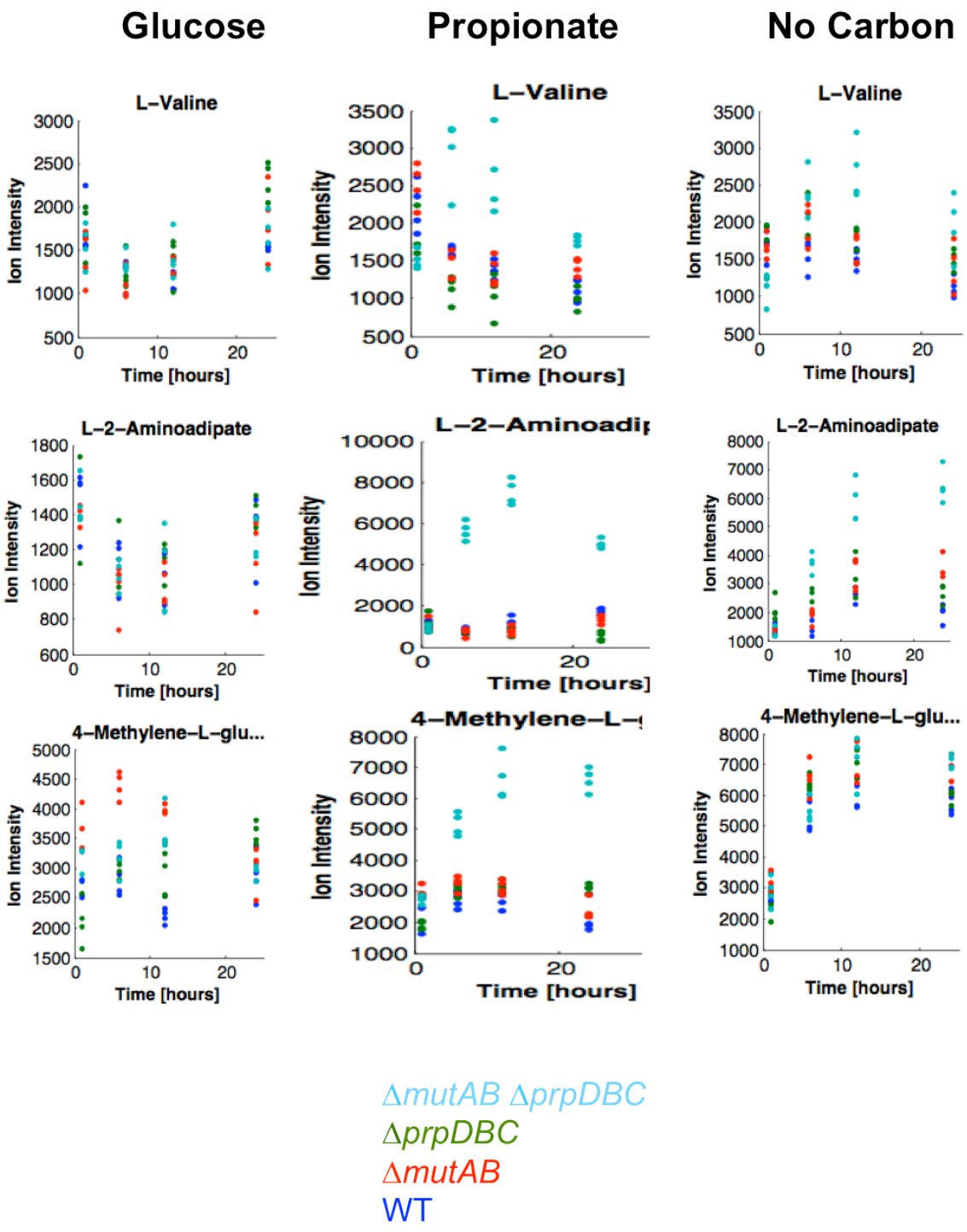

Figure 2.20 FI-TOF-MS detection of untargeted metabolites from strains of *M. smegmatis* grown in M9 + 0.5% glucose, M9 + 0.5% propionate, or M9 (no-carbon) and sampled over a time course (0 hr, 6 hr, 12 hr, 24 hr); 4 points per strain represent 2 replicates with repeat injections.

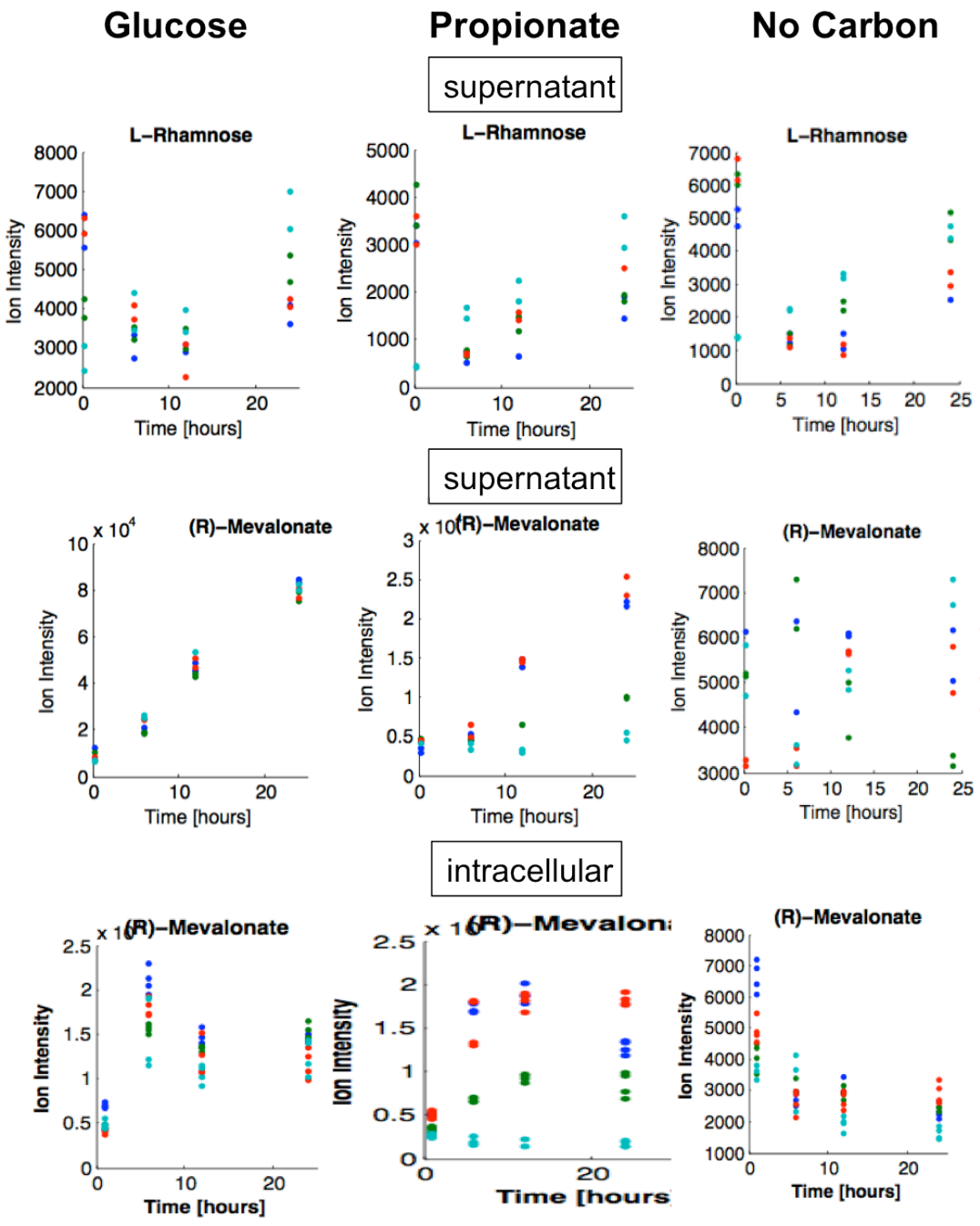

Figure 2.21 FI-TOF-MS detection of untargeted metabolites from *M. smegmatis* strains grown in M9 + 0.5% glucose, M9 + 0.5% propionate, or M9 (no-carbon) and sampled over a time course (0 hr, 6 hr, 12 hr, 24 hr); supernatant points are double injections of a single sample, 4 points per strain represent 2 replicates with repeat injections. WT (blue), Δ*mutAB* (red), Δ*prpDBC* (green), Δ*mutAB* Δ*prpDBC* (teal).

A comparison can be made between metabolites found both the cell-associated and culture supernatant fractions. During growth on propionate, mevalonate was identified in the culture supernatant in correspondence to the cell-associated levels, such that the WT and Δ*mutAB* strains contained the highest levels in both fractions, the Δ*mutAB* Δ*prpDBC* strain was lowest, and the Δ*prpDBC* strain was in between. Under no-carbon conditions, while the cell-associated levels of mevalonate declined for all strains, the levels in the culture supernatant varied throughout the time course and the apparent 'grouping' of strains was different at subsequent time-points. (Figure 2.21)

2.2.5 Discussion

The targeted metabolite approach to characterizing the propionate pathway mutant strains of *M. smegmatis* has yielded valuable insights into the dynamic metabolic content of the cell and offers some potential explanations for the surprising growth phenotypes described in the previous section. The application of this technique to mutant strains that cannot metabolize propionate has provided evidence of accumulating metabolic pathway intermediates to fulfill a prerequisite of the hypothesis that propionate toxicity towards these strains is due to accumulation of toxic metabolites, namely, that the corresponding metabolites do, in fact, accumulate.

A mutant strain of both propionate metabolic pathways contained higher levels of the intermediates upstream of the lesions, propionyl-CoA and

methylmalonyl-CoA, but also showed significant levels of intermediates downstream of the enzymes that the Δ*mutAB* Δ*prpDBC* mutant lacks. It is proposed that the citric acid cycle enzymes are able to perform the analogous transformations on propionate pathway intermediates when these intermediates are in excess. This has been observed for the *gltA*-encoded citrate synthase in *S.* Typhimurium (Rocco and Escalante-Semerena 2010). Perhaps most convincing is the formation of 2-methylcitrate, which is detected in the urine of human patients suffering from methylmalonyl aciduria with concomitantly high levels of propionyl-CoA present in the body. As humans do not possess the methylcitrate cycle, this transformation is believed to be catalyzed by the human citrate synthase enzyme (Ando et al 1972).

Of note is the stereospecificity of the reactions catalyzed by the canonical versus promiscuous enzymes. It has been suggested that producing a mix of stereoisomers that cannot be utilized by the next enzyme in the pathway might result in binding and inhibition and thus provides a putative mechanism of toxicity (van Rooyen et al 1994). To this effect, the 2-methylcitrate formed by the *gltA*-encoding citrate synthase of *Salmonella enterica* serovar Typhimurium was demonstrated to be more inhibitory to the cell than the methylcitrate formed by the canonical methylcitrate synthase (Rocco and Escalante-Semerena 2010). Interestingly, the settings for 2-methylcitrate / 2-methylisocitrate as well as for 2-methyl-cis-aconitate were associated with multiple peaks on the LC column. This

could conceivably correspond to stereoisomers that could differ between MCS- and CS-catalyzed reactions.

Testing this phenomenon genetically, by making additional deletions of the suspected citric acid cycle enzymes in the Δ*mutAB* Δ*prpDBC* strain background, could result in further metabolic defects that would be difficult to uncouple. Moreover, *M. smegmatis* encodes three putative citrate synthase homologs, which might require multiple deletion steps. Another approach might be the real-time MS-enabled detection of the formation of 2-methylcitrate when propionyl-CoA is added to cell-free protein extracts of the *M. smegmatis* Δ*mutAB* Δ*prpDBC* strain.

While the TCA cycle enzymes are implicated in forming a toxic intermediate, there is also evidence to support the idea that inhibition of TCA cycle function is what contributes to the toxic effects seen. In addition to the levels of the metabolites of the TCA cycle that were reduced in the Δ*muAB* Δ*prpDBC* mutant cultured in propionate-containing medium, the levels of PEP and pyruvate on propionate were lower than other strains. In glucose, propionate, and no-carbon media, the Δ*muAB* Δ*prpDBC* mutant had lower levels of acetyl-CoA. This might point to inhibition of the gluconeogenic pathway as part of the toxic effect (Rocco and Escalante-Semerena 2010). Clarification of these points will require further studies with alternative carbon sources.

The accumulation of propionate pathway metabolites during growth of Δ*mutAB* Δ*prpDBC* cells in glucose-containing medium was unexpected. This

corresponds to the otherwise difficult-to-interpret glucose growth phenotype described in the previous section. Moreover, the similar loss of viability (CFU) seen for the Δ*mutAB* Δ*prpDBC* strain incubated in either propionate or no-carbon medium is supported by the accumulation of propionate pathway metabolites under both conditions.

A GC-MS based investigation in the closely related species *Corynebacterium glutamicum* also demonstrated the formation of methylcitrate cycle intermediates during growth on glucose (Plassmeier et al 2007). While the endogenous source of propionyl-CoA has not been identified, some clues are provided by the apparent accumulation of aromatic amino acids, which may be indicative of a general amino acid degradation response to starvation.

In support of this idea, valine was seen to transiently accumulate in the Δ*mutAB* Δ*prpDBC* strain under both propionate and no-carbon conditions. Thus, the absence of a usable carbon substrate in both cases could lead to amino acid breakdown, which from valine would generate propionyl-CoA and further toxicity. Of note, the MCL enzyme of *S. cerevisiae* was found to be induced when threonine was provided with limiting glucose (Luttik et al 2000). As threonine degradation results in formation of propionyl-CoA, and a *tcdE*-encoded propionyl-CoA synthase of *E. coli* is encoded in a cluster of genes involved in threonine degradation, the use of propionate pathways for endogenous amino acid metabolism under starvation conditions is further suggested.

The observed accumulation of disaccharides under carbon starvation conditions for all strains, including wild-type – as well as for Δ*mutAB* Δ*prpDBC*, and to a lesser extent, Δ*prpDBC* strains incubated in propionate-containing medium – might point to the mobilization of trehalose, a disaccharide compound that is known to be stored during carbon sufficiency and catabolized during carbon starvation, or utilized as an osmoprotectant in cells exposed to propionate (Woodruff et al 2004).

The relevance of arginine metabolism to propionate metabolism in mycobacteria is not known, but as these metabolites are coordinately reduced in a Δ*mutAB* Δ*prpDBC* strain under propionate stress, this presents an interesting avenue for further investigation. Interestingly, arginine was unexpectedly able to rescue the ability of a MCS-deficient strain of *A. nidulans* to form a polyketide precursor (Zhang et al 2004). Perhaps of relevance is that hyperammonemia is a complication of propionic and methylmalonic acidemia in humans and inhibition of ureagenesis is one of the proposed routes of propionate toxicity in hepatocytes (Glasgow and Chase 1976, Coude et al 1979).

The apparent release of rhamnose into the media may be an indication of cell wall remodeling or cell lysis, which could also provide a source of propionyl-CoA for the remaining intact cells. This and other untargeted metabolites have provided additional 'hits' to follow up on to help elucidate the 'toxic' effect seen *in vitro*.

A functional link between the *in vitro* observations and the underlying metabolite profiles could be established by the isolation of 'suppressor' mutations that bypass the toxic effect of propionate on cells lacking the methylcitrate and methylmalonyl-CoA pathways. However, given the 'semi-dominant' inhibitory effect of propionate on *M. smegmatis*, as described in the previous section of this thesis, it might be preferable to focus these studies on *M. tuberculosis*, where the much stronger effects of propionate *in vitro* and relevance *in vivo* will be described in the next section.

2.3 Studies of the propionate metabolism pathways of *M. tuberculosis*

While *Mycobacterium smegmatis* is a useful model for *in vitro* studies, for questions of *in vivo* relevance, the use of the pathogenic *M. tuberculosis* becomes indispensable. Previous studies with *M. tuberculosis* have demonstrated the upregulation of the methylcitrate cycle genes *prpD* and *prpC* in *ex vivo*-infected macrophages and in infected mouse lungs (Schnappinger et al 2003, Shi et al 2010), suggesting a role for this pathway during infection.

A mutant strain, with a deletion of the *prpC* and *prpD* genes encoding the methylcitrate cycle specific enzymes methylcitrate synthase (MCS) and methylcitrate dehydratase (MCD), respectively, was previously generated in the Erdman strain of *M. tuberculosis*. The Δ*prpDC* mutant was found to resemble the

icl1::hyg icl2::aph strain in its inability to utilize propionate and attenuation in bone marrow-derived macrophages, yet was unaffected in its ability to grow and cause tissue pathology in the mouse infection model (Munoz-Elias et al 2006).

The disparity between the requirement for *prpDC in vitro* for growth on propionate and *ex vivo* for growth in cultured macrophages vs. the dispensability of *prpDC in vivo* for growth in the lungs of mice can be reconciled by any of the following possibilities (discussed in Munoz-Elias et al 2006):

- The ability to metabolize propionyl-CoA is dispensable for infection and the phenotype of the ICL/MCL-deficient mutant (Δ*icl1* Δ*icl2*) could be ascribed to its role in the glyoxylate shunt;

- A 'cryptic' pathway for propionate metabolism is able to buffer the loss of the methylcitrate cycle *in vivo* but not *in vitro* or *ex vivo*;

- The methylcitrate cycle could serve as a detoxification route for propionyl-CoA, where the pathway can be removed without consequence *in vivo* (as in a Δ*prpDC* strain), perhaps due to functional redundancy, but cannot be lesioned (as in an *icl1::hyg icl2*::*aph* strain), due to the formation of toxic intermediates.

The first hypothesis would be straightforward to test by generating an independent lesion of the glyoxylate cycle, via a malate synthase (MLS)-deficient strain, and interrogating its ability to phenocopy the ICL/MCL-deficient strain *in vivo*. However, on-going efforts suggest that the *glcB* gene encoding MLS is likely essential (E.J. Munoz-Elias PhD thesis, 2005, N. Dhar, personal

communication, S. Ehrt, personal communication, Griffin et al 2011). The apparent essentiality of MLS is surprising in light of the fact that the ICL/MCL, which acts in the same pathway, is not required under standard *in vitro* culture conditions. The MLS could be essential if glyoxylate buildup in its absence is toxic. Alternatively, MLS could possess a yet unknown, essential, secondary 'moonlighting' function (Kinhikar et al. 2006). In either case, the interpretation of the phenotype of a conditional knockout would be less than straightforward.

Addressing the second hypothesis, the methylmalonyl-CoA pathway could conceivably provide an alternative route of propionate metabolism. The putative buffering capacity *in vivo* but not *ex vivo* or *in vitro* might reflect a difference in the production or availability of the B12 (adenosylcobalamin) co-factor of the methylmalonyl-CoA mutase (MCM) enzyme of this pathway in murine lungs as compared to the conditions in culture media and within macrophages.

The requirement for *in vitro* supplementation of cyanocobalamin (vitamin B12) for obtaining growth of the Δ*prpDC* mutant on propionate, in an MCM-dependent manner, was demonstrated in studies carried out in the H37Rv strain of *M. tuberculosis* (Savvi et al 2008). Moreover, the ability of the B12-activated methylmalonyl-CoA pathway to bypass the growth defect in propionate of an ICL/MCL-chemically inhibited strain was also established, suggesting that the glyoxylate cycle was not required as an anaplerotic route for growth on propionate by this pathway.

The ability of mutant strains impaired in both pathways of propionyl-CoA metabolism to establish an infection could not previously be tested in the mouse model as these strains, along with the parental H37Rv 'wild-type' strain used in these studies, had spontaneously lost the ability to produce phthiocerol dimycocerosates (PDIM) (Savvi et al 2008). PDIM deficiency, in itself, is known to cause attenuation in animal infection models (Goren et al 1974, Cox et al 1999) and would confound interpretation of any potential *in vivo* phenotype of propionyl-CoA metabolic mutant strains.

Spontaneous loss of PDIM production arises rapidly from *in vitro* passaging of *M. tuberculosis* and appears to confer a slight, but reproducible *in vitro* growth advantage. The apparent selection against PDIM production *in vitro* is attributed to the large costs of its synthesis, in terms of the 15 separate ORFs and over 15 catalytic steps involved. (Domenech and Reed 2009, Trivedi et al 2005). This is now widely recognized as a common problem encountered during the *in vitro* passaging and bottlenecks that necessarily occurs with genetic manipulation of *M. tuberculosis* (Ioerger et al 2010, Kirksey et al 2011).

As described above, the wild-type and propionyl-CoA pathway mutant strains examined *in vitro* in the work of Savvi *et al*. were unsuitable for further *in vivo* studies. Therefore, the construction of PDIM-proficient propionate pathway mutants was pursued in collaboration with Prof. Valerie Mizrahi at the University of Cape Town, whose laboratory studies the vitamin B12-dependent enzymes in *M. tuberculosis*. The mutants were generated in parallel in the H37Rv (at UCT

by Dr. Krishnamoorthy Gopinath) and Erdman (work presented here) strain backgrounds of *M. tuberculosis* in order to assess the contribution of these pathways to growth and virulence in the mouse model.

Complementary investigations into the third possible role of the methylcitrate cycle in *M. tuberculosis*, that of propionyl-CoA detoxification, would involve testing the second postulate of the 'toxic metabolite' hypothesis (i.e., that the accumulation and adverse effects of the putative metabolite are alleviated by blocking its formation). However, to do so, it would be necessary to introduce the putative 'suppressor' mutation of Δ*prpDC*, catalyzing the upstream steps of the methylcitrate cycle, into the ICL/MCL-deficient background. As the ICL/MCL-deficient strain used previously in this lab, in studies by Munoz-Elias *et al*, was generated by allelic-replacement with a copy of the gene containing insertions of antibiotic resistance cassettes, *icl1* with *hyg* and *icl2* with *aph*, the resulting strain is doubly-marked. (Munoz-Elias and McKinney 2005) As antibiotic resistance markers are few and far between in mycobacteria (perhaps not surprisingly, given their natural drug resistance), this strain is difficult to use for additional genetic interventions, such as subsequent allelic exchange, transposon mutagenesis, or introduction of plasmids.

With these downstream applications in mind, in-frame, unmarked, PDIM-proficient deletion mutants were generated in the Erdman background of *M. tuberculosis*, yielding the following mutant strains:

- Δ*icl1* Δ*icl2* = methylcitrate cycle interrupted (MCL-deficiency) and glyoxylate cycle interrupted (ICL-deficiency);

- Δ*prpDC* Δ*icl1* Δ*icl2* = methylcitrate cycle removed (MCS/MCD/MCL-deficiency) and glyoxylate cycle interrupted (ICL-deficiency);

- Δ*mutAB* = methylmalonyl-CoA pathway interrupted (MCM-deficiency);

- Δ*mutAB* Δ*prpDC* = methylmalonyl-CoA pathway interrupted (MCM-deficiency) and methylcitrate cycle interrupted (MCS/MCD-deficiency).

The work presented here set out to test the relative contributions of the methylcitrate cycle and the methylmalonyl-CoA pathway to *M. tuberculosis* growth and survival *in vitro* and *in vivo*. A second aim was to test whether deletion of the upstream steps of the methylcitrate cycle (MCS/MCD) might, paradoxically, improve the fitness of an ICL/MCL-deficient strain by preventing the accumulation of toxic metabolites. A third aim was to address the question of whether the bifunctional ICL/MCL enzymes are essential for infection because of their function in the glyoxylate cycle, the methylcitrate cycle, or, quite possibly, an as yet unrecognized role.

2.3.1 Methylmalonyl-CoA Mutase (MCM) in *M. tuberculosis*

The genes encoding the small and large subunits of methylmalonyl-CoA mutase were previously identified in the *M. tuberculosis* genome, located 190 bp downstream of a divergently transcribed open reading frame (Rv1491c) encoding a ‘conserved hypothetical’ protein of 252 aa. The *mutA* (Rv1492) gene encoding

the small subunit (615 aa) is directly followed by the start codon of the *mutB* (Rv1493) gene encoding the large subunit (750 aa). Rather than lying adjacent to the *meaB*-encoded protection factor, the *mutAB* locus is situated 13 bp upstream of the genes *mazE4* and *mazF4* (Rv1494-Rv1495) encoding a putative toxin-antitoxin module. The *mazF4* gene overlaps 4 bp with the start of the *meaB* (Rv1496) gene encoding a protein of 334 aa, which is misannotated as a 'transport system kinase' (Savvi et al 2008). (Figure 2.1B)

2.3.2 Deletion of *mutAB* in *M. tuberculosis*

Unmarked in-frame deletions of the *mutAB* genes were made by allelic exchange using the two-step counter-selection method (Pelicic et al 1996a, Pelicic et al 1996b). Homologous flanking regions were amplified from genomic DNA and ligated into a plasmid, forming an in-frame deletion, fusing the first 4 codons of *mutA* to the last 6 codons in *mutB* with an AvrII site, to replace the native copy of the gene. This deletion construct was also used by the Mizrahi lab to generate the corresponding deletion in the H37Rv background. The *mutAB* genes were deleted in the Erdman wild-type (WT) and Δ*prpDC* (MunozElias et al 2006) strain backgrounds. The deletion was confirmed with PCR reactions, using primers that hybridized outside the cloned region, as well as by Southern blot. (Figure 2.22)

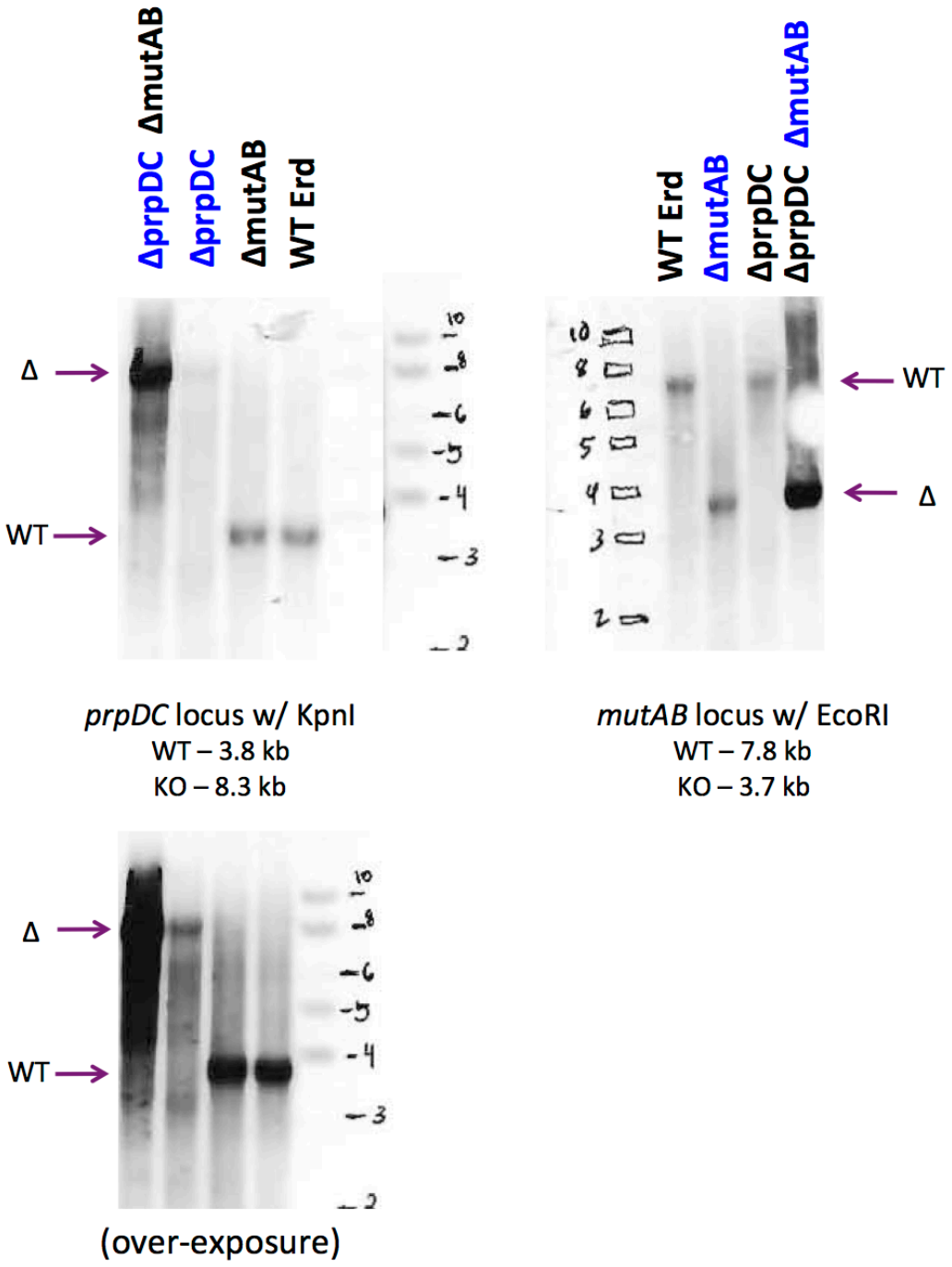

Figure 2.22 Southern blot of genomic DNA from WT, Δ*mutAB*, Δ*prpDC*, and Δ*mutAB* Δ*prpDC* strains in *M.* tuberculosis Erdman background, digested and probed as indicated. Arrows indicate expected fragments for wild-type (WT) or deleted (Δ) genes. An overexposure of the *prpDC* locus blot is shown to visualize KO band of the underloaded Δ*prpDC* strain.

2.3.3 Deletion of *icl1* and *icl2* in *M. tuberculosis*

Unmarked in-frame deletions of *icl1* (Rv0465) and *icl2* (Rv1915/Rv1916) were generated in the Erdman WT and Δ*prpDC* strain backgrounds using plasmids prepared as described above, except containing homologous genomic DNA forming an in-frame deletion of all but 10 codons for *icl1* and an in-frame deletion of all but 15 codons for *icl2.* The Δ*icl2* and Δ*prpDC*Δ*icl2* strains were used for subsequent transformation with the *icl1* knockout plasmid, as Δ*icl1* strains have a slight growth defect on glucose and passaging should be limited to avoid the potential selection of spontaneous suppressor mutations. The deletions were confirmed by PCR reactions using primers that hybridized outside the cloned region as well as by Southern blot. (Figure 2.23)

2.3.4 PDIM production

Prior to their use in experiments, all strains were tested for the ability to incorporate radioactive [14C]-propionate into the phthiocerol dimycocerosates (PDIM), assessed by thin layer chromatography (TLC) of extracted lipids. All the strains were found to be competent for PDIM production, as seen by the labeled DIM A and DIM B spots. (Figure 2.24)

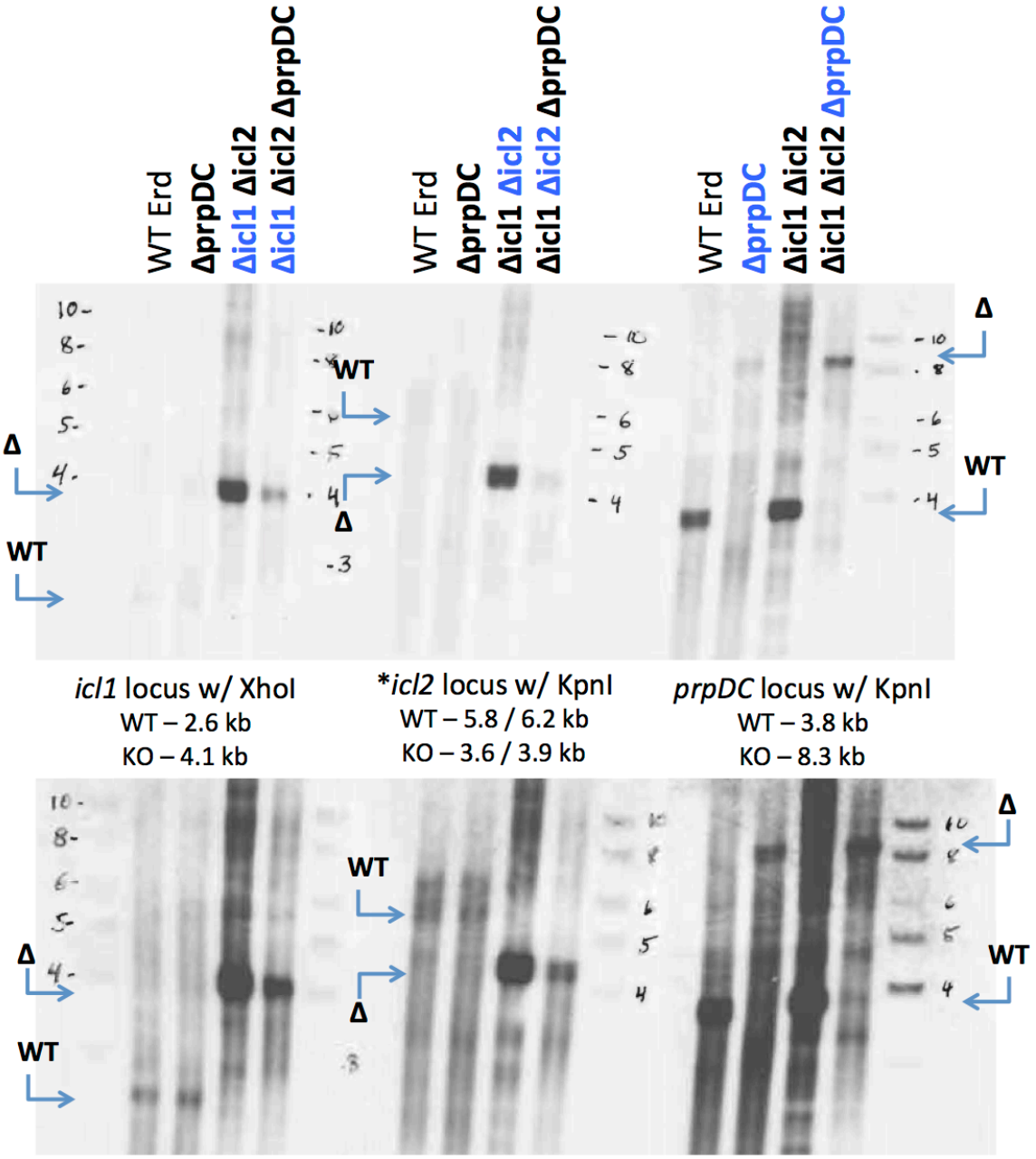

Figure 2.23 Southern blot of genomic DNA from WT, Δ*prpDC*, Δ*icl1* Δ*icl2*, and Δ*prpDC* Δ*icl1* Δ*icl2* strains in *M.* tuberculosis Erdman background, digested and probed as indicated. Arrows indicate expected fragments for wild-type (WT) or deleted (Δ) genes. An overexposure of the three blots is shown to visualize the smaller, divided, and underloaded bands of WT *icl1*, WT *icl2*, and Δ*prpDC*, respectively. *size differences due to repeat region of unknown number for unsequenced Erdman genome

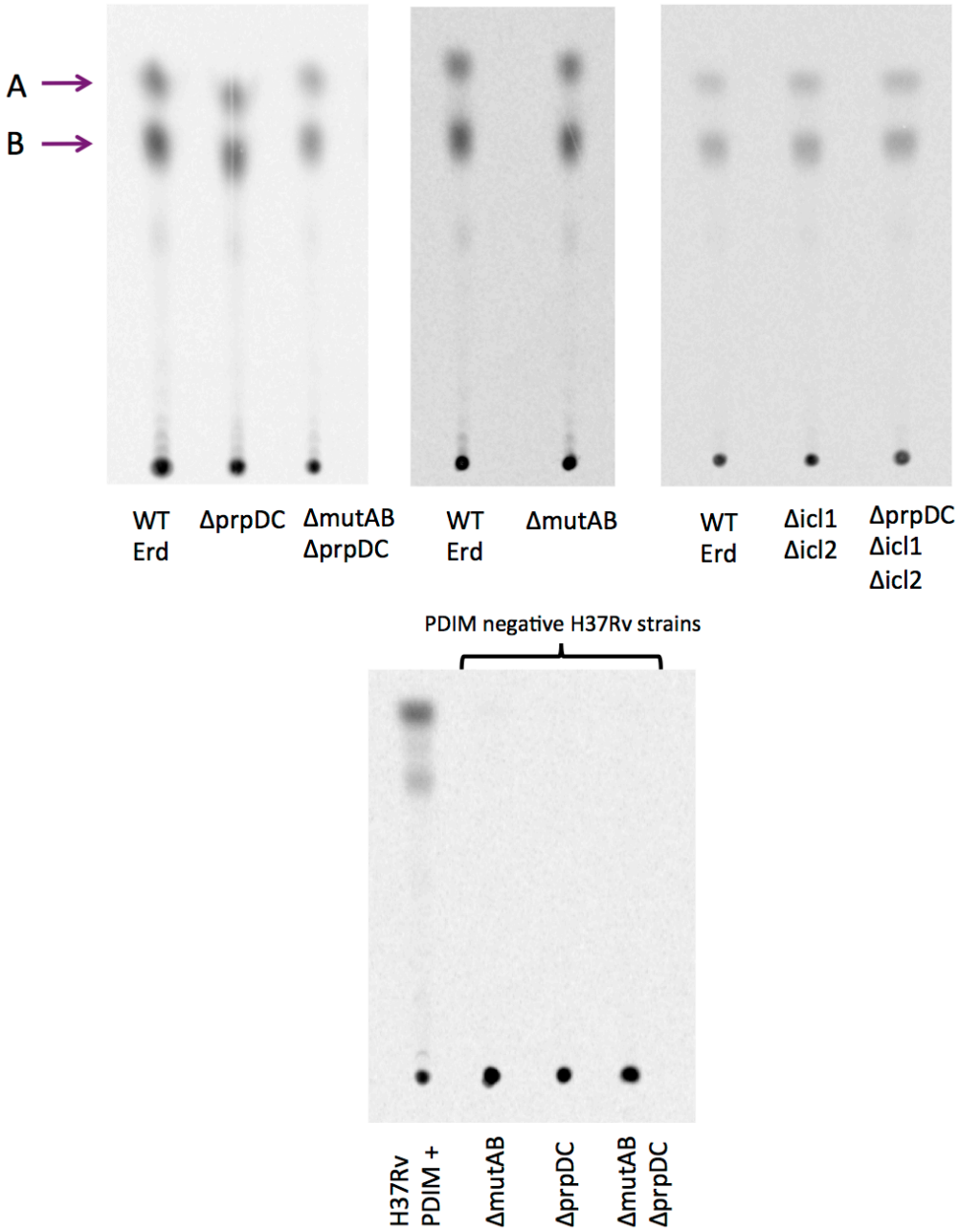

Figure 2.24 TLC analysis of ^{14}C-labeled phthiocerol dimycocerosate (PDIM) production from mutant strains of *M. tuberculosis* with arrows indicating DIM A (A) and DIM B (B) spots. PDIM-negative H37Rv-based strains from Savvi *et al* 2008 tested below.

2.3.5 *in vitro* characterization by growth curve analysis

- Relative contributions of the methylcitrate and methylmalonyl-CoA pathways

Wild-type *M. tuberculosis* Erdman is able to grow robustly on propionate-containing media, provided the concentrations are not so high as to be inhibitory; 0.2% propionate was the highest concentration tested and resulted in a slight lag relative to growth on 0.1% (data not shown). A Δ*mutAB* strain was able to grow as well as WT on propionate-containing media. (Figure 2.25A) In keeping with previous findings (Savvi et al 2008), a Δ*prpDC* strain was unable to grow on propionate unless the methylmalonyl-CoA pathway was activated by exogenous supplementation of cyanocobalamin, which is presumably activated by the bacterium to the adenosylcobalamin cofactor for the MCM. (Figure 2.25A-B)

Although the Δ*prpDC* strain responded to B12 supplementation in a dose-dependent manner (Figure 2.26A), the addition of B12 could not rescue the double mutant strain Δ*mutAB* Δ*prpDC* for growth on propionate (Figure 2.25B). These results suggest that the methylcitrate cycle and methylmalonyl-CoA pathway are the only routes for propionate metabolism in *M. tuberculosis*, although the existence of an additional 'cryptic' pathway that is not active under standard *in vitro* growth conditions cannot be ruled out.

Of note, addition of B12 to the WT strain did not change the growth kinetics (Figure 2.26B), as seen with *M. smegmatis*. However, this observation differs from mutants in the H37Rv strain background of *M. tuberculosis*, where

addition of vitamin B12 stimulates the growth of the WT and Δ*prpDC* strains above the levels shown by the WT strain in the absence of B12 (Savvi et al 2008, K. Gopinath, personal communication). If these contrasting results are not simply due to differences in experimental techniques and reagents, a confirmed difference between the strains would indicate that the methylcitrate cycle alone is sufficient for optimal growth on propionate in Erdman but not in H37Rv, which also requires activation of the methylmalonyl-CoA pathway for achieving maximal yield.

All of the propionate pathway mutants grew similarly to WT on glucose- or acetate- containing media. (Figure 2.27A-B) The addition of vitamin B12 to these cultures did not appear to alter the growth kinetics of any of the strains (data not shown). Notably, the slight defect of the *M. smegmatis* Δ*mutAB* Δ*prpDBC* mutant for growth on glucose-containing medium was not recapitulated by the *M. tuberculosis* Δ*mutAB* Δ*prpDC* mutant. These results suggest that either the putative 'basal' propionyl-CoA generating activity is not present in this species, the metabolite does not accumulate, or it is not inhibitory to *M. tuberculosis*.

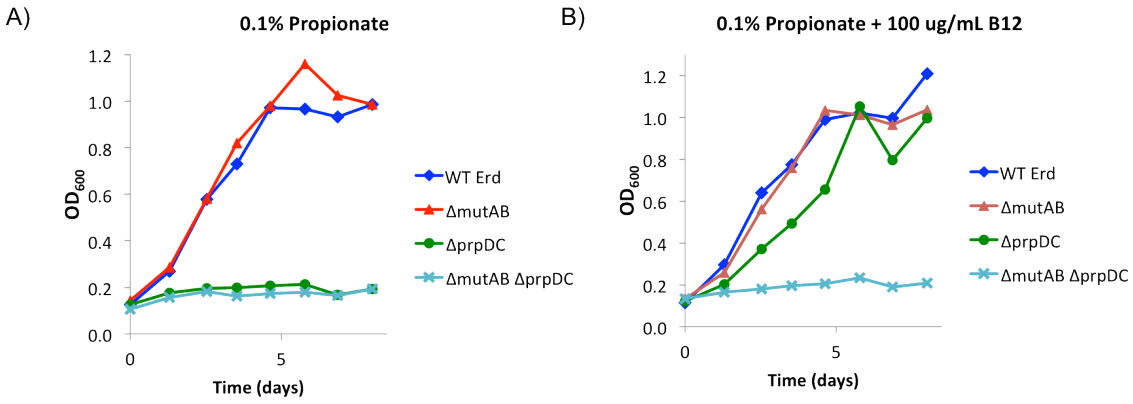

Figure 2.25 Growth of *M. tuberculosis* strains in 7H9 base + albumin-saline (AS) + 0.02% Tyloxapol + 0.1% propionate (A) without or (B) with addition of 100 *μ*g/mL cyanocobalamin (vitamin B12).

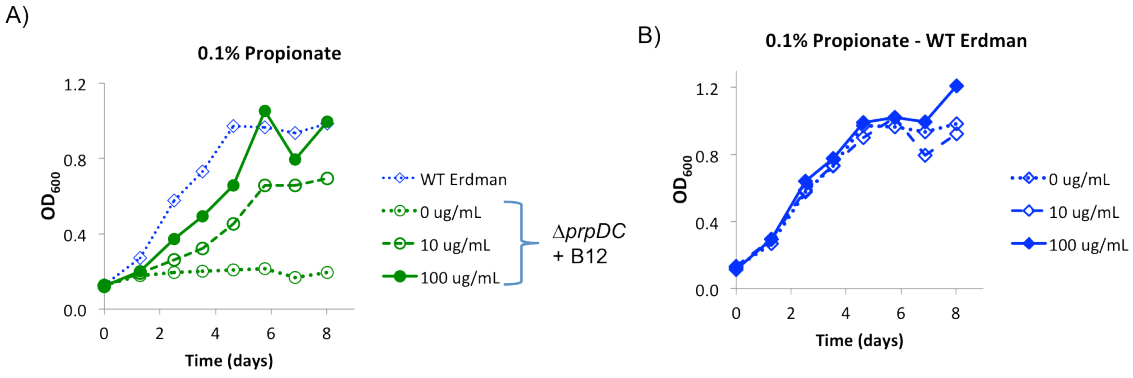

Figure 2.26 (A) Addition of cyanocobalamin (vitamin B12) to *M. tuberculosis* Δ*prpDC* in comparison to WT with 0 ug/mL (from B) grown in 7H9 base + albumin-saline + 0.02% Tyloxapol + 0.1% propionate. (B) Addition of cyanocobalamin (Vitamin B12) in *μ*g/mL to WT *M. tuberculosis* grown in 7H9 base + albumin-saline + 0.02% Tyloxapol + 0.1% propionate.

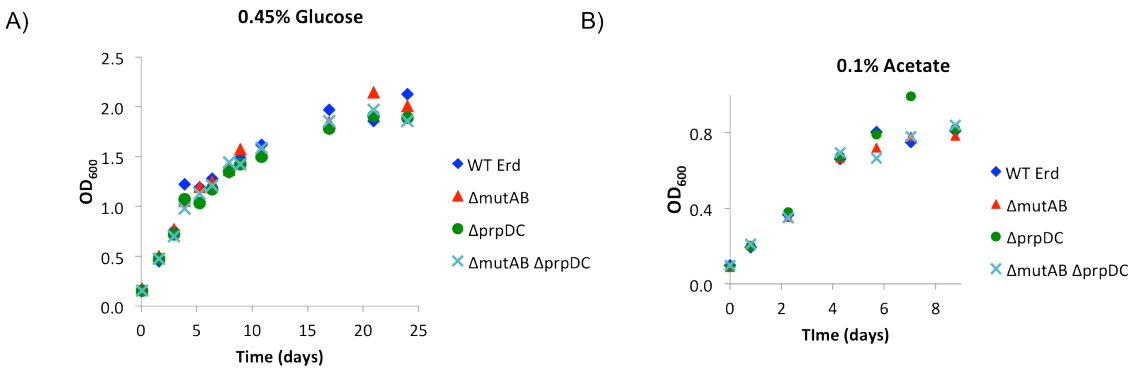

Figure 2.27 Growth of *M. tuberculosis* strains in 7H9 base + albumin-saline + 0.02% Tyloxapol with (A) 0.45% glucose or (B) 0.1% acetate.

- Effects of pathway interruption and pathway suppression on growth

In contrast to the findings above, the MCL/ICL-deficient strain (*icl1::hyg icl2::aph*) was previously shown to exhibit a growth defect on glucose-containing media, in both liquid and solid culture media (Munoz-Elias and McKinney 2005). The same was found to be true for the Δ*icl1* Δ*icl2* unmarked, in-frame deletion strain generated in these studies (Figure 2.28A), which required 4-5 weeks, in contrast to 3-4 weeks for WT, for all CFU to appear on solid agar medium. This growth phenotype of the ICL/MCL-deficient, Δ*icl1* Δ*icl2* strain suggests that ICL or MCL activity, or both, somehow contributes to optimal growth on glucose. The methylcitrate cycle *per se* is not required for normal growth on glucose because deletion of the genes encoding MCS and MCD (Δ*prpDC* strain), which function upstream of MCL in the methylcitrate cycle, had no effect (Munoz-Elias et al 2006). However, it was hypothesized that the growth defect caused by ICL/MCL deficiency (Δ*icl1* Δ*icl2* strain) might be due to accumulation of toxic intermediates

of the methylcitrate cycle. This hypothesis was tested and ruled out by demonstrating that MCS/MCD deficiency did not suppress the growth defect caused by ICL/MCL deficiency (Δ*prpDC* Δ*icl1* Δ*icl2* strain). (Figure 2.28A) Thus, impaired growth of the Δ*icl1* Δ*icl2* strain on glucose is likely due to loss of ICL activity (glyoxylate cycle) rather than loss of MCL activity (methylcitrate cycle).

Consistent with the bifunctional role of ICL/MCL in the glyoxylate and methylcitrate cycles, the Δ*icl1* Δ*icl2* strain was unable to grow on propionate unless supplemented with vitamin B12. (Figure 2.29A) These observations are consistent with the conclusions that (i) B12-mediated activation of the methylmalonyl-CoA pathway can compensate for loss of the methylcitrate cycle to support growth on propionate, and (ii) the glyoxylate cycle is not required for optimal growth on propionate (Savvi et al 2008).

Interestingly, addition of vitamin B12 to propionate-grown cultures resulted in better rescue of the Δ*prpDC* Δ*icl1* Δ*icl2* strain as compared to the Δ*icl1* Δ*icl2* strain. (Figure 2.29A) This surprising result suggests that formation of inhibitory upstream metabolites in the MCL/ICL-deficient strain can be rescued only partially by activation of the methylmalonyl-CoA pathway. Consistent with this interpretation, the Δ*prpDC* Δ*icl1* Δ*icl2* strain, which should not form these intermediates (because the entire pathway is missing), approximated WT growth rates on propionate with exogenously added vitamin B12. In contrast, addition of vitamin B12 to glucose-grown cultures did not rescue the defect of either the Δ*icl1* Δ*icl2* or Δ*prpDC* Δ*icl1* Δ*icl2* strains. (Figure 2.29B) These results suggest

that if growth impairment in these strains is caused by accumulation of toxic metabolites, then formation of these metabolites is not completely prevented by the activitation of the methylmalonyl-CoA pathway.

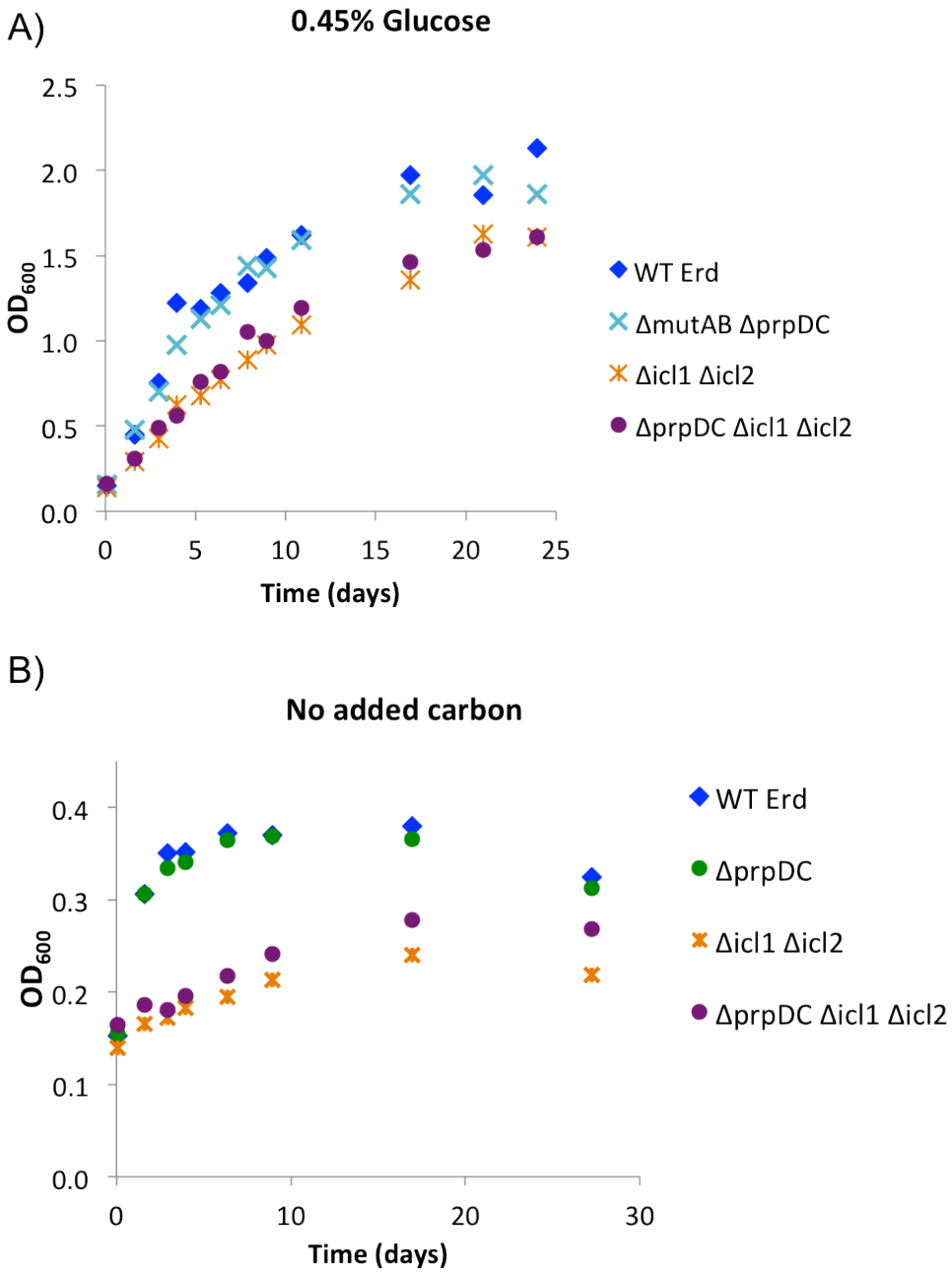

Figure 2.28 Growth of *M. tuberculosis* strains in 7H9 base + albumin-saline + 0.02% Tyloxapol with (A) 0.45% glucose (WT from Figure 2.27A), or (B) no added carbon source.

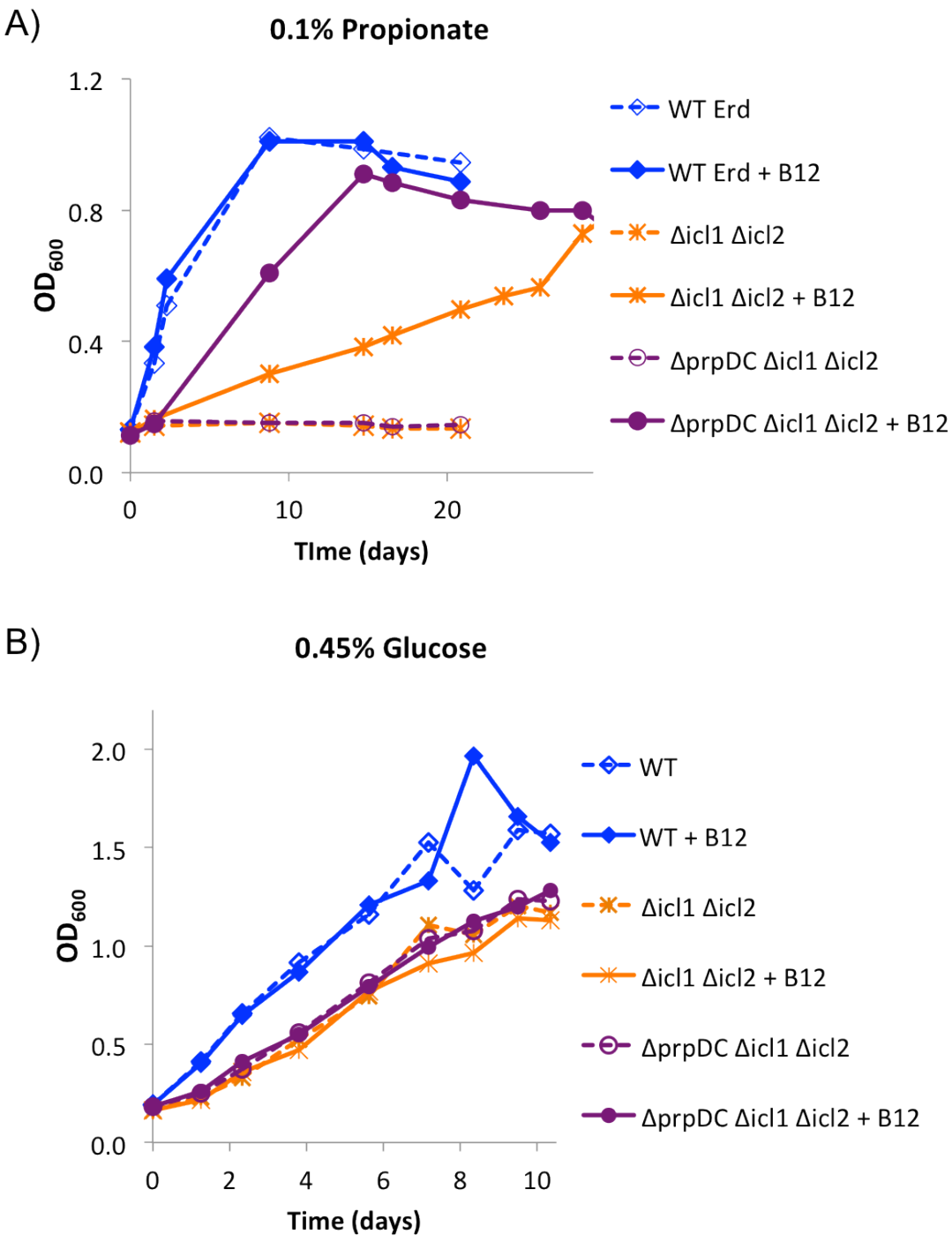

Figure 2.29 Growth of *M. tuberculosis* strains in 7H9 base + albumin-saline + 0.02% Tyloxapol with or without addition of 100 μg/mL cyanocobalamin (vitamin B12) on (A) 0.1% propionate, or (B) 0.45% glucose.

On media with 'no-carbon' added, the Δ*icl1* Δ*icl2* strain exhibited lower ODs than the WT or Δ*prpDC* strains, suggesting a potential role for MCL/ICL under carbon starvation conditions. However, as the elimination of the upstream steps of the methylcitrate cycle, in a Δ*prpDC* Δ*icl1* Δ*icl2* strain, did not significantly alleviate this difference, it is likely the role of the ICL in the glyoxylate cycle that is responsible for the phenotype. (Figure 2.28B)

- Dominant growth inhibition by propionate

The inability of the Δ*prpDC* strain to utilize glucose in the presence of propionate was previously shown (Munoz-Elias et al 2006) and is suggestive of intermediates, formed from propionate, exerting dominant inhibition over the ability to use alternative substrates. Here, the dominant inhibitory effect of 0.2% propionate on the ability to use 0.45% glucose was confirmed for all of the mutant strains that were unable to grow on propionate alone. (Figure 2.30) Whether the methylmalonyl-CoA pathway, activated by B12 supplementation, can rescue this phenotype, remains to be tested.

2.3.6 Animal infection phenotype

Given that the Δ*prpDC* strain was shown to mount an infection indistinguishable from that of wild-type (Muñoz-Elías et al 2006), the potential role of the methylmalonyl-CoA pathway in buffering the loss of the methylcitrate cycle was tested by infection of C57BL/6 mice with the Erdman WT, Δ*mutAB*,

and Δ*mutAB* Δ*prpDC* strains, delivered via the aerosol route. Groups of four mice were sacrificed at each time point to determine the bacterial load in the lungs by plating organ homogenates and enumerating the recovered CFU. It was found that methylmalonyl-CoA mutase was apparently dispensable for infection, as the Δ*mutAB* strain exhibited no difference from WT in the mouse infection model in terms of CFU burden or tissue pathology. (Figure 2.31 A-B, D-F)

In contrast, the Δ*mutAB* Δ*prpDC* strain of *M. tuberculosis* was attenuated during the acute phase of infection, exhibiting a 2.0-2.5 log difference in CFU at 2 weeks. (Figure 2.31A) Moreover, the lungs of mice infected with the Δ*mutAB* Δ*prpDC* strain exhibited no visible lesions throughout the 20 week time course, even after the 10 week time point, when the bacterial burden of the mutant strain matched the WT levels. Histopathological analysis at 12 weeks confirmed that the lung samples from mice infected with Δ*mutAB* Δ*prpDC* had less inflammation than those from WT or Δ*mutAB*-infected mice. In contrast, the WT and Δ*mutAB* exhibited immunopathology that was indistinguishable by either quantitative or semi-quantitative methods in a blinded assessment. (Figure 2.31B-F)

The finding that the methylcitrate cycle (Munoz-Elias et al 2006) and methylmalonyl-CoA pathway are individually dispensable but jointly required for normal growth and virulence in mice suggests that vitamin B12 is either acquired from the host or synthesized by *M. tuberculosis* during infection (or both). Although the Δ*prpDC* Δ*mutAB* mutant was attenuated for *in vivo* growth and

virulence, clearly this strain did not recapitulate the rapid clearance from the lungs observed after intravenous infection of mice with the Δ*icl1* Δ*icl2* strain (Muñoz-Elías and McKinney 2005). This contrast suggests that severe attenuation of the Δ*icl1* Δ*icl2* strain *in vivo* might be due primarily to ICL-deficiency (glyoxylate cycle) rather than MCL-deficiency (methylcitrate cycle).

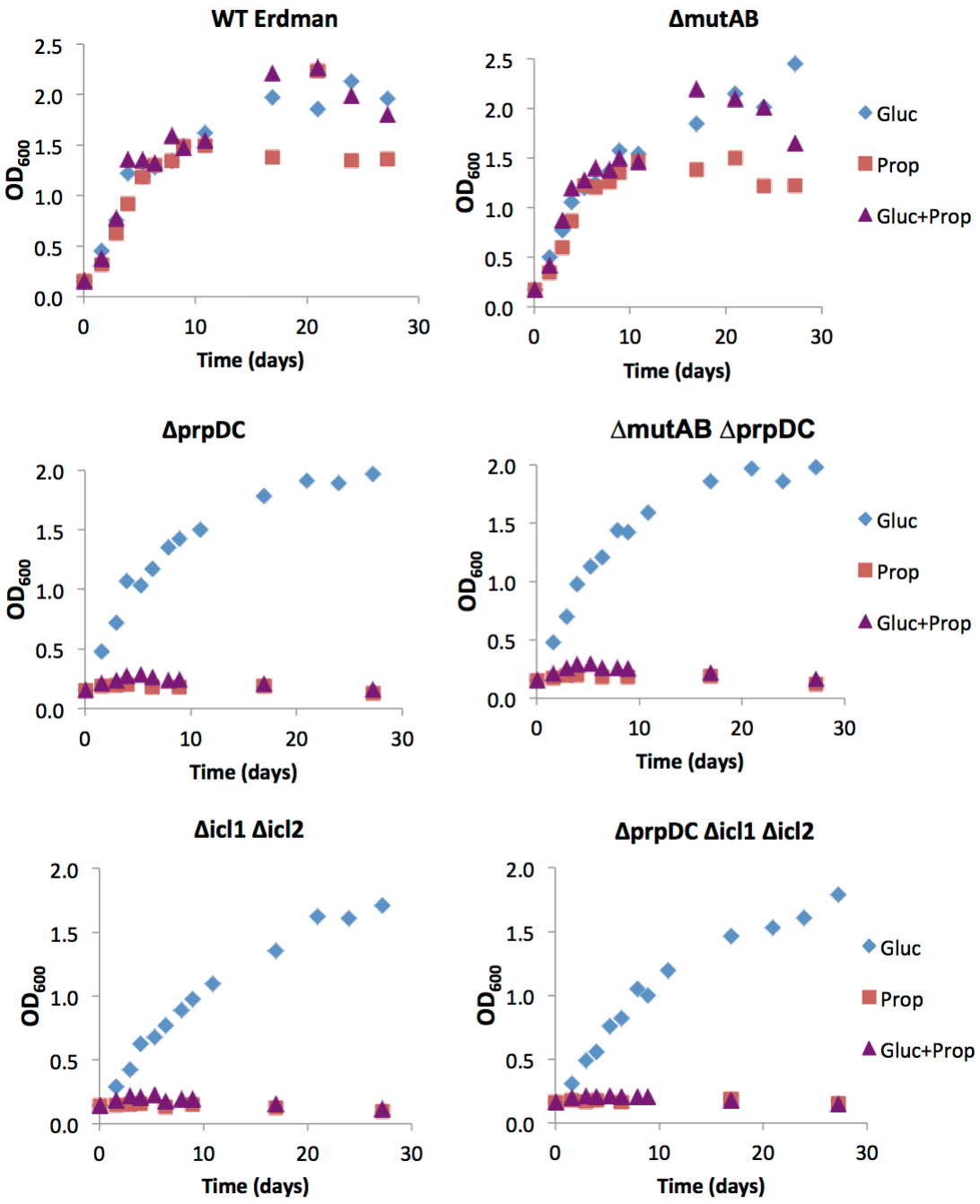

Figure 2.30 Growth of *M. tuberculosis* strains in 7H9 base + albumin-saline + 0.02% Tyloxapol with 0.45% glucose (Gluc) or 0.2% propionate (Prop) or 0.45% glucose + 0.2% propionate (Gluc + Prop).

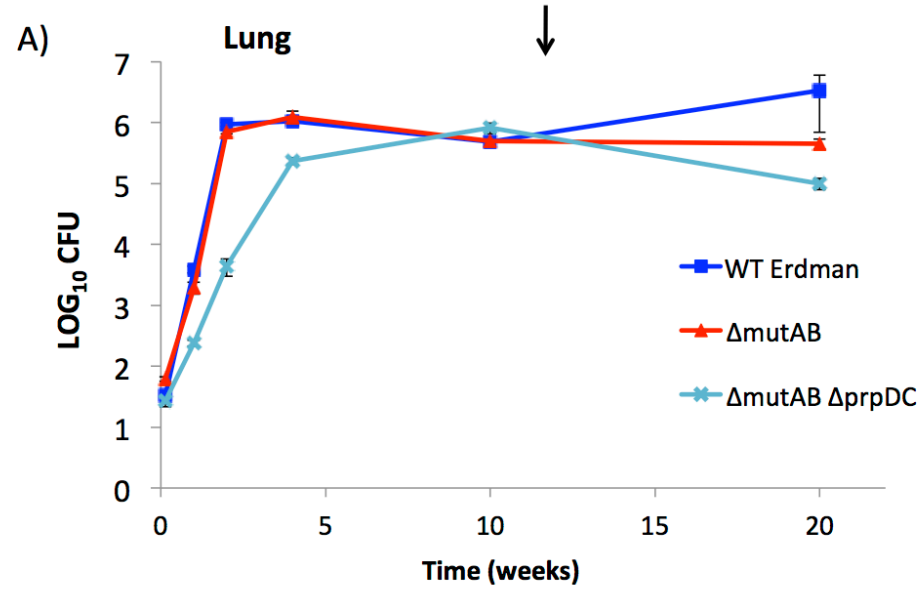

B)

Semiquantitative score		
Lung specimen	Score	Category
ΔmutAB ΔprpDC IV	1	mild
ΔmutAB ΔprpDC III	1	mild
ΔmutAB ΔprpDC II	1	mild
ΔmutAB ΔprpDC I	1	mild
ΔmutAB I	2	moderate
WT II	2	moderate
ΔmutAB IV	2.5	moderate + necrosis
ΔmutAB III	3	marked
WT III	3	marked
ΔmutAB II	3.5	marked + necrosis
WT I	3.5	marked + necrosis

Quantitative score	Inflammation
Lung specimen	Avg Pixel Area
ΔmutAB ΔprpDC II	3149
ΔmutAB ΔprpDC III	7951
ΔmutAB ΔprpDC I	18076
ΔmutAB ΔprpDC IV	18781
WT II	104301
ΔmutAB IV	109168
WT I	130636
ΔmutAB I	143347
ΔmutAB II	151380
WT III	232024
ΔmutAB III	296292

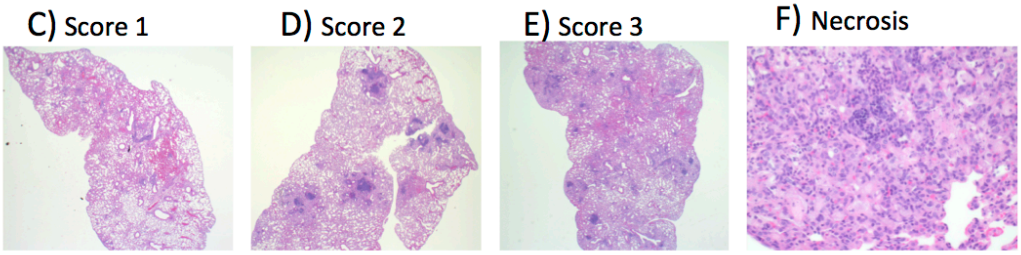

Figure 2.31 (A) Growth of *M. tuberculosis* strains in lungs of C57/BL6 mice. Each point is the average of 4 mice (WT 20 week point is 3 mice) with error bars representing standard error of the mean (SEM). Arrow indicates when samples were taken for histopathology (at 12 weeks). (B) Blind scoring of histopathology specimens by independent methods. (C-E) Representative images of categories 1 (Δ*mutAB* Δ*prpDC* IV), 2 (Δ*mutAB* I), and 3 (WT I). (F) Enlargement of necrotic region of (E).

2.3.7 Discussion

The disparities between the *in vitro* culture conditions in which we study pathogens and the conditions that prevail in their natural host environment become evident in cases where a pathway that appears to be essential for growth under defined conditions *in vitro* is shown to be dispensable for growth *in vivo*. An example is provided by earlier studies of the methylcitrate cycle, which is essential for growth *in vitro* on propionate-containing medium but dispensable for growth in the lungs of mice (Munoz-Elias et al 2006). Subsequent studies have characterized the methylmalonyl-CoA pathway as a 'cryptic' pathway that requires exogenous B12 *in vitro*, and thus might be functional *in vivo* depending on B12 availability or biosynthesis by *M. tuberculosis* during infection (Savvi et al 2008).

The early and transient growth defect of the Δ*mutAB* Δ*prpDC* strain in the lungs of acutely infected mice suggests a role for propionyl-CoA metabolism at this stage of infection. Apparently this role can be fulfilled by either the methylcitrate cycle or the methylmalonyl-CoA pathway, as evidenced by the apparently normal course of infection exhibited by the Δ*prpDC* (Munoz-Elias et al 2006) and Δ*mutAB* strains, as demonstrated here. In speculating on the cause of attenuation, it might be reasoned that a strain that is unable to process propionyl-CoA beyond the points of methylcitrate synthase or methylmalonyl-CoA epimerase would channel the excess into methyl-branched fatty acid synthesis. However, in terms of the impact this has on *in vivo* growth, the putative change in

cell wall composition could potentially increase virulence by enhancing the immunomodulatory effects of cell wall components or, conversely, attenuate virulence by stimulating immune recognition (Camacho et al 1999, Mendelson et al 2005). Alternatively, the altered routing of carbon could cause an imbalance between cataplerosis and anaplerosis, resulting in a general growth defect (Jain et al 2007).

The attenuation of lung pathology caused by the Δ*mutAB* Δ*prpDC* strain may directly result from early growth attenuation of the strain and the onset of the immune response before a 'critical mass' of bacteria is reached. However, the possibility exists that the strain itself induces a less robust inflammatory response on a 'per cell' basis. The latter possibility could be further investigated by careful evaluation of the immune responses induced by the Δ*mutAB* Δ*prpDC* strain or in a long-term survival time course.

Although methylmalonyl-CoA mutase (MCM) was found to be dispensable for infection, the entire methylmalonyl-CoA pathway is probably not dispensable because the formation of methyl-branched lipids from the action of propionyl-CoA carboxylase (PCC) should be essential for cell wall formation in mycobacteria. Consistent with this idea, genes encoding components of PCC are predicted to be essential by transposon mutagenesis (Sassetti and Rubin 2003). It is not clear whether PCC's function could be bypassed by overexpression of MCM and running the pathway in the other direction, although this has been shown not to be the favored direction in the presence of propionyl-CoA in rat tissues (Reszko

et al 2003). Attempts to overexpress *mutAB* in otherwise WT *M. tuberculosis* led to a reduction in CFU in the lungs of mice during the later stages of infection and a selection against the plasmid encoding this activity even though the overexpressing strain displayed lipidomic profiles similar to those of lung-isolated bacteria; depletion of TCA cycle intermediates was speculated to be a contributing factor (Jain et al 2007).

In light of the abovementioned findings, the severe *in vivo* attenuation of the Δ*icl1* Δ*icl2* strain cannot be attributed to the absolute requirement for propionyl-CoA metabolism during infection. However, it cannot yet be ruled out that the *in vivo* requirement for the bifunctional ICL/MCL enzymes at least partially reflects their role in metabolizing toxic intermediates of the methylcitrate cycle, thus fulfilling a detoxification role rather than a nutritional requirement.

However, it is still possible that the action of the citric acid cycle enzymes on propionyl-CoA and derived metabolites might be a source of toxic intermediates even in the absence of the initial steps of the canonical methylcitrate cycle, as suggested by studies in *M. smegmatis* presented in this thesis. An alternative explanation may be that optimal growth on glucose in *M. tuberculosis* somehow relies on the glyoxylate bypass of the TCA cycle, as a branched functioning seemed to be indicated in metabolomic studies (de Carvalho et al 2010b).

In contrast, the ability of vitamin B12 supplementation to rescue a Δ*prpDC* Δ*icl1* Δ*icl2* strain to a greater extent than a Δ*icl1* Δ*icl2* strain for growth on

propionate does suggest that in the presence of propionate, methylcitrate cycle intermediates are formed by the action of MCS (*prpC*) and MCD (*prpD*) and 'trapped' by the absence of MCL activity (*icl1 icl2*). Accumulation of these intermediates in the Δ*icl1* Δ*icl2* strain would not be alleviated by the methylmalonyl-CoA pathway, whereas accumulation of propionyl-CoA in the Δ*prpDC* Δ*icl1* Δ*icl2* strain presumably would be. This is a compelling point in terms of a potential role for ICL/MCL in detoxification of propionate breakdown products during infection, even in the presence of a functional methylmalonyl-CoA pathway.

Recently, the epistatic effect of upstream lesions on downstream lesions was also demonstrated for *M. tuberculosis* ICL/MCL-deficiency and MCD/MCS-deficiency with respect to cholesterol utilization, where the survival and growth defects in macrophages were alleviated by deletion of *mce4*, a putative cholesterol transporter (Griffin et al 2012).

Metabolite analysis of these *M. tuberculosis* mutants, similar to the types previously described in this thesis for *M. smegmatis*, would address these points. This information could be supplemented by functional clues that suppressor mutants or 'overexpress-or' mutants might provide. The *M. tuberculosis* Δ*icl1* Δ*icl2* strain is well suited to a suppressor screen as it is completely inhibited for growth by propionate, even in the presence of rich media, which contains glycerol in higher w/v amounts (0.5%) than propionate (0.1%), thus allowing for a clean selection of suppressor mutations. Providing a diverse array of alternative

carbon sources would, in theory, also allow for the selection of suppressor mutations in genes that would otherwise be essential for growth on minimal media *in vitro*. For example, a mutation in citrate synthase could be obtained (in theory, at least) because inclusion of glutamate in 7H9 and 7H10 media would supplement the inherent glutamate auxotrophy caused by citrate synthase deficiency (Rocco and Escalante-Semerena 2010). If the same degree of dominant inhibition can be shown for Δ*mutAB* Δ*prpDC*, than this strain could also be used in a genetic screen to interrogate the mechanisms of inhibition by propionate.

The *in vivo* relevance of the hypothesized detoxification role of ICL/MCL remains to be established, but could now be tested by comparing the kinetics of growth and survival of the Δ*icl1* Δ*icl2* and Δ*prpDC* Δ*icl1* Δ*icl2* strains in infected mice. Deciphering the required *in vivo* role of this enzyme would yield invaluable insight into the host environment that *Mycobacterium tuberculosis* inhabits.

3. Conclusions

The work presented in this thesis involved the examination of two routes of propionate metabolism in two species of mycobacteria. When studying the similar pathways in different organisms, it is often useful to make comparisons. In the case of the pathogen *Mycobacterium tuberculosis* and the free-living saprophyte *Mycobacterium smegmatis*, differences can be postulated to be adaptive for their respective lifestyles.

Both mycobacteria encode the methylcitrate cycle and methylmalonyl-CoA pathways of propionate metabolism. However, there are notable differences in the genomic loci and mutant phenotypes. *M. smegmatis* encodes the more canonical *prpDBC* operon, consisting of the three enzymatic activities unique to the methylcitrate cycle: MCD, MCL, and MCS (Upton and McKinney 2007). However, *M. tuberculosis* is lacking the *prpB* homolog for the methylisocitrate lyase, and instead utilizes a bifunctional isocitrate lyase / methylisocitrate lyase that acts in both the glyoxylate cycle and the methylcitrate cycle. While the *prp* operon lies downstream of the *prpR* regulator (Datta et al 2011, Griffin et al 2012), the *icl1* and *icl2* genes are located in disparate regions. It is of interest to know how the regulation of the different loci is achieved for growth on propionate.

A comparison also reveals a difference at the *mutAB*-encoding loci. While the *meaB* gene lies in the well-conserved position adjacent to the *mutAB* of *M. smegmatis*, it is separated from *mutAB* in the *M. tuberculosis* genome by a *mazEF* toxin-antitoxin module. While the functions of these genes are not yet

fully understood, a recent study suggested that the *vapBC* of *M. smegmatis* targeted a number of metabolic genes, and may play a post-transcriptional role for regulation (McKenzie et al 2012). It is tempting to speculate on the possible effect of this module in the *mutAB* locus of *M. tuberculosis*, either in regulation or on the interaction between *mutAB* and *meaB*.

The two mycobacteria also differ with respect to propionate tolerance. Wild-type *M. smegmatis* grow robustly at 0.5% w/v concentrations of propionate, whereas, a slight lag is already noticeable when culturing *M. tuberculosis* in media containing 0.2% of the substrate. There is also a difference in the inhibitory effects of propionate in the presence of alternative carbon sources. While *M. smegmatis* Δ*mutAB* Δ*prpDBC* can utilize the glucose in mixtures with propionate for growth, albeit with a lag and with reduced yields, *M. tuberculosis* Δ*mutAB* Δ*prpDC* cannot.

Based on the metabolite analysis of *M. smegmatis* and the slight defect in growth of Δ*mutAB* Δ*prpDBC* in glucose-containing media, there is an apparent basal use of the propionate pathways, perhaps for metabolism of endogenous sources of propionyl-CoA. In contrast, the Δ*mutAB* Δ*prpDC* strain of *M. tuberculosis* grows indistinguishably from WT on glucose. This suggests that there is less basal propionyl-CoA generation, that it is less toxic, or that it can be more effectively used by the propionyl-CoA carboxylase for channeling into methyl-branched lipids (Jain et al 2007). The basis of these differences will be better understood with metabolite-based analysis of *M. tuberculosis*.

In contrast, the Δ*icl1* Δ*icl2* strain of *M. tuberculosis* does have a growth phenotype on glucose, whereas the Δ*icl1* Δ*icl2* of *M. smegmatis* does not. As a Δ*prpDC* Δ*icl1* Δ*icl2* of *M. tuberculosis* shares the defect, it does not seem to be caused by accumulating methylcitrate cycle metabolites. Therefore, it seems optimal growth on glucose of *M. tuberculosis*, but not *M. smegmatis*, requires the glyoxylate cycle. A role of the glyoxylate cycle for growth in glucose was inferred from the basal activity of the ICL enzyme on glucose (Kujau et al 1992) as well as a growth phenotype on glucose for an ICL-deficient strain of *Yarrowia lipolytica* (Barth and Scheuber 1993). It was suggested that the role of ICL under glucose growth may be to produce glyoxylate, which can contribute, along with serine, to the formation of glycine (Barth and Scheuber 1993). Conversely, the derepression of ICL, in an Δ*iclR* strain of *E. coli*, led to an increase in biomass yield on glucose. A comparison of the metabolic fluxes determined that carbon was 'saved' from the bypass of CO_2 loss that the glyoxylate cycle enables (Waegeman et al 2011).

This study also reveals a difference in *M. smegmatis* and *M. tuberculosis* with respect to the *in vitro* 'inducibility' of the methylmalonyl-CoA mutase. While a Δ*prpDBC* strain of *M. smegmatis*, lacking only the methylcitrate cycle, will grow on propionate after a lag period, the Δ*prpDC* strain of *M. tuberculosis* will not. By supplementing the media with the B12 cofactor for the methylmalonyl-CoA mutase, both strains are able to utilize propionate without a lag. This suggests that under *in vitro* conditions, *M. smegmatis* can eventually activate the

methylmalonyl-CoA pathway, presumably after synthesis of B12, whereas *M. tuberculosis* cannot. As both encode the full complement of B12 synthesis genes, the difference in regulation of these pathways warrants further investigation.

The 'paradox' of vitamin B12 synthesis revolves around the seemingly large cost of encoding over 25 genes for the activation of enzymes and pathways that, *in vitro*, are largely dispensable (Lawrence and Roth 1996). In testing the *in vivo* relevance, the loss of vitamin B12 synthesis in *S*. Typhimurium and other serovars did not lead to a defect in virulence (Bjorkman et al 1996, Paiva et al 2011). While the *cob* operon for B12 biosyntheis was not upregulated in *S.* Typhimurium during colonization of the host, the *btuF* B12 transport gene was. Yet, the *btuF* mutant strain did not have a phenotype during infection (Harvey et al 2011). While the *M. tuberculosis* genome encodes both B12-independent (*metE*) and B12-dependent (*metH*) methyltransferases, clinical strains have been identified with *metH* defects. As they were isolated from patients, these isolates have retained their pathogenicity. Counter-intuitively, the CDC1551 strain, which has a disrupted *metH*, is known to be more virulent (Warner et al 2007).

Interestingly, *M. tuberculosis* Δ*mutAB* Δ*prpDC* is capable of growing and persisting in the mouse infection model, although with a defect during the acute phase. As neither the Δ*prpDC* nor Δ*mutAB* strains have this defect, there is a role for propionyl-CoA metabolism at this stage of infection. Moreover, the Δ*prpDC* strain, which is fully virulent *in vivo*, must be capable of metabolism through the alternative route of the methylmalonyl-CoA pathway, suggesting the

ability to acquire or synthesize the B12 cofactor in the host. To distinguish between the two possibilities, B12 synthesis and B12 transport mutants would need to be constructed in the Δ*prpDC* strain background and tested in mice. What the *in vivo* requirements might be of the other B12-dependent enzymes, the *metH*-encoded methionine synthase and the *nrdZ*-encoded type II ribonucleotide reductase, should be taken into account for such experiments.

The Δ*mutAB* Δ*prpDC* strain also elicits less tissue pathology during the course of infection, despite eventually reaching wild-type colonization levels. While the lower levels of inflammation could simply be a result of the initial attenuated growth levels, the role of MCM in forming methyl-branched lipid precursors might suggest an alteration of lipid profile in this mutant strain. Therefore, lipidomic and immunogenicity assays of the Δ*mutAB* Δ*prpDC* strain may clarify these aspects of the infection phenotype.

The presence of two routes of propionate metabolism is of interest, especially considering the *in vivo* dispensability of either. While the methylcitrate cycle seems to be the default route of both organisms for growth under *in vitro* conditions, the methylmalonyl-CoA pathway is the route that produces the likely essential precursors for methyl-branched lipids, although the MCM-role is not required for this. The retention of the large number of B12 biosynthetic genes in both *M. smegmatis* and *M. tuberculosis*, despite the apparent non-functionality of this pathway for *in vitro* growth of *M. tuberculosis*, also remains a mystery.

The presence of seemingly redundant pathways may be understood in terms of differential use, allowing for flexibility under a variety of conditions, as shown for the aconitase enzymes of *E. coli* (Gruer and Guest 1994, Gruer et al 1997) and the malate synthases of *S. cerevisiae* (Hartig et al 1992, Fernandez et al 1993, Wong and Wolfe 2005). The benefits of a B12-dependent enzyme for resistance to reactive oxygen species and reactive nitrogen species were suggested for the ribonucleotide reductase of *Sinorhizobium meiloti* (Taga and Walker 2010).

The results of this work corroborate the idea that how pathways are interrupted affects the phenotype. An MCL/ICL-deficient strain (Δ*icl1* Δ*icl2*) of *M. tuberculosis* was not completely rescued for growth on propionate by the activation of the methylmalonyl-CoA pathway. In contrast, the additional lesion of the upstream steps of the methylcitrate cycle in this background (Δ*prpDC* Δ*icl1* Δ*icl2*) allowed for improved rescue, suggesting that it was better to eliminate a pathway entirely than to disrupt it, as was seen for *M. smegmatis* previously (Upton and McKinney 2007).

Toxic metabolite accumulation has been shown for *M. tuberculosis* in the case of maltose-1-phosphate buildup in a glucan metabolic pathway. Suppression of toxicity was mediated by the conditional inactivation of the enzyme that forms maltose-1-phosphate (Kalscheuer et al 2010). In *S. typhimurium*, the inhibition of the acetohydroxy acid synthase I (AHAS I) caused accumulation of alpha-ketobutyrate, which can reportedly affect a number of

metabolic pathways, in addition to the branched-chain amino acid synthetic pathway that produces it (Daniel et al 1984, LaRossa et al 1987). Homocysteine, an intermediate of methionine biosynthesis, which accumulated in media containing acetate, appears to exert toxicity on the formation of the branched-chain amino acids isoleucine and valine in *E. coli* (Roe et al 2002, Tuite et al 2005). Notably, homocysteine levels increased substantially after treatment of *M. tuberculosis* with trimethoprim or following depletion of dihydrofolate reductase levels (Wei et al 2011).

The findings here support a re-evaluation of the *in vivo* phenotype of the ICL/MCL-deficient strain of *M. tuberculosis*. While neither route of propionyl-CoA metabolism was required, even the joint loss of the pathways did not recapitulate the clearance from the lungs seen for the ICL/MCL-deficient strain (Munoz-Elias and McKinney 2005). It has been suggested that the role of propionate metabolic pathways may be for detoxification, rather than primary metabolism. The correlation of accumulation of intermediates with growth defects has been shown here for the Δ*prpDBC* and Δ*mutAB* Δ*prpDBC* strains of *M. smegmatis*, using metabolite analysis. The corresponding examination will need to be done in *M. tuberculosis* with the Δ*mutAB* Δ*prpDC*, Δ*icl1* Δ*icl2*, and Δ*prpDC* Δ*icl1* Δ*icl2* strains generated as part of this study. Understanding the mechanisms by which the accumulating propionate metabolites exert their toxicity can be addressed in a genetic screen to isolate suppressor mutants of this phenotype. These strains would have additional lesions in the Δ*icl1* Δ*icl2* or Δ*mutAB* Δ*prpDC* background

that would allow for a bypass of the formation of, or an alleviation of the effects of, the toxic metabolites.

Other data shown here support a role of the glyoxylate cycle in *M. tuberculosis* for growth on glucose and no carbon (Munoz-Elias et al 2005, Gengenbacher et al 2010). Under these conditions, the phenotypes of the Δ*icl1* Δ*icl2* strain are not relieved in the Δ*prpDC* Δ*icl1* Δ*icl2* strain. An independent lesion of the glyoxyle cycle would be key in proving this, but is complicated by the apparent essentiality of MLS (E.J. Munoz-Elias Ph.D thesis, 2005, N. Dhar personal communication, S. Ehrt personal communication, Griffin et al 2011). It is possible that MLS is required to prevent a toxic buildup of glyoxylate. If so, it may be possible to construct this mutant in a Δ*icl1* Δ*icl2* background. However, this strain would not address the independent role of the glyoxylate cycle, as it leaves the function of the ICL/MCL coupled. A possible alternative may be to 'complement' the Δ*icl1* Δ*icl2* strain with a monofunctional MCL, such as that encoded by the *prpB* of *M. smegmatis.* This would conceivably reconstitute the methylcitrate cycle while leaving the glyoxylate cycle lesioned.

There remains the possibility that the essentiality for the MCL/ICL *in vivo* stems from its role in both these pathways, or, perhaps, an additional role, yet undiscovered. As the Δ*lpdC* strain is also subject to rapid clearance from the lungs of infected mice, it supports the idea that the most severe defects may result from deletion of components that lie at the junction of multiple pathways. It may be that the role of the bifunctional ICL/MCL of *M. tuberculosis* is required *in*

vivo because it plays a role in the metabolism of multiple carbon sources, including even-chain length fatty acids, odd-chain length fatty acids, cholesterol, and amino acids (Munoz-Elias and McKinney 2005, Venugopal et al 2010, Griffin et al 2012)

Thus, in targeting metabolism for drug development, identifying enzymes that contribute to multiple pathways, or that produce toxic intermediates that can dominantly inhibit metabolism, might be a promising approach. These aspects are not always clearly evident from phenotypic analysis. In this work, a role for metabolite analysis has been demonstrated in revealing the convergence of pathways and identifying these intermediates.

4. Materials & Methods

- Media and chemical reagents

Percentages are weight/volume (w/v). All non-salt reagents were filter sterilized. 7H9 based media, AS, ADS, ADC, OADC, and Tyloxapol, were all stored at 4 deg C.

Stocks of Kanamycin and cyanocobalamin (vitamin B12) were stored in aliquots at -20 deg and then at 4 deg C for use.

Carbon sources of (D+)Dextrose (glucose), sodium propionate, and sodium acetate were made as 20% (w/v) stock solutions, pH 6.8. Glycerol was made as 50% stock for media and 70% stock for freezer stocks. For electroporations, 10% glycerol was freshly made. Sucrose was made at 20%. Glycine was made at 2M. Tween80 and Tyloxapol were made as 10% solutions. Albumin-saline (AS) was made as 10X stock of 5% bovine serum albumin, Fraction V and 0.85% NaCl. Albumin-dextrose-saline (ADS) was as above, but with D-dextrose added at 2%.

7H9 media was made with Middlebrook 7H9 base, 1X ADS, 0.2% Tyloxapol.

M9 minimal salts were made as a 5X stock solution and was used at 1X with 2 mM $MgSO_4$ and 0.1 mM $CaCl_2$ (optional: carbon sources added at appropriate concentration). Solid media made with Bacto agar.

LB media was made with Luria Miller broth.

Antibiotics stock solutions were 25 mg/mL Kanamycin sulfate salt (Sigma), 50 mg/mL Hygromycin (Roche) and used at 50 ug/mL and 150 ug/mL for *E. coli*, 15 ug/mL and 50 ug/mL for *M. smegmatis*, 25 ug/mL and 50 ug/mL for *M. tuberculosis*.

Cyanocobalamin stocks were made at 10 mg/mL and kept protected from light.
Cycloheximide stock was made at 10 mg/mL and kept protected from light.
'X-Gal' stock was 40 mg/mL solution of 5-Bromo-4-chloro-3-indolyl beta-D-galactopyranoside in N'N' Dimethylformamide.

Plate media included LB agar, 1X M9 agar (1.5% Bacto agar with 2 mM $MgSO_4$ and 0.1 mM $CaCl_2$ and carbon source added to 0.1% or 0.5%, and 7H10 Middlebrook base with 10% OADC or ADC, 0.5% glycerol.

- Making bacterial stocks

Single colonies of *M. smegmatis* mutants generated in this study were selected from sucrose counter-selection plates (or antibiotic electroporation plates for plasmid integration) into 2 mL 7H9 AS + 0.2% glucose + 0.02% Tyloxapol in 15 mL culture polystyrene tubes, grown at 37 degrees, shaking at 180 rpm, to an OD_{600} of ~ 0.8 - 1. Frozen stocks in 15% glycerol were made and the remainder

of the culture was used to inoculate a 10 mL volume of 1X M9 with 0.2 or 0.5% glucose in 100 mL glass flasks with metal caps, sealed with Parafilm, grown as above, to an OD_{600} of ~0.6 - 0.9. This culture was divided into aliquots and frozen without glycerol as inocula for M9 starter cultures.

Single colonies of *M. tuberculosis* mutants generated in this study were selected from sucrose counter-selection plates into 5-10 mL 7H9 ADS + 0.5% glycerol + 0.02% Tyloxapol in 30 mL PETG square 'inkwell' bottles (Nalgene), grown at 37 degrees, shaking at 100 rpm, to an OD_{600} of ~0.8 - 1. Frozen stocks in 15% glycerol were made. 1 tube was thawed to start a culture of 1 mL in 9 mL 7H9 AS + 0.2% glucose + 0.02% Tyloxapol, grown as above to an OD_{600} of ~0.8, divided into 1 mL aliquots, and frozen without glycerol as inocula for 'minimal media' starter cultures. A culture in 7H9 ADS + 0.5% glycerol + 0.02% Tyloxapol was grown in parallel to an OD_{600} of ~0.8, divided into 1 mL aliquots, and frozen with 15% glycerol as inocula for PDIM analysis, mouse infections, and subsequent transformations.

- Bacterial growth conditions

Starter cultures of *M. smegmatis* were inoculated with 0.5 mL M9 frozen stock in 9.5 mL 1X M9 0.2 or 0.5% glucose, into glass flasks as above, and grown to OD_{600} of ~ 0.7 - 1. Cells were harvested by centrifugation in 15 mL polypropylene tubes, at 4000 rpm, for 12 minutes. The supernatant was decanted

and the pellets resuspended in 1X M9 base. OD_{600} was measured and the appropriate volume was inoculated into glass culture flasks containing 1X M9 base with carbon source added at 0.1% or 0.5% to an OD_{600} of ~0.05 in 15 - 20 mL. (Alternatively 1X M9 with carbon source pre-added at the appropriate concentration was used for resuspension and dilution). Cultures were incubated at 37 deg, shaking, with Parafilm around metal cap.

Starter cultures of *M. tuberculosis* were inoculated with 1 mL 'minimal' frozen stock in 9 mL 7H9 AS + 0.2% glucose + 0.02% Tyloxapol and grown as above to an OD_{600} of ~ 0.5 - 0.9. Cells were harvested by centrifugation in 15 mL polypropylene tubes at 3500 rpm. The supernatant was decanted and the pellets resuspended in 7H9 AS Tyloxapol base. OD_{600} was measured and the appropriate volume was used to inoculate square culture bottles at OD_{600} 0.05. Carbon source was added at appropriate concentration. Cultures were incubated at 37 deg, shaking.

- PCRs and cloning: deletion plasmids and complementation plasmids

All PCR reactions contained 0.2 mM $MgCl_2$, 0.6 uM primers, 10% glycerol, 0.5 U Taq

'Homology arms' upstream and downstream of the gene, including the codons to be retained in the fused, 'truncated' deletion allele, were amplified from genomic

DNA by primers containing 5' restriction sites. The 'upstream' F primer contained a 5' PacI site and the R primer a 5' AvrII site. The 'downstream' F primer contained a 5' AvrII site and the R primer a 3' AscI site. Invitrogen High Fidelity Taq was used.

The PCR products were cloned into the pCR2.1 TOPO vector topoisomerase-based TA cloning and transformed into TOP10 chemically competent *E. coli* cells. Transformants were selected on LB plates containing Kan and X-Gal. Clones were grown in 2.7 mL LB, stocks frozen in 15% glycerol, and the remainder used for a plasmid miniprep using the Qiagen QiaPrep spin kit. Clones containing the insert by restriction digest were sent for sequencing using the M13 and M13rev primers sites in the TOPO vector.

The homology arms in error-free clones were digested out of the TOPO vector using the PacI / AvrII and AvrII / AscI primer pairs. The pJG1100 and pJG1111 (gift of L. Merkov) vectors were digested using PacI and AvrII and AvrII and PacI and treated with calf intestinal phosphatase (NEB) for 1 hr. The dephosphorylated digested vector and the inserts were separated on a 0.85% TBE gel and bands extracted using the Qiagen QiaQuick kit.

The ligation reactions for the homology arm into the vector were done stepwise in 2 ligations, using the NEB T4 DNA ligation kit, letting the reactions go overnight

starting in a ice bath kept at room temperature. Ligations were transformed into TOP10 cells, selected as above, and checked by restriction digest with PacI / AscI, PacI / AvrII, and AvrII / AscI.

For cloning the *mutAB* complementation construct, the 4292 bp product was amplified with the Finnzyme Phusion DNA polymerase was used with the HF (High Fidelity) buffer, to avoid errors in the product. Primers containing 5' NotI sites were used to amplify the full-length genes including 174 bp of the upstream region. The PCR products were cloned, checked for insert, and sequenced as above. The insert in an error-free clone was digested out of the TOPO vector using NotI and AseI. The *attB*-integrating vector containing a gene encoding GFP expressed under a strong synthetic promoter (pND235, gift of N. Dhar) was digested using NotI-HF and treated with calf intestinal phosphatase (NEB) for 1 hr. The fragments of the insert and the vector were separated and extracted as above, and ligated.

To generate the upstream merodiploid complementation vector, the region upstream from *mutAB* was cloned using primers with 5' NsiI and 5' BsrGI sites and subcloned into the pCR2.1 TOPO clone containing *mutAB*, digested with the same enzymes. The upstream region and *mutAB* genes were excised using XbaI/SpeI. The pJG1111 vector was digested with XbaI (SpeI-compatible), eliminating the *sacB* and *hyg*-resistance cassette, and dephosphorylated. After

gel extraction of both components, the insert was ligated within and the final vector pJG1111 :: Up comp *mutAB* was used for allelic exchange.

To generate the *mutAB meaB* complementation vector, a primer located upstream of an FseI site and a primer with a 5' SpeI site were used to amplify *meaB*. This fragment was subcloned into the pCR2.1 TOPO clone containing *mutAB*, digested with the same enzymes. The original pND235 :: *mutAB* complementation construct was digested with KpnI and SpeI and the *meaB* fragment was ligated within.

- Competent cell preparation, electroporation, and counter-selection

For *M. smegmatis*, a competent cell culture was grown from 1 vial of glycerol frozen stock in 49 mL 7H9 ADS 0.02% Tyloxapol in 250 mL glass flask with metal cap, shaking at 37 deg to an OD_{600} of ~ 0.8.

Cells were kept on ice for 1 - 2 hr, spun down at 3,000 rpm, 10 min, thrice washed with ice cold 10% glycerol, resuspended in 1/25 vol 10% ice cold glycerol for allelic exchange (or 1/15 vol 10% glycerol for site-specific plasmids), aliquoted 385 uL into cuvette, added 1 - 2 ug DNA, pulsed at 2.5 kV, 1000 Ohms, 25uF in a 2 mm-gap cuvette.

Electroporations were recovered in 2.5 mL 7H9 ADS + 0.02% Tyloxapol (from 4 deg) for 2 hours, in 15 mL polypropylene tube shaking at 37 deg, before centrifuging and plating onto selective media.

For *M. tuberculosis*, cells were grown in 7H9 ADS + 0.5% glycerol + 0.02% Tyloxapol in a roller bottle to an OD_{600} ~ 0.4 - 0.6. 10 mL of 2 M glycine was added and incubated for a further 24 hr, rolling.

Cells were harvested at 3,800 rpm, 12 min. Cells were thrice washed with room temperature 10% glycerol, resuspended in 1/50 vol 10% glycerol for allelic exchange (or 1/25 vol 10% glycerol for site-specific plasmids), aliquoted 385 uL into cuvette, added 1 - 2 ug DNA, pulsed at 2.5 kV, 1000 Ohms, 25uF in a 2 mm-gap cuvette.

Electroporations were recovered in 2 mL 7H9 ADS + 0.05% glycerol + 0.02% Tyloxapol (from 4 deg), in small square bottles, shaking at 37 deg for 24 hours before centrifuging and plating onto selective media.

For *M. smegmatis*, single transformant colonies were inoculated into 2 mL 7H9 ADS + 0.02% Tyloxapol with appropriate antibiotics and incubated, shaking, until an OD_{600} ~ 0.5 - 0.8. Aliquots were frozen in 15% glycerol and remainder was pelleted in a microfuge, media removed with a pipette, and the cells resuspended

in 2 mL 7H9 ADS + 0.02% Tyloxapol (without antibiotics). The culture was incubated at 37 deg, shaking. Serial dilutions and plating onto LB agar with 5% sucrose and 25 ug/mL X-Gal was done after 4 hr and 8 hr of incubation.

For *M. tuberculosis*, single transformant colonies were inoculated into 6 mL 7H9 ADS + 0.5% glycerol + 0.02% Tyloxapol with appropriate antibiotics and incubated, shaking, until an OD_{600} ~ 0.5 - 0.8. Aliquots were frozen in 15% glycerol. For generating second recombination, one tube was thawed and the contents pelleted in a microfuge, the media removed in a pipette, and the cells resuspended in 6 mL into 6 mL 7H9 ADS + 0.5% glycerol + 0.02% Tyloxapol (without antibiotics). The culture was incubated at 37 deg, shaking. Serial dilutions and plating onto LB agar with 5% sucrose and 25 ug/mL X-Gal was done after 1.5 days and 3 days of incubation.

- Culture conditions / growth curves

Growth was measured by optical density (absorbance at 600 nm) on a spectrophotometer, using 1 mL cuvettes. Dilutions were made in 1X PBS 0.02% Tyloxapol (for *M. smegmatis*) or 1X PBS 10% formalin (for *M. tuberculosis*), to keep the reading between 0.05 and 0.2. A standard curve for B12 absorbance was made and subtracted as applicable.

- CFU assay

Serial ten-fold dilutions were made using 100 uL culture and 900 uL 1X PBS 0.02% Tyloxapol in 5 mL polypropylene tubes and vortexed. 100 uL of appropriate dilutions were plated onto agar-based media and incubated to enumerate colonies formed.

- PI staining protocol

Propidium iodide (PI) was stored frozen as 2 mM stock solution. PI staining solution was made at 0.4 uM in 1X PBS 0.02% Tyloxapol and stored at 4 deg. Samples from the culture were taken of 150 uL, 333 uL, 500 uL, or 1 mL, depending on relative OD_{600}, and pelleted in a microfuge at 10,000 rpm, for 3 min. The supernatant was removed with a pipette and the pellet resuspended in 6 uL of PI staining solution. Sample was stored covered for 15 - 30 min. 1 - 2 uL was placed on a glass coverslip and covered with a glass slide.

- Microscopy imaging

Images were taken using and Olympus IX81S1F-ZDC motorized inverted microscope equipped with a Hamamatsu ORCA/ER CCD camera. Bacteria are visualized with a 100X oil immersion lens (total magnification of 1000X). Images were taken using 20 ms exposures on phase contrast to image the cells and 100 ms exposures on the red channel to visualize PI staining. No further image processing was done.

- Cultures for metabolomics experiments

Started cultures for metabolomics experiments were grown in M9 0.5% glucose as described previously, but after the cultures reached OD_{600} ~0.9 - 1.1, the culture volume was increased to 120 mL in a 250 mL glass flask. Cells were pelleted in 50 mL polypropylene tubes, the media poured off, and the pellets resuspended in 1X M9 'no carbon' media. Flasks were set up with 1X M9 'no carbon' media and appropriate carbon source added. OD_{600} of the resuspended culture was measured and the inoculum was added to the flasks to get a starting OD_{600} of ~ 0.15 - 0.25.

- Metabolite extraction

For each timepoint, the OD_{600} was measured and the volume used for sampling adjusted to give 2 OD * mL. At each timepoint, 500 uL of culture was centrifuged at top speed rpm for 3 min, the supernatant decanted into a fresh tube and stored at -80 deg. (Longer spins should be used, as subsequent centrifugation after thawing indicated residual bacteria).

After addition of inoculum, 2 OD*mL equivalent of culture was filtered onto a 25 mm diameter, 0.45 um pore size nitrocellulose membrane (Whatman) using a 125 mL filter flask, attached to a Laboport N820FTP vacuum pump (KNF).

Each filter was submerged into a 2 mL microfuge tube containing 1.5 mL of 40:40:20 acetonitrile : methanol : water, 10 mM formic acid buffer, pre-incubated at 78 deg C. Samples containing the filter were held at 78 deg 1 min, then vortexed, returned to 78 deg for 2 min, and then placed on ice, and stored at -80 deg C for the duration of the time course. Samples at each timepoint were filtered in duplicate and independently extracted.

0.1M ammonium hydroxide (NH_4OH) was added to neutralize the formic acid in the sample (Rabinowitz and Kimball 2007), although this led to excessive salt in the sample and should be omitted. Samples were divided in 2 parts and 50 uL of 13C-labelled yeast extract (gift of the Sauer Lab) was added as an internal standard to one set (to be used for LC-MS/MS). The unlabelled set would be used for FI-TOF-MS. Samples were stored at -80 deg C until dried. Samples were evaporated in an Eppendorf DNA concentrator and returned to -80 deg C.

Before analysis, dried extract was resuspended in 100 uL 'nanopure water' (purified with greater than 18.1 MΩ resistivity), vortexed, and the debris pelleted. The supernatant was loaded into a 96-well plate, in randomized order.

For the alternative 'rapid spin' protocol, 1 mL * OD of culture was pelleted in a microfuge set to max speed for 30 seconds. The culture supernatant was poured off and the excess tapped out. The microfuge tube was closed and submerged

into liquid nitrogen. The tubes remained in liquid nitrogen until all sampling was completed. Tubes were then removed and 500 uL of 60:40 ethanol : water, 10 mM ammonium acetate buffer, pH 7.2, pre-incubated at 78 deg C was added. The tubes were vortexed and placed in an Eppendorf 'thermomixer' set to 78 deg, for 1 min. The tubes were centrifuged, the supernatant moved to a tube on ice, and the procedure repeated twice, pooling the extracts into the same tube, for ~1.5 mL total extract. (When 13C-labeled extract is used as a standard, it is added at the first extraction step). Samples on ice are then stored at -80 deg C or evaporated and then stored at -80 deg.

This protocol is not amenable to the larger culture volumes required for non-growing cultures whose OD_{600} declines over the timecourse.

- Targeted LC-MS/MS

Separation of 10 uL of sample was done using an ion-pairing method for a Waters Acquity T3 end-capped reverse phase column (150 mm × 2.1 mm × 1.8 µm) run on a gradient of mobile phases A (10 mM tributylamine, 15 mM acetic acid, 5% (v/v) methanol) and B (2-propanol). The LC was coupled to a Thermo TSQ Quantum Ultra triple quadrupole instrument, with electrospray injection, run in negative mode, using multiple reaction monitoring (MRM), detecting the parent ion in Q1, fragmenting the sample in Q2, and detecting the daughter ion in Q3.

Data was analyzed using Xcalibur and ETHZ in-house integration software (Buescher et al 2010).

- Untargeted FI-TOF

Sample was directly injected into the electrospray source of an Agilent 6520 Series Quadrupole Time-of-Flight mass spectrometer in negative mode, using a mobile phase of isopropanol/water (60:40, v/v) buffered with 5 mM ammonium carbonate at pH 9. Data was analyzed using ETHZ-developed Matlab-based software (Fuhrer et al 2011).

- PDIM labeling protocol

10 uCi of [1-14C]-propionate (specific activity of 55.9 uCi mol-1 [Campro Scientific]) was added to ~10 ml of culture at OD_{600} ~0.4 - 0.7 and incubated for 48 hr. Apolar lipids were extracted by pelleting cells, removing supernatant, resuspending in 5 mL of 10:1 (vol/vol) methanol/0.3% NaCl. After addition of 5 mL petroleum ether, samples were vortexed for 4 minutes to separate the phases. The upper phase was collected and the the lower phase was re-extracted with 5 mL petroleum ether. The upper phases were pooled and 10 mL chloroform was added to kill any residual bacteria. Samples were removed from Biosafety Level 3 facility and allowed to concentrate overnight to ~ 10 mL in a chemical hood. ~25 uL of each extract was spotted onto a 5 cm x 10 cm silica gel 60 F254 TLC plate (Merck) and run in a 9:1 (vol/vol) petroleum ether / diethyl ether mixture.

Plates were air-dried, exposed overnight to a Phosphor screen, and imaged on a Typhoon scanner (Amersham Biosciences) (Kirksey et al 2011).

- DNA digestion & Southern blot

Genomic DNA was extracted from 6 - 10 mL cultures at OD_{600} ~0.5-1.0 using lysozyme treatment, proteinase K digestion, Cetrimide (hexadecyltrimethylammonium bromide (CTAB)) saline, and chloroform extraction (Belisle and Sonnenberg 1998). 1 ug of genomic DNA was digested with 10 U of restriction enzyme overnight (~16 hr). Fragments were separated on a 0.7% TAE agarose gel. The gel was depurinated, denatured, and neutralized. The fragments were transferred to a Hybond N+ nylon membrane by capillary transfer or vacuum transfer and UV cross-linked. The membrane was pre-incubated with hybridization buffer (GE Healthcare) for over 1 hours. A DNA probe was amplified by PCR, denatured, and labeled with a horseradish peroxidase-based reagent according to the manufacturer's recommendations. (GE Healthcare) The probe was hybridized to the blot overnight. After 3 washes in SDS / urea / salt solution and 3 washes in salt solution, the blot was incubated with the detection reagents and exposed to a sheet of Hyperfilm for 1 min, 2 min, 5 min, and 10 min.

- Aerosol infection and plating for CFU

A 1 mL frozen aliquot of the appropriate strain was thawed and inoculated into a roller bottle culture of 49 mL 7H9 ADS + 0.5% glycerol + 0.02% Tyloxapol. The culture was grown to an OD_{600} of ~0.4 - 0.6. Clumps were pelleted by centrifugation at 2,000 rpm for 5 min. The OD_{600} was measured, the culture diluted to OD_{600} 0.05. This was used as the inoculum.

C57/BL6 female mice (Jackson Laboratories), 5-8 weeks of age, were infected by the aerosol route using a custom-built aerosol exposure chamber (Department of Mechanical Engineering, University of Wisconsin, Madison, WI). At each timepoint, 4 mice were euthanized by CO_2 overdose. Lungs were excised and homogenized in PBS + 0.05% Tween80. Homogenates were plated in their entirety or in serial ten-fold dilutions onto 7H10 agar + OADC + 0.5% glycerol + 100 ug/mL cycloheximide.

The animal protocols used were reviewed and approved by the chief veterinarian of EPFL and the Swiss Office Vétérinaire Fédéral.

- Histopathology

One cage of mice for each strain, at 12 weeks, was used for histological analysis. Following euthanasia with CO_2 overdose, the left lung was placed in 5 mL of 1X PBS 10% formalin and subsequently stored at 4 deg. Before removal from the

biosafety level 3 (BSL3) facility, the buffer was replaced with fresh 1X PBS 10% formalin for 24 hours.

Samples were processed by the Histology Core Facility at EPFL, which performed embedding, sectioning, and staining with hematoxylin and eosin and Ziehl–Neelsen. 1 of 2 sections through the lung were used for analysis. Samples were assigned random numbers and evaluated by a veterinary pathologist. A semiquantitative analysis involved a graded scale from 1 to 3 based on the severity of the inflammation (the extent of the lesions seen). An independent quantitative assessment used ImageJ software to calculate the size of inflamed areas, performed three times and averaged.

- Primers used for cloning

Primers to PCR amplify *M. smegmatis* homology arms for *mutAB* deletion plasmid

MSM mutA_ascI-F : GGC GCG CCG TCA GAG ATT GGA G

MSM mutA_avrII-R : CCT AGG CAC CCG CAT CTC CTG TT

MSM mutB_avrII-R : CCT AGG CTC GGC TAC GAG CTG

MSM mutB_pacI-R : TTA ATT AAT CCG GCG GAC CTC GG

Primers to PCR amplify check for WT vs Δ at *mutAB* locus:

SM mutAB X up F : CGC TCT ATT TCC TGC TTG

SM mutAB X up R : CTA GCT CAG CTC GTA GCC

SM mutAB X dn F : TTA GCC TGA TCT GCA AGC

SM mutAB X dn R : GAT CCT CGT ACC GTC CTT

Primers to PCR amplify *M. smegmatis mutAB* for complementation

SMmutABcomp_Not-F : GCG GCC GCA AGT GTG CTG ACT ACG GCT TTC

SMmutABcomp_Not-R : GCG GCC GCC TAG CTC AGC TCG TAG CC

mut Up comp_Nsi-F : GGA TGC ATA GCC GGT CAA CGC AAT TC

mut Up comp-R : ACC AGA TCG AGG AAG ACA CCT TCG

SMmutB-pre-FseI-F : ATC TCC GAC ATC TTC GCC TAC

SM meaB_SpeI-R : GGA CTA GTA CTT TCT GGT GCC GGT TGT G

Primers to PCR amplify *M. tuberculosis* homology arms for *mutAB* deletion plasmid

MTB mutA_ascI-F : GGC GCG CCG AAG GTT TAT CA

MTB mutA_avrII-R : CCT AGG ATC AAT GGA CAC CGA CTG

MTB mutB_avrII-F : CCT AGG GGG TAC ACG CTG GAT

MTB mutB_pacI-R : TTA ATT AAC CAA GGT CAG CAA CAC GAA C

Primers to PCR amplify probe for Southern blot

TB mutAB probe-F : ATG AAC GGT GCG GTG CTG

TB mutAB probe-R : GCC CCA GAA GAA CGA TAG CC

Primers to PCR amplify *M. tuberculosis* homology arms for *icl1* deletion plasmid

icl1_PacI-F : TTA ATT AAC ATC CAG GAC ATC GGT CAG

icl1_AvrII-R : CCT AGG GAC AGA CAT AGA CAA CTC CTT AAC G

icl1_AvrII-F : CCT AGG GGC CAG TTC CAC TAG TCT GC

icl1_AscI -R : GGC GCG CCG TTC ATA CAC TTC AGT ACG

Primers to PCR amplify *M. tuberculosis* homology arms for *icl2* deletion plasmid

icl2_PacI-F : TTA ATT AAC GCT GAC CCA CAA TTC G

icl2_AvrII-R : CCT AGG GTC CGT TTC GGC GAT GG

icl2_NheI- F : GCT AGC ATC ACG AAG GAG GCG TAG C

icl2_AscI -R : GGC GCG CCA TCC CGA TCA ACA TCA CGA G

References Cited

Alland, D., Steyn, A.J., Weisbrod, T., Aldrich, K., and Jacobs, W.R. (2000). Characterization of the Mycobacterium tuberculosis iniBAC promoter, a promoter that responds to cell wall biosynthesis inhibition. Journal of Bacteriology 182, 1802–1811.

Ando, T., Rasmussen, K., Wright, J.M., and Nyhan, W.L. (1972). Isolation and identification of methylcitrate, a major metabolic product of propionate in patients with propionic acidemia. J. Biol. Chem. 247, 2200–2204.

Anthony, C. (2011). How half a century of research was required to understand bacterial growth on C1 and C2 compounds; the story of the serine cycle and the ethylmalonyl-CoA pathway. Sci Prog 94, 109–137.

Appelberg, R. (2006). Macrophage nutriprive antimicrobial mechanisms. J. Leukoc. Biol. 79, 1117–1128.

Armitt, S., Roberts, C.F., and Kornberg, H.L. (1970). The role of isocitrate lyase in Aspergillus Nidulans. FEBS Lett. 7, 231–234.

Armitt, S., Roberts, C.F., and Kornberg, H.L. (1971). Mutants of Aspergillus nidulans lacking malate synthase. FEBS Lett. 12, 276–278.

Balasubramanian, S., Kim, S.J., and Podila, G.K. (2002). Differential expression of a malate synthase gene during the preinfection stage of symbiosis in the ectomycorrhizal fungus Laccaria bicolor. New Phytologist 154, 517–527.

Baldomà, L., Badía, J., Obradors, N., and Aguilar, J. (1988). Aerobic excretion of 1,2-propanediol by Salmonella typhimurium. Journal of Bacteriology 170, 2884–2885.

Baqui, S.M., Mattoo, A., and Modi, V. (1977). Glyoxylate metabolism and fatty acid oxidation in mango fruit during development and ripening. Phytochemistry 16, 51–54.

Baronofsky, J.J., Schreurs, W.J., and Kashket, E.R. (1984). Uncoupling by Acetic Acid Limits Growth of and Acetogenesis by Clostridium thermoaceticum. Appl. Environ. Microbiol. 48, 1134–1139.

Barth, G., and Scheuber, T. (1993). Cloning of the isocitrate lyase gene (ICL1) from Yarrowia lipolytica and characterization of the deduced protein. Mol. Gen. Genet. 241, 422–430.

Baughn, A.D., Garforth, S.J., Vilchèze, C., and Jacobs, W.R. (2009). An anaerobic-type alpha-ketoglutarate ferredoxin oxidoreductase completes the oxidative tricarboxylic acid cycle of Mycobacterium tuberculosis. PLoS Pathog 5, e1000662.

Baumgart, M., Mustafi, N., Krug, A., and Bott, M. (2011). Deletion of the aconitase gene in Corynebacterium glutamicum causes strong selection pressure for secondary mutations inactivating citrate synthase. Journal of Bacteriology 193, 6864–6873.

Beach, R.L., Aogaichi, T., and Plaut, G.W. (1977). Identification of D-threo-alpha-methylisocitrate as stereochemically specific substrate for bovine heart aconitase and inhibitor of TPN-linked isocitrate dehydrogenase. Journal of Biological Chemistry 252, 2702–2709.

Behr, M.A., and Small, P.M. (1997). Has BCG attenuated to impotence? Nature 389, 133–134.

Belisle, J.T., and Sonnenberg, M.G. (1998). Isolation of Genomic DNA from Mycobacteria. In Methods in Molecular Biology, Vol. 101: Mycobacteria Protocols, T. Parish, and N.G. Stoker, eds. (Totowa, NJ: Humana Press), pp. 31–44.

Bell, S.C., and Turner, J.M. (1976). Bacterial catabolism of threonine. Threonine degradation initiated by L-threonine-NAD+ oxidoreductase. Biochem. J. 156, 449–458.

Bigger, J.W. (1944). Treatment of staphylococcal infections with penicillin by intermittent sterilisation. The Lancet 244, 497–500.

Birch, A., Leiser, A., and Robinson, J.A. (1993). Cloning, sequencing, and expression of the gene encoding methylmalonyl-coenzyme A mutase from Streptomyces cinnamonensis. Journal of Bacteriology 175, 3511–3519.

Björkman, J., Rhen, M., and Andersson, D.I. (1996). Salmonella typhimurium cob mutants are not hyper-virulent. FEMS Microbiology Letters 139, 121–126.

Blank, L., Green, J., and Guest, J.R. (2002). AcnC of Escherichia coli is a 2-methylcitrate dehydratase (PrpD) that can use citrate and isocitrate as substrates. Microbiology (Reading, Engl.) 148, 133–146.

Bloch, H., and Segal, W. (1956). Biochemical differentiation of Mycobacterium tuberculosis grown in vivo and in vitro. Journal of Bacteriology 72, 132–141.

Bloom, B.R. (1994). Tuberculosis: Pathogenesis, Protection, and Control (Washington, DC: American Society for Microbiology).

Bobik, T.A., and Rasche, M.E. (2001). Identification of the human methylmalonyl-CoA racemase gene based on the analysis of prokaryotic gene arrangements. Implications for decoding the human genome. J. Biol. Chem. 276, 37194–37198.

Bobik, T.A., and Rasche, M.E. (2004). Purification and partial characterization of the Pyrococcus horikoshii methylmalonyl-CoA epimerase. Appl Microbiol Biotechnol 63, 682–685.

Bobik, T.A., Havemann, G.D., Busch, R.J., Williams, D.S., and Aldrich, H.C. (1999). The propanediol utilization (pdu) operon of Salmonella enterica serovar Typhimurium LT2 includes genes necessary for formation of polyhedral organelles involved in coenzyme B(12)-dependent 1, 2-propanediol degradation. Journal of Bacteriology 181, 5967–5975.

Bott, M., Pfister, K., Burda, P., Kalbermatter, O., Woehlke, G., and Dimroth, P. (1997). Methylmalonyl-CoA decarboxylase from Propionigenium modestum--cloning and sequencing of the structural genes and purification of the enzyme complex. Eur. J. Biochem. 250, 590–599.

Brass, E.P. (1992). Interaction of carnitine and propionate with pyruvate oxidation by hepatocytes from clofibrate-treated rats: importance of coenzyme A availability. J. Nutr. 122, 234–240.

Brämer, C.O., and Steinbüchel, A. (2001). The methylcitric acid pathway in Ralstonia eutropha: new genes identified involved in propionate metabolism. Microbiology (Reading, Engl.) 147, 2203–2214.

Brämer, C.O., and Steinbüchel, A. (2002). The malate dehydrogenase of Ralstonia eutropha and functionality of the C(3)/C(4) metabolism in a Tn5-induced mdh mutant. FEMS Microbiology Letters 212, 159–164.

Brämer, C.O., Silva, L.F., Gomez, J.G.C., Priefert, H., and Steinbüchel, A. (2002). Identification of the 2-methylcitrate pathway involved in the catabolism of propionate in the polyhydroxyalkanoate-producing strain Burkholderia sacchari IPT101(T) and analysis of a mutant accumulating a copolyester with higher 3-hydroxyvalerate content. Appl. Environ. Microbiol. 68, 271–279.

Brennan, P.J. (2003). Structure, function, and biogenesis of the cell wall of Mycobacterium tuberculosis. Tuberculosis (Edinb) 83, 91–97.

Brock, M. (2005). Generation and phenotypic characterization of Aspergillus nidulans methylisocitrate lyase deletion mutants: methylisocitrate inhibits growth and conidiation. Appl. Environ. Microbiol. 71, 5465–5475.

Brock, M., and Buckel, W. (2004). On the mechanism of action of the antifungal agent propionate. Eur. J. Biochem. 271, 3227–3241.

Brock, M., Darley, D., Textor, S., and Buckel, W. (2001). 2-Methylisocitrate lyases from the bacterium Escherichia coli and the filamentous fungus Aspergillus nidulans: characterization and comparison of both enzymes. Eur. J. Biochem. 268, 3577–3586.

Brock, M., Fischer, R., Linder, D., and Buckel, W. (2000). Methylcitrate synthase from Aspergillus nidulans: implications for propionate as an antifungal agent. Mol Microbiol 35, 961–973.

Brock, M., Maerker, C., Schütz, A., Völker, U., and Buckel, W. (2002). Oxidation of propionate to pyruvate in Escherichia coli. Involvement of methylcitrate dehydratase and aconitase. Eur. J. Biochem. 269, 6184–6194.

Brubaker, R.R., and Sulen, A. (1971). Mutations Influencing the Assimilation of Nitrogen by Yersinia pestis. Infection and Immunity 3, 580–588.

Brzostek, A., Dziadek, B., Rumijowska-Galewicz, A., Pawelczyk, J., and Dziadek, J. (2007). Cholesterol oxidase is required for virulence of Mycobacterium tuberculosis. FEMS Microbiology Letters 275, 106–112.

Buchanan, B., Gruissem, W., and Jones, R. (2002). Biochemistry & Molecular Biology of Plants (Wiley).

Buchmeier, N., Blanc-Potard, A., Ehrt, S., Piddington, D., Riley, L., and Groisman, E.A. (2000). A parallel intraphagosomal survival strategy shared by mycobacterium tuberculosis and Salmonella enterica. Mol Microbiol 35, 1375–1382.

Buescher, J.M., Moco, S., Sauer, U., and Zamboni, N. (2010). Ultrahigh performance liquid chromatography-tandem mass spectrometry method for fast and robust quantification of anionic and aromatic metabolites. Anal. Chem. 82, 4403–4412.

Camacho, L.R. (2001). Analysis of the Phthiocerol Dimycocerosate Locus of Mycobacterium tuberculosis. Journal of Biological Chemistry 276, 19845–19854.

Camacho, L.R., Ensergueix, D., Perez, E., Gicquel, B., and Guilhot, C. (1999). Identification of a virulence gene cluster of Mycobacterium tuberculosis by signature-tagged transposon mutagenesis. Mol Microbiol 34, 257–267.

Celis, R.T., Leadlay, P.F., Roy, I., and Hansen, A. (1998). Phosphorylation of the periplasmic binding protein in two transport systems for arginine incorporation in Escherichia coli K-12 is unrelated to the function of the transport system. Journal of Bacteriology 180, 4828–4833.

Chan, M., and Sim, T.S. (1998). Malate synthase from Streptomyces clavuligerus NRRL3585: cloning, molecular characterization and its control by acetate. Microbiology (Reading, Engl.) 144 (Pt 11), 3229–3237.

Chang, J.C., Harik, N.S., Liao, R.P., and Sherman, D.R. (2007). Identification of Mycobacterial genes that alter growth and pathology in macrophages and in mice. J Infect Dis 196, 788–795.

Charles, T.C., and Aneja, P. (1999). Methylmalonyl-CoA mutase encoding gene of Sinorhizobium meliloti. Gene 226, 121–127.

Cheema-Dhadli, S., Leznoff, C.C., and Halperin, M.L. (1975). Effect of 2-methylcitrate on citrate metabolism: implications for the management of patients with propionic acidemia and methylmalonic aciduria. Pediatr. Res. 9, 905–908.

Cherrington, C.A., Hinton, M., Mead, G.C., and Chopra, I. (1991). Organic acids: chemistry, antibacterial activity and practical applications. Adv. Microb. Physiol. 32, 87–108.

Chin, K.J., and Conrad, R. (1995). Intermediary metabolism in methanogenic paddy soil and the influence of temperature. FEMS Microbiology Ecology 18, 85–102.

Chou, T.C., and Lipmann, F. (1952). Separation of acetyl transfer enzymes in pigeon liver extract. J. Biol. Chem. 196, 89–103.

Claes, W.A., Pühler, A., and Kalinowski, J. (2002). Identification of two prpDBC gene clusters in Corynebacterium glutamicum and their involvement in propionate degradation via the 2-methylcitrate cycle. Journal of Bacteriology 184, 2728–2739.

Cole, S.T. (1999). Learning from the genome sequence of Mycobacterium tuberculosis H37Rv. FEBS Lett. 452, 7–10.

Cole, S.T., Brosch, R., Parkhill, J., Garnier, T., Churcher, C., Harris, D., Gordon, S.V., Eiglmeier, K., Gas, S., Barry, C.E., et al. (1998). Deciphering the biology of Mycobacterium tuberculosis from the complete genome sequence. Nature 393, 537–544.

Cole, S.T., Eiglmeier, K., Parkhill, J., James, K.D., Thomson, N.R., Wheeler, P.R., Honoré, N., Garnier, T., Churcher, C., Harris, D., et al. (2001). Massive gene decay in the leprosy bacillus. Nature 409, 1007–1011.

Collins, D.M., Wilson, T., Campbell, S., Buddle, B.M., Wards, B.J., Hotter, G., and De Lisle, G.W. (2002). Production of avirulent mutants of Mycobacterium bovis with vaccine properties by the use of illegitimate recombination and screening of stationary-phase cultures. Microbiology (Reading, Engl.) 148, 3019–3027.

Cordwell, S.J. (1999). Microbial genomes and “missing” enzymes: redefining biochemical pathways. Arch. Microbiol. 172, 269–279.

Coude, F.X., Sweetman, L., and Nyhan, W.L. (1979). Inhibition by propionyl-coenzyme A of N-acetylglutamate synthetase in rat liver mitochondria. A possible explanation for hyperammonemia in propionic and methylmalonic acidemia. J. Clin. Invest. 64, 1544–1551.

Cox, J.S., Chen, B., McNeil, M., and Jacobs, W.R. (1999). Complex lipid determines tissue-specific replication of Mycobacterium tuberculosis in mice. Nature 402, 79–83.

Cracan, V., Padovani, D., and Banerjee, R. (2010). IcmF is a fusion between the radical B12 enzyme isobutyryl-CoA mutase and its G-protein chaperone. J. Biol. Chem. 285, 655–666.

Cronan, J.E., and LaPorte, D.C. (1996). Tricarboxylic acid cycle and glyoxylate bypass. In Escherichia Coli and Salmonella: Cellular and Molecular Biology, F. Neidhardt, R. Curtiss, J. Ingraham, E.C. Lin, K.B. Low, and B. Magasanik, eds. (Washington, DC: ASM Press), pp. 206–216.

Cummings, J.H., Pomare, E.W., Branch, W.J., Naylor, C.P., and Macfarlane, G.T. (1987). Short chain fatty acids in human large intestine, portal, hepatic and venous blood. Gut 28, 1221–1227.

da Silva Neto, B.R., de Fátima da Silva, J., Mendes-Giannini, M.J.S., Lenzi, H.L., de Almeida Soares, C.M., and Pereira, M. (2009). The malate synthase of Paracoccidioides brasiliensis is a linked surface protein that behaves as an anchorless adhesin. BMC Microbiol 9, 272.

Danson, M.J., Harford, S., and Weitzman, P.D. (1979). Studies on a mutant form of Escherichia coli citrate synthase desensitised to allosteric effectors. Eur. J. Biochem. 101, 515–521.

Datta, P., Shi, L., Bibi, N., Balázsi, G., and Gennaro, M.L. (2011). Regulation of central metabolism genes of Mycobacterium tuberculosis by parallel feed-forward loops controlled by sigma factor E (σ(E)). Journal of Bacteriology 193, 1154–1160.

Dayem, L.C., Carney, J.R., Santi, D.V., Pfeifer, B.A., Khosla, C., and Kealey, J.T. (2002). Metabolic Engineering of a Methylmalonyl-CoA Mutase−Epimerase Pathway for Complex Polyketide Biosynthesis in Escherichia coli†,‡. Biochemistry 41, 5193–5201.

de Carvalho, L.P.S., Fischer, S.M., Marrero, J., Nathan, C., Ehrt, S., and Rhee, K.Y. (2010a). Metabolomics of Mycobacterium tuberculosis reveals compartmentalized co-catabolism of carbon substrates. Chemistry & Biology 17, 1122–1131.

de Carvalho, L.P.S., Zhao, H., Dickinson, C.E., Arango, N.M., Lima, C.D., Fischer, S.M., Ouerfelli, O., Nathan, C., and Rhee, K.Y. (2010b). Activity-based metabolomic profiling of enzymatic function: identification of Rv1248c as a mycobacterial 2-hydroxy-3-oxoadipate synthase. Chemistry & Biology 17, 323–332.

Dhar, N., and McKinney, J.D. (2007). Microbial phenotypic heterogeneity and antibiotic tolerance. Current Opinion in Microbiology 10, 30–38.

Dhar, N., and McKinney, J.D. (2010). Mycobacterium tuberculosis persistence mutants identified by screening in isoniazid-treated mice. Proc. Natl. Acad. Sci. U.S.a. 107, 12275–12280.

Diacovich, L., Peirú, S., Kurth, D., Rodríguez, E., Podestá, F., Khosla, C., and Gramajo, H. (2002). Kinetic and structural analysis of a new group of Acyl-CoA carboxylases found in Streptomyces coelicolor A3(2). J. Biol. Chem. 277, 31228–31236.

Dobson, C.M., Wai, T., Leclerc, D., Wilson, A., Wu, X., Doré, C., Hudson, T., Rosenblatt, D.S., and Gravel, R.A. (2002). Identification of the gene responsible for the cblA complementation group of vitamin B12-responsive methylmalonic acidemia based on analysis of prokaryotic gene arrangements. Proc. Natl. Acad. Sci. U.S.a. 99, 15554–15559.

Domenech, P., and Reed, M.B. (2009). Rapid and spontaneous loss of phthiocerol dimycocerosate (PDIM) from Mycobacterium tuberculosis grown in vitro: implications for virulence studies. Microbiology 155, 3532–3543.

Dubey, V.S. (2002). Mevalonate-independent pathway of isoprenoids synthesis: A potential target in some human pathogens. Current Science 83, 685–687.

Dubey, V.S., Sirakova, T.D., and Kolattukudy, P.E. (2002). Disruption of msl3 abolishes the synthesis of mycolipanoic and mycolipenic acids required for polyacyltrehalose synthesis in Mycobacterium tuberculosis H37Rv and causes cell aggregation. Mol Microbiol 45, 1451–1459.

Dubnau, E., Fontán, P., Manganelli, R., Soares-Appel, S., and Smith, I. (2002). Mycobacterium tuberculosis genes induced during infection of human macrophages. Infection and Immunity 70, 2787–2795.

Eisenreich, W., Strauss, G., Werz, U., Fuchs, G., and Bacher, A. (1993). Retrobiosynthetic analysis of carbon fixation in the phototrophic eubacterium Chloroflexus aurantiacus. Eur. J. Biochem. 215, 619–632.

Erb, T.J., Rétey, J., Fuchs, G., and Alber, B.E. (2008). Ethylmalonyl-CoA mutase from Rhodobacter sphaeroides defines a new subclade of coenzyme B12-dependent acyl-CoA mutases. J. Biol. Chem. 283, 32283–32293.

Erfle, J.D. (1973). Acetyl-CoA and propionyl-CoA carboxylation by Mycobacterium phlei. Partial purification and some properties of the enzyme. Biochim. Biophys. Acta 316, 143–155.

Eschenmoser, A. (1988). Vitamin B12: experiments concerning the origin of its molecular structure. Angewandte Chemie International Edition in English 27, 5–39.

Evans, C.T., Sumegi, B., Srere, P.A., Sherry, A.D., and Malloy, C.R. (1993). [13C]propionate oxidation in wild-type and citrate synthase mutant Escherichia coli: evidence for multiple pathways of propionate utilization. Biochem. J. 291 (Pt 3), 927–932.

Falentin, H., Deutsch, S.-M., Jan, G., Loux, V., Thierry, A., Parayre, S., Maillard, M.-B., Dherbécourt, J., Cousin, F.J., Jardin, J., et al. (2010). The complete genome of Propionibacterium freudenreichii CIRM-BIA1, a hardy actinobacterium with food and probiotic applications. PLoS ONE 5, e11748.

Fenhalls, G., Stevens, L., Moses, L., Bezuidenhout, J., Betts, J.C., Helden Pv, P.V., Lukey, P.T., and Duncan, K. (2002). In situ detection of Mycobacterium tuberculosis transcripts in human lung granulomas reveals differential gene expression in necrotic lesions. Infection and Immunity 70, 6330–6338.

Fenton, W.A., Gravel, R.A., and Rosenblatt, D.S. (2001). Disorders of propionate and methylmalonate metabolism. The Metabolic and Molecular Bases of Inherited Disease 2, 2165–2193.

Fernandes, N.D., and Kolattukudy, P.E. (1997). Methylmalonyl coenzyme A selectivity of cloned and expressed acyltransferase and beta-ketoacyl synthase domains of mycocerosic acid synthase from Mycobacterium bovis BCG. Journal of Bacteriology 179, 7538–7543.

Fernandez, E., Fernandez, M., and Rodicio, R. (1993). Two structural genes are encoding malate synthase isoenzymes in Saccharomyces cerevisiae. FEBS Lett. 320, 271–275.

Fiehn, O. (2002). Metabolomics--the link between genotypes and phenotypes. Plant Mol. Biol. 48, 155–171.

Fleck, C.B., and Brock, M. (2008). Characterization of an acyl-CoA: carboxylate CoA-transferase from Aspergillus nidulans involved in propionyl-CoA detoxification. Mol Microbiol 68, 642–656.

Fraenkel, D.G. (1996). Glycolysis. In Escherichia Coli And Salmonella: Cellular and Molecular Biology, F. Neidhardt, R. Curtiss, J. Ingraham, E.C. Lin, K.B. Low, and B. Magasanik, eds. (Washington, DC: ASM Press), pp. 189–198.

Froese, D.S., Dobson, C.M., White, A.P., Wu, X., Padovani, D., Banerjee, R., Haller, T., Gerlt, J.A., Surette, M.G., and Gravel, R.A. (2009). Sleeping beauty mutase (sbm) is expressed and interacts with ygfd in Escherichia coli. Microbiol. Res. 164, 1–8.

Fuhrer, T., Heer, D., Begemann, B., and Zamboni, N. (2011). High-throughput, accurate mass metabolome profiling of cellular extracts by flow injection-time-of-flight mass spectrometry. Anal. Chem. 83, 7074–7080.

Gago, G., Kurth, D., Diacovich, L., Tsai, S.-C., and Gramajo, H. (2006). Biochemical and structural characterization of an essential acyl coenzyme A carboxylase from Mycobacterium tuberculosis. Journal of Bacteriology 188, 477–486.

Gande, R., Gibson, K.J.C., Brown, A.K., Krumbach, K., Dover, L.G., Sahm, H., Shioyama, S., Oikawa, T., Besra, G.S., and Eggeling, L. (2004). Acyl-CoA carboxylases (accD2 and accD3), together with a unique polyketide synthase (Cg-pks), are key to mycolic acid biosynthesis in Corynebacterianeae such as Corynebacterium glutamicum and Mycobacterium tuberculosis. J. Biol. Chem. 279, 44847–44857.

Gatfield, J., and Pieters, J. (2000). Essential role for cholesterol in entry of mycobacteria into macrophages. Science 288, 1647–1650.

Gawron, O., and Mahajan, K.P. (1966a). Alpha-methyl-cis-aconitic acid, cis-aconitase substrate. I. Synthesis. Biochemistry 5, 2335–2342.

Gawron, O., and Mahajan, K.P. (1966b). alpha-Methyl-cis-aconitic acid. Aconitase substrate. II. Substrate properties and aconitase mechanism. Biochemistry 5, 2343–2350.

Gengenbacher, M., Rao, S.P.S., Pethe, K., and Dick, T. (2010). Nutrient-starved, non-replicating Mycobacterium tuberculosis requires respiration, ATP synthase and isocitrate lyase for maintenance of ATP homeostasis and viability. Microbiology 156, 81–87.

Gerike, U., Danson, M.J., and Hough, D.W. (2001). Cold-active citrate synthase: mutagenesis of active-site residues. Protein Eng. 14, 655–661.

Gerike, U., Hough, D.W., Russell, N.J., Dyall-Smith, M.L., and Danson, M.J. (1998). Citrate synthase and 2-methylcitrate synthase: structural, functional and evolutionary relationships. Microbiology (Reading, Engl.) 144 (Pt 4), 929–935.

Gerstmeir, R., Wendisch, V.F., Schnicke, S., Ruan, H., Farwick, M., Reinscheid, D., and Eikmanns, B.J. (2003). Acetate metabolism and its regulation in Corynebacterium glutamicum. Journal of Biotechnology 104, 99–122.

Glasgow, A.M., and Chase, H.P. (1976). Effect of propionic acid on fatty acid oxidation and ureagenesis. Pediatr. Res. 10, 683–686.

Goren, M.B., Brokl, O., and Schaefer, W.B. (1974). Lipids of putative relevance to virulence in Mycobacterium tuberculosis: correlation of virulence with elaboration of sulfatides and strongly acidic lipids. Infection and Immunity 9, 142–149.

Gould, T.A., van de Langemheen, H., Munoz-Elias, E.J., McKinney, J.D., and Sacchettini, J.C. (2006). Dual role of isocitrate lyase 1 in the glyoxylate and methylcitrate cycles in Mycobacterium tuberculosis. Mol Microbiol 61, 940–947.

Grabner, R., and Meerbach, W. (1991). Phagocytosis of surfactant by alveolar macrophages in vitro. Am. J. Physiol. 261, L472–L477.

Graham, I.A., Leaver, C.J., and Smith, S.M. (1992). Induction of Malate Synthase Gene Expression in Senescent and Detached Organs of Cucumber. Plant Cell 4, 349–357.

Graham, J.E., and Clark-Curtiss, J.E. (1999). Identification of Mycobacterium tuberculosis RNAs synthesized in response to phagocytosis by human macrophages by selective capture of transcribed sequences (SCOTS). Proc. Natl. Acad. Sci. U.S.a. 96, 11554–11559.

Griffin, J.E., Gawronski, J.D., DeJesus, M.A., Ioerger, T.R., Akerley, B.J., and Sassetti, C.M. (2011). High-resolution phenotypic profiling defines genes essential for mycobacterial growth and cholesterol catabolism. PLoS Pathog 7, e1002251.

Griffin, J.E., Pandey, A.K., Gilmore, S.A., Mizrahi, V., McKinney, J.D., Bertozzi, C.R., and Sassetti, C.M. (2012). Cholesterol Catabolism by Mycobacterium tuberculosis Requires Transcriptional and Metabolic Adaptations. Chemistry & Biology 19, 218–227.

Grimek, T.L., and Escalante-Semerena, J.C. (2004). The acnD genes of Shewenella oneidensis and Vibrio cholerae encode a new Fe/S-dependent 2-methylcitrate dehydratase enzyme that requires prpF function in vivo. Journal of Bacteriology 186, 454–462.

Grimek, T.L., Holden, H., Rayment, I., and Escalante-Semerena, J.C. (2003). Residues C123 and D58 of the 2-methylisocitrate lyase (PrpB) enzyme of Salmonella enterica are essential for catalysis. Journal of Bacteriology 185, 4837–4843.

Grimm, C., Evers, A., Brock, M., Maerker, C., Klebe, G., Buckel, W., and Reuter, K. (2003). Crystal structure of 2-methylisocitrate lyase (PrpB) from Escherichia coli and modelling of its ligand bound active centre. J. Mol. Biol. 328, 609–621.

Gross, F., Ring, M.W., Perlova, O., Fu, J., Schneider, S., Gerth, K., Kuhlmann, S., Stewart, A.F., Zhang, Y., and Müller, R. (2006). Metabolic engineering of Pseudomonas putida for methylmalonyl-CoA biosynthesis to enable complex heterologous secondary metabolite formation. Chemistry & Biology 13, 1253–1264.

Gruer, M.J., and Guest, J.R. (1994). Two genetically-distinct and differentially-regulated aconitases (AcnA and AcnB) in Escherichia coli. Microbiology (Reading, Engl.) 140 (Pt 10), 2531–2541.

Gruer, M.J., Artymiuk, P.J., and Guest, J.R. (1997a). The aconitase family: three structural variations on a common theme. Trends Biochem. Sci. 22, 3–6.

Gruer, M.J., Bradbury, A.J., and Guest, J.R. (1997b). Construction and properties of aconitase mutants of Escherichia coli. Microbiology (Reading, Engl.) 143 (Pt 6), 1837–1846.

Haller, T., Buckel, T., Rétey, J., and Gerlt, J.A. (2000). Discovering new enzymes and metabolic pathways: conversion of succinate to propionate by Escherichia coli. Biochemistry 39, 4622–4629.

Hammelman, T.A., O'Toole, G.A., Trzebiatowski, J.R., Tsang, A.W., Rank, D., and Escalante-Semerena, J.C. (1996). Identification of a new prp locus required for propionate catabolism in Salmonella typhimurium LT2. FEMS Microbiology Letters 137, 233–239.

Hartig, A., Simon, M.M., Schuster, T., Daugherty, J.R., Yoo, H.S., and Cooper, T.G. (1992). Differentially regulated malate synthase genes participate in carbon and nitrogen metabolism of S. cerevisiae. Nucleic Acids Research 20, 5677–5686.

Harvey, P.C., Watson, M., Hulme, S., Jones, M.A., Lovell, M., Berchieri, A., Young, J., Bumstead, N., and Barrow, P. (2011). Salmonella enterica serovar typhimurium colonizing the lumen of the chicken intestine grows slowly and upregulates a unique set of virulence and metabolism genes. Infection and Immunity 79, 4105–4121.

Haydock, S.F., Mironenko, T., Ghoorahoo, H.I., and Leadlay, P.F. (2004). The putative elaiophylin biosynthetic gene cluster in Streptomyces sp. DSM4137 is adjacent to genes encoding adenosylcobalamin-dependent methylmalonyl CoA mutase and to genes for synthesis of cobalamin. Journal of Biotechnology 113, 55–68.

Heider, J. (2001). A new family of CoA-transferases. FEBS Lett. 509, 345–349.

Heinisch, J.J., Valdés, E., Alvarez, J., and Rodicio, R. (1996). Molecular genetics of ICL2, encoding a non-functional isocitrate lyase in Saccharomyces cerevisiae. Yeast 12, 1285–1295.

Helliwell, K.E., Wheeler, G.L., Leptos, K.C., Goldstein, R.E., and Smith, A.G. (2011). Insights into the evolution of vitamin B12 auxotrophy from sequenced algal genomes. Mol. Biol. Evol. 28, 2921–2933.

Henrikson, K.P., and Allen, S.H. (1979). Purification and subunit structure of propionyl coenzyme A carboxylase of Mycobacterium smegmatis. J. Biol. Chem. 254, 5888–5891.

Hesslinger, C., Fairhurst, S.A., and Sawers, G. (1998). Novel keto acid formate-lyase and propionate kinase enzymes are components of an anaerobic pathway in Escherichia coli that degrades L-threonine to propionate. Mol Microbiol 27, 477–492.

Hill, C.H. (1952). Studies on the inhibition of growth of Streptococcus faecalis by sodium propionate. J. Biol. Chem. 199, 329–332.

Hines, J.K. (2006). Novel Allosteric Activation Site in Escherichia coli Fructose-1,6-bisphosphatase. Journal of Biological Chemistry 281, 18386–18393.

Hines, J.K., Fromm, H.J., and Honzatko, R.B. (2007). Structures of activated fructose-1,6-bisphosphatase from Escherichia coli. Coordinate regulation of bacterial metabolism and the conservation of the R-state. J. Biol. Chem. 282, 11696–11704.

Horswill, A.R., and Escalante-Semerena, J.C. (1997). Propionate catabolism in Salmonella typhimurium LT2: two divergently transcribed units comprise the prp locus at 8.5 centisomes, prpR encodes a member of the sigma-54 family of activators, and the prpBCDE genes constitute an operon. Journal of Bacteriology 179, 928–940.

Horswill, A.R., and Escalante-Semerena, J.C. (1999a). Salmonella typhimurium LT2 catabolizes propionate via the 2-methylcitric acid cycle. Journal of Bacteriology 181, 5615–5623.

Horswill, A.R., and Escalante-Semerena, J.C. (1999b). The prpE gene of Salmonella typhimurium LT2 encodes propionyl-CoA synthetase. Microbiology (Reading, Engl.) 145 (Pt 6), 1381–1388.

Horswill, A.R., and Escalante-Semerena, J.C. (2001). In vitro conversion of propionate to pyruvate by Salmonella enterica enzymes: 2-methylcitrate dehydratase (PrpD) and aconitase Enzymes catalyze the conversion of 2-methylcitrate to 2-methylisocitrate. Biochemistry 40, 4703–4713.

Horswill, A.R., and Escalante-Semerena, J.C. (2002). Characterization of the propionyl-CoA synthetase (PrpE) enzyme of Salmonella enterica: residue Lys592 is required for propionyl-AMP synthesis. Biochemistry 41, 2379–2387.

Horswill, A.R., Dudding, A.R., and Escalante-Semerena, J.C. (2001). Studies of propionate toxicity in Salmonella enterica identify 2-methylcitrate as a potent inhibitor of cell growth. Journal of Biological Chemistry 276, 19094–19101.

Hu, Y., van der Geize, R., Besra, G.S., Gurcha, S.S., Liu, A., Rohde, M., Singh, M., and Coates, A. (2010). 3-Ketosteroid 9alpha-hydroxylase is an essential factor in the pathogenesis of Mycobacterium tuberculosis. Mol Microbiol 75, 107–121.

Huang, C.S., Sadre-Bazzaz, K., Shen, Y., Deng, B., Zhou, Z.H., and Tong, L. (2010). Crystal structure of the alpha(6)beta(6) holoenzyme of propionyl-coenzyme A carboxylase. Nature 466, 1001–1005.

Huberts, D.H.E.W., and van der Klei, I.J. (2010). Moonlighting proteins: an intriguing mode of multitasking. Biochim. Biophys. Acta 1803, 520–525.

Huder, J.B., and Dimroth, P. (1993). Sequence of the sodium ion pump methylmalonyl-CoA decarboxylase from Veillonella parvula. J. Biol. Chem. 268, 24564–24571.

Hunaiti, A.R., and Kolattukudy, P.E. (1982). Isolation and characterization of an acyl-coenzyme A carboxylase from an erythromycin-producing Streptomyces erythreus. Arch. Biochem. Biophys. 216, 362–371.

Huynen, M.A., Dandekar, T., and Bork, P. (1999). Variation and evolution of the citric-acid cycle: a genomic perspective. Trends Microbiol. 7, 281–291.

Hüser, A.T., Becker, A., Brune, I., Dondrup, M., Kalinowski, J., Plassmeier, J., Pühler, A., Wiegräbe, I., and Tauch, A. (2003). Development of a Corynebacterium glutamicum DNA microarray and validation by genome-wide expression profiling during growth with propionate as carbon source. Journal of Biotechnology 106, 269–286.

Ibrahim-Granet, O., Dubourdeau, M., Latgé, J.-P., Avé, P., Huerre, M., Brakhage, A.A., and Brock, M. (2008). Methylcitrate synthase from Aspergillus fumigatus is essential for manifestation of invasive aspergillosis. Cell. Microbiol. 10, 134–148.

Idnurm, A., and Howlett, B.J. (2002). Isocitrate lyase is essential for pathogenicity of the fungus Leptosphaeria maculans to canola (Brassica napus). Eukaryotic Cell 1, 719–724.

Ioerger, T.R., Feng, Y., Ganesula, K., Chen, X., Dobos, K.M., Fortune, S., Jacobs, W.R., Mizrahi, V., Parish, T., Rubin, E., et al. (2010). Variation among genome sequences of H37Rv strains of Mycobacterium tuberculosis from multiple laboratories. Journal of Bacteriology 192, 3645–3653.

Jackson, C.A., Kirszbaum, L., Dashper, S., and Reynolds, E.C. (1995). Cloning, expression and sequence analysis of the genes encoding the heterodimeric methylmalonyl-CoA mutase of Porphyromonas gingivalis W50. Gene 167, 127–132.

Jacobs, W.R., Jr (2000). Mycobacterium tuberculosis: a Once Genetically Intractable Organism. In Molecular Gentics of Mycobacteria, G.F. Hatfull, and W.R. Jacobs Jr, eds. (Washington, DC: ASM Press), pp. 4–6.

Jain, M., Petzold, C.J., Schelle, M.W., Leavell, M.D., Mougous, J.D., Bertozzi, C.R., Leary, J.A., and Cox, J.S. (2007a). Lipidomics reveals control of Mycobacterium tuberculosis virulence lipids via metabolic coupling. Proc. Natl. Acad. Sci. U.S.a. 104, 5133–5138.

Jain, S.K., Hernandez Abanto, S.M., Cheng, Q.J., Singh, P., Ly, L.H., Klinkenberg, L.G., Morrison, N.E., Converse, P.J., Nuermberger, E., Grosset, J., et al. (2007b). Accelerated detection of Mycobacterium tuberculosis genes essential for bacterial survival in guinea pigs, compared with mice. J Infect Dis 195, 1634–1642.

Jansen, R., Kalousek, F., Fenton, W.A., Rosenberg, L.E., and Ledley, F.D. (1989). Cloning of full-length methylmalonyl-CoA mutase from a cDNA library using the polymerase chain reaction. Genomics 4, 198–205.

Jeter, R.M., Olivera, B.M., and Roth, J.R. (1984). Salmonella typhimurium synthesizes cobalamin (vitamin B12) de novo under anaerobic growth conditions. Journal of Bacteriology 159, 206–213.

Johnston, J.B., Ouellet, H., and Ortiz de Montellano, P.R. (2010). Functional redundancy of steroid C26-monooxygenase activity in Mycobacterium tuberculosis revealed by biochemical and genetic analyses. J. Biol. Chem. 285, 36352–36360.

Kalscheuer, R., Syson, K., Veeraraghavan, U., Weinrick, B., Biermann, K.E., Liu, Z., Sacchettini, J.C., Besra, G., Bornemann, S., and Jacobs, W.R. (2010). Self-poisoning of Mycobacterium tuberculosis by targeting GlgE in an alpha-glucan pathway. Nat. Chem. Biol. 6, 376–384.

Kamihara, T. (1969). Role of pyruvate metabolism in the growth of Streptococcus faecalis in the presence of propionate. Journal of Bacteriology 97, 151–155.

Kay, W.W. (1972). Genetic control of the metabolism of propionate by Escherichia coli K12. Biochim. Biophys. Acta 264, 508–521.

Keating, L.A., Wheeler, P.R., Mansoor, H., Inwald, J.K., Dale, J., Hewinson, R.G., and Gordon, S.V. (2005). The pyruvate requirement of some members of the Mycobacterium tuberculosis complex is due to an inactive pyruvate kinase: implications for in vivo growth. Mol Microbiol 56, 163–174.

Kelly, J.M., and Hynes, M.J. (1977). Increased and decreased sensitivity to carbon catabolite repression of enzymes of acetate metabolism in mutants of Aspergillus nidulans. Mol. Gen. Genet. 156, 87–92.

Khosla, C., Gokhale, R.S., Jacobsen, J.R., and Cane, D.E. (1999). Tolerance and specificity of polyketide synthases. Annu. Rev. Biochem. 68, 219–253.

Kim, Y.R., Brinsmade, S.R., Yang, Z., Escalante-Semerena, J.C., and Fierer, J. (2006). Mutation of phosphotransacetylase but not isocitrate lyase reduces the virulence of Salmonella enterica serovar Typhimurium in mice. Infection and Immunity 74, 2498–2502.

King, T.E., and Cheldelin, V.H. (1948). Pantothenic acid studies; propionic acid and beta-alanine utilization. J. Biol. Chem. 174, 273–279.

Kinhikar, A.G., Vargas, D., Li, H., Mahaffey, S.B., Hinds, L., Belisle, J.T., and Laal, S. (2006). Mycobacterium tuberculosis malate synthase is a laminin-binding adhesin. Mol Microbiol 60, 999–1013.

Kirksey, M.A., Tischler, A.D., Siméone, R., Hisert, K.B., Uplekar, S., Guilhot, C., and McKinney, J.D. (2011). Spontaneous phthiocerol dimycocerosate-deficient variants of Mycobacterium tuberculosis are susceptible to gamma interferon-mediated immunity. Infection and Immunity 79, 2829–2838.

Kornberg, H.L. (1965). Anaplerotic sequences in microbial metabolism. Angewandte Chemie International Edition in English 4, 558–565.

Kornberg, H.L., and Beevers, H. (1957). The glyoxylate cycle as a stage in the conversion of fat to carbohydrate in castor beans. Biochim. Biophys. Acta 26, 531–537.

Korotkova, N., and Lidstrom, M.E. (2004). MeaB is a component of the methylmalonyl-CoA mutase complex required for protection of the enzyme from inactivation. J. Biol. Chem. 279, 13652–13658.

Korotkova, N., Chistoserdova, L., Kuksa, V., and Lidstrom, M.E. (2002). Glyoxylate regeneration pathway in the methylotroph Methylobacterium extorquens AM1. Journal of Bacteriology 184, 1750–1758.

Koziol, U., Hannibal, L., Rodríguez, M.C., Fabiano, E., Kahn, M.L., and Noya, F. (2009). Deletion of citrate synthase restores growth of Sinorhizobium meliloti 1021 aconitase mutants. Journal of Bacteriology 191, 7581–7586.

Kujau, M., Weber, H., and Barth, G. (1992). Characterization of mutants of the yeast Yarrowia lipolytica defective in acetyl-coenzyme A synthetase. Yeast 8, 193–203.

Kurth, D.G., Gago, G.M., la Iglesia, de, A., Bazet Lyonnet, B., Lin, T.-W., Morbidoni, H.R., Tsai, S.-C., and Gramajo, H. (2009). ACCase 6 is the essential acetyl-CoA carboxylase involved in fatty acid and mycolic acid biosynthesis in mycobacteria. Microbiology (Reading, Engl.) 155, 2664–2675.

la Paz Santangelo, de, M., Gest, P.M., Guerin, M.E., Coinçon, M., Pham, H., Ryan, G., Puckett, S.E., Spencer, J.S., Gonzalez-Juarrero, M., Daher, R., et al. (2011). Glycolytic and non-glycolytic functions of Mycobacterium tuberculosis fructose-1,6-bisphosphate aldolase, an essential enzyme produced by replicating and non-replicating bacilli. J. Biol. Chem. 286, 40219–40231.

Laal, S., Samanich, K.M., Sonnenberg, M.G., Zolla-Pazner, S., Phadtare, J.M., and Belisle, J.T. (1997). Human humoral responses to antigens of Mycobacterium tuberculosis: immunodominance of high-molecular-mass antigens. Clin. Diagn. Lab. Immunol. 4, 49–56.

LaPorte, D.C. (1993). The isocitrate dehydrogenase phosphorylation cycle: regulation and enzymology. J. Cell. Biochem. 51, 14–18.

LaRossa, R.A., Van Dyk, T.K., and Smulski, D.R. (1987). Toxic accumulation of alpha-ketobutyrate caused by inhibition of the branched-chain amino acid biosynthetic enzyme acetolactate synthase in Salmonella typhimurium. Journal of Bacteriology 169, 1372–1378.

Lauble, H., and Stout, C.D. (1995). Steric and conformational features of the aconitase mechanism. Proteins 22, 1–11.

Lauble, H., Kennedy, M.C., Beinert, H., and Stout, C.D. (1992). Crystal structures of aconitase with isocitrate and nitroisocitrate bound. Biochemistry 31, 2735–2748.

Lawrence, J.G., and Roth, J.R. (1996a). Evolution of coenzyme B12 synthesis among enteric bacteria: evidence for loss and reacquisition of a multigene complex. Genetics 142, 11–24.

Lawrence, J.G., and Roth, J.R. (1996b). Selfish operons: horizontal transfer may drive the evolution of gene clusters. Genetics 143, 1843–1860.

Leadlay, P.F. (1981). Purification and characterization of methylmalonyl-CoA epimerase from Propionibacterium shermanii. Biochem. J. 197, 413–419.

Lee, H.-S., Lee, T.-H., Lee, J.H., Chae, C.-S., Chung, S.-C., Shin, D.-S., Shin, J., and Oh, K.-B. (2007). Inhibition of the pathogenicity of Magnaporthe grisea by bromophenols, isocitrate lyase inhibitors, from the red alga Odonthalia corymbifera. J. Agric. Food Chem. 55, 6923–6928.

Lee, S.-H., Han, Y.-K., Yun, S.-H., and Lee, Y.-W. (2009). Roles of the glyoxylate and methylcitrate cycles in sexual development and virulence in the cereal pathogen Gibberella zeae. Eukaryotic Cell 8, 1155–1164.

Lee, S.K., Newman, J.D., and Keasling, J.D. (2005). Catabolite repression of the propionate catabolic genes in Escherichia coli and Salmonella enterica: evidence for involvement of the cyclic AMP receptor protein. Journal of Bacteriology 187, 2793–2800.

Leipe, D., Wolf, Y., Koonin, E., and Aravind, L. (2002). Classification and evolution of P-loop GTPases and related ATPases. J. Mol. Biol. 317, 41–72.

Li, C., Florova, G., Akopiants, K., and Reynolds, K.A. (2004). Crotonyl-coenzyme A reductase provides methylmalonyl-CoA precursors for monensin biosynthesis by Streptomyces cinnamonensis in an oil-based extended fermentation. Microbiology (Reading, Engl.) 150, 3463–3472.

Lin, T.-W., Melgar, M.M., Kurth, D., Swamidass, S.J., Purdon, J., Tseng, T., Gago, G., Baldi, P., Gramajo, H., and Tsai, S.-C. (2006). Structure-based inhibitor design of AccD5, an essential acyl-CoA carboxylase carboxyltransferase domain of Mycobacterium tuberculosis. Proc. Natl. Acad. Sci. U.S.a. 103, 3072–3077.

Liu, F., Thatcher, J.D., Barral, J.M., and Epstein, H.F. (1995). Bifunctional glyoxylate cycle protein of Caenorhabditis elegans: a developmentally regulated protein of intestine and muscle. Dev. Biol. 169, 399–414.

Lombard, J., and Moreira, D. (2011). Early evolution of the biotin-dependent carboxylase family. BMC Evol. Biol. 11, 232.

Lorenz, M.C., and Fink, G.R. (2001). The glyoxylate cycle is required for fungal virulence. Nature 412, 83–86.

Luttik, M.A., Kötter, P., Salomons, F.A., van der Klei, I.J., van Dijken, J.P., and Pronk, J.T. (2000). The Saccharomyces cerevisiae ICL2 gene encodes a mitochondrial 2-methylisocitrate lyase involved in propionyl-coenzyme A metabolism. Journal of Bacteriology 182, 7007–7013.

Ma, Y., Pan, F., and McNeil, M. (2002). Formation of dTDP-Rhamnose Is Essential for Growth of Mycobacteria. Journal of Bacteriology 184, 3392–3395.

Maerker, C., Rohde, M., Brakhage, A.A., and Brock, M. (2005). Methylcitrate synthase from Aspergillus fumigatus. Propionyl-CoA affects polyketide synthesis, growth and morphology of conidia. Febs J. 272, 3615–3630.

Man, W.J., Li, Y., O'Connor, C.D., and Wilton, D.C. (1995). The binding of propionyl-CoA and carboxymethyl-CoA to Escherichia coli citrate synthase. Biochim. Biophys. Acta 1250, 69–75.

Mancia, F., Keep, N.H., Nakagawa, A., Leadlay, P.F., McSweeney, S., Rasmussen, B., Bösecke, P., Diat, O., and Evans, P.R. (1996). How coenzyme B12 radicals are generated: the crystal structure of methylmalonyl-coenzyme A mutase at 2 A resolution. Structure 4, 339–350.

Marrero, J., Rhee, K.Y., Schnappinger, D., Pethe, K., and Ehrt, S. (2010). Gluconeogenic carbon flow of tricarboxylic acid cycle intermediates is critical for Mycobacterium tuberculosis to establish and maintain infection. Proc. Natl. Acad. Sci. U.S.a. 107, 9819–9824.

Marsh, E.N., McKie, N., Davis, N.K., and Leadlay, P.F. (1989). Cloning and structural characterization of the genes coding for adenosylcobalamin-dependent methylmalonyl-CoA mutase from Propionibacterium shermanii. Biochem. J. 260, 345–352.

Martens, J.H., Barg, H., Warren, M.J., and Jahn, D. (2002). Microbial production of vitamin B12. Appl Microbiol Biotechnol 58, 275–285.

Maruyama, K., and Kitamura, H. (1975). Some Effects of Propionate on the Growth of Rhodopseudomonas spheroides S. Agricultural and Biological Chemistry 39, 1521–1526.

Maruyama, K., and Kitamura, H. (1985). Mechanisms of growth inhibition by propionate and restoration of the growth by sodium bicarbonate or acetate in Rhodopseudomonas sphaeroides S. J. Biochem. 98, 819–824.

Mason, R.J., Stossel, T.P., and Vaughan, M. (1972). Lipids of alveolar macrophages, polymorphonuclear leukocytes, and their phagocytic vesicles. J. Clin. Invest. 51, 2399–2407.

Massey, L.K., Sokatch, J.R., and Conrad, R.S. (1976). Branched-chain amino acid catabolism in bacteria. Bacteriol Rev 40, 42–54.

Matthies, C., and Schink, B. (1992). Reciprocal isomerization of butyrate and isobutyrate by the strictly anaerobic bacterium strain WoG13 and methanogenic isobutyrate degradation by a defined triculture. Appl. Environ. Microbiol. 58, 1435–1439.

Mattow, J., Siejak, F., Hagens, K., Becher, D., Albrecht, D., Krah, A., Schmidt, F., Jungblut, P.R., Kaufmann, S.H.E., and Schaible, U.E. (2006). Proteins unique to intraphagosomally grown Mycobacterium tuberculosis. Proteomics 6, 2485–2494.

McCarthy, A.A., Baker, H.M., Shewry, S.C., Patchett, M.L., and Baker, E.N. (2001). Crystal structure of methylmalonyl-coenzyme A epimerase from P. shermanii: a novel enzymatic function on an ancient metal binding scaffold. Structure 9, 637–646.

McKenzie, J.L., Robson, J., Berney, M., Smith, T.C., Ruthe, A., Gardner, P.P., Arcus, V.L., and Cook, G.M. (2012). A VapBC Toxin-Antitoxin Module Is a Posttranscriptional Regulator of Metabolic Flux in Mycobacteria. Journal of Bacteriology 194, 2189–2204.

Micklinghoff, J.C., Breitinger, K.J., Schmidt, M., Geffers, R., Eikmanns, B.J., and Bange, F.-C. (2009). Role of the transcriptional regulator RamB (Rv0465c) in the control of the glyoxylate cycle in Mycobacterium tuberculosis. Journal of Bacteriology 191, 7260–7269.

Middlebrook, G., and Cohn, M.L. (1958). Bacteriology of tuberculosis: laboratory methods. Am J Public Health Nations Health 48, 844–853.

Miles, P.R., Ma, J.Y., and Bowman, L. (1988). Degradation of pulmonary surfactant disaturated phosphatidylcholines by alveolar macrophages. J. Appl. Physiol. 64, 2474–2481.

Miyamoto, E., Watanabe, F., Charles, T.C., Yamaji, R., INUI, H., and Nakano, Y. (2003). Purification and characterization of homodimeric methylmalonyl-CoA mutase from Sinorhizobium meliloti. Arch. Microbiol. 180, 151–154.

Molina, I., Pellicer, M.T., Badía, J., Aguilar, J., and Baldomà, L. (1994). Molecular characterization of Escherichia coli malate synthase G. Differentiation with the malate synthase A isoenzyme. Eur. J. Biochem. 224, 541–548.

Moran, L.A., Horton, H.R., Scrimgeour, K.G., and Perry, M.D. (2011). Principles of Biochemistry (Prentice Hall).

Mori, K., Tobimatsu, T., Hara, T., and Toraya, T. (1997). Characterization, sequencing, and expression of the genes encoding a reactivating factor for glycerol-inactivated adenosylcobalamin-dependent diol dehydratase. J. Biol. Chem. 272, 32034–32041.

Mueller, G., Zipfel, F., Hlineny, K., Savvidis, E., Hertle, R., Traub-Eberhard, U., Scott, A.I., Williams, H.J., and Stolowich, N.J. (1991). Timing of cobalt insertion in vitamin B12 biosynthesis. J. Am. Chem. Soc. 113, 9893–9895.

Munoz-Elias, E.J., and McKinney, J.D. (2005). Mycobacterium tuberculosis isocitrate lyases 1 and 2 are jointly required for in vivo growth and virulence. Nat Med 11, 638–644.

Munoz-Elias, E.J., and McKinney, J.D. (2006). Carbon metabolism of intracellular bacteria. Cell. Microbiol. 8, 10–22.

Munoz-Elias, E.J., Upton, A.M., Cherian, J., and McKinney, J.D. (2006). Role of the methylcitrate cycle in Mycobacterium tuberculosis metabolism, intracellular growth, and virulence. Mol Microbiol 60, 1109–1122.

Murray, S.L., and Hynes, M.J. (2010). Metabolic and developmental effects resulting from deletion of the citA gene encoding citrate synthase in Aspergillus nidulans. Eukaryotic Cell 9, 656–666.

Mutka, S.C., Bondi, S.M., Carney, J.R., Da Silva, N.A., and Kealey, J.T. (2006). Metabolic pathway engineering for complex polyketide biosynthesis in Saccharomyces cerevisiae. FEMS Yeast Res. 6, 40–47.

Nakazawa, M., Minami, T., Teramura, K., Kumamoto, S., Hanato, S., Takenaka, S., Ueda, M., INUI, H., Nakano, Y., and Miyatake, K. (2005). Molecular characterization of a bifunctional glyoxylate cycle enzyme, malate synthase/isocitrate lyase, in Euglena gracilis. Comp. Biochem. Physiol. B, Biochem. Mol. Biol. 141, 445–452.

Nesbitt, N.M., Yang, X., Fontán, P., Kolesnikova, I., Smith, I., Sampson, N.S., and Dubnau, E. (2010). A thiolase of Mycobacterium tuberculosis is required for virulence and production of androstenedione and androstadienedione from cholesterol. Infection and Immunity 78, 275–282.

Nichayapun, P. (2005). Indentification and Characterization of Rhamnolipid Operon in Burkholderia pseudomallei. Mahidol University.

Nowrousian, M., Masloff, S., Pöggeler, S., and Kück, U. (1999). Cell differentiation during sexual development of the fungus Sordaria macrospora requires ATP citrate lyase activity. Mol. Cell. Biol. 19, 450–460.

Obradors, N., Badía, J., Baldomà, L., and Aguilar, J. (1988). Anaerobic metabolism of the L-rhamnose fermentation product 1,2-propanediol in Salmonella typhimurium. Journal of Bacteriology 170, 2159–2162.

Oh, T.-J., Daniel, J., Kim, H.-J., Sirakova, T.D., and Kolattukudy, P.E. (2006). Identification and characterization of Rv3281 as a novel subunit of a biotin-dependent acyl-CoA Carboxylase in Mycobacterium tuberculosis H37Rv. J. Biol. Chem. 281, 3899–3908.

Olivas, I., Royuela, M., Romero, B., Monteiro, M.C., Mínguez, J.M., Laborda, F., and De Lucas, J.R. (2008). Ability to grow on lipids accounts for the fully virulent phenotype in neutropenic mice of Aspergillus fumigatus null mutants in the key glyoxylate cycle enzymes. Fungal Genet. Biol. 45, 45–60.

Olszewski, K.L., Mather, M.W., Morrisey, J.M., Garcia, B.A., Vaidya, A.B., Rabinowitz, J.D., and Llinás, M. (2010). Branched tricarboxylic acid metabolism in Plasmodium falciparum. Nature 466, 774–778.

Padovani, D., and Banerjee, R. (2006). Assembly and protection of the radical enzyme, methylmalonyl-CoA mutase, by its chaperone. Biochemistry 45, 9300–9306.

Padovani, D., Labunska, T., and Banerjee, R. (2006). Energetics of interaction between the G-protein chaperone, MeaB, and B12-dependent methylmalonyl-CoA mutase. J. Biol. Chem. 281, 17838–17844.

Paiva, J.B., Penha Filho, R.A.C., Berchieri Junior, A., and Lemos, M.V.F. (2011). Requirement for cobalamin by Salmonella enterica serovars Typhimurium, Pullorum, Gallinarum and Enteritidis during infection in chickens. Brazilian Journal of Microbiology 42, 1409–1419.

Palacios, S., and Escalante-Semerena, J.C. (2000). prpR, ntrA, and ihf functions are required for expression of the prpBCDE operon, encoding enzymes that catabolize propionate in Salmonella enterica serovar typhimurium LT2. Journal of Bacteriology 182, 905–910.

Palacios, S., Starai, V.J., and Escalante-Semerena, J.C. (2003). Propionyl coenzyme A is a common intermediate in the 1,2-propanediol and propionate catabolic pathways needed for expression of the prpBCDE operon during growth of Salmonella enterica on 1,2-propanediol. Journal of Bacteriology 185, 2802–2810.

Pandey, A.K., and Sassetti, C.M. (2008). Mycobacterial persistence requires the utilization of host cholesterol. Proc. Natl. Acad. Sci. U.S.a. 105, 4376–4380.

Patton, A.J., Hough, D.W., Towner, P., and Danson, M.J. (1993). Does Escherichia coli possess a second citrate synthase gene? Eur. J. Biochem. 214, 75–81.

Peirs, P., Lefevre, P., Boarbi, S., Wang, X.M., Denis, O., Braibant, M., Pethe, K., Locht, C., Huygen, K., and Content, J. (2005). Mycobacterium tuberculosis with Disruption in Genes Encoding the Phosphate Binding Proteins PstS1 and PstS2 Is Deficient in Phosphate Uptake and Demonstrates Reduced In Vivo Virulence. Infection and Immunity 73, 1898–1902.

Pelicic, V., Reyrat, J.M., and Gicquel, B. (1996a). Expression of the Bacillus subtilis sacB gene confers sucrose sensitivity on mycobacteria. Journal of Bacteriology 178, 1197–1199.

Pelicic, V., Reyrat, J.M., and Gicquel, B. (1996b). Generation of unmarked directed mutations in mycobacteria, using sucrose counter-selectable suicide vectors. Mol Microbiol 20, 919–925.

Pethe, K., Sequeira, P.C., Agarwalla, S., Rhee, K., Kuhen, K., Phong, W.Y., Patel, V., Beer, D., Walker, J.R., Duraiswamy, J., et al. (2010). A chemical genetic screen in Mycobacterium tuberculosis identifies carbon-source-dependent growth inhibitors devoid of in vivo efficacy. Nat Commun 1, 57.

Peyron, P., Vaubourgeix, J., Poquet, Y., Levillain, F., Botanch, C., Bardou, F., Daffé, M., Emile, J.-F., Marchou, B., Cardona, P.-J., et al. (2008). Foamy macrophages from tuberculous patients' granulomas constitute a nutrient-rich reservoir for M. tuberculosis persistence. PLoS Pathog 4, e1000204.

Plassmeier, J., Barsch, A., Persicke, M., Niehaus, K., and Kalinowski, J. (2007). Investigation of central carbon metabolism and the 2-methylcitrate cycle in Corynebacterium glutamicum by metabolic profiling using gas chromatography-mass spectrometry. Journal of Biotechnology 130, 354–363.

Plassmeier, J., Persicke, M., Pühler, A., Sterthoff, C., Rückert, C., and Kalinowski, J. (2011). Molecular characterization of PrpR, the transcriptional activator of propionate catabolism in Corynebacterium glutamicum. Journal of Biotechnology.

Plassmeier, J., Persicke, M., Pühler, A., Sterthoff, C., Rückert, C., and Kalinowski, J. (2012). Molecular characterization of PrpR, the transcriptional activator of propionate catabolism in Corynebacterium glutamicum. Journal of Biotechnology 159, 1–11.

Plaut, G.W., Beach, R.L., and Aogaichi, T. (1975). Alpha-methylisocitrate. A selective inhibitor of TPN-linked isocitrate dehydrogenase from bovine heart and rat liver. Journal of Biological Chemistry 250, 6351–6354.

Portevin, D., de Sousa-D'Auria, C., Montrozier, H., Houssin, C., Stella, A., Lanéelle, M.-A., Bardou, F., Guilhot, C., and Daffé, M. (2005). The acyl-AMP ligase FadD32 and AccD4-containing acyl-CoA carboxylase are required for the synthesis of mycolic acids and essential for mycobacterial growth: identification of the carboxylation product and determination of the acyl-CoA carboxylase components. J. Biol. Chem. 280, 8862–8874.

Price, C.T.D., Al-Quadan, T., Santic, M., Rosenshine, I., and Abu Kwaik, Y. (2011). Host Proteasomal Degradation Generates Amino Acids Essential for Intracellular Bacterial Growth. Science 334, 1553–1557.

Price-Carter, M., Tingey, J., Bobik, T.A., and Roth, J.R. (2001). The Alternative Electron Acceptor Tetrathionate Supports B12-Dependent Anaerobic Growth of Salmonella enterica Serovar Typhimurium on Ethanolamine or 1,2-Propanediol. Journal of Bacteriology 183, 2463–2475.

Rabinowitz, J.D., and Kimball, E. (2007). Acidic acetonitrile for cellular metabolome extraction from Escherichia coli. Anal. Chem. 79, 6167–6173.

Radmacher, E., and Eggeling, L. (2007). The three tricarboxylate synthase activities of Corynebacterium glutamicum and increase of L-lysine synthesis. Appl Microbiol Biotechnol 76, 587–595.

Rajni, Rao, N., and Meena, L.S. (2011). Biosynthesis and Virulent Behavior of Lipids Produced by Mycobacterium tuberculosis: LAM and Cord Factor: An Overview. Biotechnology Research International 2011, 1–7.

Raux, E., Schubert, H.L., and Warren, M.J. (2000). Biosynthesis of cobalamin (vitamin B12): a bacterial conundrum. Cell. Mol. Life Sci. 57, 1880–1893.

Raynaud, C., Guilhot, C., Rauzier, J., Bordat, Y., Pelicic, V., Manganelli, R., Smith, I., Gicquel, B., and Jackson, M. (2002). Phospholipases C are involved in the virulence of Mycobacterium tuberculosis. Mol Microbiol 45, 203–217.

Reeves, A.R., Brikun, I.A., Cernota, W.H., Leach, B.I., Gonzalez, M.C., and Weber, J.M. (2007). Engineering of the methylmalonyl-CoA metabolite node of Saccharopolyspora erythraea for increased erythromycin production. Metabolic Engineering 9, 293–303.

Rehman, A., and McFadden, B.A. (1997). Lysine 194 is functional in isocitrate lyase from Escherichia coli. Curr. Microbiol. 35, 14–17.

Reinscheid, D.J., Schnicke, S., Rittmann, D., Zahnow, U., Sahm, H., and Eikmanns, B.J. (1999). Cloning, sequence analysis, expression and inactivation of the Corynebacterium glutamicum pta-ack operon encoding phosphotransacetylase and acetate kinase. Microbiology (Reading, Engl.) 145 (Pt 2), 503–513.

Rengarajan, J., Bloom, B.R., and Rubin, E.J. (2005). Genome-wide requirements for Mycobacterium tuberculosis adaptation and survival in macrophages. Proc. Natl. Acad. Sci. U.S.a. 102, 8327–8332.

Reszko, A.E., Kasumov, T., Pierce, B.A., David, F., Hoppel, C.L., Stanley, W.C., Rosiers, Des, C., and Brunengraber, H. (2003). Assessing the reversibility of the anaplerotic reactions of the propionyl-CoA pathway in heart and liver. J. Biol. Chem. 278, 34959–34965.

Rocco, C.J., and Escalante-Semerena, J.C. (2010). In Salmonella enterica, 2-methylcitrate blocks gluconeogenesis. Journal of Bacteriology 192, 771–778.

Rodionov, D.A., Vitreschak, A.G., Mironov, A.A., and Gelfand, M.S. (2003). Comparative genomics of the vitamin B12 metabolism and regulation in prokaryotes. Journal of Biological Chemistry 278, 41148–41159.

Rodríguez, E., and Gramajo, H. (1999). Genetic and biochemical characterization of the alpha and beta components of a propionyl-CoA carboxylase complex of Streptomyces coelicolor A3(2). Microbiology (Reading, Engl.) 145 (Pt 11), 3109–3119.

Rodríguez, E., Banchio, C., Diacovich, L., Bibb, M.J., and Gramajo, H. (2001). Role of an essential acyl coenzyme A carboxylase in the primary and secondary metabolism of Streptomyces coelicolor A3(2). Appl. Environ. Microbiol. 67, 4166–4176.

Roe, A.J., O'Byrne, C., McLaggan, D., and Booth, I.R. (2002). Inhibition of Escherichia coli growth by acetic acid: a problem with methionine biosynthesis and homocysteine toxicity. Microbiology (Reading, Engl.) 148, 2215–2222.

Roessner, C.A., Huang, K.-X., Warren, M.J., Raux, E., and Scott, A.I. (2002). Isolation and characterization of 14 additional genes specifying the anaerobic biosynthesis of cobalamin (vitamin B12) in Propionibacterium freudenreichii (P. shermanii). Microbiology (Reading, Engl.) 148, 1845–1853.

Romano, A.H., and Conway, T. (1996). Evolution of carbohydrate metabolic pathways. Res. Microbiol. 147, 448–455.

Rondon, M.R., and Escalante-Semerena, J.C. (1992). The poc locus is required for 1,2-propanediol-dependent transcription of the cobalamin biosynthetic (cob) and propanediol utilization (pdu) genes of Salmonella typhimurium. Journal of Bacteriology 174, 2267–2272.

Roth, J.R., Lawrence, J.G., and Bobik, T.A. (1996). Cobalamin (coenzyme B12): synthesis and biological significance. Annu. Rev. Microbiol. 50, 137–181.

Roy, I., and Leadlay, P.F. (1992). Physical map location of the new Escherichia coli gene sbm. Journal of Bacteriology 174, 5763–5764.

Rude, T.H., Toffaletti, D.L., Cox, G.M., and Perfect, J.R. (2002). Relationship of the glyoxylate pathway to the pathogenesis of Cryptococcus neoformans. Infection and Immunity 70, 5684–5694.

Russell, J. (1992). Another explanation for the toxicity of fermentation acids at low pH: anion accumulation versus uncoupling. J. Appl. Microbiol. 73, 363–370.

Salmond, C.V., Kroll, R.G., and Booth, I.R. (1984). The effect of food preservatives on pH homeostasis in Escherichia coli. J. Gen. Microbiol. 130, 2845–2850.

Samanich, K., Belisle, J.T., and Laal, S. (2001). Homogeneity of Antibody Responses in Tuberculosis Patients. Infection and Immunity 69, 4600–4609.

Sampson, B.A., and Gotschlich, E.C. (1992). Elimination of the vitamin B12 uptake or synthesis pathway does not diminish the virulence of Escherichia coli K1 or Salmonella typhimurium in three model systems. Infection and Immunity 60, 3518–3522.

Sandeman, R.A., and Hynes, M.J. (1989). Isolation of the facA (acetyl-coenzyme A synthetase) and acuE (malate synthase) genes of Aspergillus nidulans. Mol. Gen. Genet. 218, 87–92.

Sassetti, C.M., and Rubin, E.J. (2003). Genetic requirements for mycobacterial survival during infection. Proc. Natl. Acad. Sci. U.S.a. 100, 12989–12994.

Sassetti, C.M., Boyd, D.H., and Rubin, E.J. (2003). Genes required for mycobacterial growth defined by high density mutagenesis. Mol Microbiol 48, 77–84.

Savvi, S., Warner, D.F., Kana, B.D., McKinney, J.D., Mizrahi, V., and Dawes, S.S. (2008). Functional characterization of a vitamin B12-dependent methylmalonyl pathway in Mycobacterium tuberculosis: implications for propionate metabolism during growth on fatty acids. Journal of Bacteriology 190, 3886–3895.

Schnappinger, D., Ehrt, S., Voskuil, M.I., Liu, Y., Mangan, J.A., Monahan, I.M., Dolganov, G., Efron, B., Butcher, P.D., Nathan, C., et al. (2003). Transcriptional Adaptation of Mycobacterium tuberculosis within Macrophages: Insights into the Phagosomal Environment. J. Exp. Med. 198, 693–704.

Schobert, P., and Bowien, B. (1984). Unusual C3 and C4 metabolism in the chemoautotroph Alcaligenes eutrophus. Journal of Bacteriology 159, 167–172.

Schöbel, F., Ibrahim-Granet, O., Avé, P., Latgé, J.-P., Brakhage, A.A., and Brock, M. (2007). Aspergillus fumigatus does not require fatty acid metabolism via isocitrate lyase for development of invasive aspergillosis. Infection and Immunity 75, 1237–1244.

Sealy-Lewis, H.M. (1994). A new selection method for isolating mutants defective in acetate utilisation in Aspergillus nidulans. Curr. Genet. 25, 47–48.

Sharma, V., Sharma, S., Hoener zu Bentrup, K., McKinney, J.D., Russell, D.G., Jacobs, W.R., and Sacchettini, J.C. (2000). Structure of isocitrate lyase, a persistence factor of Mycobacterium tuberculosis. Nat. Struct. Biol. 7, 663–668.

Shi, L., Sohaskey, C.D., Pfeiffer, C., Datta, P., Parks, M., McFadden, J., North, R.J., and Gennaro, M.L. (2010). Carbon flux rerouting during Mycobacterium tuberculosis growth arrest. Mol Microbiol 78, 1199–1215.

Sirakova, T.D. (2001). The Mycobacterium tuberculosis pks2 Gene Encodes the Synthase for the Hepta- and Octamethyl-branched Fatty Acids Required for Sulfolipid Synthesis. Journal of Biological Chemistry 276, 16833–16839.

Sirakova, T.D., Dubey, V.S., Kim, H.J., Cynamon, M.H., and Kolattukudy, P.E. (2003). The Largest Open Reading Frame (pks12) in the Mycobacterium tuberculosis Genome Is Involved in Pathogenesis and Dimycocerosyl Phthiocerol Synthesis. Infection and Immunity 71, 3794–3801.

Smith, A.J., and Lucas, C. (1971). Propionate resistance in blue-green algae. Biochem. J. 124, 23P–24P.

Smith, C.V., Huang, C.-C., Miczak, A., Russell, D.G., Sacchettini, J.C., and Höner zu Bentrup, K. (2003). Biochemical and structural studies of malate synthase from Mycobacterium tuberculosis. Journal of Biological Chemistry 278, 1735–1743.

Snapper, S.B., Melton, R.E., Mustafa, S., Kieser, T., and Jacobs, W.R. (1990). Isolation and characterization of efficient plasmid transformation mutants of Mycobacterium smegmatis. Mol Microbiol 4, 1911–1919.

Solomon, P.S., Lee, R.C., Wilson, T.J.G., and Oliver, R.P. (2004). Pathogenicity of Stagonospora nodorum requires malate synthase. Mol Microbiol 53, 1065–1073.

Somashekar, B.S., Amin, A.G., Rithner, C.D., Troudt, J., Basaraba, R., Izzo, A., Crick, D.C., and Chatterjee, D. (2011). Metabolic profiling of lung granuloma in Mycobacterium tuberculosis infected guinea pigs: ex vivo 1H magic angle spinning NMR studies. J. Proteome Res. 10, 4186–4195.

Somerville, G.A., Saïd-Salim, B., Wickman, J.M., Raffel, S.J., Kreiswirth, B.N., and Musser, J.M. (2003). Correlation of acetate catabolism and growth yield in Staphylococcus aureus: implications for host-pathogen interactions. Infection and Immunity 71, 4724–4732.

Sonnenberg, M.G., and Belisle, J.T. (1997). Definition of Mycobacterium tuberculosis culture filtrate proteins by two-dimensional polyacrylamide gel electrophoresis, N-terminal amino acid sequencing, and electrospray mass spectrometry. Infection and Immunity 65, 4515–4524.

Srinivasan, V., and Morowitz, H.J. (2006). Ancient genes in contemporary persistent microbial pathogens. Biol. Bull. 210, 1–9.

Stone, B.J., Brier, A., and Kwaik, Y.A. (1999). The Legionella pneumophila prp locus; required during infection of macrophages and amoebae. Microb. Pathog. 27, 369–376.

Tabuchi, T., and Serizawa, N. (1975). A hypothetical cyclic pathway for the metabolism of odd-carbon n-alkanes or propionyl-CoA via seven-carbon tricarboxylic acids in yeasts. Agricultural and Biological Chemistry 39, 1055–1061.

Tabuchi, T., Aoki, H., Uchiyama, H., and Nakahara, T. (1981). 2-Methylcitrate dehydratase, a new enzyme functioning at the methylcitric acid cycle of propionate metabolism. Agricultural and Biological Chemistry 45, 2823–2829.

Tabuchi, T., Umetsu, H., Aoki, H., and Uchiyama, H. (1995). Characteristics of 2-methylisocitrate dehydratase, isolated from Yallowia lipolytica, in comparison with aconitase. Biosci. Biotechnol. Biochem. 59, 2013–2017.

Taga, M.E., and Walker, G.C. (2010). Sinorhizobium meliloti requires a cobalamin-dependent ribonucleotide reductase for symbiosis with its plant host. Mol. Plant Microbe Interact. 23, 1643–1654.

Takahashi-Iñiguez, T., Garcia-Hernandez, E., Arreguin-Espinosa, R., and Flores, M.E. (2012). The role of vitamin B 12 on methylmalonyl-CoA mutase activity. Journal of Zhejiang University.

Takahashi-Iñiguez, T., García-Arellano, H., Trujillo-Roldán, M.A., and Flores, M.E. (2011). Protection and reactivation of human methylmalonyl-CoA mutase by MMAA protein. Biochem. Biophys. Res. Commun. 404, 443–447.

Textor, S., Wendisch, V.F., De Graaf, A.A., Müller, U., Linder, M.I., Linder, D., and Buckel, W. (1997). Propionate oxidation in Escherichia coli: evidence for operation of a methylcitrate cycle in bacteria. Arch. Microbiol. 168, 428–436.

Tholozan, J., Samain, E., Grivet, J.P., and Albagnac, G. (1990). Propionate metabolism in a methanogenic enrichment culture. Direct reductive carboxylation and acetogenesis pathways. FEMS Microbiology Letters 73, 291–297.

Tian, J., Bryk, R., Itoh, M., Suematsu, M., and Nathan, C. (2005). Variant tricarboxylic acid cycle in Mycobacterium tuberculosis: identification of alpha-ketoglutarate decarboxylase. Proc. Natl. Acad. Sci. U.S.a. 102, 10670–10675.

Timm, J., Post, F.A., Bekker, L.-G., Walther, G.B., Wainwright, H.C., Manganelli, R., Chan, W.-T., Tsenova, L., Gold, B., Smith, I., et al. (2003). Differential expression of iron-, carbon-, and oxygen-responsive mycobacterial genes in the lungs of chronically infected mice and tuberculosis patients. Proc. Natl. Acad. Sci. U.S.a. 100, 14321–14326.

Toraya, T., and Mori, K. (1999). A reactivating factor for coenzyme B12-dependent diol dehydratase. J. Biol. Chem. 274, 3372–3377.

Trivedi, O.A., Arora, P., Vats, A., Ansari, M.Z., Tickoo, R., Sridharan, V., Mohanty, D., and Gokhale, R.S. (2005). Dissecting the mechanism and assembly of a complex virulence mycobacterial lipid. Mol. Cell 17, 631–643.

Tsang, A.W., Horswill, A.R., and Escalante-Semerena, J.C. (1998). Studies of regulation of expression of the propionate (prpBCDE) operon provide insights into how Salmonella typhimurium LT2 integrates its 1,2-propanediol and propionate catabolic pathways. Journal of Bacteriology 180, 6511–6518.

Tuite, N.L., Fraser, K.R., and O'byrne, C.P. (2005). Homocysteine toxicity in Escherichia coli is caused by a perturbation of branched-chain amino acid biosynthesis. Journal of Bacteriology 187, 4362–4371.

Upton, A.M., and McKinney, J.D. (2007). Role of the methylcitrate cycle in propionate metabolism and detoxification in Mycobacterium smegmatis. Microbiology (Reading, Engl.) 153, 3973–3982.

Vagelos, P.R., and Earl, J.M. (1959). Propionic acid metabolism. III. beta-Hydroxypropionyl coenzyme A and malonyl semialdehyde coenzyme A, intermediates in propionate oxidation by Clostridium kluyveri. J. Biol. Chem. 234, 2272–2280.

van der Geize, R., Yam, K., Heuser, T., Wilbrink, M.H., Hara, H., Anderton, M.C., Sim, E., Dijkhuizen, L., Davies, J.E., Mohn, W.W., et al. (2007). A gene cluster encoding cholesterol catabolism in a soil actinomycete provides insight into Mycobacterium tuberculosis survival in macrophages. Proc. Natl. Acad. Sci. U.S.a. 104, 1947–1952.

van Rooyen, J.P., Mienie, L.J., Erasmus, E., De Wet, W.J., Ketting, D., Duran, M., and Wadman, S.K. (1994). Identification of the stereoisomeric configurations of methylcitric acid produced by si-citrate synthase and methylcitrate synthase using capillary gas chromatography-mass spectrometry. J. Inherit. Metab. Dis. 17, 738–747.

Vanderwinkel, E., and Vlieghere, M. (1968). Physiologie et génétique de l'isocitritase et des malate synthases chez Escherichia coli. European Journal of Biochemistry 5, 81–90.

Veit, A., Rittmann, D., Georgi, T., Youn, J.-W., Eikmanns, B.J., and Wendisch, V.F. (2009). Pathway identification combining metabolic flux and functional genomics analyses: acetate and propionate activation by Corynebacterium glutamicum. Journal of Biotechnology 140, 75–83.

Venugopal, A., Bryk, R., Shi, S., Rhee, K., Rath, P., Schnappinger, D., Ehrt, S., and Nathan, C. (2011). Virulence of Mycobacterium tuberculosis depends on lipoamide dehydrogenase, a member of three multienzyme complexes. Cell Host and Microbe 9, 21–31.

Vereecke, D., Cornelis, K., Temmerman, W., Holsters, M., and Goethals, K. (2002a). Versatile persistence pathways for pathogens of animals and plants. Trends Microbiol. 10, 485–488.

Vereecke, D., Cornelis, K., Temmerman, W., Jaziri, M., Van Montagu, M., Holsters, M., and Goethals, K. (2002b). Chromosomal locus that affects pathogenicity of Rhodococcus fascians. Journal of Bacteriology 184, 1112–1120.

Viollier, P.H., Nguyen, K.T., Minas, W., Folcher, M., Dale, G.E., and Thompson, C.J. (2001). Roles of aconitase in growth, metabolism, and morphological differentiation of Streptomyces coelicolor. Journal of Bacteriology 183, 3193–3203.

Voellym, R., and Leisinger, T. (1976). Role of 4-aminobutyrate aminotransferase in the arginine metabolism of Pseudomonas aeruginosa. Journal of Bacteriology 128, 722–729.

Volcani, B.E., Toohey, J.I., and Barker, H.A. (1961). Detection of cobamide coenzymes in microorganisms by the ionophoretic bioautographic method. Arch. Biochem. Biophys. 92, 381–391.

Waegeman, H., Beauprez, J., Moens, H., Maertens, J., De Mey, M., Foulquié-Moreno, M.R., Heijnen, J.J., Charlier, D., and Soetaert, W. (2011). Effect of iclR and arcA knockouts on biomass formation and metabolic fluxes in Escherichia coli K12 and its implications on understanding the metabolism of Escherichia coli BL21 (DE3). BMC Microbiol 11, 70.

Wagner, D., Maser, J., Lai, B., Cai, Z., Barry, C.E., Höner zu Bentrup, K., Russell, D.G., and Bermudez, L.E. (2005). Elemental analysis of Mycobacterium avium-, Mycobacterium tuberculosis-, and Mycobacterium smegmatis-containing phagosomes indicates pathogen-induced microenvironments within the host cell's endosomal system. J. Immunol. 174, 1491–1500.

Wall, D.M., Duffy, P.S., Dupont, C., Prescott, J.F., and Meijer, W.G. (2005). Isocitrate lyase activity is required for virulence of the intracellular pathogen Rhodococcus equi. Infection and Immunity 73, 6736–6741.

Walsh, K., and Koshland, D.E. (1985). Characterization of rate-controlling steps in vivo by use of an adjustable expression vector. Proc. Natl. Acad. Sci. U.S.a. 82, 3577–3581.

Wang, Z.-X., Brämer, C.O., and Steinbüchel, A. (2003). The glyoxylate bypass of Ralstonia eutropha. FEMS Microbiology Letters 228, 63–71.

Warner, D.F., Savvi, S., Mizrahi, V., and Dawes, S.S. (2007). A riboswitch regulates expression of the coenzyme B12-independent methionine synthase in Mycobacterium tuberculosis: implications for differential methionine synthase function in strains H37Rv and CDC1551. Journal of Bacteriology 189, 3655–3659.

Wayne, L.G., and Lin, K.Y. (1982). Glyoxylate metabolism and adaptation of Mycobacterium tuberculosis to survival under anaerobic conditions. Infection and Immunity 37, 1042–1049.

Wayne, L.G., and Sohaskey, C.D. (2001). Nonreplicating persistence of mycobacterium tuberculosis. Annu. Rev. Microbiol. 55, 139–163.

Wegener, W.S., Reeves, H.C., and Ajl, S.J. (1968a). Propionate metabolism. 3. Studies on the significance of the alpha-hydroxyglutarate pathway. Arch. Biochem. Biophys. 123, 62–65.

Wegener, W.S., Reeves, H.C., Rabin, R., and Ajl, S.J. (1968b). Alternate pathways of metabolism of short-chain fatty acids. Bacteriol Rev 32, 1–26.

Wei, J.-R., Krishnamoorthy, V., Murphy, K., Kim, J.-H., Schnappinger, D., Alber, T., Sassetti, C.M., Rhee, K.Y., and Rubin, E.J. (2011). Depletion of antibiotic targets has widely varying effects on growth. Proc. Natl. Acad. Sci. U.S.a. 108, 4176–4181.

Wheeler, P.R., Bulmer, K., Ratledge, C., Dale, J.W., and Norman, E. (1992). Control of acyl-CoA carboxylase activity in mycobacteria. FEMS Microbiology Letters 69, 169–172.

Wilkemeyer, M.F., Crane, A.M., and Ledley, F.D. (1990). Primary structure and activity of mouse methylmalonyl-CoA mutase. Biochem. J. 271, 449–455.

Winter, S.E., Thiennimitr, P., Winter, M.G., Butler, B.P., Huseby, D.L., Crawford, R.W., Russell, J.M., Bevins, C.L., Adams, L.G., Tsolis, R.M., et al. (2010). Gut inflammation provides a respiratory electron acceptor for Salmonella. Nature 467, 426–429.

Wong, S., and Wolfe, K.H. (2005). Birth of a metabolic gene cluster in yeast by adaptive gene relocation. Nat. Genet. 37, 777–782.

Woodruff, P.J., Carlson, B.L., Siridechadilok, B., Pratt, M.R., Senaratne, R.H., Mougous, J.D., Riley, L.W., Williams, S.J., and Bertozzi, C.R. (2004). Trehalose is required for growth of Mycobacterium smegmatis. J. Biol. Chem. 279, 28835–28843.

Wright, L.D., and Skeggs, H.R. (1946). Reversal of sodium propionate inhibition of Escherichia coli with beta-alanine. Arch Biochem 10, 383–386.

Yam, K.C., D'Angelo, I., Kalscheuer, R., Zhu, H., Wang, J.-X., Snieckus, V., Ly, L.H., Converse, P.J., Jacobs, W.R., Strynadka, N., et al. (2009). Studies of a ring-cleaving dioxygenase illuminate the role of cholesterol metabolism in the pathogenesis of Mycobacterium tuberculosis. PLoS Pathog 5, e1000344.

Yang, X., Gao, J., Smith, I., Dubnau, E., and Sampson, N.S. (2011). Cholesterol is not an essential source of nutrition for Mycobacterium tuberculosis during infection. Journal of Bacteriology 193, 1473–1476.

Yang, X., Nesbitt, N.M., Dubnau, E., Smith, I., and Sampson, N.S. (2009). Cholesterol metabolism increases the metabolic pool of propionate in Mycobacterium tuberculosis. Biochemistry 48, 3819–3821.

Zerbe-Burkhardt, K., Ratnatilleke, A., Philippon, N., Birch, A., Leiser, A., Vrijbloed, J.W., Hess, D., Hunziker, P., and Robinson, J.A. (1998). Cloning, sequencing, expression, and insertional inactivation of the gene for the large subunit of the coenzyme B12-dependent isobutyryl-CoA mutase from Streptomyces cinnamonensis. J. Biol. Chem. 273, 6508–6517.

Zhang, H., Boghigian, B.A., and Pfeifer, B.A. (2010). Investigating the role of native propionyl-CoA and methylmalonyl-CoA metabolism on heterologous polyketide production in Escherichia coli. Biotechnol. Bioeng. 105, 567–573.

Zhang, Y., Rodionov, D.A., Gelfand, M.S., and Gladyshev, V.N. (2009). Comparative genomic analyses of nickel, cobalt and vitamin B12 utilization. BMC Genomics 10, 78.

Zhang, Y.-Q., and Keller, N.P. (2004). Blockage of methylcitrate cycle inhibits polyketide production in Aspergillus nidulans. Mol Microbiol 52, 541–550.

Zhang, Y.-Q., Brock, M., and Keller, N.P. (2004). Connection of propionyl-CoA metabolism to polyketide biosynthesis in Aspergillus nidulans. Genetics 168, 785–794.